



# Lecture notes for the 2011 RAL School for Experimental High Energy Physics Students

MA Thomson (ed)

August 2011

**©2011 Science and Technology Facilities Council**

Enquiries about copyright, reproduction and requests for additional copies of this report should be addressed to:

RAL Library  
STFC Rutherford Appleton Laboratory  
R61  
Harwell Oxford  
Didcot  
OX11 0QX

Tel: +44(0)1235 445384  
Fax: +44(0)1235 446403  
email: [libraryral@stfc.ac.uk](mailto:libraryral@stfc.ac.uk)

Science and Technology Facilities Council reports are available online at: <http://epubs.stfc.ac.uk>

**ISSN 1358- 6254**

Neither the Council nor the Laboratory accept any responsibility for loss or damage arising from the use of information contained in any of their reports or in any communication about their tests or investigations.

**RAL-TR-2011-014**  
Science and Technology Facilities Council

## **Rutherford Appleton Laboratory**

Harwell Oxford, DIDCOT Oxon OX11 0QX

# **Lecture Notes for the 2011 RAL School for Experimental High Energy Physics Students**

**Editor:** MA Thomson  
**Compilers:** G Birch and J Graham

**Rutherford Appleton Laboratory**  
**4 - 16 September 2011**



# CONTENTS

# Pages

## LECTURE COURSES

Quantum Field Theory Dr C White	1 - 47
An Introduction to QED & QCD Dr F Hautmann	49 - 115
The Standard Model Dr C Maxwell	117 - 146
Phenomenology Dr P Richardson	147 - 218



# QUANTUM FIELD THEORY

Dr Chris White (University of Glasgow)

Lecture presented at the School for Experimental High Energy Physics Students  
Somerville College, Oxford, September 2010





# Contents

<b>1</b>	<b>Introduction .....</b>	<b>5</b>
1.1	Classical Mechanics .....	6
1.2	Quantum mechanics .....	8
1.3	The Schrödinger picture.....	10
1.4	The Heisenberg picture .....	11
1.5	The quantum harmonic oscillator .....	11
1.6	Relativistic Quantum Mechanics .....	12
<b>2</b>	<b>Classical Field Theory .....</b>	<b>14</b>
2.1	Example: Model of an Elastic Rod.....	14
2.2	Relativistic Fields .....	15
2.3	Plane wave solutions to the Klein-Gordon equation.....	17
2.4	Symmetries and Conservation Laws .....	18
<b>3</b>	<b>Quantum Field Theory: Free Fields.....</b>	<b>19</b>
3.1	Canonical Field Quantisation.....	19
3.2	Creation and annihilation operators .....	21
3.3	Energy of the vacuum state and renormalisation .....	22
3.4	Fock space and Particles .....	24
<b>4</b>	<b>Quantum Field Theory: Interacting Fields .....</b>	<b>26</b>
4.1	The $S$ -matrix.....	26
4.2	More on time evolution: Dirac picture .....	28
4.3	$S$ -matrix and Green's functions .....	31
4.4	How to compute Green's functions .....	33
<b>5</b>	<b>Perturbation Theory .....</b>	<b>35</b>
5.1	Wick's Theorem.....	36
5.2	The Feynman propagator .....	37
5.3	Two-particle scattering to $O(\lambda)$ .....	38
5.4	Graphical representation of the Wick expansion: Feynman rules.....	40
5.5	Feynman rules in momentum space .....	41
5.6	$S$ -matrix and truncated Green's functions .....	42
<b>6</b>	<b>Summary.....</b>	<b>44</b>
	<b>Acknowledgments .....</b>	<b>45</b>
<b>A</b>	<b>Books on QFT .....</b>	<b>46</b>
	<b>References.....</b>	<b>46</b>
<b>B</b>	<b>Notation and conventions .....</b>	<b>47</b>



# Quantum Field Theory - Notes

Chris White (University of Glasgow)

## Abstract

These notes are a write-up of lectures given at the RAL school for High Energy Physicists, which took place at Somerville College, Oxford in September 2010. The aim is to introduce the canonical quantisation approach to QFT, and derive the Feynman rules for a scalar field.

## 1 Introduction

Quantum Field Theory is a highly important cornerstone of modern physics. It underlies, for example, the description of elementary particles i.e. the Standard Model of particle physics is a QFT. There is currently no observational evidence to suggest that QFT is insufficient in describing particle behaviour, and indeed many theories for beyond the Standard Model physics (e.g. supersymmetry, extra dimensions) are QFTs. There are some theoretical reasons, however, for believing that QFT will not work at energies above the Planck scale, at which gravity becomes important. Aside from particle physics, QFT is also widely used in the description of condensed matter systems, and there has been a fruitful interplay between the fields of condensed matter and high energy physics.

We will see that the need for QFT arises when one tries to unify special relativity and quantum mechanics, which explains why theories of use in high energy particle physics are quantum field theories. Historically, Quantum Electrodynamics (QED) emerged as the prototype of modern QFT's. It was developed in the late 1940s and early 1950s chiefly by Feynman, Schwinger and Tomonaga, and has the distinction of being the most accurately verified theory of all time: the anomalous magnetic dipole moment of the electron predicted by QED agrees with experiment with a stunning accuracy of one part in  $10^{10}$ ! Since then, QED has been understood as forming part of a larger theory, the Standard Model of particle physics, which also describes the weak and strong nuclear forces. As you will learn at this school, electromagnetism and the weak interaction can be unified into a single “electroweak” theory, and the theory of the strong force is described by Quantum Chromodynamics (QCD). QCD has been verified in a wide range of contexts, albeit not as accurately as QED (due to the fact that the QED force is much weaker, allowing more accurate calculations to be carried out).

As is clear from the above discussion, QFT is a type of theory, rather than a particular theory. In this course, our aim is to introduce what a QFT is, and how to derive scattering amplitudes in perturbation theory (in the form of Feynman rules). For this purpose, it is sufficient to consider the simple example of a single, real scalar field. More physically relevant examples will be dealt with in the other courses. Throughout, we will follow the so-called canonical quantisation approach to QFT, rather than the path integral approach. Although the latter approach is more elegant, it is less easily presented in such a short course.

The structure of these notes is as follows. In the rest of the introduction, we review those aspects of classical and quantum mechanics which are relevant in discussing QFT. In particular, we go over the Lagrangian formalism in point particle mechanics, and see how this can also be used to describe classical fields. We then look at the quantum mechanics of non-relativistic point

particles, and recall the properties of the quantum harmonic oscillator, which will be useful in what follows. We then briefly show how attempts to construct a relativistic analogue of the Schrödinger equation lead to inconsistencies. Next, we discuss classical field theory, deriving the equations of motion that a relativistic scalar field theory has to satisfy, and examining the relationship between symmetries and conservation laws. We then discuss the quantum theory of free fields, and interpret the resulting theory in terms of particles, before showing how to describe interactions via the  $S$ -matrix and its relation to Green's functions. Finally, we describe how to obtain explicit results for scattering amplitudes using perturbation theory, which leads (via Wick's theorem) to Feynman diagrams.

## 1.1 Classical Mechanics

Let us begin this little review by considering the simplest possible system in classical mechanics, a single point particle of mass  $m$  in one dimension, whose coordinate and velocity are functions of time,  $x(t)$  and  $\dot{x}(t) = dx(t)/dt$ , respectively. Let the particle be exposed to a time-independent potential  $V(x)$ . Its motion is then governed by Newton's law

$$m \frac{d^2 x}{dt^2} = -\frac{\partial V}{\partial x} = F(x), \quad (1)$$

where  $F(x)$  is the force exerted on the particle. Solving this equation of motion involves two integrations, and hence two arbitrary integration constants to be fixed by initial conditions. Specifying, e.g., the position  $x(t_0)$  and velocity  $\dot{x}(t_0)$  of the particle at some initial time  $t_0$  completely determines its motion: knowing the initial conditions and the equations of motion, we also know the evolution of the particle at all times (provided we can solve the equations of motion).

We can also derive the equation of motion using an entirely different approach, via the Lagrangian formalism. This is perhaps more abstract than Newton's force-based approach, but in fact is easier to generalise and technically more simple in complicated systems (such as field theory!), not least because it avoids us having to think about forces at all.

First, we introduce the *Lagrangian*

$$L(x, \dot{x}) = T - V = \frac{1}{2} m \dot{x}^2 - V(x), \quad (2)$$

which is a function of coordinates and velocities, and given by the difference between the kinetic and potential energies of the particle. Next, we define the *action*

$$S = \int_{t_0}^{t_1} dt L(x, \dot{x}). \quad (3)$$

The equations of motion are then given by the *principle of least action*, which says that the trajectory  $x(t)$  followed by the particle is precisely that such that  $S$  is extremised<sup>1</sup>. To verify this in the present case, let us rederive Newton's Second Law.

First let us suppose that  $x(t)$  is indeed the trajectory that extremises the action, and then introduce a small perturbation

$$x(t) \rightarrow x(t) + \delta x(t), \quad (4)$$

such that the end points are fixed:

$$\left. \begin{array}{l} x'(t_1) = x(t_1) \\ x'(t_2) = x(t_2) \end{array} \right\} \Rightarrow \delta x(t_1) = \delta x(t_2) = 0. \quad (5)$$

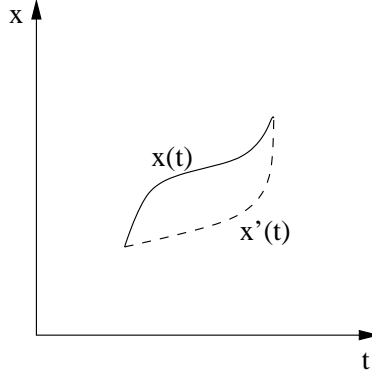


Figure 1: *Variation of particle trajectory with identified initial and end points.*

This sends  $S$  to some  $S + \delta S$ , where  $\delta S = 0$  if  $S$  is extremised. One may Taylor expand to give

$$\begin{aligned}
 S + \delta S &= \int_{t_1}^{t_2} L(x + \delta x, \dot{x} + \delta \dot{x}) dt, \quad \delta \dot{x} = \frac{d}{dt} \delta x \\
 &= \int_{t_1}^{t_2} \left\{ L(x, \dot{x}) + \frac{\partial L}{\partial x} \delta x + \frac{\partial L}{\partial \dot{x}} \delta \dot{x} + \dots \right\} dt \\
 &= S + \frac{\partial L}{\partial \dot{x}} \delta x \Big|_{t_1}^{t_2} + \int_{t_1}^{t_2} \left\{ \frac{\partial L}{\partial x} - \frac{d}{dt} \frac{\partial L}{\partial \dot{x}} \right\} \delta x dt,
 \end{aligned} \tag{6}$$

where we performed an integration by parts on the last term in the second line. The second and third term in the last line are the variation of the action,  $\delta S$ , under variations of the trajectory,  $\delta x$ . The second term vanishes because of the boundary conditions for the variation, and we are left with the third. Now the Principle of Least Action demands  $\delta S = 0$ . For the remaining integral to vanish for arbitrary  $\delta x$  is only possible if the integrand vanishes, leaving us with the Euler-Lagrange equation:

$$\frac{\partial L}{\partial x} - \frac{d}{dt} \frac{\partial L}{\partial \dot{x}} = 0. \tag{7}$$

If we insert the Lagrangian of our point particle, Eq. (2), into the Euler-Lagrange equation we obtain

$$\begin{aligned}
 \frac{\partial L}{\partial x} &= -\frac{\partial V(x)}{\partial x} = F \\
 \frac{d}{dt} \frac{\partial L}{\partial \dot{x}} &= \frac{d}{dt} m\dot{x} = m\ddot{x} \\
 \Rightarrow m\ddot{x} &= F = -\frac{\partial V}{\partial x} \quad (\text{Newton's law}).
 \end{aligned} \tag{8}$$

Hence, we have derived the equation of motion (the Euler-Lagrange equation) using the Principle of Least Action and found it to be equivalent to Newton's Second Law. The benefit of the former is that it can be easily generalised to other systems in any number of dimensions, multi-particle systems, or systems with an infinite number of degrees of freedom, where the latter are needed for field theory.

---

<sup>1</sup>The name of the principle comes from the fact that, in most cases,  $S$  is indeed minimised.

For example, a general system of point particles has a set  $\{q_i\}$  of *generalised coordinates*, which may not be simple positions but also angles etc. The equations of motion are then given by

$$\frac{d}{dt} \frac{\partial L}{\partial \dot{q}_i} = \frac{\partial L}{\partial q_i},$$

by analogy with the one-dimensional case. That is, each coordinate has its own Euler-Lagrange equation (which may nevertheless depend on the other coordinates, so that the equations of motion are coupled). Another advantage of the Lagrangian formalism is that the relationship between symmetries and conserved quantities is readily understood - more on this later.

First, let us note that there is yet another way to think about classical mechanics (that we will see again in quantum mechanics / field theory), namely via the Hamiltonian formalism. Given a Lagrangian depending on generalised coordinates  $\{q_i\}$ , we may define the *conjugate momenta*

$$p_i = \frac{\partial L}{\partial \dot{q}_i}$$

e.g. in the simple one-dimensional example given above, there is a single momentum  $p = m\dot{x}$  conjugate to  $x$ . We recognise as the familiar definition of momentum, but it is not always true that  $p_i = m\dot{q}_i$ .

We may now define the *Hamiltonian*

$$H(\{q_i\}, \{p_i\}) = \sum_i \dot{q}_i p_i - L(\{q_i\}, \{\dot{q}_i\}).$$

As an example, consider again

$$L = \frac{1}{2} m \dot{x}^2 - V(x).$$

It is easy to show from the above definition that

$$H = \frac{1}{2} m \dot{x}^2 + V(x),$$

which we recognise as the total energy of the system. From the definition of the Hamiltonian one may derive (problem 1.1)

$$\frac{\partial H}{\partial q_i} = -\dot{p}_i, \quad \frac{\partial H}{\partial p_i} = \dot{q}_i,$$

which constitute *Hamilton's equations*. These are useful in proving the relation between symmetries and conserved quantities. For example, one readily sees from the above equations that the momentum  $p_i$  is conserved if  $H$  does not depend explicitly on  $q_i$ . That is, conservation of momentum is related to invariance under spatial translations, if  $q_i$  can be interpreted as a simple position coordinate.

## 1.2 Quantum mechanics

Having set up some basic formalism for classical mechanics, let us now move on to quantum mechanics. In doing so we shall use *canonical quantisation*, which is historically what was used first and what we shall later use to quantise fields as well. We remark, however, that one can also quantise a theory using path integrals.

Canonical quantisation consists of two steps. Firstly, the dynamical variables of a system are replaced by operators, which we denote by a hat. Secondly, one imposes commutation relations on these operators,

$$[\hat{x}_i, \hat{p}_j] = i\hbar \delta_{ij} \tag{9}$$

$$[\hat{x}_i, \hat{x}_j] = [\hat{p}_i, \hat{p}_j] = 0. \tag{10}$$

The physical state of a quantum mechanical system is encoded in state vectors  $|\psi\rangle$ , which are elements of a Hilbert space  $\mathcal{H}$ . The hermitian conjugate state is  $\langle\psi| = (|\psi\rangle)^\dagger$ , and the modulus squared of the scalar product between two states gives the probability for the system to go from state 1 to state 2,

$$|\langle\psi_1|\psi_2\rangle|^2 = \text{probability for } |\psi_1\rangle \rightarrow |\psi_2\rangle. \quad (11)$$

On the other hand physical observables  $O$ , i.e. measurable quantities, are given by the expectation values of hermitian operators,  $\hat{O} = \hat{O}^\dagger$ ,

$$O = \langle\psi|\hat{O}|\psi\rangle, \quad O_{12} = \langle\psi_2|\hat{O}|\psi_1\rangle. \quad (12)$$

Hermiticity ensures that expectation values are real, as required for measurable quantities. Due to the probabilistic nature of quantum mechanics, expectation values correspond to statistical averages, or mean values, with a variance

$$(\Delta O)^2 = \langle\psi|(\hat{O} - O)^2|\psi\rangle = \langle\psi|\hat{O}^2|\psi\rangle - \langle\psi|\hat{O}|\psi\rangle^2. \quad (13)$$

An important concept in quantum mechanics is that of eigenstates of an operator, defined by

$$\hat{O}|\psi\rangle = O|\psi\rangle. \quad (14)$$

Evidently, between eigenstates we have  $\Delta O = 0$ . Examples are coordinate eigenstates,  $\hat{\mathbf{x}}|\mathbf{x}\rangle = \mathbf{x}|\mathbf{x}\rangle$ , and momentum eigenstates,  $\hat{\mathbf{p}}|\mathbf{p}\rangle = \mathbf{p}|\mathbf{p}\rangle$ , describing a particle at position  $\mathbf{x}$  or with momentum  $\mathbf{p}$ , respectively. However, a state vector cannot be simultaneous eigenstate of non-commuting operators. This leads to the Heisenberg uncertainty relation for any two non-commuting operators  $\hat{A}, \hat{B}$ ,

$$\Delta A \Delta B \geq \frac{1}{2} |\langle\psi|[\hat{A}, \hat{B}]|\psi\rangle|. \quad (15)$$

Finally, sets of eigenstates can be orthonormalized and we assume completeness, i.e. they span the entire Hilbert space,

$$\langle\mathbf{p}'|\mathbf{p}\rangle = \delta(\mathbf{p} - \mathbf{p}'), \quad 1 = \int d^3p |\mathbf{p}\rangle\langle\mathbf{p}|. \quad (16)$$

As a consequence, an arbitrary state vector can always be expanded in terms of a set of eigenstates. We may then define the *position space wavefunction*

$$\psi(\mathbf{x}) = \langle\mathbf{x}|\psi\rangle,$$

so that

$$\begin{aligned} \langle\psi_1|\psi_2\rangle &= \int d^3\mathbf{x} \langle\psi_1|\mathbf{x}\rangle\langle\mathbf{x}|\psi_2\rangle \\ &= \int d^3\mathbf{x} \psi_1^*(\mathbf{x})\psi_2(\mathbf{x}). \end{aligned} \quad (17)$$

Acting on the wavefunction, the explicit form of the position and momentum operators is

$$\hat{\mathbf{x}} = \mathbf{x}, \quad \hat{\mathbf{p}} = -i\hbar\nabla, \quad (18)$$

so that the Hamiltonian operator is

$$\hat{H} = \frac{\hat{\mathbf{p}}^2}{2m} + V(\mathbf{x}) = -\frac{\hbar^2\nabla^2}{2m} + V(\mathbf{x}). \quad (19)$$

Having quantised our system, we now want to describe its time evolution. This can be done in different “pictures”, depending on whether we consider the state vectors or the operators (or both) to depend explicitly on  $t$ , such that expectation values remain the same. Two extreme cases are those where the operators do not depend on time (the *Schrödinger picture*), and when the state vectors do not depend on time (the *Heisenberg picture*). We discuss these two choices in the following sections.

### 1.3 The Schrödinger picture

In this approach state vectors are functions of time,  $|\psi(t)\rangle$ , while operators are time independent,  $\partial_t \hat{O} = 0$ . The time evolution of a system is described by the Schrödinger equation<sup>2</sup>,

$$i\hbar \frac{\partial}{\partial t} \psi(\mathbf{x}, t) = \hat{H} \psi(\mathbf{x}, t). \quad (20)$$

If at some initial time  $t_0$  our system is in the state  $\Psi(\mathbf{x}, t_0)$ , then the time dependent state vector

$$\Psi(\mathbf{x}, t) = e^{-\frac{i}{\hbar} \hat{H}(t-t_0)} \Psi(\mathbf{x}, t_0) \quad (21)$$

solves the Schrödinger equation for all later times  $t$ .

The expectation value of some hermitian operator  $\hat{O}$  at a given time  $t$  is then defined as

$$\langle \hat{O} \rangle_t = \int d^3x \Psi^*(\mathbf{x}, t) \hat{O} \Psi(\mathbf{x}, t), \quad (22)$$

and the normalisation of the wavefunction is given by

$$\int d^3x \Psi^*(\mathbf{x}, t) \Psi(\mathbf{x}, t) = \langle 1 \rangle_t. \quad (23)$$

Since  $\Psi^* \Psi$  is positive, it is natural to interpret it as the probability density for finding a particle at position  $\mathbf{x}$ . Furthermore one can derive a conserved current  $\mathbf{j}$ , as well as a continuity equation by considering

$$\Psi^* \times (\text{Schr.Eq.}) - \Psi \times (\text{Schr.Eq.})^*. \quad (24)$$

The continuity equation reads

$$\frac{\partial}{\partial t} \rho = -\nabla \cdot \mathbf{j} \quad (25)$$

where the density  $\rho$  and the current  $\mathbf{j}$  are given by

$$\rho = \Psi^* \Psi \quad (\text{positive}), \quad (26)$$

$$\mathbf{j} = \frac{\hbar}{2im} (\Psi^* \nabla \Psi - (\nabla \Psi^*) \Psi) \quad (\text{real}). \quad (27)$$

Now that we have derived the continuity equation let us discuss the probability interpretation of Quantum Mechanics in more detail. Consider a finite volume  $V$  with boundary  $S$ . The integrated continuity equation is

$$\begin{aligned} \int_V \frac{\partial \rho}{\partial t} d^3x &= - \int_V \nabla \cdot \mathbf{j} d^3x \\ &= - \int_S \mathbf{j} \cdot \underline{dS} \end{aligned} \quad (28)$$

where in the last line we have used Gauss's theorem. Using Eq. (23) the left-hand side can be rewritten and we obtain

$$\frac{\partial}{\partial t} \langle 1 \rangle_t = - \int_S \mathbf{j} \cdot \underline{dS} = 0. \quad (29)$$

In other words, provided that  $\mathbf{j} = 0$  everywhere at the boundary  $S$ , we find that the time derivative of  $\langle 1 \rangle_t$  vanishes. Since  $\langle 1 \rangle_t$  represents the total probability for finding the particle anywhere inside the volume  $V$ , we conclude that this probability must be conserved: particles cannot be created or destroyed in our theory. Non-relativistic Quantum Mechanics thus provides a consistent formalism to describe a single particle. The quantity  $\Psi(\mathbf{x}, t)$  is interpreted as a one-particle wave function.

---

<sup>2</sup>Note that the Hamiltonian could itself have some time dependence in general, even in the Schrödinger picture, if the potential of a system depends on time. Here we assume that this is not the case.



## 1.4 The Heisenberg picture

Here the situation is the opposite to that in the Schrödinger picture, with the state vectors regarded as constant,  $\partial_t|\Psi_H\rangle = 0$ , and operators which carry the time dependence,  $\hat{O}_H(t)$ . This is the concept which later generalises most readily to field theory. We make use of the solution Eq. (21) to the Schrödinger equation in order to *define* a Heisenberg state vector through

$$\Psi(x, t) = e^{-\frac{i}{\hbar}\hat{H}(t-t_0)}\Psi(x, t_0) \equiv e^{-\frac{i}{\hbar}\hat{H}(t-t_0)}\Psi_H(x), \quad (30)$$

i.e.  $\Psi_H(\mathbf{x}) = \Psi(\mathbf{x}, t_0)$ . In other words, the Schrödinger vector at some time  $t_0$  is defined to be equivalent to the Heisenberg vector, and the solution to the Schrödinger equation provides the transformation law between the two for all times. This transformation of course leaves the physics, i.e. expectation values, invariant,

$$\langle\Psi(t)|\hat{O}|\Psi(t)\rangle = \langle\Psi(t_0)|e^{\frac{i}{\hbar}\hat{H}(t-t_0)}\hat{O}e^{-\frac{i}{\hbar}\hat{H}(t-t_0)}|\Psi(t_0)\rangle = \langle\Psi_H|\hat{O}_H(t)|\Psi_H\rangle, \quad (31)$$

with

$$\hat{O}_H(t) = e^{\frac{i}{\hbar}\hat{H}(t-t_0)}\hat{O}e^{-\frac{i}{\hbar}\hat{H}(t-t_0)}. \quad (32)$$

From this last equation it is now easy to derive the equivalent of the Schrödinger equation for the Heisenberg picture, the Heisenberg equation of motion for operators:

$$i\hbar\frac{d\hat{O}_H(t)}{dt} = [\hat{O}_H, \hat{H}]. \quad (33)$$

Note that all commutation relations, like Eq. (9), with time dependent operators are now intended to be valid for all times. Substituting  $\hat{x}, \hat{p}$  for  $\hat{O}$  into the Heisenberg equation readily leads to

$$\begin{aligned} \frac{d\hat{x}_i}{dt} &= \frac{\partial\hat{H}}{\partial\hat{p}_i}, \\ \frac{d\hat{p}_i}{dt} &= -\frac{\partial\hat{H}}{\partial\hat{x}_i}, \end{aligned} \quad (34)$$

the quantum mechanical equivalent of the Hamilton equations of classical mechanics.

## 1.5 The quantum harmonic oscillator

Because of similar structures later in quantum field theory, it is instructive to also briefly recall the harmonic oscillator in one dimension. Its Hamiltonian is given by

$$\hat{H}(\hat{x}, \hat{p}) = \frac{1}{2} \left( \frac{\hat{p}^2}{m} + m\omega^2\hat{x}^2 \right). \quad (35)$$

Employing the canonical formalism we have just set up, we easily identify the momentum operator to be  $\hat{p}(t) = m\partial_t\hat{x}(t)$ , and from the Hamilton equations we find the equation of motion to be  $\partial_t^2\hat{x} = -\omega^2\hat{x}$ , which has the well known plane wave solution  $\hat{x} \sim \exp i\omega t$ .

An alternative path useful for later field theory applications is to introduce new operators, expressed in terms of the old ones,

$$\hat{a} = \frac{1}{\sqrt{2}} \left( \sqrt{\frac{m\omega}{\hbar}}\hat{x} + i\sqrt{\frac{1}{m\omega\hbar}}\hat{p} \right), \quad \hat{a}^\dagger = \frac{1}{\sqrt{2}} \left( \sqrt{\frac{m\omega}{\hbar}}\hat{x} - i\sqrt{\frac{1}{m\omega\hbar}}\hat{p} \right). \quad (36)$$

Using the commutation relation for  $\hat{x}, \hat{p}$ , one readily derives (see the preschool problems)

$$[\hat{a}, \hat{a}^\dagger] = 1, \quad [\hat{H}, \hat{a}] = -\hbar\omega\hat{a}, \quad [\hat{H}, \hat{a}^\dagger] = \hbar\omega\hat{a}^\dagger. \quad (37)$$

With the help of these the Hamiltonian can be rewritten in terms of the new operators:

$$\hat{H} = \frac{1}{2}\hbar\omega (\hat{a}^\dagger\hat{a} + \hat{a}\hat{a}^\dagger) = \left(\hat{a}^\dagger\hat{a} + \frac{1}{2}\right)\hbar\omega. \quad (38)$$

With this form of the Hamiltonian it is easy to construct a complete basis of energy eigenstates  $|n\rangle$ ,

$$\hat{H}|n\rangle = E_n|n\rangle. \quad (39)$$

Using the above commutation relations, one finds

$$\hat{a}^\dagger\hat{H}|n\rangle = (\hat{H}\hat{a}^\dagger - \hbar\omega\hat{a}^\dagger)|n\rangle = E_n\hat{a}^\dagger|n\rangle, \quad (40)$$

and therefore

$$\hat{H}\hat{a}^\dagger|n\rangle = (E_n + \hbar\omega)\hat{a}^\dagger|n\rangle. \quad (41)$$

Thus, the state  $\hat{a}^\dagger|n\rangle$  has energy  $E_n + \hbar\omega$ , so that  $\hat{a}^\dagger$  may be regarded as a “creation operator” for a quantum with energy  $\hbar\omega$ . Along the same lines one finds that  $\hat{a}|n\rangle$  has energy  $E_n - \hbar\omega$ , and  $\hat{a}$  is an “annihilation operator”.

Let us introduce a vacuum state  $|0\rangle$  with no quanta excited, for which  $\hat{a}|0\rangle = 0$ , because there cannot be any negative energy states. Acting with the Hamiltonian on that state we find

$$\hat{H}|0\rangle = \hbar\omega/2, \quad (42)$$

i.e. the quantum mechanical vacuum has a non-zero energy, known as vacuum oscillation or *zero point energy*. Acting with a creation operator onto the vacuum state one easily finds the state with one quantum excited, and this can be repeated  $n$  times to get

$$\begin{aligned} |1\rangle &= \hat{a}^\dagger|0\rangle \quad , \quad E_1 = (1 + \frac{1}{2})\hbar\omega, \quad \dots \\ |n\rangle &= \frac{\hat{a}^\dagger}{\sqrt{n}}|n-1\rangle = \frac{1}{\sqrt{n!}}(\hat{a}^\dagger)^n|0\rangle \quad , \quad E_n = (n + \frac{1}{2})\hbar\omega. \end{aligned} \quad (43)$$

The root of the factorial is there to normalise all eigenstates to one. Finally, the *number operator*  $\hat{N} = \hat{a}^\dagger\hat{a}$  returns the number of quanta in a given energy eigenstate,

$$\hat{N}|n\rangle = n|n\rangle. \quad (44)$$

## 1.6 Relativistic Quantum Mechanics

So far we have only considered non-relativistic particles. In this section, we see what happens when we try to formulate a relativistic analogue of the Schrödinger equation. First, note that we can derive the non-relativistic equation starting from the energy relation

$$E = \frac{\mathbf{p}^2}{2m} + V(\mathbf{x}) \quad (45)$$

and replacing variables by their appropriate operators acting on a position space wavefunction  $\psi(\mathbf{x}, t)$

$$E \rightarrow i\hbar\frac{\partial}{\partial t}, \quad \mathbf{p} \rightarrow -i\hbar\nabla, \quad \mathbf{x} \rightarrow \mathbf{x} \quad (46)$$

to give

$$\left[-\frac{\hbar^2}{2m}\nabla^2 + V(\mathbf{x})\right]\psi(\mathbf{x}, t) = i\hbar\frac{\partial\psi(\mathbf{x}, t)}{\partial t}. \quad (47)$$

As we have already seen, there is a corresponding positive definite probability density

$$\rho = |\psi(\mathbf{x}, t)|^2 \geq 0, \quad (48)$$

with corresponding current

$$\mathbf{j} = \frac{\hbar}{2im} (\psi^* \nabla \psi - (\nabla \psi^*) \psi). \quad (49)$$

Can we also make a relativistic equation? By analogy with the above, we may start with the relativistic energy relation

$$E^2 = c^2 \mathbf{p}^2 + m^2 c^4, \quad (50)$$

and making the appropriate operator replacements leads to the equation

$$\left( \frac{1}{c^2} \frac{\partial^2}{\partial t^2} - \nabla^2 + \frac{m^2 c^2}{\hbar^2} \right) \phi(\mathbf{x}, t) \quad (51)$$

for some wavefunction  $\phi(\mathbf{x}, t)$ . This is the *Klein-Gordon* equation, and one may try to form a probability density and current, as in the non-relativistic case. Firstly, one notes that to satisfy relativistic invariance, the probability density should be the zeroth component of a 4-vector  $j^\mu = (\rho, \mathbf{j})$  satisfying

$$\partial_\mu j^\mu = 0. \quad (52)$$

In fact, one finds

$$\rho = \frac{i\hbar}{2m} \left( \phi^* \frac{\partial \phi}{\partial t} - \phi \frac{\partial \phi^*}{\partial t} \right), \quad (53)$$

with  $\mathbf{j}$  given as before. This is not positive definite! That is, this may (and will) become negative in general, so we cannot interpret this as the probability density of a single particle.

There is another problem with the Klein-Gordon equation as it stands, that is perhaps less abstract to appreciate. The relativistic energy relation gives

$$E = \pm \sqrt{c^2 \mathbf{p}^2 + m^2 c^4}, \quad (54)$$

and thus one has positive and negative energy solutions. For a free particle, one could restrict to having positive energy states only. However, an interacting particle may exchange energy with its environment, and there is nothing to stop it cascading down to energy states of more and more negative energy, thus emitting infinite amounts of energy.

We conclude that the Klein-Gordon equation does not make sense as a consistent quantum theory of a single particle. We thus need a different approach in unifying special relativity and quantum mechanics. This, as we will see, is QFT, in which we will be able to reinterpret the Klein-Gordon function as a field  $\phi(\mathbf{x}, t)$  describing many particles.

From now on, it will be extremely convenient to work in *natural units*, in which one sets  $\hbar = c = 1$ . The correct factors can always be reinstated by dimensional analysis. In these units, the Klein-Gordon equation becomes

$$(\square + m^2) \phi(\mathbf{x}, t) = 0, \quad (55)$$

where

$$\square = \partial^\mu \partial_\mu = \frac{\partial^2}{\partial t^2} - \nabla^2. \quad (56)$$

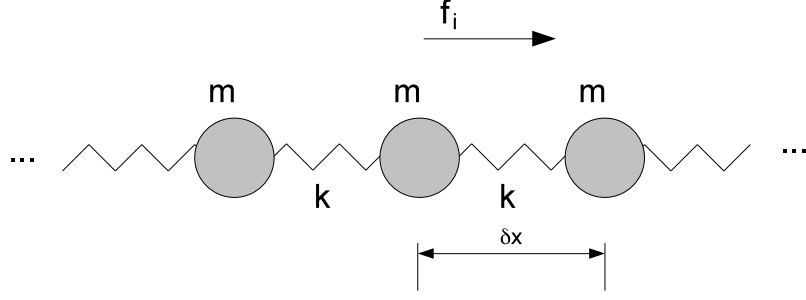


Figure 2: System of masses  $m$  joined by springs (of constant  $k$ ), whose longitudinal displacements are  $\{f_i\}$ , and whose separation at rest is  $\delta x$ .

## 2 Classical Field Theory

In the previous section, we have seen how to describe point particles, both classically and quantum mechanically. In this section, we discuss classical field theory, as a precursor to considering quantum fields. A *field* associates a mathematical object (e.g. scalar, vector, tensor, spinor...) with every point in spacetime. Examples are the temperature distribution in a room (a scalar field), or the  $\mathbf{E}$  and  $\mathbf{B}$  fields in electromagnetism (vector fields). Just as point particles can be described by Lagrangians, so can fields, although it is more natural to think in terms of *Lagrangian densities*.

### 2.1 Example: Model of an Elastic Rod

Let us consider a particular example, namely a set of point masses connected together by springs, as shown in figure 2. Assume the masses  $m$  are equal, as also are the force constants of the springs  $k$ . Furthermore, we assume that the masses may move only longitudinally, where the  $i^{\text{th}}$  displacement is  $f_i$ , and that the separation of adjacent masses is  $\delta x$  when all  $f_i$  are zero. This system is an approximation to an elastic rod, with a displacement field  $f(x, t)$ . To see what this field theory looks like, we may first write the total kinetic and potential energies as

$$T = \sum_i \frac{1}{2} m \dot{f}_i^2, \quad V = \sum_i \frac{1}{2} k (f_{i+1} - f_i)^2 \quad (57)$$

respectively, where we have used Hooke's Law for the potential energy. Thus, the Lagrangian is

$$L = T - V = \sum_i \left[ \frac{1}{2} m \dot{f}_i^2 - \frac{1}{2} k (f_{i+1} - f_i)^2 \right]. \quad (58)$$

Clearly this system becomes a better approximation to an elastic rod as the continuum limit is approached, in which the number of masses  $N \rightarrow \infty$  and the separation  $\delta x \rightarrow 0$ . We can then rewrite the Lagrangian as

$$L = \sum_i \delta x \left[ \frac{1}{2} \left( \frac{m}{\delta x} \right) \dot{f}_i^2 - \frac{1}{2} (k \delta x) \left( \frac{f_{i+1} - f_i}{\delta x} \right)^2 \right]. \quad (59)$$

We may recognise

$$\lim_{\delta x \rightarrow 0} m / \delta x = \rho \quad (60)$$

as the density of the rod, and also define the tension

$$\kappa = \lim_{\delta x \rightarrow 0} k \delta x. \quad (61)$$

Furthermore, the position index  $i$  gets replaced by the continuous variable  $x$ , and one has

$$\lim_{\delta x \rightarrow 0} \frac{f_{i+1} - f_i}{\delta x} = \frac{\partial f(x, t)}{\partial x}. \quad (62)$$

Finally, the sum over  $i$  becomes an integral so that the continuum Lagrangian is

$$L = \int dx \left[ \frac{1}{2} \rho \dot{f}(x, t)^2 - \frac{1}{2} \kappa \left( \frac{\partial f}{\partial x} \right)^2 \right]. \quad (63)$$

This is the Lagrangian for the displacement field  $f(x, t)$ . It depends on a function of  $f$  and  $\dot{f}$  which is integrated over all space coordinates (in this case there is only one, the position along the rod). We may therefore write the Lagrangian manifestly as

$$L = \int dx \mathcal{L}[f(x, t), \dot{f}(x, t)], \quad (64)$$

where  $\mathcal{L}$  is the *Lagrangian density*

$$\mathcal{L}[f(x, t), \dot{f}(x, t)] = \frac{1}{2} \rho \dot{f}^2(x, t) - \frac{1}{2} \kappa \left( \frac{\partial f}{\partial x} \right)^2. \quad (65)$$

It is perhaps clear from the above example that for any field, there will always be an integration over all space dimensions, and thus it is more natural to think about the Lagrangian density rather than the Lagrangian itself. Indeed, we may construct the following dictionary between quantities in point particle mechanics, and corresponding field theory quantities (which may or may not be helpful to you in remembering the differences between particles and fields...!).

Classical Mechanics:	Classical Field Theory:	
$x(t)$	$\longrightarrow \phi(x, t)$	(66)
$\dot{x}(t)$	$\longrightarrow \dot{\phi}(x, t)$	

Index $i$	$\longrightarrow$ Coordinate $x$	(67)
-----------	----------------------------------	------

$L(x, \dot{x})$	$\longrightarrow \mathcal{L}[\phi, \dot{\phi}]$	(68)
-----------------	---	------

Note that the action for the above field theory is given, as usual, by the time integral of the Lagrangian:

$$S = \int dt L = \int dt \int dx \mathcal{L}[f, \dot{f}]. \quad (69)$$

## 2.2 Relativistic Fields

In the previous section we saw how fields can be described using Lagrangian densities, and illustrated this with a non-relativistic example. Rather than derive the field equations for this case, we do this explicitly here for relativistic theories, which we will be concerned with for the rest of the course (and, indeed, the school).

In special relativity, coordinates are combined into four-vectors,  $x^\mu = (t, x_i)$  or  $x = (t, \mathbf{x})$ , whose length  $x^2 = t^2 - \mathbf{x}^2$  is invariant under Lorentz transformations

$$x'^\mu = \Lambda^\mu{}_\nu x^\nu. \quad (70)$$

A general function transforms as  $f(x) \rightarrow f'(x')$ , i.e. both the function and its argument transform. A Lorentz scalar is a function  $\phi(x)$  which at any given point in space-time will have the same amplitude, regardless of which inertial frame it is observed in. Consider a space-time point given by  $x$  in the unprimed frame, and  $x'(x)$  in the primed frame, where the function  $x'(x)$  can be derived from eq. (70). Observers in both the primed and unprimed frames will see the same amplitude  $\phi(x)$ , although an observer in the primed frame will prefer to express this in terms of his or her own coordinate system  $x'$ , hence will see

$$\phi(x) = \phi(x(x')) = \phi'(x'), \quad (71)$$

where the latter equality defines  $\phi'$ .

Equation (71) defines the transformation law for a Lorentz scalar. A vector function transforms as

$$V'^{\mu}(x') = \Lambda^{\mu}{}_{\nu} V^{\nu}(x). \quad (72)$$

We will work in particular with  $\partial_{\mu}\phi(x)$ , where  $x \equiv x^{\mu}$  denotes the 4-position. Note in particular that

$$\begin{aligned} (\partial_{\mu}\phi)(\partial^{\mu}\phi) &= \left(\frac{\partial\phi}{\partial t}\right)^2 - \nabla\phi \cdot \nabla\phi \\ \partial_{\mu}\partial^{\mu}\phi &= \frac{\partial^2\phi}{\partial t^2} - \nabla^2\phi. \end{aligned}$$

In general, a relativistically invariant scalar field theory has action

$$S = \int d^4x \mathcal{L}[\phi, \partial_{\mu}\phi], \quad (73)$$

where

$$\int d^4x \equiv \int dt d^3\mathbf{x}, \quad (74)$$

and  $\mathcal{L}$  is the appropriate Lagrangian density. We can find the equations of motion satisfied by the field  $\phi$  using, as in point particle mechanics, the principle of least action. The field theory form of this is that the field  $\phi(x)$  is such that the action of eq. (73) is extremised. Assuming  $\phi(x)$  is indeed such a field, we may introduce a small perturbation

$$\phi(x) \rightarrow \phi(x) + \delta\phi(x), \quad (75)$$

which correspondingly perturbs the action according to

$$S \rightarrow S + \delta S = \int d^4x \left[ \mathcal{L}(\phi, \partial_{\mu}\phi) + \frac{\partial\mathcal{L}}{\partial\phi}\delta\phi + \frac{\partial\mathcal{L}}{\partial(\partial_{\mu}\phi)}\delta(\partial_{\mu}\phi) \right]. \quad (76)$$

Recognising the first term as the unperturbed action, one thus finds

$$\begin{aligned} \delta S &= \int d^4x \left[ \frac{\partial\mathcal{L}}{\partial\phi}\delta\phi + \frac{\partial\mathcal{L}}{\partial(\partial_{\mu}\phi)}\delta(\partial_{\mu}\phi) \right] \\ &= \left[ \frac{\partial\mathcal{L}}{\partial(\partial_{\mu}\phi)}\delta\phi \right]_{\text{boundary}} + \int d^4x \left[ \frac{\partial\mathcal{L}}{\partial\phi} - \partial_{\mu} \left( \frac{\partial\mathcal{L}}{\partial(\partial_{\mu}\phi)} \right) \right] \delta\phi, \end{aligned}$$

where we have integrated by parts in the second line. Assuming the fields die away at infinity so that  $\delta\phi = 0$  at the boundary of spacetime, the principle of least action  $\delta S = 0$  implies

$$\partial_{\mu} \left( \frac{\partial\mathcal{L}}{\partial(\partial_{\mu}\phi)} \right) = \frac{\partial\mathcal{L}}{\partial\phi}. \quad (77)$$

This is the *Euler-Lagrange field equation*. It tells us, given a particular Lagrangian density (which defines a particular field theory) the classical equation of motion which must be satisfied by the field  $\phi$ . As a specific example, let us consider the Lagrangian density

$$\mathcal{L} = \frac{1}{2}(\partial_\mu \phi)(\partial^\mu \phi) - \frac{1}{2}m^2 \phi^2, \quad (78)$$

from which one finds

$$\frac{\partial \mathcal{L}}{\partial(\partial_\mu \phi)} = \partial^\mu \phi, \quad \frac{\partial \mathcal{L}}{\partial \phi} = -m^2 \phi, \quad (79)$$

so that the Euler-Lagrange equation gives

$$\partial_\mu \partial^\mu \phi + m^2 \phi = (\square + m^2)\phi(x) = 0. \quad (80)$$

This is the Klein-Gordon equation! The above Lagrangian density thus corresponds to the classical field theory of a Klein-Gordon field. We see in particular that the coefficient of the quadratic term in the Lagrangian can be interpreted as the mass.

By analogy with point particle mechanics, one can define a *canonical momentum field* conjugate to  $\phi$ :

$$\pi(x) = \frac{\partial \mathcal{L}}{\partial \dot{\phi}}. \quad (81)$$

Then one can define the *Hamiltonian density*

$$\mathcal{H}[\phi, \pi] = \pi \dot{\phi} - \mathcal{L}, \quad (82)$$

such that

$$H = \int d^3\mathbf{x} \mathcal{H}(\pi, \phi) \quad (83)$$

is the Hamiltonian (total energy carried by the field). For example, the Klein-Gordon field has conjugate momentum  $\pi = \dot{\phi}$ , and Hamiltonian density

$$\mathcal{H} = \frac{1}{2} [\pi^2(x) + (\nabla \phi)^2 + m^2 \phi^2]. \quad (84)$$

### 2.3 Plane wave solutions to the Klein-Gordon equation

Let us consider real solutions to Eq. (80), characterised by  $\phi^*(x) = \phi(x)$ . To find them we try an ansatz of plane waves

$$\phi(x) \propto e^{i(k^0 t - \mathbf{k} \cdot \mathbf{x})}. \quad (85)$$

The Klein-Gordon equation is satisfied if  $(k^0)^2 - \mathbf{k}^2 = m^2$  so that

$$k^0 = \pm \sqrt{\mathbf{k}^2 + m^2}. \quad (86)$$

Defining the energy as

$$E(\mathbf{k}) = \sqrt{\mathbf{k}^2 + m^2} > 0, \quad (87)$$

we obtain two types of solution which read

$$\phi_+(x) \propto e^{i(E(\mathbf{k})t - \mathbf{k} \cdot \mathbf{x})}, \quad \phi_-(x) \propto e^{-i(E(\mathbf{k})t - \mathbf{k} \cdot \mathbf{x})}. \quad (88)$$

We may interpret these as positive and negative energy solutions, such that it does not matter which branch of the square root we take in eq. (87) (it is conventional, however, to define energy as a positive quantity). The general solution is a superposition of  $\phi_+$  and  $\phi_-$ . Using

$$E(\mathbf{k})t - \mathbf{k} \cdot \mathbf{x} = k^\mu k_\mu = k_\mu k^\mu = k \cdot x \quad (89)$$

this solution reads

$$\phi(x) = \int \frac{d^3k}{(2\pi)^3 2E(\mathbf{k})} (e^{ik \cdot x} \alpha^*(\mathbf{k}) + e^{-ik \cdot x} \alpha(\mathbf{k})), \quad (90)$$

where  $\alpha(\mathbf{k})$  is an arbitrary complex coefficient. Note that the coefficients of the positive and negative exponentials are related by complex conjugation. This ensures that the field  $\phi(x)$  is real (as can be easily verified from eq. (90)), consistent with the Lagrangian we wrote down. Such a field has applications in e.g. the description of neutral mesons. We can also write down a Klein-Gordon Lagrangian for a complex field  $\phi$ . This is really two independent fields (i.e.  $\phi$  and  $\phi^*$ ), and thus can be used to describe a system of two particles (e.g. charged meson pairs). To simplify the discussion in this course, we will explicitly consider the real Klein-Gordon field. Note that the factors of 2 and  $\pi$  in eq. (90) are conventional, and the inverse power of the energy is such that the measure of integration is Lorentz invariant (problem 2.1), so that the whole solution is written in a manifestly Lorentz invariant way.

## 2.4 Symmetries and Conservation Laws

As was the case in point particle mechanics, one may relate symmetries of the Lagrangian density to conserved quantities in field theory. For example, consider the invariance of  $\mathcal{L}$  under space-time translations

$$x^\mu \rightarrow x^\mu + \epsilon^\mu, \quad (91)$$

where  $\epsilon^\mu$  is constant. Under such a transformation one has

$$\mathcal{L}(x^\mu + \epsilon^\mu) = \mathcal{L}(x^\mu) + \epsilon^\mu \partial_\mu \mathcal{L}(x^\mu) + \dots \quad (92)$$

$$\phi(x^\mu + \epsilon^\mu) = \phi(x^\mu) + \epsilon^\mu \partial_\mu \phi(x^\mu) + \dots \quad (93)$$

$$\partial_\nu \phi(x^\mu + \epsilon^\mu) = \partial_\nu \phi(x^\mu) + \epsilon^\mu \partial_\mu \partial_\nu \phi(x^\mu) + \dots, \quad (94)$$

$$(95)$$

where we have used Taylor's theorem. But if  $\mathcal{L}$  does not explicitly depend on  $x^\mu$  (i.e. only through  $\phi$  and  $\partial_\mu \phi$ ) then one has

$$\begin{aligned} \mathcal{L}(x^\mu + \epsilon^\mu) &= \mathcal{L}[\phi(x^\mu + \epsilon^\mu), \partial_\nu \phi(x^\mu + \epsilon^\mu)] \\ &= \mathcal{L} + \frac{\partial \mathcal{L}}{\partial \phi} \delta \phi + \frac{\partial \mathcal{L}}{\partial (\partial_\nu \phi)} \delta (\partial_\nu \phi) + \dots \end{aligned} \quad (96)$$

$$= \mathcal{L} + \frac{\partial \mathcal{L}}{\partial \phi} \epsilon^\mu \partial_\mu \phi + \frac{\partial \mathcal{L}}{\partial (\partial_\nu \phi)} \epsilon^\mu \partial_\mu \partial_\nu \phi + \dots, \quad (97)$$

where we have used the fact that  $\delta \phi = \epsilon^\mu \partial_\mu \phi$  in the third line, and all functions on the right-hand side are evaluated at  $x^\mu$ . One may replace  $\partial \mathcal{L} / \partial \phi$  by the LHS of the Euler-Lagrange equation to get

$$\begin{aligned} \mathcal{L}(x^\mu + \epsilon^\mu) &= \mathcal{L} + \partial_\nu \frac{\partial \mathcal{L}}{\partial (\partial_\nu \phi)} \epsilon^\mu \partial_\mu \phi + \frac{\partial \mathcal{L}}{\partial (\partial_\nu \phi)} \epsilon^\mu \partial_\mu \partial_\nu \phi + \dots \\ &= \mathcal{L} + \partial_\nu \left[ \frac{\partial \mathcal{L}}{\partial (\partial_\nu \phi)} \partial_\mu \phi \right] \epsilon^\mu, \end{aligned} \quad (98)$$

and equating this with the alternative expression above, one finds

$$\partial_\nu \left[ \frac{\partial \mathcal{L}}{\partial (\partial_\nu \phi)} \partial_\mu \phi \right] \epsilon^\mu = \epsilon^\mu \partial_\mu \mathcal{L}. \quad (99)$$



If this is true for all  $\epsilon^\mu$ , then one has

$$\partial^\nu \Theta_{\nu\mu} = 0, \quad (100)$$

where

$$\Theta_{\nu\mu} = \frac{\partial \mathcal{L}}{\partial(\partial_\nu \phi)} \partial_\mu \phi - g_{\mu\nu} \mathcal{L} \quad (101)$$

is the *energy-momentum tensor*. We can see how this name arises by considering the components explicitly, for the case of the Klein Gordon field. One then finds

$$\Theta_{00} = \frac{\partial \mathcal{L}}{\partial \dot{\phi}} \dot{\phi} - g_{00} \mathcal{L} = \pi \dot{\phi} - \mathcal{L} = \mathcal{H}, \quad (102)$$

$$\Theta_{0j} = \frac{\partial \mathcal{L}}{\partial \dot{\phi}} \partial_j \phi - g_{0j} \mathcal{L} = \pi \partial_j \phi \quad (j = 1 \dots 3). \quad (103)$$

One then sees that  $\Theta_{00}$  is the energy density carried by the field. Its conservation can then be shown by considering

$$\begin{aligned} \frac{\partial}{\partial t} \int_V d^3x \Theta_{00} &= \int_V d^3x \partial^0 \Theta_{00} \\ &= \int_V d^3x \partial^j \Theta_{j0} = \int_S dS_j \cdot \Theta_{0j} = 0, \end{aligned} \quad (104)$$

where we have used Eq. (100) in the second line. The Hamiltonian density is a conserved quantity, provided that there is no energy flow through the surface  $S$  which encloses the volume  $V$ . In a similar manner one can show that the 3-momentum  $p_j$ , which is related to  $\Theta_{0j}$ , is conserved as well. It is then useful to define a conserved energy-momentum four-vector

$$P_\mu = \int d^3x \Theta_{0\mu}. \quad (105)$$

In analogy to point particle mechanics, we thus see that invariances of the Lagrangian density correspond to conservation laws. An entirely analogous procedure leads to conserved quantities like angular momentum and spin. Furthermore one can study so-called internal symmetries, i.e. ones which are not related to coordinate but other transformations. Examples are conservation of all kinds of charges, isospin, etc.

We have thus established the Lagrange-Hamilton formalism for classical field theory: we derived the equation of motion (Euler-Lagrange equation) from the Lagrangian and introduced the conjugate momentum. We then defined the Hamiltonian (density) and considered conservation laws by studying the energy-momentum tensor  $\Theta_{\mu\nu}$ .

## 3 Quantum Field Theory: Free Fields

### 3.1 Canonical Field Quantisation

In the previous sections we have reviewed the classical and quantum mechanics of point particles, and also classical field theory. We used the canonical quantisation procedure in discussing quantum mechanics, whereby classical variables are replaced by operators, which have non-trivial commutation relations. In this section, we see how to apply this procedure to fields, taking the explicit example of the Klein-Gordon field discussed previously. This is, as yet, a non-interacting field theory, and we will discuss how to deal with interactions later on in the course.

The Klein-Gordon Lagrangian density has the form

$$\mathcal{L} = \frac{1}{2} \partial^\mu \phi \partial_\mu \phi - \frac{1}{2} m^2 \phi^2. \quad (106)$$

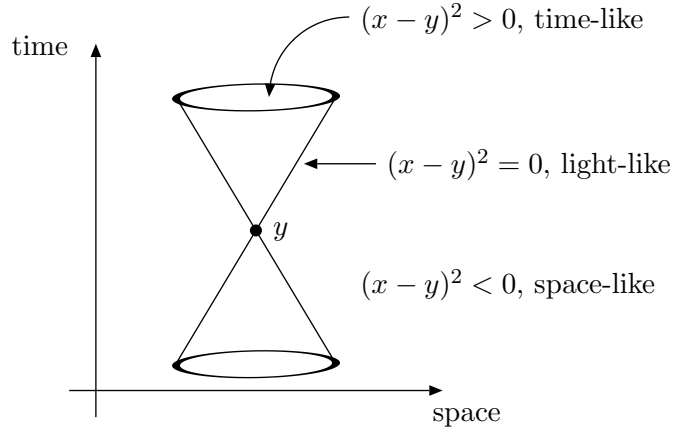


Figure 3: The light cone about  $y$ . Events occurring at points  $x$  and  $y$  are said to be time-like (space-like) if  $x$  is inside (outside) the light cone about  $y$ .

We have seen that in field theory the field  $\phi(x)$  plays the role of the coordinates in ordinary point particle mechanics, and we defined a canonically conjugate momentum,  $\pi(x) = \partial\mathcal{L}/\partial\dot{\phi} = \dot{\phi}(x)$ . We then continue the analogy to point mechanics through the quantisation procedure, i.e. we now take our canonical variables to be operators,

$$\phi(x) \rightarrow \hat{\phi}(x), \quad \pi(x) \rightarrow \hat{\pi}(x). \quad (107)$$

Next we impose equal-time commutation relations on them,

$$[\hat{\phi}(\mathbf{x}, t), \hat{\pi}(\mathbf{y}, t)] = i\delta^3(\mathbf{x} - \mathbf{y}), \quad (108)$$

$$[\hat{\phi}(\mathbf{x}, t), \hat{\phi}(\mathbf{y}, t)] = [\hat{\pi}(\mathbf{x}, t), \hat{\pi}(\mathbf{y}, t)] = 0. \quad (109)$$

As in the case of quantum mechanics, the canonical variables commute among themselves, but not the canonical coordinate and momentum with each other. Note that the commutation relation is entirely analogous to the quantum mechanical case. There would be an  $\hbar$ , if it hadn't been set to one earlier, and the delta-function accounts for the fact that we are dealing with fields. It is zero if the fields are evaluated at different space-time points.

After quantisation, our fields have turned into field operators. Note that within the relativistic formulation they depend on time, and hence they are Heisenberg operators.

In the previous paragraph we have formulated commutation relations for fields evaluated at equal time, which is clearly a special case when considering fields at general  $x, y$ . The reason has to do with maintaining causality in a relativistic theory. Let us recall the light cone about an event at  $y$ , as in Fig. 3. One important postulate of special relativity states that no signal and no interaction can travel faster than the speed of light. This has important consequences about the way in which different events can affect each other. For instance, two events which are characterised by space-time points  $x^\mu$  and  $y^\mu$  are said to be causal if the distance  $(x - y)^2$  is time-like, i.e.  $(x - y)^2 > 0$ . By contrast, two events characterised by a space-like separation, i.e.  $(x - y)^2 < 0$ , cannot affect each other, since the point  $x$  is not contained inside the light cone about  $y$ .

In non-relativistic Quantum Mechanics the commutation relations among operators indicate whether precise and independent measurements of the corresponding observables can be made. If the commutator does not vanish, then a measurement of one observable affects that of the

other. From the above it is then clear that the issue of causality must be incorporated into the commutation relations of the relativistic version of our quantum theory: whether or not independent and precise measurements of two observables can be made depends also on the separation of the 4-vectors characterising the points at which these measurements occur. Clearly, events with space-like separations cannot affect each other, and hence all fields must commute,

$$\left[\hat{\phi}(x), \hat{\phi}(y)\right] = [\hat{\pi}(x), \hat{\pi}(y)] = \left[\hat{\phi}(x), \hat{\pi}(y)\right] = 0 \quad \text{for} \quad (x - y)^2 < 0. \quad (110)$$

This condition is sometimes called micro-causality. Writing out the four-components of the time interval, we see that as long as  $|t' - t| < |\mathbf{x} - \mathbf{y}|$ , the commutator vanishes in a finite interval  $|t' - t|$ . It also vanishes for  $t' = t$ , as long as  $\mathbf{x} \neq \mathbf{y}$ . Only if the fields are evaluated at an equal space-time point can they affect each other, which leads to the equal-time commutation relations above. They can also affect each other everywhere within the light cone, i.e. for time-like intervals. It is not hard to show that in this case (e.g. problem 3.1)

$$\left[\hat{\phi}(x), \hat{\phi}(y)\right] = [\hat{\pi}(x), \hat{\pi}(y)] = 0, \quad \text{for} \quad (x - y)^2 > 0 \quad (111)$$

$$\left[\hat{\phi}(x), \hat{\pi}(y)\right] = \frac{i}{2} \int \frac{d^3 \mathbf{p}}{(2\pi)^3} \left( e^{ip \cdot (x-y)} + e^{-ip \cdot (x-y)} \right). \quad (112)$$

n.b. since the 4-vector dot product  $p \cdot (x - y)$  depends on  $p_0 = \sqrt{\mathbf{p}^2 + m^2}$ , one cannot trivially carry out the integrals over  $d^3 \mathbf{p}$  here.

### 3.2 Creation and annihilation operators

After quantisation, the Klein-Gordon equation we derived earlier turns into an equation for operators. For its solution we simply promote the classical plane wave solution, Eq. (90), to operator status,

$$\hat{\phi}(x) = \int \frac{d^3 k}{(2\pi)^3 2E(\mathbf{k})} \left( e^{ik \cdot x} \hat{a}^\dagger(\mathbf{k}) + e^{-ik \cdot x} \hat{a}(\mathbf{k}) \right). \quad (113)$$

Note that the complex conjugation of the Fourier coefficient turned into hermitian conjugation for an operator.

Let us now solve for the operator coefficients of the positive and negative energy solutions. In order to do so, we invert the Fourier integrals for the field and its time derivative,

$$\int d^3 x \hat{\phi}(\mathbf{x}, t) e^{ikx} = \frac{1}{2E} \left[ \hat{a}(\mathbf{k}) + \hat{a}^\dagger(\mathbf{k}) e^{2ik_0 x_0} \right], \quad (114)$$

$$\int d^3 x \dot{\hat{\phi}}(\mathbf{x}, t) e^{ikx} = -\frac{i}{2} \left[ \hat{a}(\mathbf{k}) - \hat{a}^\dagger(\mathbf{k}) e^{2ik_0 x_0} \right], \quad (115)$$

and then build the linear combination  $iE(k)(114)-(115)$  to find

$$\int d^3 x \left[ iE(k) \hat{\phi}(\mathbf{x}, t) - \dot{\hat{\phi}}(\mathbf{x}, t) \right] e^{ikx} = i\hat{a}(\mathbf{k}), \quad (116)$$

Following a similar procedure for  $\hat{a}^\dagger(k)$ , and using  $\hat{\pi}(x) = \dot{\hat{\phi}}(x)$  we find

$$\hat{a}(\mathbf{k}) = \int d^3 x \left[ E(k) \hat{\phi}(\mathbf{x}, t) + i\hat{\pi}(\mathbf{x}, t) \right] e^{ikx}, \quad (117)$$

$$\hat{a}^\dagger(\mathbf{k}) = \int d^3 x \left[ E(k) \hat{\phi}(\mathbf{x}, t) - i\hat{\pi}(\mathbf{x}, t) \right] e^{-ikx}. \quad (118)$$

Note that, as Fourier coefficients, these operators do not depend on time, even though the right hand side does contain time variables. Having expressions in terms of the canonical

field variables  $\hat{\phi}(x), \hat{\pi}(x)$ , we can now evaluate the commutators for the Fourier coefficients. Expanding everything out and using the commutation relations Eq. (109), we find

$$[\hat{a}^\dagger(\mathbf{k}_1), \hat{a}^\dagger(\mathbf{k}_2)] = 0 \quad (119)$$

$$[\hat{a}(\mathbf{k}_1), \hat{a}(\mathbf{k}_2)] = 0 \quad (120)$$

$$[\hat{a}(\mathbf{k}_1), \hat{a}^\dagger(\mathbf{k}_2)] = (2\pi)^3 2E(\mathbf{k}_1) \delta^3(\mathbf{k}_1 - \mathbf{k}_2) \quad (121)$$

We easily recognise these for every  $\mathbf{k}$  to correspond to the commutation relations for the harmonic oscillator, Eq. (37). This motivates us to also express the Hamiltonian and the energy momentum four-vector of our quantum field theory in terms of these operators. To do this, first note that the Hamiltonian is given by the integral of the Hamiltonian density (eq. (84)) over all space. One may then substitute eq. (113) to yield (see the problem sheet)

$$\hat{H} = \frac{1}{2} \int \frac{d^3k}{(2\pi)^3 2E(\mathbf{k})} E(\mathbf{k}) (\hat{a}^\dagger(\mathbf{k})\hat{a}(\mathbf{k}) + \hat{a}(\mathbf{k})\hat{a}^\dagger(\mathbf{k})), \quad (122)$$

$$\hat{\mathbf{P}} = \frac{1}{2} \int \frac{d^3k}{(2\pi)^3 2E(\mathbf{k})} \mathbf{k} (\hat{a}^\dagger(\mathbf{k})\hat{a}(\mathbf{k}) + \hat{a}(\mathbf{k})\hat{a}^\dagger(\mathbf{k})). \quad (123)$$

We thus find that the Hamiltonian and the momentum operator are nothing but a continuous sum of excitation energies/momenta of one-dimensional harmonic oscillators! After a minute of thought this is not so surprising. We expanded the solution of the Klein-Gordon equation into a superposition of plane waves with momenta  $\mathbf{k}$ . But of course a plane wave solution with energy  $E(\mathbf{k})$  is also the solution to a one-dimensional harmonic oscillator with the same energy. Hence, our free scalar field is simply a collection of infinitely many harmonic oscillators distributed over the whole energy/momentum range. These energies sum up to that of the entire system. We have thus reduced the problem of handling our field theory to oscillator algebra. From the harmonic oscillator we know already how to construct a complete basis of energy eigenstates, and thanks to the analogy of the previous section we can take this over to our quantum field theory.

### 3.3 Energy of the vacuum state and renormalisation

In complete analogy we begin again with the postulate of a vacuum state  $|0\rangle$  with norm one, which is annihilated by the action of the operator  $a$ ,

$$\langle 0|0\rangle = 1, \quad \hat{a}(\mathbf{k})|0\rangle = 0 \quad \text{for all } \mathbf{k}. \quad (124)$$

Let us next evaluate the energy of this vacuum state, by taking the expectation value of the Hamiltonian,

$$E_0 = \langle 0|\hat{H}|0\rangle = \frac{1}{2} \int \frac{d^3k}{(2\pi)^3 2E(\mathbf{k})} E(\mathbf{k}) \{ \langle 0|\hat{a}^\dagger(\mathbf{k})\hat{a}(\mathbf{k})|0\rangle + \langle 0|\hat{a}(\mathbf{k})\hat{a}^\dagger(\mathbf{k})|0\rangle \}. \quad (125)$$

The first term in curly brackets vanishes, since  $a$  annihilates the vacuum. The second can be rewritten as

$$\hat{a}(\mathbf{k})\hat{a}^\dagger(\mathbf{k})|0\rangle = \{ [\hat{a}(\mathbf{k}), \hat{a}^\dagger(\mathbf{k})] + \hat{a}^\dagger(\mathbf{k})\hat{a}(\mathbf{k}) \} |0\rangle. \quad (126)$$

It is now the second term which vanishes, whereas the first can be replaced by the value of the commutator. Thus we obtain

$$E_0 = \langle 0|\hat{H}|0\rangle = \delta^3(0) \frac{1}{2} \int d^3k E(\mathbf{k}) = \delta^3(0) \frac{1}{2} \int d^3k \sqrt{\mathbf{k}^2 + m^2} = \infty, \quad (127)$$

which means that the energy of the ground state is infinite! This result seems rather paradoxical, but it can be understood again in terms of the harmonic oscillator. Recall that the simple

quantum mechanical oscillator has a finite zero-point energy. As we have seen above, our field theory corresponds to an infinite collection of harmonic oscillators, i.e. the vacuum receives an infinite number of zero point contributions, and its energy thus diverges.

This is the first of frequent occurrences of infinities in quantum field theory. Fortunately, it is not too hard to work around this particular one. Firstly, we note that nowhere in nature can we observe absolute values of energy, all we can measure are energy differences relative to some reference scale, at best the one of the vacuum state,  $|0\rangle$ . In this case it does not really matter what the energy of the vacuum is. This then allows us to redefine the energy scale, by always subtracting the (infinite) vacuum energy from any energy we compute. This process is called “renormalisation”.

We then *define* the renormalised vacuum energy to be zero, and take it to be the expectation value of a renormalised Hamiltonian,

$$E_0^R \equiv \langle 0 | \hat{H}^R | 0 \rangle = 0. \quad (128)$$

According to this recipe, the renormalised Hamiltonian is our original one, minus the (unrenormalised) vacuum energy,

$$\hat{H}^R = \hat{H} - E_0 \quad (129)$$

$$\begin{aligned} &= \frac{1}{2} \int \frac{d^3 k}{(2\pi)^3 2E(\mathbf{k})} E(\mathbf{k}) \{ \hat{a}^\dagger(\mathbf{k}) \hat{a}(\mathbf{k}) + \hat{a}(\mathbf{k}) \hat{a}^\dagger(\mathbf{k}) - \langle 0 | \hat{a}^\dagger(\mathbf{k}) \hat{a}(\mathbf{k}) + \hat{a}(\mathbf{k}) \hat{a}^\dagger(\mathbf{k}) | 0 \rangle \} \\ &= \frac{1}{2} \int \frac{d^3 k}{(2\pi)^3 2E(\mathbf{k})} E(\mathbf{k}) \{ 2\hat{a}^\dagger(\mathbf{k}) \hat{a}(\mathbf{k}) + [\hat{a}(\mathbf{k}), \hat{a}^\dagger(\mathbf{k})] - \langle 0 | [\hat{a}(\mathbf{k}), \hat{a}^\dagger(\mathbf{k})] | 0 \rangle \}. \end{aligned} \quad (130)$$

Here the subtraction of the vacuum energy is shown explicitly, and we can rewrite it as

$$\begin{aligned} \hat{H}^R &= \int \frac{d^3 p}{(2\pi)^3 2E(\mathbf{p})} E(\mathbf{p}) \hat{a}^\dagger(\mathbf{p}) \hat{a}(\mathbf{p}) \\ &\quad + \frac{1}{2} \int \frac{d^3 p}{(2\pi)^3 2E(\mathbf{p})} E(\mathbf{p}) \{ [\hat{a}(\mathbf{p}), \hat{a}^\dagger(\mathbf{p})] - \langle 0 | [\hat{a}(\mathbf{p}), \hat{a}^\dagger(\mathbf{p})] | 0 \rangle \}. \\ &= \int \frac{d^3 p}{(2\pi)^3 2E(\mathbf{p})} E(\mathbf{p}) \hat{a}^\dagger(\mathbf{p}) \hat{a}(\mathbf{p}) + \hat{H}^{\text{vac}} \end{aligned} \quad (131)$$

The operator  $\hat{H}^{\text{vac}}$  ensures that the vacuum energy is properly subtracted: if  $|\psi\rangle$  and  $|\psi'\rangle$  denote arbitrary  $N$ -particle states, then one can convince oneself that  $\langle \psi' | \hat{H}^{\text{vac}} | \psi \rangle = 0$ . In particular we now find that

$$\langle 0 | \hat{H}^R | 0 \rangle = 0, \quad (132)$$

as we wanted. A simple way to automatise the removal of the vacuum contribution is to introduce *normal ordering*. Normal ordering means that all annihilation operators appear to the right of any creation operator. The notation is

$$: \hat{a} \hat{a}^\dagger : = \hat{a}^\dagger \hat{a}, \quad (133)$$

i.e. the normal-ordered operators are enclosed within colons. For instance

$$: \frac{1}{2} (\hat{a}^\dagger(\mathbf{p}) \hat{a}(\mathbf{p}) + \hat{a}(\mathbf{p}) \hat{a}^\dagger(\mathbf{p})) : = \hat{a}^\dagger(\mathbf{p}) \hat{a}(\mathbf{p}). \quad (134)$$

It is important to keep in mind that  $\hat{a}$  and  $\hat{a}^\dagger$  *always* commute inside  $: \dots :$ . This is true for an arbitrary string of  $\hat{a}$  and  $\hat{a}^\dagger$ . With this definition we can write the normal-ordered Hamiltonian as

$$\begin{aligned} : \hat{H} : &= : \frac{1}{2} \int \frac{d^3 p}{(2\pi)^3 2E(\mathbf{p})} E(\mathbf{p}) (\hat{a}^\dagger(\mathbf{p}) \hat{a}(\mathbf{p}) + \hat{a}(\mathbf{p}) \hat{a}^\dagger(\mathbf{p})) : \\ &= \int \frac{d^3 p}{(2\pi)^3 2E(\mathbf{p})} E(\mathbf{p}) \hat{a}^\dagger(\mathbf{p}) \hat{a}(\mathbf{p}), \end{aligned} \quad (135)$$

and thus have the relation

$$\hat{H}^R =: \hat{H} : + \hat{H}^{\text{vac}}. \quad (136)$$

Hence, we find that

$$\langle \psi' | : \hat{H} : | \psi \rangle = \langle \psi' | \hat{H}^R | \psi \rangle, \quad (137)$$

and, in particular,  $\langle 0 | : \hat{H} : | 0 \rangle = 0$ . The normal ordered Hamiltonian thus produces a renormalised, sensible result for the vacuum energy.

### 3.4 Fock space and Particles

After this lengthy grappling with the vacuum state, we can continue to construct our basis of states in analogy to the harmonic oscillator, making use of the commutation relations for the operators  $\hat{a}, \hat{a}^\dagger$ . In particular, we define the state  $|\mathbf{k}\rangle$  to be the one obtained by acting with the operator  $\hat{a}^\dagger(\mathbf{k})$  on the vacuum,

$$|\mathbf{k}\rangle = \hat{a}^\dagger(\mathbf{k})|0\rangle. \quad (138)$$

Using the commutator, its norm is found to be

$$\langle \mathbf{k} | \mathbf{k}' \rangle = \langle 0 | \hat{a}(\mathbf{k}) \hat{a}^\dagger(\mathbf{k}') | 0 \rangle = \langle 0 | [\hat{a}(\mathbf{k}), \hat{a}^\dagger(\mathbf{k}')] | 0 \rangle + \langle 0 | \hat{a}^\dagger(\mathbf{k}') \hat{a}(\mathbf{k}) | 0 \rangle \quad (139)$$

$$= (2\pi)^3 2E(\mathbf{k}) \delta^3(\mathbf{k} - \mathbf{k}'), \quad (140)$$

since the last term in the first line vanishes ( $\hat{a}(\mathbf{k})$  acting on the vacuum). Next we compute the energy of this state, making use of the normal ordered Hamiltonian,

$$: \hat{H} : |\mathbf{k}\rangle = \int \frac{d^3 k'}{(2\pi)^3 2E(\mathbf{k}')} E(\mathbf{k}') \hat{a}^\dagger(\mathbf{k}') \hat{a}(\mathbf{k}') \hat{a}^\dagger(\mathbf{k}) | 0 \rangle \quad (141)$$

$$= \int \frac{d^3 k'}{(2\pi)^3 2E(\mathbf{k}')} E(\mathbf{k}') (2\pi)^3 2E(\mathbf{k}) \delta^3(\mathbf{k} - \mathbf{k}') \hat{a}^\dagger(\mathbf{k}) | 0 \rangle \quad (142)$$

$$= E(\mathbf{k}) \hat{a}^\dagger(\mathbf{k}) | 0 \rangle = E(\mathbf{k}) |\mathbf{k}\rangle, \quad (143)$$

and similarly one finds

$$: \hat{\mathbf{P}} : |\mathbf{k}\rangle = \mathbf{k} |\mathbf{k}\rangle. \quad (144)$$

Observing that the normal ordering did its job and we obtain renormalised, finite results, we may now interpret the state  $|\mathbf{k}\rangle$ . It is a one-particle state for a relativistic particle of mass  $m$  and momentum  $\mathbf{k}$ , since acting on it with the energy-momentum operator returns the relativistic one particle energy-momentum dispersion relation,  $E(\mathbf{k}) = \sqrt{\mathbf{k}^2 + m^2}$ . The  $\hat{a}^\dagger(\mathbf{k}), \hat{a}(\mathbf{k})$  are creation and annihilation operators for particles of momentum  $\mathbf{k}$ .

In analogy to the harmonic oscillator, the procedure can be continued to higher states. One easily checks that (problem 3.4)

$$: \hat{P}^\mu : \hat{a}^\dagger(\mathbf{k}_2) \hat{a}^\dagger(\mathbf{k}_1) | 0 \rangle = (k_1^\mu + k_2^\mu) \hat{a}^\dagger(\mathbf{k}_2) \hat{a}^\dagger(\mathbf{k}_1) | 0 \rangle, \quad (145)$$

and so the state

$$|\mathbf{k}_2, \mathbf{k}_1\rangle = \frac{1}{\sqrt{2!}} \hat{a}^\dagger(\mathbf{k}_2) \hat{a}^\dagger(\mathbf{k}_1) | 0 \rangle \quad (146)$$

is a two-particle state (the factorial is there to have it normalised in the same way as the one-particle state), and so on for higher states. These are called *Fock states* in the textbooks (formally speaking, a Fock space is a tensor product of Hilbert spaces, where the latter occur in ordinary Quantum Mechanics).

At long last we can now see how the field in our free quantum field theory is related to particles. A particle of momentum  $\mathbf{k}$  corresponds to an excited Fourier mode of a field. Since the field is a superposition of all possible Fourier modes, one field is enough to describe all possible

configurations representing one or many particles of the same kind in any desired momentum state.

There are some rather profound ideas here about how nature works at fundamental scales. In classical physics we have matter particles, and forces which act on those particles. These forces can be represented by fields, such that fields and particles are distinct concepts. In non-relativistic quantum mechanics, one unifies the concept of waves and particles (particles can have wave-like characteristics), but fields are still distinct (e.g. one may quantise a particle in an electromagnetic field in QM, provided the latter is treated classically). Taking into account the effects of relativity for both particles and fields, one finds in QFT that all particles are excitation quanta of fields. That is, the concepts of *field* and *particle* are no longer distinct, but actually manifestations of the same thing, namely quantum fields. In this sense, QFT is more fundamental than either of its preceding theories. Each force field and each matter field have particles associated with it.

Returning to our theory for the free Klein-Gordon field, let us investigate what happens under interchange of the two particles. Since  $[\hat{a}^\dagger(\mathbf{k}_1), \hat{a}^\dagger(\mathbf{k}_2)] = 0$  for all  $\mathbf{k}_1, \mathbf{k}_2$ , we see that

$$|\mathbf{k}_2, \mathbf{k}_1\rangle = |\mathbf{k}_1, \mathbf{k}_2\rangle, \quad (147)$$

and hence the state is symmetric under interchange of the two particles. Thus, the particles described by the scalar field are bosons.

Finally we complete the analogy to the harmonic oscillator by introducing a number operator

$$\hat{N}(\mathbf{k}) = \hat{a}^\dagger(\mathbf{k})\hat{a}(\mathbf{k}), \quad \hat{\mathcal{N}} = \int d^3k \hat{a}^\dagger(\mathbf{k})\hat{a}(\mathbf{k}), \quad (148)$$

which gives us the number of bosons described by a particular Fock state,

$$\hat{\mathcal{N}}|0\rangle = 0, \quad \hat{\mathcal{N}}|\mathbf{k}\rangle = |\mathbf{k}\rangle, \quad \hat{\mathcal{N}}|\mathbf{k}_1 \dots \mathbf{k}_n\rangle = n|\mathbf{k}_1 \dots \mathbf{k}_n\rangle. \quad (149)$$

Of course the normal-ordered Hamiltonian can now simply be given in terms of this operator,

$$:\hat{H} := \int \frac{d^3k}{(2\pi)^3} \frac{1}{2E(\mathbf{k})} E(\mathbf{k}) \hat{N}(\mathbf{k}), \quad (150)$$

i.e. when acting on a Fock state it simply sums up the energies of the individual particles to give

$$:\hat{H} : |\mathbf{k}_1 \dots \mathbf{k}_n\rangle = (E(\mathbf{k}_1) + \dots E(\mathbf{k}_n)) |\mathbf{k}_1 \dots \mathbf{k}_n\rangle. \quad (151)$$

This concludes the quantisation of our free scalar field theory. We have followed the canonical quantisation procedure familiar from quantum mechanics. Due to the infinite number of degrees of freedom, we encountered a divergent vacuum energy, which we had to renormalise. The renormalised Hamiltonian and the Fock states that we constructed describe free relativistic, uncharged spin zero particles of mass  $m$ , such as neutral pions, for example.

If we want to describe charged pions as well, we need to introduce complex scalar fields, the real and imaginary parts being necessary to describe opposite charges. For particles with spin we need still more degrees of freedom and use vector or spinor fields, which have the appropriate rotation and Lorentz transformation properties. For fermion fields (which satisfy the Dirac equation rather than the Klein-Gordon equation), one finds that the condition of a positive-definite energy density requires that one impose anti-commutation relations rather than commutation relations. This in turn implies that multiparticle states are antisymmetric under interchange of identical fermions, which we recognise as the Pauli exclusion principle. Thus, not only does QFT provide a consistent theory of relativistic multiparticle systems; it also allows us to “derive” the Pauli principle, which is put in by hand in non-relativistic quantum mechanics.

More details on vector and spinor fields can be found in the other courses at this school. Here, we continue to restrict our attention to scalar fields, so as to more clearly illustrate what happens when interactions are present.

## 4 Quantum Field Theory: Interacting Fields

So far we have seen how to quantise the Klein-Gordon Lagrangian, and seen that this describes free scalar particles. For interesting physics, however, we need to know how to describe interactions, which lead to nontrivial scattering processes. This is the subject of this section.

From now on we shall always discuss quantised real scalar fields. It is then convenient to drop the “hats” on the operators that we have considered up to now. Interactions can be described by adding a term  $\mathcal{L}_{\text{int}}$  to the Lagrangian density, so that the full result  $\mathcal{L}$  is given by

$$\mathcal{L} = \mathcal{L}_0 + \mathcal{L}_{\text{int}} \quad (152)$$

where

$$\mathcal{L}_0 = \frac{1}{2} \partial_\mu \phi \partial^\mu \phi - \frac{1}{2} m^2 \phi^2 \quad (153)$$

is the free Lagrangian density discussed before. The Hamiltonian density of the interaction is related to  $\mathcal{L}_{\text{int}}$  simply by

$$\mathcal{H}_{\text{int}} = \mathcal{H} - \mathcal{H}_0, \quad (154)$$

where  $\mathcal{H}_0$  is the free Hamiltonian. If the interaction Lagrangian only depends on  $\phi$  (we will consider such a case later in the course), one has

$$\mathcal{H}_{\text{int}} = -\mathcal{L}_{\text{int}}, \quad (155)$$

as can be easily shown from the definition above. We shall leave the details of  $\mathcal{L}_{\text{int}}$  unspecified for the moment. What we will be concerned with mostly are scattering processes, in which two initial particles with momenta  $\mathbf{p}_1$  and  $\mathbf{p}_2$  scatter, thereby producing a number of particles in the final state, characterised by momenta  $\mathbf{k}_1, \dots, \mathbf{k}_n$ . This is schematically shown in Fig. 4. Our task is to find a description of such a scattering process in terms of the underlying quantum field theory.

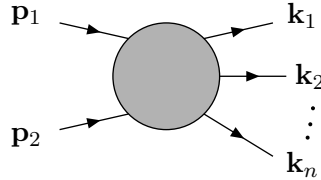


Figure 4: Scattering of two initial particles with momenta  $\mathbf{p}_1$  and  $\mathbf{p}_2$  into  $n$  particles with momenta  $\mathbf{k}_1, \dots, \mathbf{k}_n$  in the final state.

### 4.1 The $S$ -matrix

The timescales over which interactions happen are extremely short. The scattering (interaction) process takes place during a short interval around some particular time  $t$  with  $-\infty \ll t \ll \infty$ .



Long before  $t$ , the incoming particles evolve independently and freely. They are described by a field operator  $\phi_{\text{in}}$  defined through

$$\lim_{t \rightarrow -\infty} \phi(x) = \phi_{\text{in}}(x), \quad (156)$$

which acts on a corresponding basis of  $|\text{in}\rangle$  states. Long after the collision the particles in the final state evolve again like in the free theory, and the corresponding operator is

$$\lim_{t \rightarrow +\infty} \phi(x) = \phi_{\text{out}}(x), \quad (157)$$

acting on states  $|\text{out}\rangle$ . The fields  $\phi_{\text{in}}$ ,  $\phi_{\text{out}}$  are the asymptotic limits of the Heisenberg operator  $\phi$ . They both satisfy the free Klein-Gordon equation, i.e.

$$(\square + m^2)\phi_{\text{in}}(x) = 0, \quad (\square + m^2)\phi_{\text{out}}(x) = 0. \quad (158)$$

Operators describing free fields can be expressed as a superposition of plane waves (see Eq. (113)). Thus, for  $\phi_{\text{in}}$  we have

$$\phi_{\text{in}}(x) = \int \frac{d^3k}{(2\pi)^3 2E(\mathbf{k})} \left( e^{ik \cdot x} a_{\text{in}}^\dagger(\mathbf{k}) + e^{-ik \cdot x} a_{\text{in}}(\mathbf{k}) \right), \quad (159)$$

with an entirely analogous expression for  $\phi_{\text{out}}(x)$ . Note that the operators  $a^\dagger$  and  $a$  also carry subscripts “in” and “out”.

The above discussion assumes that the interaction is such that we can talk about free particles at asymptotic times  $t \rightarrow \pm\infty$  i.e. that the interaction is only present at intermediate times. This is not always a reasonable assumption e.g. it does not encompass the phenomenon of bound states, in which incident particles form a composite object at late times, which no longer consists of free particles. Nevertheless, the assumption will indeed allow us to discuss scattering processes, which is the aim of this course. Note that we can only talk about well-defined particle states at  $t \rightarrow \pm\infty$  (the states labelled by “in” and “out” above), as only at these times do we have a free theory, and thus know what the spectrum of states is (using the methods of section 3). At general times  $t$ , the interaction is present, and it is not possible in general to solve for the states of the quantum field theory. Remarkably, we will end up seeing that we can ignore all the complicated stuff at intermediate times, and solve for scattering probabilities purely using the properties of the asymptotic fields.

At the asymptotic times  $t = \pm\infty$ , we can use the creation operators  $a_{\text{in}}^\dagger$  and  $a_{\text{out}}^\dagger$  to build up Fock states from the vacuum. For instance

$$a_{\text{in}}^\dagger(\mathbf{p}_1) a_{\text{in}}^\dagger(\mathbf{p}_2) |0\rangle = |\mathbf{p}_1, \mathbf{p}_2; \text{in}\rangle, \quad (160)$$

$$a_{\text{out}}^\dagger(\mathbf{k}_1) \cdots a_{\text{out}}^\dagger(\mathbf{k}_n) |0\rangle = |\mathbf{k}_1, \dots, \mathbf{k}_n; \text{out}\rangle. \quad (161)$$

We must now distinguish between Fock states generated by  $a_{\text{in}}^\dagger$  and  $a_{\text{out}}^\dagger$ , and therefore we have labelled the Fock states accordingly. In eqs. (160) and (161) we have assumed that there is a stable and unique vacuum state of the free theory (the vacuum at general times  $t$  will be that of the full interacting theory, and thus differ from this in general):

$$|0\rangle = |0; \text{in}\rangle = |0; \text{out}\rangle. \quad (162)$$

Mathematically speaking, the  $a_{\text{in}}^\dagger$ ’s and  $a_{\text{out}}^\dagger$ ’s generate two different bases of the Fock space. Since the physics that we want to describe must be independent of the choice of basis, expectation values expressed in terms of “in” and “out” operators and states must satisfy

$$\langle \text{in} | \phi_{\text{in}}(x) | \text{in} \rangle = \langle \text{out} | \phi_{\text{out}}(x) | \text{out} \rangle. \quad (163)$$

Here  $|\text{in}\rangle$  and  $|\text{out}\rangle$  denote generic “in” and “out” states. We can relate the two bases by introducing a unitary operator  $S$  such that

$$\phi_{\text{in}}(x) = S \phi_{\text{out}}(x) S^\dagger \quad (164)$$

$$|\text{in}\rangle = S |\text{out}\rangle, \quad |\text{out}\rangle = S^\dagger |\text{in}\rangle, \quad S^\dagger S = 1. \quad (165)$$

$S$  is called the  $S$ -matrix or  $S$ -operator. Note that the plane wave solutions of  $\phi_{\text{in}}$  and  $\phi_{\text{out}}$  also imply that

$$a_{\text{in}}^\dagger = S a_{\text{out}}^\dagger S^\dagger, \quad \hat{a}_{\text{in}} = S \hat{a}_{\text{out}} S^\dagger. \quad (166)$$

By comparing “in” with “out” states one can extract information about the interaction – this is the very essence of detector experiments, where one tries to infer the nature of the interaction by studying the products of the scattering of particles that have been collided with known energies. As we will see below, this information is contained in the elements of the  $S$ -matrix.

By contrast, in the absence of any interaction, i.e. for  $\mathcal{L}_{\text{int}} = 0$  the distinction between  $\phi_{\text{in}}$  and  $\phi_{\text{out}}$  is not necessary. They can thus be identified, and then the relation between different bases of the Fock space becomes trivial,  $S = 1$ , as one would expect.

What we are ultimately interested in are transition amplitudes between an initial state  $i$  of, say, two particles of momenta  $\mathbf{p}_1, \mathbf{p}_2$ , and a final state  $f$ , for instance  $n$  particles of unequal momenta. The transition amplitude is then given by

$$\langle f, \text{out} | i, \text{in} \rangle = \langle f, \text{out} | S | i, \text{out} \rangle = \langle f, \text{in} | S | i, \text{in} \rangle \equiv S_{fi}. \quad (167)$$

The  $S$ -matrix element  $S_{fi}$  therefore describes the transition amplitude for the scattering process in question. The scattering cross section, which is a measurable quantity, is then proportional to  $|S_{fi}|^2$ . All information about the scattering is thus encoded in the  $S$ -matrix, which must therefore be closely related to the interaction Hamiltonian density  $\mathcal{H}_{\text{int}}$ . However, before we try to derive the relation between  $S$  and  $\mathcal{H}_{\text{int}}$  we have to take a slight detour.

## 4.2 More on time evolution: Dirac picture

The operators  $\phi(\mathbf{x}, t)$  and  $\pi(\mathbf{x}, t)$  which we have encountered are Heisenberg fields and thus time-dependent. The state vectors are time-independent in the sense that they do not satisfy a non-trivial equation of motion. Nevertheless, state vectors in the Heisenberg picture can carry a time label. For instance, the “in”-states of the previous subsection are defined at  $t = -\infty$ . The relation of the Heisenberg operator  $\phi_H(x)$  with its counterpart  $\phi_S$  in the Schrödinger picture is given by

$$\phi_H(\mathbf{x}, t) = e^{iHt} \phi_S e^{-iHt}, \quad H = H_0 + H_{\text{int}}, \quad (168)$$

Note that this relation involves the *full* Hamiltonian  $H = H_0 + H_{\text{int}}$  in the interacting theory. We have so far found solutions to the Klein-Gordon equation in the free theory, and so we know how to handle time evolution in this case. However, in the interacting case the Klein-Gordon equation has an extra term,

$$(\square + m^2)\phi(x) + \frac{\partial V_{\text{int}}(\phi)}{\partial \phi} = 0, \quad (169)$$

due to the potential of the interactions. Apart from very special cases of this potential, the equation cannot be solved anymore in closed form, and thus we no longer know the time evolution. It is therefore useful to introduce a new quantum picture for the interacting theory, in which the time dependence is governed by  $H_0$  only. This is the so-called Dirac or Interaction picture. The relation between fields in the Interaction picture,  $\phi_I$ , and in the Schrödinger picture,  $\phi_S$ , is given by

$$\phi_I(\mathbf{x}, t) = e^{iH_0 t} \phi_S e^{-iH_0 t}. \quad (170)$$

At  $t = -\infty$  the interaction vanishes, i.e.  $H_{\text{int}} = 0$ , and hence the fields in the Interaction and Heisenberg pictures are identical, i.e.  $\phi_H(\mathbf{x}, t) = \phi_I(\mathbf{x}, t)$  for  $t \rightarrow -\infty$ . The relation between  $\phi_H$  and  $\phi_I$  can be worked out easily:

$$\begin{aligned}\phi_H(\mathbf{x}, t) &= e^{iHt} \phi_S e^{-iHt} \\ &= e^{iHt} e^{-iH_0 t} \underbrace{e^{iH_0 t} \phi_S e^{-iH_0 t}}_{\phi_I(\mathbf{x}, t)} e^{iH_0 t} e^{-iHt} \\ &= U^{-1}(t) \phi_I(\mathbf{x}, t) U(t),\end{aligned}\tag{171}$$

where we have introduced the unitary operator  $U(t)$

$$U(t) = e^{iH_0 t} e^{-iHt}, \quad U^\dagger U = 1.\tag{172}$$

The field  $\phi_H(\mathbf{x}, t)$  contains the information about the interaction, since it evolves over time with the full Hamiltonian. In order to describe the “in” and “out” field operators, we can now make the following identifications:

$$t \rightarrow -\infty : \quad \phi_{\text{in}}(\mathbf{x}, t) = \phi_I(\mathbf{x}, t) = \phi_H(\mathbf{x}, t),\tag{173}$$

$$t \rightarrow +\infty : \quad \phi_{\text{out}}(\mathbf{x}, t) = \phi_H(\mathbf{x}, t).\tag{174}$$

Furthermore, since the fields  $\phi_I$  evolve over time with the free Hamiltonian  $H_0$ , they always act in the basis of “in” vectors, such that

$$\phi_{\text{in}}(\mathbf{x}, t) = \phi_I(\mathbf{x}, t), \quad -\infty < t < \infty.\tag{175}$$

The relation between  $\phi_I$  and  $\phi_H$  at any time  $t$  is given by

$$\phi_I(\mathbf{x}, t) = U(t) \phi_H(\mathbf{x}, t) U^{-1}(t).\tag{176}$$

As  $t \rightarrow \infty$  the identifications of eqs. (174) and (175) yield

$$\phi_{\text{in}} = U(\infty) \phi_{\text{out}} U^\dagger(\infty).\tag{177}$$

From the definition of the  $S$ -matrix, Eq. (164) we then read off that

$$\lim_{t \rightarrow \infty} U(t) = S.\tag{178}$$

We have thus derived a formal expression for the  $S$ -matrix in terms of the operator  $U(t)$ , which tells us how operators and state vectors deviate from the free theory at time  $t$ , measured relative to  $t_0 = -\infty$ , i.e. long before the interaction process.

An important boundary condition for  $U(t)$  is

$$\lim_{t \rightarrow -\infty} U(t) = 1.\tag{179}$$

What we mean here is the following: the operator  $U$  actually describes the evolution relative to some initial time  $t_0$ , which we will normally suppress, i.e. we write  $U(t)$  instead of  $U(t, t_0)$ . We regard  $t_0$  merely as a time label and fix it at  $-\infty$ , where the interaction vanishes. Equation (179) then simply states that  $U$  becomes unity as  $t \rightarrow t_0$ , which means that in this limit there is no distinction between Heisenberg and Dirac fields.

Using the definition of  $U(t)$ , Eq. (172), it is an easy exercise to derive the equation of motion for  $U(t)$ :

$$i \frac{d}{dt} U(t) = H_{\text{int}}(t) U(t), \quad H_{\text{int}}(t) = e^{iH_0 t} H_{\text{int}} e^{-iH_0 t}.\tag{180}$$

The time-dependent operator  $H_{\text{int}}(t)$  is defined in the interaction picture, and depends on the fields  $\phi_{\text{in}}, \pi_{\text{in}}$  in the “in” basis. Let us now solve the equation of motion for  $U(t)$  with the boundary condition  $\lim_{t \rightarrow -\infty} U(t) = 1$ . Integrating Eq. (180) gives

$$\begin{aligned} \int_{-\infty}^t \frac{d}{dt_1} U(t_1) dt_1 &= -i \int_{-\infty}^t H_{\text{int}}(t_1) U(t_1) dt_1 \\ U(t) - U(-\infty) &= -i \int_{-\infty}^t H_{\text{int}}(t_1) U(t_1) dt_1 \\ \Rightarrow U(t) &= 1 - i \int_{-\infty}^t H_{\text{int}}(t_1) U(t_1) dt_1. \end{aligned} \quad (181)$$

The right-hand side still depends on  $U$ , but we can substitute our new expression for  $U(t)$  into the integrand, which gives

$$\begin{aligned} U(t) &= 1 - i \int_{-\infty}^t H_{\text{int}}(t_1) \left\{ 1 - i \int_{-\infty}^{t_1} H_{\text{int}}(t_2) U(t_2) dt_2 \right\} dt_1 \\ &= 1 - i \int_{-\infty}^t H_{\text{int}}(t_1) dt_1 - \int_{-\infty}^t dt_1 H_{\text{int}}(t_1) \int_{-\infty}^{t_1} dt_2 H_{\text{int}}(t_2) U(t_2), \end{aligned} \quad (182)$$

where  $t_2 < t_1 < t$ . This procedure can be iterated further, so that the  $n$ th term in the sum is

$$(-i)^n \int_{-\infty}^t dt_1 \int_{-\infty}^{t_1} dt_2 \cdots \int_{-\infty}^{t_{n-1}} dt_n H_{\text{int}}(t_1) H_{\text{int}}(t_2) \cdots H_{\text{int}}(t_n). \quad (183)$$

This iterative solution could be written in much more compact form, were it not for the fact that the upper integration bounds were all different, and that the ordering  $t_n < t_{n-1} < \dots < t_1 < t$  had to be obeyed. Time ordering is an important issue, since one has to ensure that the interaction Hamiltonians act at the proper time, thereby ensuring the causality of the theory. By introducing the time-ordered product of operators, one can use a compact notation, such that the resulting expressions still obey causality. The time-ordered product of two fields  $\phi(t_1)$  and  $\phi(t_2)$  is defined as

$$\begin{aligned} T \{ \phi(t_1) \phi(t_2) \} &= \begin{cases} \phi(t_1) \phi(t_2) & t_1 > t_2 \\ \phi(t_2) \phi(t_1) & t_1 < t_2 \end{cases} \\ &\equiv \theta(t_1 - t_2) \phi(t_1) \phi(t_2) + \theta(t_2 - t_1) \phi(t_2) \phi(t_1), \end{aligned} \quad (184)$$

where  $\theta$  denotes the step function. The generalisation to products of  $n$  operators is obvious. Using time ordering for the  $n$ th term of Eq. (183) we obtain

$$\frac{(-i)^n}{n!} \prod_{i=1}^n \int_{-\infty}^t dt_i T \{ H_{\text{int}}(t_1) H_{\text{int}}(t_2) \cdots H_{\text{int}}(t_n) \}. \quad (185)$$

Here we have replaced each upper limit of integration with  $t$ . Each specific ordering in the time-ordered product gives a term identical to eq. (183), where applying the  $T$  operator corresponds to setting the upper limit of integration to the relevant  $t_i$  in each integral. However, we have overcounted by a factor  $n!$ , corresponding to the number of ways of ordering the fields in the time ordered product. Thus one must divide by  $n!$  as shown. We may recognise eq. (185) as the  $n$ th term in the series expansion of an exponential, and thus can finally rewrite the solution for  $U(t)$  in compact form as

$$U(t) = T \exp \left\{ -i \int_{-\infty}^t H_{\text{int}}(t') dt' \right\}, \quad (186)$$

where the “ $T$ ” in front ensures the correct time ordering.

### 4.3 $S$ -matrix and Green's functions

The  $S$ -matrix, which relates the “in” and “out” fields before and after the scattering process, can be written as

$$S = 1 + iT, \quad (187)$$

where  $T$  is commonly called the  $T$ -matrix. The fact that  $S$  contains the unit operator means that also the case where none of the particles scatter is encoded in  $S$ . On the other hand, the non-trivial case is described by the  $T$ -matrix, and this is what we are interested in. So far we have derived an expression for the  $S$ -matrix in terms of the interaction Hamiltonian, and we could use this in principle to calculate scattering processes. However, there is a slight complication owing to the fact that the vacuum of the free theory is not the same as the true vacuum of the full, interacting theory. Instead, we will follow the approach of Lehmann, Symanzik and Zimmerman, which relates the  $S$ -matrix to  $n$ -point Green's functions

$$G_n(x_1, \dots, x_n) = \langle 0 | T(\phi(x_1) \dots \phi(x_n)) | 0 \rangle \quad (188)$$

i.e. vacuum expectation values of Heisenberg fields. We will see later how to calculate these in terms of vacuum expectation values of “in” fields (i.e. in the free theory).

In order to relate  $S$ -matrix elements to Green's functions, we have to express the “in/out”-states in terms of creation operators  $a_{\text{in/out}}^\dagger$  and the vacuum, then express the creation operators by the fields  $\phi_{\text{in/out}}$ , and finally use the time evolution to connect those with the fields  $\phi$  in our Lagrangian.

Let us consider again the scattering process depicted in Fig. 4. The  $S$ -matrix element in this case is

$$\begin{aligned} S_{\text{fi}} &= \langle \mathbf{k}_1, \mathbf{k}_2, \dots, \mathbf{k}_n; \text{out} | \mathbf{p}_1, \mathbf{p}_2; \text{in} \rangle \\ &= \langle \mathbf{k}_1, \mathbf{k}_2, \dots, \mathbf{k}_n; \text{out} | a_{\text{in}}^\dagger(\mathbf{p}_1) | \mathbf{p}_2; \text{in} \rangle, \end{aligned} \quad (189)$$

where  $a_{\text{in}}^\dagger$  is the creation operator pertaining to the “in” field  $\phi_{\text{in}}$ . Our task is now to express  $a_{\text{in}}^\dagger$  in terms of  $\phi_{\text{in}}$ , and repeat this procedure for all other momenta labelling our Fock states.

The following identities will prove useful

$$\begin{aligned} a^\dagger(\mathbf{p}) &= i \int d^3x \{ (\partial_0 e^{-iq \cdot x}) \phi(x) - e^{-iq \cdot x} (\partial_0 \phi(x)) \} \\ &\equiv -i \int d^3x e^{-iq \cdot x} \overleftrightarrow{\partial}_0 \phi(x), \end{aligned} \quad (190)$$

$$\begin{aligned} \hat{a}(\mathbf{p}) &= -i \int d^3x \{ (\partial_0 e^{iq \cdot x}) \phi(x) - e^{iq \cdot x} (\partial_0 \phi(x)) \} \\ &\equiv i \int d^3x e^{iq \cdot x} \overleftrightarrow{\partial}_0 \phi(x). \end{aligned} \quad (191)$$

The  $S$ -matrix element can then be rewritten as

$$\begin{aligned} S_{\text{fi}} &= -i \int d^3x_1 e^{-ip_1 \cdot x_1} \overleftrightarrow{\partial}_0 \langle \mathbf{k}_1, \dots, \mathbf{k}_n; \text{out} | \phi_{\text{in}}(x_1) | \mathbf{p}_2; \text{in} \rangle \\ &= -i \lim_{t_1 \rightarrow -\infty} \int d^3x_1 e^{-ip_1 \cdot x_1} \overleftrightarrow{\partial}_0 \langle \mathbf{k}_1, \dots, \mathbf{k}_n; \text{out} | \phi(x_1) | \mathbf{p}_2; \text{in} \rangle, \end{aligned} \quad (192)$$

where in the last line we have used Eq. (156) to replace  $\phi_{\text{in}}$  by  $\phi$ . We can now rewrite  $\lim_{t_1 \rightarrow -\infty}$  using the following identity, which holds for an arbitrary, differentiable function  $f(t)$ , whose limit  $t \rightarrow \pm\infty$  exists:

$$\lim_{t \rightarrow -\infty} f(t) = \lim_{t \rightarrow +\infty} f(t) - \int_{-\infty}^{+\infty} \frac{df}{dt} dt. \quad (193)$$

The  $S$ -matrix element then reads

$$S_{\text{fi}} = -i \lim_{t_1 \rightarrow +\infty} \int d^3 x_1 e^{-ip_1 \cdot x_1} \overleftrightarrow{\partial}_0 \left\langle \mathbf{k}_1, \dots, \mathbf{k}_n; \text{out} \left| \phi(x_1) \right| \mathbf{p}_2; \text{in} \right\rangle \\ + i \int_{-\infty}^{+\infty} dt_1 \frac{\partial}{\partial t_1} \left\{ \int d^3 x_1 e^{-ip_1 \cdot x_1} \overleftrightarrow{\partial}_0 \left\langle \mathbf{k}_1, \dots, \mathbf{k}_n; \text{out} \left| \phi(x_1) \right| \mathbf{p}_2; \text{in} \right\rangle \right\}. \quad (194)$$

The first term in this expression involves  $\lim_{t_1 \rightarrow +\infty} \phi = \phi_{\text{out}}$ , which gives rise to a contribution

$$\propto \left\langle \mathbf{k}_1, \dots, \mathbf{k}_n; \text{out} \left| a_{\text{out}}^\dagger(\mathbf{p}_1) \right| \mathbf{p}_2; \text{in} \right\rangle. \quad (195)$$

This is non-zero only if  $\mathbf{p}_1$  is equal to one of  $\mathbf{k}_1, \dots, \mathbf{k}_n$ . This, however, means that the particle with momentum  $\mathbf{p}_1$  does not scatter, and hence the first term does not contribute to the  $T$ -matrix of Eq. (187). We are then left with the following expression for  $S_{\text{fi}}$ :

$$S_{\text{fi}} = -i \int d^4 x_1 \left\langle \mathbf{k}_1, \dots, \mathbf{k}_n; \text{out} \left| \partial_0 \left\{ (\partial_0 e^{-ip_1 \cdot x_1}) \phi(x_1) - e^{-ip_1 \cdot x_1} (\partial_0 \phi(x_1)) \right\} \right| \mathbf{p}_2; \text{in} \right\rangle. \quad (196)$$

The time derivatives in the integrand can be worked out:

$$\begin{aligned} & \partial_0 \left\{ (\partial_0 e^{-ip_1 \cdot x_1}) \phi(x_1) - e^{-ip_1 \cdot x_1} (\partial_0 \phi(x_1)) \right\} \\ &= -[E(\mathbf{p}_1)]^2 e^{-ip_1 \cdot x_1} \phi(x_1) - e^{-ip_1 \cdot x_1} \partial_0^2 \phi(x_1) \\ &= -\left\{ ((-\nabla^2 + m^2) e^{-ip_1 \cdot x_1}) \phi(x_1) + e^{-ip_1 \cdot x_1} \partial_0^2 \phi(x_1) \right\}, \end{aligned} \quad (197)$$

where we have used that  $-\nabla^2 e^{-ip_1 \cdot x_1} = \mathbf{p}_1^2 e^{-ip_1 \cdot x_1}$ . For the  $S$ -matrix element one obtains

$$\begin{aligned} S_{\text{fi}} &= i \int d^4 x_1 e^{-ip_1 \cdot x_1} \left\langle \mathbf{k}_1, \dots, \mathbf{k}_n; \text{out} \left| (\partial_0^2 - \nabla^2 + m^2) \phi(x_1) \right| \mathbf{p}_2; \text{in} \right\rangle \\ &= i \int d^4 x_1 e^{-ip_1 \cdot x_1} (\Box_{x_1} + m^2) \left\langle \mathbf{k}_1, \dots, \mathbf{k}_n; \text{out} \left| \phi(x_1) \right| \mathbf{p}_2; \text{in} \right\rangle, \end{aligned} \quad (198)$$

where we have used integration by parts twice so that  $\nabla^2$  acts on  $\phi(x_1)$  rather than on  $e^{-ip_1 \cdot x_1}$ . What we have obtained after this rather lengthy step of algebra is an expression in which the (Heisenberg) field operator is sandwiched between Fock states, one of which has been reduced to a one-particle state. We can now successively eliminate all momentum variables from the Fock states, by repeating the procedure for the momentum  $\mathbf{p}_2$ , as well as the  $n$  momenta of the “out” state. The final expression for  $S_{\text{fi}}$  is

$$\begin{aligned} S_{\text{fi}} &= (i)^{n+2} \int d^4 x_1 \int d^4 x_2 \int d^4 y_1 \cdots \int d^4 y_n e^{(-ip_1 \cdot x_1 - ip_2 \cdot x_2 + ik_1 \cdot y_1 + \cdots + ik_n \cdot y_n)} \\ &\quad \times (\Box_{x_1} + m^2) (\Box_{x_2} + m^2) (\Box_{y_1} + m^2) \cdots (\Box_{y_n} + m^2) \\ &\quad \times \left\langle 0; \text{out} \left| T\{\phi(y_1) \cdots \phi(y_n) \phi(x_1) \phi(x_2)\} \right| 0; \text{in} \right\rangle, \end{aligned} \quad (199)$$

where the time-ordering inside the vacuum expectation value (VEV) ensures that causality is obeyed. The above expression is known as the Lehmann-Symanzik-Zimmermann (LSZ) reduction formula. It relates the formal definition of the scattering amplitude to a vacuum expectation value of time-ordered fields. Since the vacuum is uniquely the same for “in/out”, the VEV in the LSZ formula for the scattering of two initial particles into  $n$  particles in the final state is recognised as the  $(n+2)$ -point Green’s function:

$$G_{n+2}(y_1, y_2, \dots, y_n, x_1, x_2) = \left\langle 0 \left| T\{\phi(y_1) \cdots \phi(y_n) \phi(x_1) \phi(x_2)\} \right| 0 \right\rangle. \quad (200)$$

You will note that we still have not calculated or evaluated anything, but merely rewritten the expression for the scattering matrix elements. Nevertheless, the LSZ formula is of tremendous importance and a central piece of QFT. It provides the link between fields in the Lagrangian and the scattering amplitude  $S_{\text{fi}}^2$ , which yields the cross section, measurable in an experiment. Up to here no assumptions or approximations have been made, so this connection between physics and formalism is rather tight. It also illustrates a profound phenomenon of QFT and particle physics: the scattering properties of particles, in other words their interactions, are encoded in the vacuum structure, i.e. the vacuum is non-trivial!

#### 4.4 How to compute Green's functions

Of course, in order to calculate cross sections, we need to compute the Green's functions. Alas, for any physically interesting and interacting theory this cannot be done exactly, contrary to the free theory discussed earlier. Instead, approximation methods have to be used in order to simplify the calculation, while hopefully still giving reliable results. Or one reformulates the entire QFT as a lattice field theory, which in principle allows to compute Green's functions without any approximations (in practice this still turns out to be a difficult task for physically relevant systems). This is what many theorists do for a living. But the formalism stands, and if there are discrepancies between theory and experiments, one “only” needs to check the accuracy with which the Green's functions have been calculated or measured, before approving or discarding a particular Lagrangian.

In the next section we shall discuss how to compute the Green's function of scalar field theory in perturbation theory. Before we can tackle the actual computation, we must take a further step. Let us consider the  $n$ -point Green's function

$$G_n(x_1, \dots, x_n) = \langle 0 | T \{ \phi(x_1) \cdots \phi(x_n) \} | 0 \rangle. \quad (201)$$

The fields  $\phi$  which appear in this expression are Heisenberg fields, whose time evolution is governed by the full Hamiltonian  $H_0 + H_{\text{int}}$ . In particular, the  $\phi$ 's are *not* the  $\phi_{\text{in}}$ 's. We know how to handle the latter, because they correspond to a free field theory, but not the former, whose time evolution is governed by the interacting theory, whose solutions we do not know. Let us thus start to isolate the dependence of the fields on the interaction Hamiltonian. Recall the relation between the Heisenberg fields  $\phi(t)$  and the “in”-fields<sup>3</sup>

$$\phi(t) = U^{-1}(t) \phi_{\text{in}}(t) U(t). \quad (202)$$

We now assume that the fields are properly time-ordered, i.e.  $t_1 > t_2 > \dots > t_n$ , so that we can forget about writing  $T(\dots)$  everywhere. After inserting Eq. (202) into the definition of  $G_n$  one obtains

$$G_n = \langle 0 | U^{-1}(t_1) \phi_{\text{in}}(t_1) U(t_1) U^{-1}(t_2) \phi_{\text{in}}(t_2) U(t_2) \cdots \times U^{-1}(t_n) \phi_{\text{in}}(t_n) U(t_n) | 0 \rangle. \quad (203)$$

Now we introduce another time label  $t$  such that  $t \gg t_1$  and  $-t \ll t_1$ . For the  $n$ -point function we now obtain

$$G_n = \langle 0 | U^{-1}(t) \left\{ U(t) U^{-1}(t_1) \phi_{\text{in}}(t_1) U(t_1) U^{-1}(t_2) \phi_{\text{in}}(t_2) U(t_2) \cdots \times U^{-1}(t_n) \phi_{\text{in}}(t_n) U(t_n) U^{-1}(-t) \right\} U(-t) | 0 \rangle. \quad (204)$$

The expression in curly braces is now time-ordered by construction. An important observation at this point is that it involves pairs of  $U$  and its inverse, for instance

$$U(t) U^{-1}(t_1) \equiv U(t, t_1). \quad (205)$$

---

<sup>3</sup>Here and in the following we suppress the spatial argument of the fields for the sake of brevity.

One can easily convince oneself that  $U(t, t_1)$  provides the net time evolution from  $t_1$  to  $t$ . We can now write  $G_n$  as

$$G_n = \langle 0 | U^{-1}(t) T \left\{ \phi_{\text{in}}(t_1) \cdots \phi_{\text{in}}(t_n) \underbrace{U(t, t_1) U(t_1, t_2) \cdots U(t_n, -t)}_{U(t, -t)} \right\} U(-t) | 0 \rangle, \quad (206)$$

where we have used the fact that we may commute the  $U$  operators within the time-ordered product. Let us now take  $t \rightarrow \infty$ . The relation between  $U(t)$  and the  $S$ -matrix Eq.(178), as well as the boundary condition Eq.(179) tell us that

$$\lim_{t \rightarrow \infty} U(-t) = 1, \quad \lim_{t \rightarrow \infty} U(t, -t) = S, \quad (207)$$

which can be inserted into the above expression. We still have to work out the meaning of  $\langle 0 | U^{-1}(\infty)$  in the expression for  $G_n$ . In a paper by Gell-Mann and Low it was argued that the time evolution operator must leave the vacuum invariant (up to a phase), which justifies the ansatz

$$\langle 0 | U^{-1}(\infty) = K \langle 0 |, \quad (208)$$

with  $K$  being the phase<sup>4</sup>. Multiplying this relation with  $|0\rangle$  from the right gives

$$\langle 0 | U^{-1}(\infty) | 0 \rangle = K \langle 0 | 0 \rangle = K. \quad (209)$$

Furthermore, Gell-Mann and Low showed that

$$\langle 0 | U^{-1}(\infty) | 0 \rangle = \frac{1}{\langle 0 | U(\infty) | 0 \rangle}, \quad (210)$$

which implies

$$K = \frac{1}{\langle 0 | S | 0 \rangle}. \quad (211)$$

After inserting all these relations into the expression for  $G_n$  we obtain

$$G_n(x_1, \dots, x_n) = \frac{\langle 0 | T \{ \phi_{\text{in}}(x_1) \cdots \phi_{\text{in}}(x_n) S \} | 0 \rangle}{\langle 0 | S | 0 \rangle}. \quad (212)$$

The  $S$ -matrix is given by

$$S = T \exp \left\{ -i \int_{-\infty}^{+\infty} H_{\text{int}}(t) dt \right\}, \quad H_{\text{int}} = H_{\text{int}}(\phi_{\text{in}}, \pi_{\text{in}}), \quad (213)$$

and thus we have finally succeeded in expressing the  $n$ -point Green's function exclusively in terms of the “in”-fields. This completes the derivation of a relation between the general definition of the scattering amplitude  $S_{\text{fi}}$  and the VEV of time-ordered “in”-fields. This has been a long and technical discussion, but the main points are the following:

*Scattering probabilities are related to  $S$ -matrix elements. To calculate  $S$ -matrix elements for an  $n$  particle scattering process, one must first calculate the  $n$  particle Green's function (eq. (212)). Then one plugs this into the LSZ formula (eq. (199)).*

In fact, the Green's functions cannot be calculated exactly using eq. (212). Instead, one can only obtain answers in the limit in which the interaction strength  $\lambda$  is small. This is the subject of the following sections.

---

<sup>4</sup>As hinted at earlier,  $K$  relates the vacuum of the free theory to the true vacuum of the interacting theory.



## 5 Perturbation Theory

In this section we are going to calculate the Green's functions of scalar quantum field theory explicitly. We will specify the interaction Lagrangian in detail and use an approximation known as perturbation theory. At the end we will derive a set of rules, which represent a systematic prescription for the calculation of Green's functions, and can be easily generalised to apply to other, more complicated field theories. These are the famous Feynman rules.

We start by making a definite choice for the interaction Lagrangian  $\mathcal{L}_{\text{int}}$ . Although one may think of many different expressions for  $\mathcal{L}_{\text{int}}$ , one has to obey some basic principles: firstly,  $\mathcal{L}_{\text{int}}$  must be chosen such that the potential it generates is bounded from below – otherwise the system has no ground state. Secondly, our interacting theory should be renormalisable. Despite being of great importance, the second issue will not be addressed in these lectures. The requirement of renormalisability arises because the non-trivial vacuum, much like a medium, interacts with particles to modify their properties. Moreover, if one computes quantities like the energy or charge of a particle, one typically obtains a divergent result<sup>5</sup>. There are classes of quantum field theories, called renormalisable, in which these divergences can be removed by suitable redefinitions of the fields and the parameters (masses and coupling constants).

For our theory of a real scalar field in four space-time dimensions, it turns out that the only interaction term which leads to a renormalisable theory must be quartic in the fields. Thus we choose

$$\mathcal{L}_{\text{int}} = -\frac{\lambda}{4!}\phi^4(x), \quad (214)$$

where the coupling constant  $\lambda$  describes the strength of the interaction between the scalar fields, much like, say, the electric charge describing the strength of the interaction between photons and electrons. The factor  $4!$  is for later convenience. The full Lagrangian of the theory then reads

$$\mathcal{L} = \mathcal{L}_0 + \mathcal{L}_{\text{int}} = \frac{1}{2}(\partial_\mu\phi)^2 - \frac{1}{2}m^2\phi^2 - \frac{\lambda}{4!}\phi^4, \quad (215)$$

and the explicit expressions for the interaction Hamiltonian and the  $S$ -matrix are

$$\begin{aligned} \mathcal{H}_{\text{int}} &= -\mathcal{L}_{\text{int}}, & H_{\text{int}} &= \frac{\lambda}{4!} \int d^3x \phi_{\text{in}}^4(\mathbf{x}, t) \\ S &= T \exp \left\{ -i \frac{\lambda}{4!} \int d^4x \phi_{\text{in}}^4(x) \right\}. \end{aligned} \quad (216)$$

The  $n$ -point Green's function is

$$\begin{aligned} G_n(x_1, \dots, x_n) &= \frac{\sum_{r=0}^{\infty} \left(-\frac{i\lambda}{4!}\right)^r \frac{1}{r!} \left\langle 0 \left| T \left\{ \phi_{\text{in}}(x_1) \cdots \phi_{\text{in}}(x_n) \left( \int d^4y \phi_{\text{in}}^4(y) \right)^r \right\} \right| 0 \right\rangle}{\sum_{r=0}^{\infty} \left(-\frac{i\lambda}{4!}\right)^r \frac{1}{r!} \left\langle 0 \left| T \left( \int d^4y \phi_{\text{in}}^4(y) \right)^r \right| 0 \right\rangle}. \end{aligned} \quad (217)$$

This expression cannot be dealt with as it stands. In order to evaluate it we must expand  $G_n$  in powers of the coupling  $\lambda$  and truncate the series after a finite number of terms. This only makes sense if  $\lambda$  is sufficiently small. In other words, the interaction Lagrangian must act as a small perturbation on the system. As a consequence, the procedure of expanding Green's functions in powers of the coupling is referred to as perturbation theory. We will see that there is a natural diagrammatic representation of this expansion (Feynman diagrams). First, we need to know how to calculate the vacuum expectation values of time ordered products. This is the subject of the next section.

---

<sup>5</sup>This is despite the subtraction of the vacuum energy discussed earlier.

## 5.1 Wick's Theorem

The  $n$ -point Green's function in Eq. (217) involves the time-ordered product over at least  $n$  fields. There is a method to express VEV's of  $n$  fields, i.e.  $\langle 0|T\{\phi_{\text{in}}(x_1)\cdots\phi_{\text{in}}(x_n)\}|0\rangle$  in terms of VEV's involving two fields only. This is known as Wick's theorem.

Let us for the moment ignore the subscript “in” and return to the definition of normal-ordered fields. The normal-ordered product  $:\phi(x_1)\phi(x_2):$  differs from  $\phi(x_1)\phi(x_2)$  by the vacuum expectation value, i.e.

$$\phi(x_1)\phi(x_2) = :\phi(x_1)\phi(x_2): + \langle 0|\phi(x_1)\phi(x_2)|0\rangle. \quad (218)$$

We are now going to combine normal-ordered products with time ordering. The time-ordered product  $T\{\phi(x_1)\phi(x_2)\}$  is given by

$$\begin{aligned} T\{\phi(x_1)\phi(x_2)\} &= \phi(x_1)\phi(x_2)\theta(t_1 - t_2) + \phi(x_2)\phi(x_1)\theta(t_2 - t_1) \\ &= :\phi(x_1)\phi(x_2): \left( \theta(t_1 - t_2) + \theta(t_2 - t_1) \right) \\ &\quad + \langle 0|\phi(x_1)\phi(x_2)\theta(t_1 - t_2) + \phi(x_2)\phi(x_1)\theta(t_2 - t_1)|0\rangle. \end{aligned} \quad (219)$$

Here we have used the important observation that

$$:\phi(x_1)\phi(x_2): = :\phi(x_2)\phi(x_1):, \quad (220)$$

which means that normal-ordered products of fields are automatically time-ordered.<sup>6</sup> Equation (219) is Wick's theorem for the case of two fields:

$$T\{\phi(x_1)\phi(x_2)\} = :\phi(x_1)\phi(x_2): + \langle 0|T\{\phi(x_1)\phi(x_2)\}|0\rangle. \quad (221)$$

For the case of three fields, Wick's theorem yields

$$\begin{aligned} T\{\phi(x_1)\phi(x_2)\phi(x_3)\} &= :\phi(x_1)\phi(x_2)\phi(x_3): + :\phi(x_1): \langle 0|T\{\phi(x_2)\phi(x_3)\}|0\rangle \\ &\quad + :\phi(x_2): \langle 0|T\{\phi(x_1)\phi(x_3)\}|0\rangle + :\phi(x_3): \langle 0|T\{\phi(x_1)\phi(x_2)\}|0\rangle \end{aligned} \quad (222)$$

At this point the general pattern becomes clear: any time-ordered product of fields is equal to its normal-ordered version plus terms in which pairs of fields are removed from the normal-ordered product and sandwiched between the vacuum to form 2-point functions. Then one sums over all permutations. Without proof we give the expression for the general case of  $n$  fields ( $n$  even):

$$\begin{aligned} T\{\phi(x_1)\cdots\phi(x_n)\} &= \\ &:\phi(x_1)\cdots\phi(x_n): \\ &+ :\phi(x_1)\cdots\widehat{\phi(x_i)}\cdots\widehat{\phi(x_j)}\cdots\phi(x_n): \langle 0|T\{\phi(x_i)\phi(x_j)\}|0\rangle + \text{perms.} \\ &+ :\phi(x_1)\cdots\widehat{\phi(x_i)}\cdots\widehat{\phi(x_j)}\cdots\widehat{\phi(x_k)}\cdots\widehat{\phi(x_l)}\cdots\phi(x_n): \\ &\quad \times \langle 0|T\{\phi(x_i)\phi(x_j)\}|0\rangle\langle 0|T\{\phi(x_k)\phi(x_l)\}|0\rangle + \text{perms.} \\ &+ \dots + \\ &+ \langle 0|T\{\phi(x_1)\phi(x_2)\}|0\rangle\langle 0|T\{\phi(x_3)\phi(x_4)\}|0\rangle\cdots\langle 0|T\{\phi(x_{n-1})\phi(x_n)\}|0\rangle \\ &\quad + \text{perms..} \end{aligned} \quad (223)$$

The symbol  $\widehat{\phi(x_i)}$  indicates that  $\phi(x_i)$  has been removed from the normal-ordered product.

Let us now go back to  $\langle 0|T\{\phi(x_1)\cdots\phi(x_n)\}|0\rangle$ . If we insert Wick's theorem, then we find that only the contribution in the last line of Eq. (223) survives: by definition the VEV of a

---

<sup>6</sup>The reverse is, however, not true!

normal-ordered product of fields vanishes, and it is precisely the last line of Wick's theorem in which no normal-ordered products are left. The only surviving contribution is that in which all fields have been paired or "contracted". Sometimes a contraction is represented by the notation:

$$\underbrace{\phi(x_i)\phi(x_j)} \equiv \langle 0|T\{\phi(x_i)\phi(x_j)\}|0\rangle, \quad (224)$$

i.e. the pair of fields which is contracted is joined by the braces. Wick's theorem can now be rephrased as

$$\langle 0|T\{\phi(x_1)\cdots\phi(x_n)\}|0\rangle = \text{sum of all possible contractions of } n \text{ fields.} \quad (225)$$

An example of this result is the 4-point function

$$\begin{aligned} \langle 0|T\{\phi(x_1)\phi(x_2)\phi(x_3)\phi(x_4)\}|0\rangle &= \underbrace{\phi(x_1)\phi(x_2)}\underbrace{\phi(x_3)\phi(x_4)} \\ &+ \underbrace{\phi(x_1)\phi(x_2)\phi(x_3)}\phi(x_4) + \underbrace{\phi(x_1)\phi(x_2)\phi(x_4)}\phi(x_3) \end{aligned} \quad (226)$$

## 5.2 The Feynman propagator

Using Wick's Theorem one can relate any  $n$ -point Green's functions to an expression involving only 2-point functions. Let us have a closer look at

$$G_2(x, y) = \langle 0|T\{\phi_{\text{in}}(x)\phi_{\text{in}}(y)\}|0\rangle. \quad (227)$$

We can now insert the solution for  $\phi$  in terms of  $\hat{a}$  and  $\hat{a}^\dagger$ . If we assume  $t_x > t_y$  then  $G_2(x, y)$  can be written as

$$\begin{aligned} G_2(x, y) &= \int \frac{d^3p \, d^3q}{(2\pi)^6 4E(\mathbf{p})E(\mathbf{q})} \\ &\times \langle 0|(\hat{a}^\dagger(\mathbf{p})e^{ip\cdot x} + \hat{a}(\mathbf{p})e^{-ip\cdot x})(\hat{a}^\dagger(\mathbf{q})e^{iq\cdot y} + \hat{a}(\mathbf{q})e^{-iq\cdot y})|0\rangle \\ &= \int \frac{d^3p \, d^3q}{(2\pi)^6 4E(\mathbf{p})E(\mathbf{q})} e^{-ip\cdot x + iq\cdot y} \langle 0|\hat{a}(\mathbf{p})\hat{a}^\dagger(\mathbf{q})|0\rangle. \end{aligned} \quad (228)$$

This shows that  $G_2$  can be interpreted as the amplitude for a meson which is created at  $y$  and destroyed again at point  $x$ . We can now replace  $\hat{a}(\mathbf{p})\hat{a}^\dagger(\mathbf{q})$  by its commutator:

$$\begin{aligned} G_2(x, y) &= \int \frac{d^3p \, d^3q}{(2\pi)^6 4E(\mathbf{p})E(\mathbf{q})} e^{-ip\cdot x + iq\cdot y} \langle 0|[\hat{a}(\mathbf{p}), \hat{a}^\dagger(\mathbf{q})]|0\rangle \\ &= \int \frac{d^3p}{(2\pi)^3 2E(\mathbf{p})} e^{-ip\cdot(x-y)}, \end{aligned} \quad (229)$$

and the general result, after restoring time-ordering, reads

$$G_2(x, y) = \int \frac{d^3p}{(2\pi)^3 2E(\mathbf{p})} \left( e^{-ip\cdot(x-y)}\theta(t_x - t_y) + e^{ip\cdot(x-y)}\theta(t_y - t_x) \right). \quad (230)$$

Furthermore, using contour integration one can show that this expression can be rewritten as a 4-dimensional integral

$$G_2(x, y) = i \int \frac{d^4p}{(2\pi)^4} \frac{e^{-ip\cdot(x-y)}}{p^2 - m^2 + i\epsilon}, \quad (231)$$

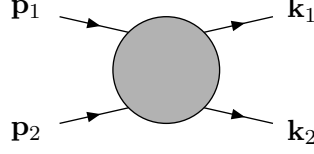


Figure 5: Scattering of two initial particles with momenta  $\mathbf{p}_1$  and  $\mathbf{p}_2$  into 2 particles with momenta  $\mathbf{k}_1$  and  $\mathbf{k}_2$ .

where  $\epsilon$  is a small parameter which ensures that  $G_2$  does not develop a pole. This calculation has established that  $G_2(x, y)$  actually depends only on the difference  $(x - y)$ . Equation (231) is called the Feynman propagator  $G_F(x - y)$ :

$$G_F(x - y) \equiv \langle 0 | T \{ \phi(x) \phi(y) \} | 0 \rangle = i \int \frac{d^4 p}{(2\pi)^4} \frac{e^{-ip \cdot (x - y)}}{p^2 - m^2 + i\epsilon}. \quad (232)$$

The Feynman propagator is a Green's function of the Klein-Gordon equation, i.e. it satisfies

$$(\square_x + m^2) G_F(x - y) = -i\delta^4(x - y), \quad (233)$$

and describes the propagation of a meson between the space-time points  $x$  and  $y$ .

### 5.3 Two-particle scattering to $\mathcal{O}(\lambda)$

Let us now consider a scattering process in which two incoming particles with momenta  $\mathbf{p}_1$  and  $\mathbf{p}_2$  scatter into two outgoing ones with momenta  $\mathbf{k}_1$  and  $\mathbf{k}_2$ , as shown in Fig. 5. The  $S$ -matrix element in this case is

$$\begin{aligned} S_{\text{fi}} &= \langle \mathbf{k}_1, \mathbf{k}_2; \text{out} | \mathbf{p}_1, \mathbf{p}_2; \text{in} \rangle \\ &= \langle \mathbf{k}_1, \mathbf{k}_2; \text{in} | S | \mathbf{p}_1, \mathbf{p}_2; \text{in} \rangle, \end{aligned} \quad (234)$$

and  $S = 1 + iT$ . The LSZ formula Eq. (199) tells us that we must compute  $G_4$  in order to obtain  $S_{\text{fi}}$ . Let us work out  $G_4$  in powers of  $\lambda$  using Wick's theorem.

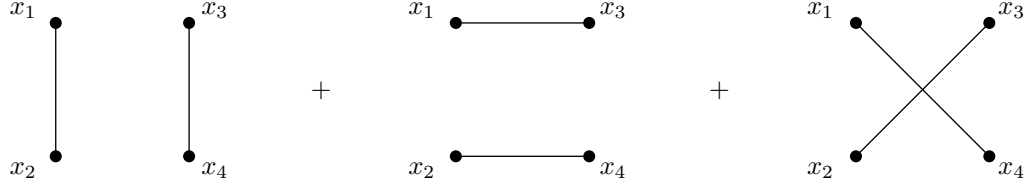
Suppressing the subscripts “in” from now on, the expression we have to evaluate order by order in  $\lambda$  is

$$\begin{aligned} G_4(x_1, \dots, x_4) &= \frac{\sum_{r=0}^{\infty} \left( -\frac{i\lambda}{4!} \right)^r \frac{1}{r!} \left\langle 0 \left| T \left\{ \phi(x_1) \phi(x_2) \phi(x_3) \phi(x_4) \left( \int d^4 y \phi^4(y) \right)^r \right\} \right| 0 \right\rangle}{\sum_{r=0}^{\infty} \left( -\frac{i\lambda}{4!} \right)^r \frac{1}{r!} \left\langle 0 \left| T \left( \int d^4 y \phi^4(y) \right)^r \right| 0 \right\rangle}. \end{aligned} \quad (235)$$

At  $\mathcal{O}(\lambda^0)$ , the denominator is 1, and the numerator gives

$$\begin{aligned} \langle 0 | T \{ \phi(x_1) \phi(x_2) \phi(x_3) \phi(x_4) \} | 0 \rangle &= G_F(x_1 - x_2) G_F(x_3 - x_4) + G_F(x_1 - x_3) G_F(x_2 - x_4) \\ &\quad + G_F(x_1 - x_4) G_F(x_2 - x_3), \end{aligned} \quad (236)$$

where we have used Wick's theorem. We may represent this graphically as follows:

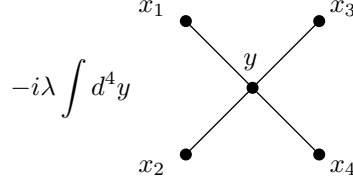


But this is the same answer as if we had set  $\lambda = 0$ , so  $\mathcal{O}(\lambda^0)$  does not describe scattering and hence is not a contribution to the  $T$ -matrix.

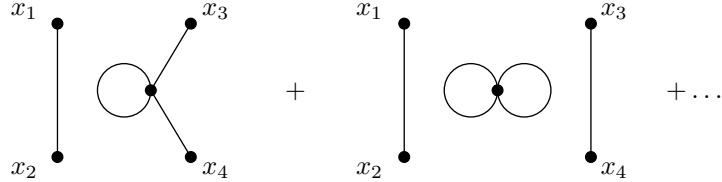
The first non-trivial scattering happens at  $\mathcal{O}(\lambda)$ . For example, the expansion of the above formula includes the contribution (from the numerator)

$$-\frac{i\lambda}{4!} \langle 0 | T[\phi(x_1) \dots \phi(x_4)] \int d^4 y \phi^4(y) | 0 \rangle = -\frac{i\lambda}{4!} \int d^4 y 4! G_F(x_1 - y) G_F(x_2 - y) G_F(x_3 - y) \times G_F(x_4 - y), \quad (237)$$

where the  $4!$  inside the integral arises from all possible contractions in Wick's theorem. This has the graphical representation



where each line corresponds to a propagator, and we have assigned a vertex to each space-time point. Also at this order, we have the graphs



We will see later on that neither of these graphs contributes to the  $S$ -matrix element (after substituting the Green's function into the LSZ formula of eq. (199)), as they are not fully connected. By this we mean that not all external particle vertices are connected to the same graph. At yet higher orders, we may have graphs which involve fully connected pieces, dressed by additional “vacuum bubbles” (such as that which is sitting in the middle of the right-most figure above). These vacuum bubbles are cancelled by the denominator in eq. (212) which, given that it contains no external fields, generates all possible vacuum graphs. The presence of these vacuum graphs explains why the vacuum of the interacting theory is different to that of the free theory, as mentioned earlier.

To summarise, the final answer for the scattering amplitude to  $\mathcal{O}(\lambda)$  is given by Eq. (237).

## 5.4 Graphical representation of the Wick expansion: Feynman rules

We have already encountered the graphical representation of the expansion of Green's functions in perturbation theory after applying Wick's theorem. It is possible to formulate a simple set of rules which allow us to draw the graphs directly without using Wick's theorem and to write down the corresponding algebraic expressions.

We again consider a neutral scalar field whose Lagrangian is

$$\mathcal{L} = \frac{1}{2} \partial_\mu \phi \partial^\mu \phi - \frac{1}{2} m^2 \phi^2 - \frac{\lambda}{4!} \phi^4. \quad (238)$$

Suppose now that we want to compute the  $O(\lambda^m)$  contribution to the  $n$ -point Green's function  $G_n(x_1, \dots, x_n)$ . This is achieved by going through the following steps:

- (1) Draw all distinct diagrams with  $n$  external lines and  $m$  4-fold vertices:
  - Draw  $n$  dots and label them  $x_1, \dots, x_n$  (external points)
  - Draw  $m$  dots and label them  $y_1, \dots, y_m$  (vertices)
  - Join the dots according to the following rules:
    - only one line emanates from each  $x_i$
    - exactly four lines run into each  $y_j$
    - the resulting diagram must be connected, i.e. there must be a continuous path between any two points.
- (2) Assign a factor  $-\frac{i\lambda}{4!} \int d^4 y_i$  to the vertex at  $y_i$
- (3) Assign a factor  $G_F(x_i - y_j)$  to the line joining  $x_i$  and  $y_j$
- (4) Multiply by the number of contractions  $\mathcal{C}$  from the Wick expansion which lead to the same diagram.

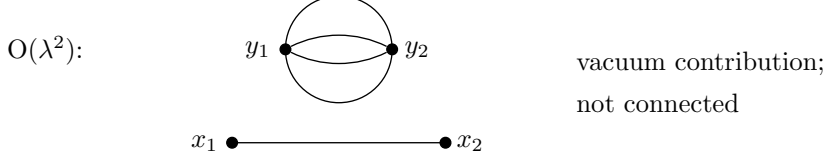
These are the Feynman rules for scalar field theory in position space.

Let us look at an example, namely the 2-point function. According to the Feynman rules the contributions up to order  $\lambda^2$  are as follows:

$$\begin{aligned}
O(1): \quad & x_1 \bullet \text{---} \bullet x_2 = G_F(x_1 - x_2) \\
O(\lambda): \quad & x_1 \bullet \text{---} \bullet y \text{---} \bigcirc \text{---} \bullet y \text{---} \bullet x_2 = \frac{i\lambda}{2} \int d^4 y G_F(x_1 - y) G_F(x_2 - y) G_F(0) \\
O(\lambda^2): \quad & x_1 \bullet \text{---} \bullet y_1 \text{---} \bigcirc \text{---} \bullet y_2 \text{---} \bigcirc \text{---} \bullet y_1 \text{---} \bullet x_2 = -\frac{\lambda^2}{4} \int d^4 y \int d^4 z G_F(x_1 - y) G_F(x_2 - y) \\
& \quad \times G_F^2(y - z) G_F(0) \\
O(\lambda^2): \quad & x_1 \bullet \text{---} \bullet y_1 \text{---} \bigcirc \text{---} \bullet y_2 \text{---} \bullet x_2 \\
& = \mathcal{C} \left( -\frac{i\lambda}{4!} \right)^2 \int d^4 y_1 d^4 y_2 G_F(x_1 - y_1) [G_F(y_1 - y_2)]^3 G_F(y_2 - x_2)
\end{aligned}$$

The combinatorial factor for this contribution is worked out as  $\mathcal{C} = 4 \cdot 4!$ . Note that the same graph, but with the positions of  $y_1$  and  $y_2$  interchanged is topologically distinct. Numerically it has the same value as the above graph, and so the corresponding expression has to be multiplied by a factor 2.

Another contribution at order  $\lambda^2$  is



This contribution must be discarded, since not all of the points are connected via a continuous line.

## 5.5 Feynman rules in momentum space

It is often simpler to work in momentum space, and hence we will discuss the derivation of Feynman rules in this case. This also reflects what is typically done in scattering experiments (i.e. incoming and outgoing particles have definite momentum). If one works in momentum space, the Green's functions are related to those in position space by a Fourier transform

$$\tilde{G}_n(p_1, \dots, p_n) = \int d^4x_1 \dots \int d^4x_n e^{ip_1 \cdot x_1 + \dots + ip_n \cdot x_n} G_n(x_1, \dots, x_n). \quad (239)$$

The Feynman rules then serve to compute the Green's function  $\tilde{G}_n(p_1, \dots, p_n)$  order by order in the coupling.

Let us see how this works for the  $2 \rightarrow 2$  scattering example we considered above. At  $\mathcal{O}(\lambda)$  this was given in eq. (237), which we may simplify slightly to

$$-i\lambda \int d^4y G_F(x_1 - y) G_F(x_2 - y) G_F(x_3 - y) G_F(x_4 - y). \quad (240)$$

We may now substitute in the momentum space form of each propagator (eq. (232)) to give

$$\begin{aligned} & -i\lambda \int d^4y \left( \prod_{i=1}^4 \int \frac{d^4p_i}{(2\pi)^4} \frac{i}{p_i^2 - m^2 + i\epsilon} \right) e^{-i \sum_i p_i \cdot (x_i - y)} \\ & = -i\lambda (2\pi)^4 \delta^4(p_1 + p_2 + p_3 + p_4) \left( \prod_{i=1}^4 \int \frac{d^4p_i}{(2\pi)^4} \frac{i}{p_i^2 - m^2 + i\epsilon} \right) e^{-i \sum_i p_i \cdot x_i}, \end{aligned}$$

where we have carried out the  $y$  integration in the second line. Substituting this into eq. (239) and carrying out the integrals over each  $x_i$ , one finds

$$\begin{aligned} \tilde{G}_4(p_1, \dots, p_n) & = -i\lambda (2\pi)^4 \delta^4(p_1 + p_2 + p_3 + p_4) \left( \prod_i \int \frac{d^4p_i}{(2\pi)^4} \frac{i}{p_i^2 - m^2 + i\epsilon} (2\pi)^4 \delta(p_i) \right) \\ & = -i\lambda (2\pi)^4 \delta^4(p_1 + p_2 + p_3 + p_4) \prod_i \frac{i}{p_i^2 - m^2 + i\epsilon} \end{aligned}$$

We will not repeat the above derivation for a general Green's function. Rather, we now state the Feynman rules in momentum space, and the reader may easily verify that the above example is

a special case.

### Feynman rules (momentum space)

(1) Draw all distinct diagrams with  $n$  external lines and  $m$  4-fold vertices:

- Assign momenta  $p_1, \dots, p_n$  to the external lines
- Assign momenta  $k_j$  to the internal lines

(2) Assign to each external line a factor

$$\frac{i}{p_k^2 - m^2 + i\epsilon}$$

(3) Assign to each internal line a factor

$$\int \frac{d^4 k_j}{(2\pi)^4} \frac{i}{k_j^2 - m^2 + i\epsilon}$$

(4) Each vertex contributes a factor

$$-\frac{i\lambda}{4!}(2\pi)^4 \delta^4 \left( \sum \text{momenta} \right),$$

(the delta function ensures that momentum is conserved at each vertex).

(5) Multiply by the combinatorial factor  $\mathcal{C}$ , which is the number of contractions leading to the same momentum space diagram (note that  $\mathcal{C}$  may be different from the combinatorial factor for the same diagram considered in position space!)

Alternatively, one may rephrase (4) and (5) as follows:

(4\*) Each vertex carries a factor

$$-i\lambda(2\pi)^4 \delta^4 \left( \sum \text{momenta} \right),$$

(5\*) Divide by the *symmetry factor* i.e. the dimension of the group of symmetry transformations that leaves the diagram invariant.

## 5.6 S-matrix and truncated Green's functions

The final topic in these lectures is the derivation of a simple relation between the  $S$ -matrix element and a particular momentum space Green's function, which has its external legs amputated: the so-called truncated Green's function. This further simplifies the calculation of scattering amplitudes using Feynman rules.

Let us return to the LSZ formalism and consider the scattering of  $m$  initial particles (momenta  $\mathbf{p}_1, \dots, \mathbf{p}_m$ ) into  $n$  final particles with momenta  $\mathbf{k}_1, \dots, \mathbf{k}_n$ . The LSZ formula (eq. (199)) tells us that the  $S$ -matrix element is given by

$$\begin{aligned} & \left\langle \mathbf{k}_1, \dots, \mathbf{k}_n; \text{out} \middle| \mathbf{p}_1, \dots, \mathbf{p}_m; \text{in} \right\rangle \\ &= (i)^{n+m} \int \prod_{i=1}^m d^4 x_i \int \prod_{j=1}^n d^4 y_j \exp \left\{ -i \sum_{i=1}^m p_i \cdot x_i + i \sum_{j=1}^n k_j \cdot y_j \right\} \\ & \quad \times \prod_{i=1}^m (\square_{x_i} + m^2) \prod_{j=1}^n (\square_{y_j} + m^2) G_{n+m}(x_1, \dots, x_m, y_1, \dots, y_n). \end{aligned} \quad (241)$$



Let us have a closer look at  $G_{n+m}(x_1, \dots, x_m, y_1, \dots, y_n)$ . As shown in Fig. 6 it can be split into Feynman propagators, which connect the external points to the vertices at  $z_1, \dots, z_{n+m}$ , and a remaining Green's function  $\overline{G}_{n+m}$ , according to

$$G_{n+m} = \int d^4 z_1 \cdots d^4 z_{n+m} G_F(x_1 - z_1) \cdots G_F(y_n - z_{n+m}) \overline{G}_{n+m}(z_1, \dots, z_{n+m}), \quad (242)$$

where, perhaps for obvious reasons,  $\overline{G}_{n+m}$  is called the truncated Green's function.

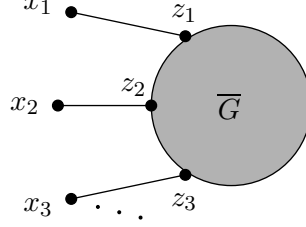


Figure 6: The construction of the truncated Green's function in position space.

Putting Eq. (242) back into the LSZ expression for the  $S$ -matrix element, and using that

$$(\square_{x_i} + m^2) G_F(x_i - z_i) = -i\delta^4(x_i - z_i) \quad (243)$$

one obtains

$$\begin{aligned} & \langle \mathbf{k}_1, \dots, \mathbf{k}_n; \text{out} | \mathbf{p}_1, \dots, \mathbf{p}_m; \text{in} \rangle \\ &= (i)^{n+m} \int \prod_{i=1}^m d^4 x_i \int \prod_{j=1}^n d^4 y_j \exp \left\{ -i \sum_{i=1}^m p_i \cdot x_i + i \sum_{j=1}^n k_j \cdot y_j \right\} \\ & \quad \times (-i)^{n+m} \int d^4 z_1 \cdots d^4 z_{n+m} \delta^4(x_1 - z_1) \cdots \delta^4(y_n - z_{n+m}) \overline{G}_{n+m}(z_1, \dots, z_{n+m}). \end{aligned} \quad (244)$$

After performing all the integrations over the  $z_k$ 's, the final relation becomes

$$\begin{aligned} & \langle \mathbf{k}_1, \dots, \mathbf{k}_n; \text{out} | \mathbf{p}_1, \dots, \mathbf{p}_m; \text{in} \rangle \\ &= \int \prod_{i=1}^m d^4 x_i \prod_{j=1}^n d^4 y_j \exp \left\{ -i \sum_{i=1}^m p_i \cdot x_i + i \sum_{j=1}^n k_j \cdot y_j \right\} \\ & \quad \times \overline{G}_{n+m}(x_1, \dots, x_m, y_1, \dots, y_n) \\ &\equiv \overline{\mathcal{G}}_{n+m}(p_1, \dots, p_m, k_1, \dots, k_n), \end{aligned} \quad (245)$$

where  $\overline{\mathcal{G}}_{n+m}$  is the truncated  $n+m$ -point function in momentum space. This result shows that the scattering matrix element is directly given by the truncated Green's function in momentum space. In other words, calculating the  $S$ -matrix is much the same as calculating the Green's function, but without the free propagators associated with the external legs. Note that this renders zero any graph which is not fully connected - any diagram in which not all external points are connected to the same graph vanishes upon multiplication by the  $(p_i^2 + m^2)$  factors. This is what allowed us to neglect such graphs in the previous section.

## 6 Summary

That completes this introductory look at quantum field theory. Although we did not get as far as some of the more relevant physical applications of QFT, we have looked in detail at what a QFT is, and how the description of scattering amplitudes leads to Feynman diagrams. To recap how we did this:

1. We reviewed the Lagrangian formalism for classical field theory, and also the canonical quantisation approach to quantum mechanics.
2. We constructed the Lagrangian for a relativistic field theory (the free Klein-Gordon field), and applied the techniques of canonical quantisation to this field theory.
3. States in this theory were found to represent particle excitations, such that a particle of momentum  $\mathbf{p}$  was found to be a quantum of excitation in the relevant Fourier mode of the field.
4. We then studied the interacting theory, arguing that at initial and final times (when the interaction dies away) we can work with free fields. These were related by an operator  $S$ , whose matrix elements represented the transition probability to go from a given initial to a given final state.
5. Using the interaction picture for time evolution, we found an expression for the  $S$  matrix in terms of an evolution operator  $U$ , describing how the fields at general time  $t$  deviate from the initial free fields.
6. We also found a formula which related  $S$  matrix elements to  $n$ -particle Green's functions (vacuum expectation values of time-ordered fields). This was the LSZ formula of eq. (199).
7. We related the Green's functions involving Heisenberg fields to those involving the "in" fields at time  $t \rightarrow -\infty$  (eq. (212)).
8. We then found how to compute these Green's functions in perturbation theory, valid when the strength of the interaction is weak. This involved having to calculate vacuum expectation values of time-ordered products, for which we could use Wick's theorem.
9. We developed a graphical representation of Wick's theorem, which led to simple rules (Feynman rules) for the calculation of Green's functions in position or momentum space.
10. These can easily be converted to  $S$  matrix elements by truncating the free propagators associated with the external lines.

Needless to say, there are many things we did not have time to talk about. Some of these will be explored by the other courses at this school:

- Here we calculated  $S$ -matrix elements without explaining how to turn these into decay rates or cross-sections, which are the measurable quantities. This is dealt with in the QED / QCD course.
- The Klein-Gordon field involves particles of spin zero, which are bosons. One may also construct field theories for fermions of spin  $\frac{1}{2}$ , and vector bosons (spin 1). Physical examples include QED and QCD.
- Fields may have internal symmetries (e.g. local gauge invariance). Again, see the QED / QCD and Standard Model courses.
- Diagrams involving loops are divergent, ultimately leading to infinite renormalisation of the couplings and masses. The renormalisation procedure can only be carried out in certain theories. The Standard Model is one example, but other well-known physical theories (e.g. general relativity) fail this criterion.

- There is an alternative formulation of QFT in terms of path integrals (i.e sums over all possible configurations of fields). This alternative formulation involves some extra conceptual overhead, but allows a much more straightforward derivation of the Feynman rules. More than this, the path integral approach makes many aspects of field theory manifest i.e. is central to our understanding of what a quantum field theory is. This will not be covered at all in this school, but the interested student will find many excellent textbooks on the subject.

There are other areas which are not covered at this school, but nonetheless are indicative of the fact that field theory is still very much an active research area, with many exciting new developments:

- Calculating Feynman diagrams at higher orders is itself a highly complicated subject, and there are a variety of interesting mathematical ideas (e.g. from number theory and complex analysis) involved in current research.
- Sometimes perturbation theory is not well-behaved, in that there are large coefficients at each order of the expansion in the coupling constant. Often the physics of these large contributions can be understood, and summed up to all orders in the coupling. This is known as *resummation*, and is crucial to obtaining sensible results for many cross-sections, especially in QCD.
- Here we have “solved” for scattering probabilities using a perturbation expansion. It is sometimes possible to numerically solve the theory fully non-perturbatively. Such approaches are known as lattice field theory, due to the fact that one discretizes space and time into a lattice of points. It is then possible (with enough supercomputing power!) to calculate things like hadron masses, which are completely incalculable in perturbation theory.
- Here we set up QFT in Minkowski (flat space). If one attempts to do the same thing in curved space (i.e. a strong gravitational field), many weird things happen that give us tantalising hints of what a quantum field of gravity should look like.
- There are some very interesting recent correspondences between certain limits of certain string theories, and a particular quantum field theory in the strong coupling limit. This has allowed us to gain new insights into nonperturbative field theory from an analytic point of view, and there have been applications in heavy ion physics and even condensed matter systems.

I could go on of course, and many of the more formal developments of current QFT research are perhaps not so interesting to a student in experimental particle physics. However, at the present time some of the more remarkable and novel extensions to the Standard Model (SUSY, extra dimensions) are not only testable, but are actively being looked for. Thus QFT, despite its age, is very much at the forefront of current research efforts and may yet surprise us!

## Acknowledgments

I am very grateful to Mrinal Dasgupta for providing a previous set of lecture notes, on which these notes are heavily based. Thanks to Mark Thomson for running a succesful school, and also to Jacqui and Gill for all of their help. Thanks to Ian Tomalin for suggesting a set of improvements to these notes, and to the other tutors for feedback at various points. Lastly many thanks to the students of the RAL HEP school 2010, whose numerous difficult and thought-provoking questions, as well as their good humour, made for a highly enjoyable fortnight in Oxford.

## A Books on QFT

There have been numerous texts on Quantum Field Theory over many decades, and a surprisingly high number are appearing all the time. Here I list some notable ones, although I have not read every page of all of them...!

In the following list, [1] is a good introductory text. So is [2], which also features reasonably accessible introductions to topics which are not normally featured in general purpose QFT books (e.g. SUSY, topological aspects). By far one of the best all-round books is [3], which many use as a standard text (it is particularly useful for looking things up in). A very good book for doing explicit calculations, especially in QCD where there is a very good coverage of advanced material (e.g. resummation), is [4]. People say nice things about [5], although I am not so familiar with this book.

For particle physics applications in particular, a very nice two volume set is that of [6]. Also of note (with a very physically motivated and Feynman diagrammatic approach to field theory) is [7], although this is hard to get hold of (an updated version is in preparation).

Finally, those who are not faint of heart and who like their field theory from the horse's mouth may like to consult Weinberg's monumental three volume set [8]!

## References

- [1] F. Mandl and G. Shaw, *Quantum Field Theory*, Wiley 1984.
- [2] L. Ryder, *Quantum Field Theory*, CUP 1985.
- [3] M.E. Peskin and D.V. Schroeder, *An Introduction to Quantum Field Theory*, Addison Wesley 1995
- [4] G. Sterman, *An Introduction to quantum field theory*, CUP 1993.
- [5] C. Itzykson and J.B. Zuber, *Quantum Field Theory*, McGraw-Hill 1987.
- [6] I. Aitchison and A. Hey, *Gauge theories in particle physics: A practical introduction. Vol. 1: From relativistic quantum mechanics to QED; Vol. 2: Non-Abelian gauge theories: QCD and the electroweak theory*, IOP 2004.
- [7] B. de Wit and J. Smith, *Field Theory in Particle Physics*, 1986.
- [8] S. Weinberg, *The Quantum Theory of Fields*, Vol. 1, CUP 1995

## B Notation and conventions

**4-vectors:**

$$\begin{aligned}x^\mu &= (x^0, \mathbf{x}) = (t, \mathbf{x}) \\x_\mu &= g_{\mu\nu} x^\nu = (x^0, -\mathbf{x}) = (t, -\mathbf{x}) \\ \text{Metric tensor: } g_{\mu\nu} &= g^{\mu\nu} = \begin{pmatrix} 1 & 0 & 0 & 0 \\ 0 & -1 & 0 & 0 \\ 0 & 0 & -1 & 0 \\ 0 & 0 & 0 & -1 \end{pmatrix}\end{aligned}$$

**Scalar product:**

$$\begin{aligned}x^\mu x_\mu &= x^0 x_0 + x^1 x_1 + x^2 x_2 + x^3 x_3 \\ &= t^2 - \mathbf{x}^2\end{aligned}$$

**Gradient operators:**

$$\begin{aligned}\partial^\mu &\equiv \frac{\partial}{\partial x_\mu} = \left( \frac{\partial}{\partial t}, -\nabla \right) \\ \partial_\mu &\equiv \frac{\partial}{\partial x^\mu} = \left( \frac{\partial}{\partial t}, \nabla \right) \\ \text{d'Alembertian: } \partial^\mu \partial_\mu &= \frac{\partial^2}{\partial t^2} - \nabla^2 \equiv \square\end{aligned}$$

**Momentum operator:**

$$\hat{p}^\mu = i\hbar \partial^\mu = \left( i\hbar \frac{\partial}{\partial t}, -i\hbar \nabla \right) = (\hat{E}, \hat{\mathbf{p}}) \quad (\text{as it should be})$$

**$\delta$ -functions:**

$$\begin{aligned}\int d^3p f(\mathbf{p}) \delta^3(\mathbf{p} - \mathbf{q}) &= f(\mathbf{q}) \\ \int d^3x e^{-i\mathbf{p}\cdot\mathbf{x}} &= (2\pi)^3 \delta^3(\mathbf{p}) \\ \int \frac{d^3p}{(2\pi)^3} e^{-i\mathbf{p}\cdot\mathbf{x}} &= \delta^3(\mathbf{x})\end{aligned}$$

(similarly in four dimensions)

**Note:**

$$\begin{aligned}\delta(x^2 - x_0^2) &= \delta\{(x - x_0)(x + x_0)\} \\ &= \frac{1}{2x} \{\delta(x - x_0) + \delta(x + x_0)\}\end{aligned}$$



# An Introduction to QED & QCD

**F Hautmann**

Department of Theoretical Physics  
University of Oxford  
Oxford OX1 3NP

Lectures presented at the RAL High Energy Physics Summer School  
Somerville College, Oxford, September 2010





# Contents

<b>1</b>	<b>Relativistic quantum mechanics .....</b>	<b>53</b>
1.1	Relativistic wave equations .....	53
1.2	The Klein-Gordon equation.....	55
1.3	The Dirac equation.....	56
1.4	The Feynman-Stueckelberg picture.....	57
<b>2</b>	<b>Spin.....</b>	<b>59</b>
2.1	Algebra of Lorentz transformations.....	59
2.2	Weyl spinors .....	61
2.3	Dirac spinors.....	61
2.4	Solutions of the Dirac equation.....	64
<b>3</b>	<b>Perturbation theory and S matrix .....</b>	<b>66</b>
3.1	Electromagnetic interaction of spinless charges.....	66
3.2	Electromagnetic interaction of spin-1/2 charges .....	68
3.3	Green's functions .....	69
3.4	From scattering matrix elements to cross sections.....	71
<b>4</b>	<b>Coulomb scattering.....</b>	<b>74</b>
4.1	Nonrelativistic case.....	74
4.2	The $e\mu$ scattering matrix element in QED.....	75
4.3	Fermionic spin sums.....	76
4.4	Elastic $e\mu$ scattering cross section .....	76
4.5	Scattering by an external Coulomb potential .....	78
4.6	Crossing symmetry: $e^+e^- \rightarrow \mu^+\mu^-$ annihilation .....	80
<b>5</b>	<b>Compton scattering.....</b>	<b>82</b>
5.1	Photon polarization sums .....	83
5.2	The $e\gamma$ unpolarized cross section.....	84
5.3	Photon polarization dependence.....	86
<b>6</b>	<b>Strong interactions.....</b>	<b>87</b>
6.1	Basic structure .....	87
6.2	Physical polarization states and ghosts .....	90
6.3	Color algebra .....	92
<b>7</b>	<b>Renormalization.....</b>	<b>94</b>
7.1	General principles.....	94
7.2	The gauge boson self-energy .....	97
7.3	Renormalization of the electromagnetic coupling .....	99
7.4	Vertex correction and anomalous magnetic moment.....	101
<b>8</b>	<b>Renormalization group.....</b>	<b>105</b>
8.1	Renormalization scale dependence and evolution equations .....	105
8.2	RG interpretation of the photon self-energy .....	107
8.3	QCD $\beta$ function at one loop.....	108
<b>8.4</b>	<b>The QCD scale <math>\Lambda</math> .....</b>	<b>111</b>
	<b>Acknowledgments .....</b>	<b>114</b>
	<b>References.....</b>	<b>115</b>

These lectures present a heuristic introduction to gauge theories of electromagnetic and strong interactions, focusing on perturbative applications of the S matrix and the use of Feynman graphs in QED and QCD. They are complementary to the presentations of field theory in the Standard Model and Quantum Field Theory courses at this School. The approach followed in these lectures may be found in the textbooks given in Ref. [1]. Quantum field theory treatments may be found in the textbooks given in Ref. [2]. Secs. 1 and 2 discuss relativistic quantum mechanics and spin. Secs. 3 to 5 are devoted to interactions and scattering processes at tree level in QED. Sec. 6 extends the discussion to QCD. Secs. 7 and 8 consider loops and give an introductory discussion to renormalization.

# 1 Relativistic quantum mechanics

In this section we present the Klein-Gordon equation and the Dirac equation as they arise from attempts to generalize quantum-mechanical wave equations to include relativity. We discuss the difficulties in interpreting these equations as single-particle wave equations, and illustrate that the Feynman-Stueckelberg causality argument points to the resolution of these difficulties by going beyond the single particle interpretation.

## 1.1 Relativistic wave equations

Let us start with the case of nonrelativistic quantum mechanics, and ask how we can generalize it to the relativistic case.

The time evolution of the state  $|\psi\rangle$  of a quantum mechanical system is given by the Schrödinger equation,

$$i \frac{\partial}{\partial t} |\psi\rangle = H |\psi\rangle \quad , \quad (1.1)$$

where  $H$  is the hamiltonian operator corresponding to the total energy.

For a free, spinless, nonrelativistic particle we have

$$H = \frac{\mathbf{p}^2}{2m} \quad , \quad (1.2)$$

where  $\mathbf{p}$  is the momentum operator, and  $m$  is the particle's mass. In the basis of eigenstates of the position operator,  $\mathbf{p}$  is represented by

$$\mathbf{p} = -i \nabla \quad , \quad (1.3)$$

and therefore the evolution equation reads

$$i \frac{\partial}{\partial t} \psi(\mathbf{x}, t) = -\frac{1}{2m} \nabla^2 \psi(\mathbf{x}, t) \quad , \quad (1.4)$$

where  $\psi(\mathbf{x}, t) = \langle \mathbf{x} | \psi \rangle$  is the position-space wave function.

The wave equation (1.4) admits a probabilistic interpretation. By taking the complex conjugate  $\psi^*$  times Eq. (1.4) and subtracting  $\psi$  times the complex conjugate equation, we obtain

$$\frac{\partial \rho}{\partial t} + \nabla \cdot \mathbf{j} = 0 \quad , \quad (1.5)$$

with

$$\rho = \psi^* \psi \quad , \quad \mathbf{j} = -\frac{i}{2m} [\psi^* (\nabla \psi) - (\nabla \psi^*) \psi] \quad . \quad (1.6)$$

Here  $\rho$  and  $\mathbf{j}$  are interpreted as probability density and current, and the continuity equation (1.5) expresses probability conservation.

How could we extend this to the relativistic case? To do this, we need to incorporate the relativistic energy-momentum relation

$$E^2 = \mathbf{p}^2 + m^2 \quad . \quad (1.7)$$

If we naively were to take

$$H = \sqrt{\mathbf{p}^2 + m^2} \quad , \quad (1.8)$$

this would yield the correct energy-momentum relation, but would give as a candidate wave equation

$$i \frac{\partial}{\partial t} \psi = \sqrt{\mathbf{p}^2 + m^2} \psi , \quad (1.9)$$

which contains space derivatives under the square root. This equation has a number of difficulties, because it treats time and space derivatives on a different footing, contrary to what one would expect of a relativistic theory, and because it is non-local in space, as the square root gives rise to an infinite number of spatial derivatives.

One possible way to overcome this is to square the differential operators in Eq. (1.9) before applying them to  $\psi$ . This gives

$$-\frac{\partial^2}{\partial t^2} \psi = (-\nabla^2 + m^2) \psi , \quad (1.10)$$

that is, using covariant notation with  $\partial^\mu = (\partial/\partial t, -\nabla)$ ,  $\partial^2 = \partial^\mu \partial_\mu$ ,

$$(\partial^2 + m^2) \psi = 0 . \quad (1.11)$$

This is the approach originally proposed by Schrödinger, Klein and Gordon, and Eq. (1.11) is referred to as the Klein-Gordon equation. This equation describes relativistic spin-0 particles. We will discuss Klein-Gordon in Subsec. 1.2. As we will see, this equation is a candidate wave equation consistent with relativity, but it runs into problems with quantum mechanics as a single-particle wave equation, because, due to the second-order time derivative, it does not lead to a positive-definite probability density.

A second possible way around the naive Eq. (1.9) is to insist on the equation being first-order in the time derivative but devise a new hamiltonian  $H_d$  which is local, linear in momentum, and such that its square returns the correct relativistic energy-momentum relation (1.7):

$$i \frac{\partial}{\partial t} \psi = H_d \psi . \quad (1.12)$$

This is the approach followed originally by Dirac. It turns out that this route is viable only if the wave function is not one-component but multi-component (which implies spin), and the new hamiltonian is of the form

$$H_d = \boldsymbol{\alpha} \cdot \mathbf{p} + \beta m , \quad (1.13)$$

where  $\alpha$  and  $\beta$  are four matrices, in a space to be determined, obeying the relations

$$\alpha_i \alpha_j + \alpha_j \alpha_i = 2\delta_{ij} , \quad \beta \alpha_i + \alpha_i \beta = 0 , \quad \beta^2 = 1 . \quad (1.14)$$

Eq. (1.12), with  $H_d$  given in Eqs. (1.13),(1.14), is the Dirac equation. This equation describes relativistic spin-1/2 particles. We will discuss it in Subsec. 1.3.

We will see that, unlike the Klein-Gordon equation, the Dirac equation, being first-order, allows one to construct a positive-definite probability density. However, we will see that both the Klein-Gordon equation and the Dirac equation have solutions corresponding to states with negative energies. In Subsec. 1.4 we discuss how this issue can be addressed via the Feynman-Stueckelberg picture of causality. This picture reinterprets negative energy states by introducing the concept of antiparticle, and leads us to think of theories that incorporate quantum mechanics and relativity as theories for which particle number is not conserved.

## 1.2 The Klein-Gordon equation

We have seen in the previous subsection that the Klein-Gordon equation emerges from requiring the relativistic energy-momentum relation and taking the square of the hamiltonian operator in the position-space wave equation. In covariant form, the Klein-Gordon equation is given by

$$(\partial^2 + m^2) \phi(x) = 0 \quad , \quad (1.15)$$

where

$$\partial^2 \equiv \partial^\mu \partial_\mu = \frac{\partial^2}{\partial t^2} - \nabla^2. \quad (1.16)$$

The Klein-Gordon equation is relativistically covariant. That is, if we start with Eq. (1.15) and make a Lorentz transformation,

$$x^\mu \rightarrow x'^\mu = \Lambda^\mu_\nu x^\nu \quad , \quad \Lambda^{\mu\rho} \Lambda^{\nu\sigma} g_{\mu\nu} = g^{\rho\sigma} \quad , \quad (1.17)$$

$$\phi(x) \rightarrow \phi'(x) = \phi(\Lambda^{-1}x) \quad , \quad (1.18)$$

in the primed coordinate system an equation of the same form holds, because

$$\begin{aligned} (\partial^2 + m^2)\phi'(x) &= [(\Lambda^{-1})^\rho_\mu \partial_\rho (\Lambda^{-1})^\sigma_\nu \partial_\sigma g^{\mu\nu} + m^2] \phi(\Lambda^{-1}x) \\ &= (\partial_\rho \partial_\sigma g^{\rho\sigma} + m^2) \phi(\Lambda^{-1}x) = (\partial^2 + m^2) \phi(\Lambda^{-1}x) = 0 \quad . \end{aligned} \quad (1.19)$$

On the other hand, interpreting the Klein-Gordon equation as a single particle relativistic wave equation leads to difficulties with quantum mechanics. As the equation is second-order in the time derivative, the norm of  $\phi$  is not conserved with time. We can see the difficulty by looking for a continuity equation for Klein-Gordon similar to Eq. (1.5) for the nonrelativistic case. Following the same steps as described for Eq. (1.5), we obtain

$$\partial_\mu j^\mu = 0 \quad , \quad j^\mu = (\rho, \mathbf{j}) \quad , \quad (1.20)$$

with

$$\rho = i \left[ \phi^* \frac{\partial \phi}{\partial t} - \frac{\partial \phi^*}{\partial t} \phi \right] \quad , \quad \mathbf{j} = -i [\phi^* (\nabla \phi) - (\nabla \phi^*) \phi] \quad . \quad (1.21)$$

The current  $\mathbf{j}$  is formally similar to that of the nonrelativistic case in Eq. (1.6). The density  $\rho$ , however, is not. Nor could it be, because  $\phi^* \phi$  would transform under Lorentz like a scalar rather than like the time component of a four-vector. Because Eq. (1.15) contains second-order time derivatives, the density  $\rho$  contains terms in  $\partial/\partial t$ , and is not positive definite.

If we look for plane wave solutions of the Klein-Gordon equation,

$$\phi(x) = N e^{-ipx} \quad , \quad (1.22)$$

where  $p^\mu = (E, \mathbf{p})$ , another difficulty arises. By substituting Eq. (1.22) into the equation, we find that Eq. (1.22) is solution if

$$p^2 = m^2 \quad , \quad (1.23)$$

that is,

$$E = \pm \sqrt{\mathbf{p}^2 + m^2} \quad . \quad (1.24)$$

The Klein-Gordon equation contains both positive-energy and negative-energy solutions. Since  $j^\mu$  in Eq. (1.20) is proportional to  $p^\mu$ , negative energy solutions also have negative probability density. We discuss in Subsec. 1.4 how to interpret negative-energy states.

### 1.3 The Dirac equation

We have seen in Eqs. (1.12),(1.13) that the Dirac equation has the form

$$i \frac{\partial}{\partial t} \psi = (-i\boldsymbol{\alpha} \cdot \boldsymbol{\nabla} + \beta m) \psi . \quad (1.25)$$

Consistency with the relativistic energy-momentum relation requires that by squaring Eq. (1.25),

$$-\frac{\partial^2 \psi}{\partial t^2} = [-\alpha^i \alpha^j \nabla^i \nabla^j - i(\beta \alpha^i + \alpha^i \beta) m \nabla^i + \beta^2 m^2] \psi , \quad (1.26)$$

we reobtain the Klein-Gordon equation,

$$-\frac{\partial^2 \psi}{\partial t^2} = [-\nabla^i \nabla^i + m^2] \psi . \quad (1.27)$$

Then  $\alpha^i$  and  $\beta$  must obey anticommutation relations,

$$\alpha^i \alpha^j + \alpha^j \alpha^i = 2\delta^{ij} , \quad \beta \alpha^i + \alpha^i \beta = 0 , \quad \beta^2 = 1 . \quad (1.28)$$

Eq. (1.28) implies that

$$\text{Tr } \alpha^i = \text{Tr } \beta = 0 , \quad (1.29)$$

and that the eigenvalues of  $\alpha^i$  and  $\beta$  are  $\pm 1$ . Then  $\alpha^i$  and  $\beta$  must be even-dimensional matrices. In two dimensions there are no four matrices satisfying Eq. (1.28) (the three Pauli  $\sigma$  matrices would be three candidate matrices but there is no fourth anticommuting  $2 \times 2$  matrix). So the minimum possible dimension is four. Then  $\psi$  in Eq. (1.25) is a four-component object, referred to as a four-component spinor.

A possible choice of  $\alpha^i$  and  $\beta$  is given by

$$\boldsymbol{\alpha} = \begin{pmatrix} 0 & \boldsymbol{\sigma} \\ \boldsymbol{\sigma} & 0 \end{pmatrix}, \quad \beta = \begin{pmatrix} 1 & 0 \\ 0 & -1 \end{pmatrix}, \quad (1.30)$$

where we use block matrix notation.

The Dirac equation can be recast in manifestly covariant form by defining four new matrices  $\gamma$  in terms of the  $\boldsymbol{\alpha}$  and  $\beta$  as

$$\gamma^0 = \beta, \quad \boldsymbol{\gamma} = \beta \boldsymbol{\alpha}, \quad (1.31)$$

and noting that Eq. (1.25), multiplied by  $\beta$ , can be compactly rewritten in terms of the  $\gamma$  matrices as

$$(i\gamma^\mu \partial_\mu - m)\psi = 0 , \quad (1.32)$$

where

$$\gamma^\mu = (\gamma^0, \boldsymbol{\gamma}) . \quad (1.33)$$

In terms of the  $\gamma$  matrices the anticommutation relations (1.28) become

$$\{\gamma^\mu, \gamma^\nu\} \equiv \gamma^\mu \gamma^\nu + \gamma^\nu \gamma^\mu = 2g^{\mu\nu} . \quad (1.34)$$

The representation (1.30) is

$$\boldsymbol{\gamma} = \begin{pmatrix} 0 & \boldsymbol{\sigma} \\ -\boldsymbol{\sigma} & 0 \end{pmatrix}, \quad \gamma^0 = \begin{pmatrix} 1 & 0 \\ 0 & -1 \end{pmatrix}. \quad (1.35)$$

Because the Dirac equation is first-order, it gives rise to a positive-definite density, unlike the Klein-Gordon equation. By manipulations analogous to those seen in the previous sections, we obtain the continuity equation

$$\partial_\mu j^\mu = 0 \quad , \quad j^\mu = (\rho, \mathbf{j}) \quad , \quad (1.36)$$

with

$$\rho = \psi^\dagger \psi, \quad \mathbf{j} = \psi^\dagger \boldsymbol{\alpha} \psi. \quad (1.37)$$

On the other hand, because  $\boldsymbol{\alpha}$  and  $\beta$  are traceless (Eq. (1.29)), the hamiltonian is traceless. Then the eigenvalues must be  $E$ ,  $-E$ . Thus the Dirac equation, like the Klein-Gordon equation, has negative energy solutions.

A first interpretation of negative energy solutions is provided by Dirac's "sea" picture. Dirac postulates the existence of a "sea" of negative energy states (Fig. 1), such that the vacuum has all the negative energy states filled with electrons. The Pauli principle forbids any positive-energy electron from falling into one of the lower states. Although the vacuum state has infinite negative charge and energy, this leads to an acceptable theory based on the fact that all observations only involve differences in energy and charge. When energy is supplied and one of the negative energy electrons is promoted to a positive energy one, an electron-hole pair is created, i.e. a positive energy electron and a hole in the negative energy sea. The hole, i.e. the absence of a negative-energy electron, is seen as the presence of a positive-energy and positive-charge state, the positron.

This picture led Dirac to postulate (1927) the existence of the positron as the electron's antiparticle, which was discovered experimentally five years later.

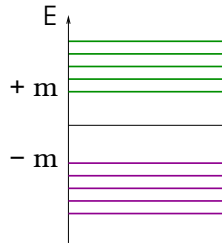


Figure 1: *Dirac sea picture of negative energy states.*

But Dirac's sea picture does not work for bosons, which have no exclusion principle. A second, more general interpretation of negative-energy states is given by Feynman's picture, which we describe in the next subsection.

## 1.4 The Feynman-Stueckelberg picture

The Feynman-Stueckelberg interpretation of negative-energy states does not appeal to the exclusion principle but rather to a causality principle. It is based on the observation that causality ensures that positive energy states, with time dependence  $e^{-iEt}$ , propagate forwards in time, and that if we impose that negative energy states propagate only backwards in time, with

$$e^{-i(-|E|)(-|t|)} \rightarrow e^{-i|E||t|} \quad , \quad (1.38)$$

we still obtain an acceptable theory, consistent with causality. In this picture the emission of a negative energy particle with momentum  $p^\mu$  is interpreted as the absorption of a positive energy antiparticle with momentum  $-p^\mu$ .

Consider for example photon-particle scattering (Fig. 2). In Fig. 2(a) a particle comes in with energy  $E_1$ , and at time  $t_1$  and point  $x_1$  it emits a photon with energy  $E_\gamma < E_1$ . It travels on forwards in time, and at time  $t_2$  and point  $x_2$  it absorbs the initial state photon, giving rise to the photon-particle final state.

Another process is shown in Fig. 2(b). In this process the particle coming in with energy  $E_1$  emits a photon with energy  $E_\gamma > E_1$ , and is thus forced to travel backwards in time. Then at an earlier time it absorbs the initial state photon at the point  $x_2$ , which renders its energy positive again.

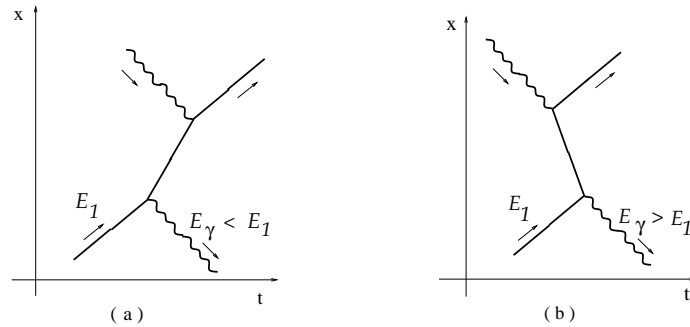


Figure 2: *Feynman interpretation of positive-energy and negative-energy states in terms of particle and antiparticle propagation.*

The process in Fig. 2(b) can be described by saying that in the initial state we have a particle and a photon, and that at point  $x_2$  the photon creates a particle-antiparticle pair, both of which propagate forwards in time. The particle ends up in the final state, whereas the antiparticle is annihilated at a later time by the initial state particle, thereby producing the final state photon. According to this picture, the negative energy state moving backwards in time is viewed as a negatively charged state with positive energy moving forwards in time.



## 2 Spin

In the previous section we have introduced Dirac spinors, which we will use to describe spin-1/2 relativistic charges. In this section we further the study of spin in the context of Dirac theory.

We start from the algebraic description of the group of Lorentz transformations and associated representations, which parallels the treatment of the group of rotations and its representations in quantum mechanics. We describe how Dirac spinors emerge from this point of view, and we discuss solutions of the Dirac equations.

### 2.1 Algebra of Lorentz transformations

Let us start with the group of rotations in three dimensions. In quantum mechanics, given a particle with spin  $s$ , the matrices that rotate its  $n$ -component wave function, where  $n = 2s + 1$ , are constructed from the angular momentum operators  $J_i$ ,  $i = 1, 2, 3$ . These satisfy the commutation relations

$$[J_i, J_j] = i\varepsilon_{ijk}J_k . \quad (2.1)$$

Rotation operators are obtained by exponentiation as

$$R = e^{-i\theta_i J_i} , \quad (2.2)$$

where the parameters  $\theta_i$  specify the rotation axis and angle. The angular momentum operators  $J_i$  are the generators of the rotation group, and have matrix representations for every dimensionality  $n$ . The representation for  $n = 2$ , corresponding to spin  $s = 1/2$ , is given by

$$J_i \rightarrow \frac{1}{2} \sigma_i , \quad (2.3)$$

where  $\sigma_i$  are the three Pauli matrices, so that

$$R_{1/2} = e^{-i\theta_i \sigma_i / 2} . \quad (2.4)$$

We can generalize this from the group of rotations to the group of Lorentz transformations. One way to obtain the commutation relations of the Lorentz generators is as follows. In the case of the rotation group, the relations (2.1) can be obtained by taking

$$\mathbf{J} = \mathbf{x} \wedge \mathbf{p} = -i\mathbf{x} \wedge \nabla , \quad (2.5)$$

and evaluating the commutators. The components of angular momentum in Eq. (2.5) can also be rewritten explicitly, using antisymmetric tensor notation, as

$$J^{ij} = -i(x^i \nabla^j - x^j \nabla^i) . \quad (2.6)$$

The generalization of this formula to the four-dimensional case,

$$L^{\mu\nu} = i(x^\mu \partial^\nu - x^\nu \partial^\mu) , \quad (2.7)$$

gives the correct generators of Lorentz transformations. As it is antisymmetric in  $\mu$  and  $\nu$ , Eq. (2.7) contains six operators, the three generators of rotations and three

generators of boosts. The commutation relations can be obtained by evaluating directly the commutators of the operators (2.7), and the result is

$$\begin{aligned}[L_{\mu\nu}, L_{\rho\sigma}] &= i(g_{\mu\sigma}L_{\nu\rho} - g_{\nu\sigma}L_{\mu\rho} - g_{\mu\rho}L_{\nu\sigma} + g_{\nu\rho}L_{\mu\sigma}) \\ &= i(g_{\mu\sigma}L_{\nu\rho} - \{\mu \leftrightarrow \nu\}) - \{\rho \leftrightarrow \sigma\} .\end{aligned}\quad (2.8)$$

Given the six operators in Eq. (2.7), it is helpful to distinguish the three operators

$$J_i = \frac{1}{2}\varepsilon_{ijk}L_{jk} \quad (2.9)$$

and the three operators

$$K_i = L_{0i} . \quad (2.10)$$

From Eq. (2.8) we get

$$[J_i, J_j] = i\varepsilon_{ijk}J_k , \quad (2.11)$$

that is, the three operators in Eq. (2.9) are the generators of rotations. The three remaining operators in Eq. (2.10) are the generators of boosts. From Eq. (2.8) we have

$$[J_i, K_j] = i\varepsilon_{ijk}K_k , \quad (2.12)$$

$$[K_i, K_j] = -i\varepsilon_{ijk}J_k . \quad (2.13)$$

The  $J$  and  $K$  operators in Eqs. (2.9),(2.10) have the clear physical interpretation of rotation and boost generators, but they are mixed by the algebra of commutation relations (2.8), as shown in Eqs. (2.12),(2.13). It is useful to disentangle the algebra by introducing the linear combinations of generators

$$A_i = \frac{1}{2}(J_i + iK_i) , \quad B_i = \frac{1}{2}(J_i - iK_i) . \quad (2.14)$$

By computing the commutators of the  $A$  and  $B$  operators in Eq. (2.14), we find

$$[A_i, A_j] = i\varepsilon_{ijk}A_k , \quad [B_i, B_j] = i\varepsilon_{ijk}B_k , \quad [A_i, B_j] = 0 . \quad (2.15)$$

That is, the  $A$  and the  $B$  operators do not mix, and each set obeys commutation relations of the form (2.1). This means that we can specify a representation of the group of Lorentz transformations by specifying a pair of rotation-group representations,

$$(a, b) , \quad \text{where} \quad A_i A_i = a(a+1) , \quad B_i B_i = b(b+1) , \quad (2.16)$$

with  $a$  and  $b$  integer or half-integer. Here  $a+b$  gives the spin quantum number: so the representation  $(0, 0)$  is spin-0 (scalar);  $(1/2, 1/2)$  is spin-1 (vector);  $(1/2, 0)$  and  $(0, 1/2)$  are spin-1/2. The latter are referred to as Weyl spinors (respectively, left-handed and right-handed). A Dirac spinor is obtained from two Weyl spinors,  $(1/2, 0) \oplus (0, 1/2)$ .

Dirac spinors are thus identified by a representation of the group of Lorentz transformations reducible to the sum of two representations (2.16),  $(1/2, 0)$  and  $(0, 1/2)$ .

We discuss Weyl and Dirac spinors in the next two subsections.

## 2.2 Weyl spinors

A left-handed Weyl spinor is defined by taking  $a = 1/2, b = 0$  in Eq. (2.16). We thus have

$$A^i = \frac{1}{2} \sigma^i, \quad B^i = 0. \quad (2.17)$$

Using Eq. (2.14), the representation of the rotation and boost generators is given by

$$J^i = \frac{1}{2} \sigma^i \quad (\text{rotation generators}), \quad K^i = -i \frac{1}{2} \sigma^i \quad (\text{boost generators}). \quad (2.18)$$

So a left-handed Weyl spinor is a two-component spinor,

$$\xi_L = \begin{pmatrix} \xi_L^1 \\ \xi_L^2 \end{pmatrix}, \quad (2.19)$$

which transforms under rotations and boosts as

$$\xi_L \rightarrow e^{-i\theta^k \sigma^k/2 - \eta^k \sigma^k/2} \xi_L. \quad (2.20)$$

A right-handed Weyl spinor is defined by taking  $a = 0, b = 1/2$  in Eq. (2.16). Then

$$A^i = 0, \quad B^i = \frac{1}{2} \sigma^i, \quad (2.21)$$

i.e.,

$$J^i = \frac{1}{2} \sigma^i \quad (\text{rotation generators}), \quad K^i = i \frac{1}{2} \sigma^i \quad (\text{boost generators}). \quad (2.22)$$

So a right-handed Weyl spinor is a two-component spinor,

$$\xi_R = \begin{pmatrix} \xi_R^1 \\ \xi_R^2 \end{pmatrix}, \quad (2.23)$$

which transforms under rotations and boosts as

$$\xi_R \rightarrow e^{-i\theta^k \sigma^k/2 + \eta^k \sigma^k/2} \xi_R. \quad (2.24)$$

Eq. (2.20) and Eq. (2.24) differ by the sign in the boost transformation.

## 2.3 Dirac spinors

A Dirac spinor is a four-component spinor built out of two Weyl spinors as

$$\psi = \begin{pmatrix} \xi_L \\ \xi_R \end{pmatrix}. \quad (2.25)$$

We can construct explicitly its Lorentz transformation matrix  $S$

$$\psi \rightarrow \psi' = S\psi \quad (2.26)$$

from those for the Weyl spinors in Sec. 2.2. We obtain

$$\psi \rightarrow \psi' = e^{-i\omega_{\mu\nu}\Sigma^{\mu\nu}}\psi \equiv S\psi , \quad (2.27)$$

where

$$\Sigma^{\mu\nu} \equiv \frac{i}{4} [\gamma^\mu, \gamma^\nu] \quad (2.28)$$

with the  $\gamma$  matrix representation

$$\gamma = \begin{pmatrix} 0 & \boldsymbol{\sigma} \\ -\boldsymbol{\sigma} & 0 \end{pmatrix}, \quad \gamma^0 = \begin{pmatrix} 0 & 1 \\ 1 & 0 \end{pmatrix}. \quad (2.29)$$

Thus the generators of boosts for Dirac spinors are

$$\Sigma^{0i} = \frac{i}{4} [\gamma^0, \gamma^i] = -\frac{i}{2} \begin{pmatrix} \sigma^i & 0 \\ 0 & -\sigma^i \end{pmatrix} \quad (\text{boost generators}), \quad (2.30)$$

and the generators of rotations are

$$\Sigma^{ij} = \frac{i}{4} [\gamma^i, \gamma^j] = \frac{1}{2} \varepsilon_{ijk} \begin{pmatrix} \sigma^k & 0 \\ 0 & \sigma^k \end{pmatrix} \quad (\text{rotation generators}). \quad (2.31)$$

An alternative method, equivalent to that given above, for constructing Dirac spinors is based on observing that if 4  $n \times n$  matrices  $\gamma^\mu$  satisfy

$$\{\gamma^\mu, \gamma^\nu\} \equiv \gamma^\mu \gamma^\nu + \gamma^\nu \gamma^\mu = 2g^{\mu\nu} , \quad (2.32)$$

then

$$\Sigma^{\mu\nu} \equiv \frac{i}{4} [\gamma^\mu, \gamma^\nu] \quad (2.33)$$

obey the Lorentz algebra (2.8). Then, by a reasoning similar to that followed in Sec. 1.3, one sees that  $n$  must be 4. By this method one arrives at Dirac spinors without going through the construction from two Weyl spinors.

Note the following two properties of the Lorentz transformation matrix  $S$  for Dirac spinors, which follow from Eqs. (2.27),(2.28). The first is that

$$S^{-1}\gamma^\mu S = \Lambda^{\mu\nu}\gamma_\nu . \quad (2.34)$$

This relation implies that the Dirac equation Eq. (1.32),

$$(i\gamma^\mu \partial_\mu - m)\psi = 0 , \quad (2.35)$$

is relativistically covariant, because under a Lorentz transformation we have

$$\begin{aligned} (i\gamma^\mu \partial_\mu - m)\psi(x) &\rightarrow [i\gamma^\mu (\Lambda^{-1})^\rho_\mu \partial_\rho - m] S\psi(\Lambda^{-1}x) \\ &= S(i\gamma^\nu \partial_\nu - m)\psi(\Lambda^{-1}x) = 0 . \end{aligned} \quad (2.36)$$

The second property is that, because boost generators (2.30) are not hermitian,  $S$  is not unitary; rather, it satisfies

$$S^\dagger = \gamma^0 S^{-1} \gamma^0 . \quad (2.37)$$

For this reason the product  $\psi^\dagger\psi$  is not Lorentz invariant. It is thus useful to define the adjoint spinor

$$\bar{\psi} \equiv \psi^\dagger \gamma^0 . \quad (2.38)$$

Using Eq. (2.37), we see that the product  $\bar{\psi}\psi$  is Lorentz invariant.

We have seen the transformation law of Dirac spinors under rotations and boosts. Lorentz transformations also include discrete transformations, space parity and time reversal. The transformation law of Dirac spinors under these are

$$P\psi(\mathbf{x}, t)P^{-1} = \eta\gamma^0\psi(-\mathbf{x}, t) , \quad P\bar{\psi}(\mathbf{x}, t)P^{-1} = \eta^*\bar{\psi}(-\mathbf{x}, t)\gamma^0 , \quad (2.39)$$

where  $\eta$  is a phase factor to be fixed, and

$$T\psi(\mathbf{x}, t)T^{-1} = -\gamma^1\gamma^3\psi(\mathbf{x}, -t) , \quad T\bar{\psi}(\mathbf{x}, t)T^{-1} = \bar{\psi}(\mathbf{x}, -t)\gamma^1\gamma^3 . \quad (2.40)$$

A third discrete symmetry is charge conjugation, exchanging particle and antiparticle,

$$C\psi C^{-1} = -i\gamma^2\psi^* , \quad C\bar{\psi} C^{-1} = -i\psi^T\gamma^2\gamma^0 . \quad (2.41)$$

Finally, it is useful to introduce a fifth  $\gamma$  matrix

$$\gamma^5 \equiv i\gamma^0\gamma^1\gamma^2\gamma^3 , \quad (2.42)$$

obeying

$$(\gamma^5)^2 = 1 , \quad \{\gamma^5, \gamma^\mu\} = 0 , \quad (\gamma^5)^\dagger = \gamma^5 . \quad (2.43)$$

Then define the projection operators

$$P_L = \frac{1 - \gamma^5}{2} , \quad P_R = \frac{1 + \gamma^5}{2} . \quad (2.44)$$

In the representation (2.29) we have

$$\gamma^5 = \begin{pmatrix} -1 & 0 \\ 0 & 1 \end{pmatrix} \implies P_L = \begin{pmatrix} 1 & 0 \\ 0 & 0 \end{pmatrix} , \quad P_R = \begin{pmatrix} 0 & 0 \\ 0 & 1 \end{pmatrix} . \quad (2.45)$$

Thus

$$\psi_L \equiv P_L\psi = \frac{1 - \gamma^5}{2} \begin{pmatrix} \xi_L \\ \xi_R \end{pmatrix} = \begin{pmatrix} \xi_L \\ 0 \end{pmatrix} , \quad \psi_R \equiv P_R\psi = \frac{1 + \gamma^5}{2} \begin{pmatrix} \xi_L \\ \xi_R \end{pmatrix} = \begin{pmatrix} 0 \\ \xi_R \end{pmatrix} . \quad (2.46)$$

Note that, because  $\gamma^5$  anticommutes with  $\gamma^0$ , for the adjoint we have

$$\bar{\psi}_L = \psi_L^\dagger \gamma^0 = \psi^\dagger P_L \gamma^0 = \psi^\dagger \gamma^0 P_R = \bar{\psi} P_R , \quad (2.47)$$

and similarly

$$\bar{\psi}_R = \bar{\psi} P_L . \quad (2.48)$$

By including  $\gamma^5$ , it is possible to see that any combination of the form

$$\bar{\psi}\Gamma\psi , \quad (2.49)$$

where  $\Gamma$  is any  $4 \times 4$  matrix, can be decomposed into terms with definite transformation properties under Lorentz, because a basis for  $4 \times 4$  matrices is given by the sixteen, linearly independent matrices

$$\mathbf{1} , \quad \gamma^5 , \quad \gamma^\mu , \quad \gamma^\mu\gamma^5 , \quad \Sigma^{\mu\nu} , \quad (2.50)$$

transforming respectively like scalar, pseudoscalar, vector, pseudovector and tensor.

## 2.4 Solutions of the Dirac equation

We can use Dirac spinors to write plane wave solutions of the Dirac equation. Consider

$$\psi(x) = \begin{pmatrix} \chi(\mathbf{p}) \\ \phi(\mathbf{p}) \end{pmatrix} e^{-ipx} , \quad (2.51)$$

where  $p^\mu = (E, \mathbf{p})$ , and  $\chi$  and  $\phi$  are two-components spinors. Substituting (2.51) into the Dirac equation (2.35) and using the representation (1.35) yields the coupled equations for  $\chi$  and  $\phi$

$$E \begin{pmatrix} \chi \\ \phi \end{pmatrix} = \begin{pmatrix} m & \boldsymbol{\sigma} \cdot \mathbf{p} \\ \boldsymbol{\sigma} \cdot \mathbf{p} & -m \end{pmatrix} \begin{pmatrix} \chi \\ \phi \end{pmatrix} , \quad (2.52)$$

that is,

$$\begin{aligned} \boldsymbol{\sigma} \cdot \mathbf{p} \phi &= (E - m) \chi \\ \boldsymbol{\sigma} \cdot \mathbf{p} \chi &= (E + m) \phi . \end{aligned} \quad (2.53)$$

These have solutions for positive and negative energies,  $E = \pm\sqrt{\mathbf{p}^2 + m^2}$ . We can write the solution for positive energies as

$$\psi_+(x) = \mathcal{N} \begin{pmatrix} \chi_r \\ \frac{\boldsymbol{\sigma} \cdot \mathbf{p}}{E+m} \chi_r \end{pmatrix} e^{-ipx} \equiv u_r(\mathbf{p}) e^{-ipx} , \quad (2.54)$$

where  $\mathcal{N} = \sqrt{E + m}$ , and the spinors  $\chi_r$  for  $r = 1, 2$  are given by

$$\chi_1 = \begin{pmatrix} 1 \\ 0 \end{pmatrix} , \quad \chi_2 = \begin{pmatrix} 0 \\ 1 \end{pmatrix} . \quad (2.55)$$

For negative energies, it is convenient to make the transformation  $p^\mu \rightarrow -p^\mu$ , so that we write the corresponding solution as

$$\psi_-(x) = \mathcal{N} \begin{pmatrix} \frac{\boldsymbol{\sigma} \cdot \mathbf{p}}{E+m} \chi_r \\ \chi_r \end{pmatrix} e^{ipx} \equiv v_r(\mathbf{p}) e^{ipx} . \quad (2.56)$$

The spinors  $u$  and  $v$  defined by Eqs. (2.54), (2.56) correspond respectively to particle and antiparticle solutions. Taking the solutions in the rest frame  $\mathbf{p} = 0$ , the top two components of  $\psi$  describe electrons with spin up and spin down, while the bottom two components describe positrons with spin up and spin down. This provides a clear physical interpretation to the four components of Dirac spinors. For arbitrary  $\mathbf{p}$ , we can study the spin content of the solutions by using the explicit expression of the spin operator

$$\mathbf{S} = \frac{1}{2} \boldsymbol{\Sigma} = \frac{1}{2} \begin{pmatrix} \boldsymbol{\sigma} & 0 \\ 0 & \boldsymbol{\sigma} \end{pmatrix} , \quad (2.57)$$

corresponding to spin 1/2,

$$\mathbf{S}^2 = \frac{1}{4} \boldsymbol{\Sigma}^2 = \frac{1}{4} \begin{pmatrix} \boldsymbol{\sigma} \cdot \boldsymbol{\sigma} & 0 \\ 0 & \boldsymbol{\sigma} \cdot \boldsymbol{\sigma} \end{pmatrix} = \frac{3}{4} \mathbf{1} , \quad (2.58)$$

and helicity operator

$$h = \frac{\mathbf{S} \cdot \mathbf{p}}{|\mathbf{p}|} = \frac{1}{2} \begin{pmatrix} \boldsymbol{\sigma} \cdot \hat{\mathbf{p}} & 0 \\ 0 & \boldsymbol{\sigma} \cdot \hat{\mathbf{p}} \end{pmatrix} . \quad (2.59)$$

The  $u$  and  $v$  spinors satisfy the Dirac equation in momentum space,

$$(\not{p} - m)u = 0 \quad , \quad (\not{p} + m)v = 0 \quad , \quad (2.60)$$

and obey orthonormality and completeness relations. The orthonormality relations are given by

$$u_r^\dagger(\mathbf{p})u_s(\mathbf{p}) = v_r^\dagger(\mathbf{p})v_s(\mathbf{p}) = 2E\delta^{rs} \quad , \quad (2.61)$$

$$u_r^\dagger(\mathbf{p})v_s(-\mathbf{p}) = v_r^\dagger(\mathbf{p})u_s(-\mathbf{p}) = 0 \quad . \quad (2.62)$$

Equivalently, in terms of the adjoint spinors  $\bar{u} = u^\dagger\gamma^0$  and  $\bar{v} = v^\dagger\gamma^0$ ,

$$\bar{u}_r(\mathbf{p})u_s(\mathbf{p}) = -\bar{v}_r(\mathbf{p})v_s(\mathbf{p}) = 2m\delta^{rs} \quad , \quad (2.63)$$

$$\bar{u}_r(\mathbf{p})v_s(\mathbf{p}) = -\bar{v}_r(\mathbf{p})u_s(\mathbf{p}) = 0 \quad , \quad (2.64)$$

The completeness relations are given by

$$\sum_{r=1}^2 u_r(\mathbf{p})\bar{u}_r(\mathbf{p}) = (\not{p} + m) \quad , \quad (2.65)$$

$$\sum_{r=1}^2 v_r(\mathbf{p})\bar{v}_r(\mathbf{p}) = (\not{p} - m) \quad . \quad (2.66)$$

### 3 Perturbation theory and S matrix

We now consider the coupling of the Klein-Gordon and the Dirac equation to electromagnetism, and study scattering processes (Fig. 3) in quantum electrodynamics, applying time-dependent perturbation theory.

We will express physical cross sections in terms of invariant scattering matrix elements. The application of perturbation theory can be encoded in the Feynman rules for the calculation of the S matrix elements.

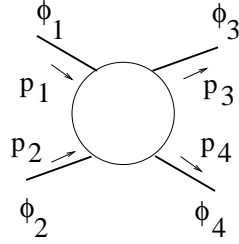


Figure 3: *The scattering process  $\phi_1 + \phi_2 \rightarrow \phi_3 + \phi_4$ .*

#### 3.1 Electromagnetic interaction of spinless charges

We consider a relativistic, spinless system described by the Klein-Gordon equation, Eq. (1.15), and we couple it to electromagnetism via the replacement

$$\partial_\mu \rightarrow \partial_\mu + ieA_\mu \quad . \quad (3.1)$$

By including the electromagnetic interaction (3.1) into Eq. (1.15), the equation of motion of the system can be written

$$(\partial^\mu \partial_\mu + m^2)\phi = -ie(\partial_\mu A^\mu + A_\mu \partial^\mu)\phi + e^2 A^2 \phi \equiv -\mathcal{V}\phi \quad , \quad (3.2)$$

where in the right hand side we identify the potential

$$\mathcal{V} = V_1 + V_2 \quad , \quad (3.3)$$

$$V_1 = ie(\partial_\mu A^\mu + A^\mu \partial_\mu) \quad , \quad (3.4)$$

$$V_2 = -e^2 A^2 \quad . \quad (3.5)$$

Let us apply first-order time-dependent perturbation theory to the transition amplitude  $\mathcal{A}$  due to the interaction given by  $\mathcal{V}$ ,

$$\mathcal{A} = -i \int d^3x \, dt \, \phi_f^* \mathcal{V} \phi_i \quad . \quad (3.6)$$

We will derive the result for the term  $V_1$  of the potential. The contribution of  $V_2$  can be treated analogously, and we will include the result later.



By inserting the potential (3.4) into Eq. (3.6) and doing an integration by parts, we can recast the transition amplitude in the form of a  $j \cdot A$  interaction,

$$\mathcal{A} = -i \int d^4x j_\mu A^\mu , \quad (3.7)$$

where the interaction current is given by

$$j_\mu = ie[\phi_3^* [\partial_\mu \phi_1] - (\partial_\mu \phi_3^*) \phi_1] . \quad (3.8)$$

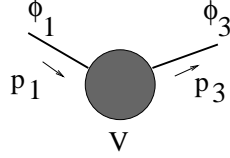


Figure 4: *The  $\phi_1 \rightarrow \phi_3$  transition subprocess by  $\mathcal{V}$  interaction.*

We take the initial and final states  $\phi_1$  and  $\phi_3$  to be given by plane waves (Fig. 4)

$$\phi_1 = N_1 e^{-ip_1 x} , \quad \phi_3 = N_3 e^{-ip_3 x} , \quad (3.9)$$

normalized in a box of volume  $V$  so that

$$N_1 = 1/\sqrt{2E_1 V}, \quad N_3 = 1/\sqrt{2E_3 V} . \quad (3.10)$$

Inserting Eqs. (3.4),(3.9) into Eq. (3.6) we obtain

$$\begin{aligned} \mathcal{A} &= -iN_1 N_3 \int d^4x e^{ip_3 x} (ie)(\partial_\mu A^\mu + A^\mu \partial_\mu) e^{-ip_1 x} \\ &= -ieN_1 N_3 (p_1 + p_3)_\mu \int d^4x e^{-iqx} A^\mu , \end{aligned} \quad (3.11)$$

where  $q = p_1 - p_3$ , and we have done an integration by parts in the second line.

Let us now determine the electromagnetic potential  $A^\mu$  in Eq. (3.11) which results from the transition  $\phi_2 \rightarrow \phi_4$ . Let us use the Lorentz gauge-fixing condition,

$$\partial^\nu A_\nu = 0 . \quad (3.12)$$

Then the equation of motion for the electromagnetic potential is given by

$$\partial^2 A^\mu = J^\mu , \quad (3.13)$$

where the current  $J^\mu$  is of the form (3.8), with the replacements  $1 \rightarrow 2, 3 \rightarrow 4$ . The states  $\phi_2$  and  $\phi_4$  are also represented by plane waves, analogously to Eqs. (3.9),(3.10). By Fourier-transforming Eq. (3.13) with respect to  $x$ , we get

$$-q^2 \tilde{A}^\mu = \tilde{J}^\mu , \quad (3.14)$$

where

$$\tilde{A}^\mu = \int d^4x e^{-iqx} A^\mu , \quad \tilde{J}^\mu = \int d^4x e^{-iqx} J^\mu . \quad (3.15)$$

That is,

$$\tilde{A}^\mu = \frac{-g^{\mu\nu}}{q^2} \tilde{J}_\nu . \quad (3.16)$$

By substituting the explicit expression of the current  $J$  and inserting the result (3.16) into Eq. (3.11), we obtain

$$\mathcal{A} = ie^2 N_1 N_3 N_2 N_4 (p_1 + p_3)_\mu (p_2 + p_4)^\mu \frac{1}{q^2} \int d^4x e^{i(p_3-p_1)x} e^{i(p_4-p_2)x} . \quad (3.17)$$


Performing the integral in  $d^4x$  in Eq. (3.17) gives  $(2\pi)^4 \delta^4(p_3+p_4-p_1-p_2)$ , which expresses four-momentum conservation in the scattering process (Fig. 3). By inserting this result and the explicit expressions of the normalization factors, we can rewrite Eq. (3.17) as

$$\mathcal{A} = (2\pi)^4 \delta^4(P_f - P_i) \frac{1}{\prod_f \sqrt{2E_f V}} \frac{1}{\prod_i \sqrt{2E_i V}} \mathcal{M}_{fi} , \quad (3.18)$$

where the products over  $i$  and  $f$  run respectively over initial and final state particles,  $P_i$  and  $P_f$  denote the total four-momentum in the initial and final state, and we have defined the scattering matrix element

$$\mathcal{M}_{fi} = -e (p_1 + p_3)_\mu \frac{-i g^{\mu\nu}}{q^2} e (p_2 + p_4)_\nu . \quad (3.19)$$

We will interpret Eq. (3.19) as resulting from associating a factor  $ie(p_1 + p_3)_\mu$  to the



$$ie (p + p')^\mu$$



$$2ie^2 g^{\mu\nu}$$

Figure 5: *Feynman rules for interaction vertices of spin-0 particles with photons.*

transition vertex in Fig. 4, an analogous factor  $ie(p_2 + p_4)_\mu$  to the  $\phi_2 \rightarrow \phi_4$  transition vertex, and the factor  $-ig^{\mu\nu}/q^2$  to the electromagnetic interaction. This gives the Feynman rules in the top row in Fig. 5 and in the top row in Fig. 8 (more comment on this in Sec. 3.3). An analogous treatment of the potential term in Eq. (3.5) gives the Feynman rule in the bottom row in Fig. 5.

### 3.2 Electromagnetic interaction of spin-1/2 charges

The case of spin 1/2 can be treated by an analysis analogous to that of the previous subsection. In this case, by including the electromagnetic interaction (3.1) into the Dirac equation (1.32),

$$(i\partial - e\mathcal{A} - m)\psi = 0 , \quad (3.20)$$

we arrive at the interaction potential

$$\mathcal{V} = -e\gamma^0\gamma^\mu A_\mu . \quad (3.21)$$

Then first-order perturbation theory gives

$$\begin{aligned} \mathcal{A} &= -i \int d^3x dt \psi_f^* \mathcal{V} \psi_i \\ &= ie \int d^4x \bar{\psi}_f \gamma^\mu \psi_i A_\mu , \end{aligned} \quad (3.22)$$

that is, a  $j \cdot A$  interaction,

$$\mathcal{A} = -i \int d^4x j^\mu A_\mu , \quad (3.23)$$

with the current given by

$$j^\mu = -e\bar{\psi}_f \gamma^\mu \psi_i . \quad (3.24)$$

Now we represent initial and final states by plane-wave solutions

$$\psi_k = N_k u(p_k) e^{-ip_k x} , \quad N_k = 1/\sqrt{2E_k V}, \quad k = 1, 2, 3, 4 . \quad (3.25)$$

By following the same steps as in the scalar case, we arrive at

$$\mathcal{A} = (2\pi)^4 \delta^4(P_f - P_i) \prod_f \left[ \frac{1}{\sqrt{2E_f V}} \right] \prod_i \left[ \frac{1}{\sqrt{2E_i V}} \right] \mathcal{M}_{fi} , \quad (3.26)$$

where now the scattering matrix element is given by

$$\mathcal{M}_{fi} = -e \bar{u}(p_3) \gamma_\mu u(p_1) \frac{-i g^{\mu\nu}}{q^2} e \bar{u}(p_4) \gamma_\nu u(p_2) . \quad (3.27)$$

The corresponding Feynman rule for the spin-1/2 transition vertex is given in Fig. 5.



Figure 6: *Feynman rule for the interaction vertex of spin-1/2 particles with photons.*

### 3.3 Green's functions

In Sec. 3.1 we have treated the equation of motion (3.13) for the electromagnetic potential by taking the Fourier transformation, and we have solved for the potential in Eq. (3.16) in terms of the Green function, or propagator, of the  $\partial^2$  differential operator, proportional to  $1/q^2$ . This function has poles for  $q^2 = q^{02} - \mathbf{q}^2 = 0$ , that is,

$$q^0 = \pm |\mathbf{q}| . \quad (3.28)$$

Therefore, when we take the inverse Fourier transform, in order to fully specify the solution we need to specify the prescription for going around these poles on the integration contour in the complex  $q^0$  plane. Different possible choices are sketched in Fig. 7, and correspond to different boundary conditions on the solutions of Eq. (3.13):

- a) vanishing fields far in the past (radiation case)
- b) vanishing fields far in the future (absorption case)
- c) propagation of positive frequencies in the future and negative frequencies in the past (Feynman)
- d) propagation of negative frequencies in the future and positive frequencies in the past (anti-Feynman)

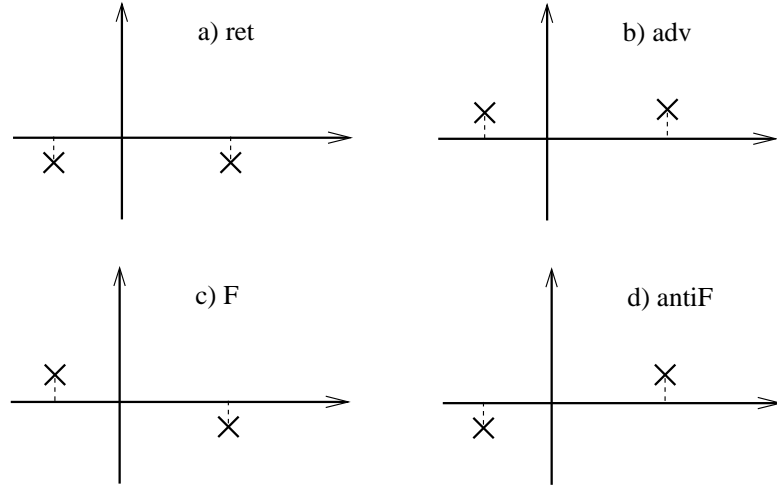


Figure 7: *Contours in the complex  $q^0$  plane: a) retarded; b) advanced; c) Feynman; d) anti-Feynman.*

The Feynman contour is obtained by taking

$$\frac{1}{q^2 + i\varepsilon} \quad (3.29)$$

in the denominator of the Green function, where  $\varepsilon$  is real and positive. We will take the Feynman prescription for the propagator, according to the causality picture in Sec. 1.4.

The same discussion applies to the Green functions for the Klein-Gordon equation and the Dirac equation. The results for the photon, Klein-Gordon and Dirac propagators are given in Fig. 8, using the Feynman prescription.

Note that Fig. 8 gives the photon propagator for a general covariant gauge-fixing condition, Eq. (3.12). This depends on the gauge parameter  $\xi$ . The value  $\xi = 1$  is the Feynman gauge choice.

$$\begin{array}{ccc}
\begin{array}{c} \mu \quad q \quad \nu \\ \text{---} \text{---} \text{---} \end{array} & -i \frac{g^{\mu\nu} - (1-\xi) q^\mu q^\nu / q^2}{q^2 + i\epsilon} \\
\begin{array}{c} q \\ \text{---} \text{---} \text{---} \end{array} & \frac{i}{q^2 - m^2 + i\epsilon} \\
\begin{array}{c} q \\ \text{---} \text{---} \end{array} & \frac{i (\not{q} + m)}{q^2 - m^2 + i\epsilon}
\end{array}$$

Figure 8: *Feynman rules for propagators: (top) photon; (middle) Klein-Gordon; (bottom) Dirac.*

### 3.4 From scattering matrix elements to cross sections

In order to go from transition amplitudes to scattering cross sections, we need to i) construct transition probabilities by squaring the amplitudes, ii) integrate over the final state phase space, iii) divide by the incident flux of particles.

To carry out step i), we evaluate the square of the  $\delta$  function, working in volume  $V$  and time interval  $T$ , as

$$\begin{aligned}
|(2\pi)^4 \delta^4(P_f - P_i)|^2 &\simeq (2\pi)^4 \delta^4(P_f - P_i) \int e^{i(P_f - P_i)x} d^4x \\
&\simeq VT (2\pi)^4 \delta^4(P_f - P_i) .
\end{aligned} \tag{3.30}$$

For step ii), we take the phase space element for each particle  $f$  in the final state,

$$d\phi_f = \frac{V d^3 p_f}{(2\pi)^3} . \tag{3.31}$$

Then the transition probability per unit time is given by

$$\begin{aligned}
dw_{fi} &= \frac{|\mathcal{A}_{fi}|^2}{T} \prod_f d\phi_f \\
&= \frac{1}{T} \prod_f \left[ \frac{1}{2E_f V} \right] \prod_i \left[ \frac{1}{2E_i V} \right] (2\pi)^4 \delta^4(P_f - P_i) |\mathcal{M}_{fi}|^2 VT \prod_f \left( \frac{V d^3 p_f}{(2\pi)^3} \right) .
\end{aligned} \tag{3.32}$$

Note that the factor of  $T$  cancels; so does each factor of  $V$  associated with final state particles.

Let us now consider the decay process in Fig. 9. The decay rate is given by

$$d\Gamma_{fi} = \frac{1}{2E_i V} |\mathcal{M}_{fi}|^2 V \prod_f \left( \frac{d^3 p_f}{(2\pi)^3 2E_f} \right) (2\pi)^4 \delta^4(P_f - P_i)$$

$$= \frac{1}{2E_i} |\mathcal{M}_{fi}|^2 \prod_f \left( \frac{d^3 p_f}{(2\pi)^3 2E_f} \right) (2\pi)^4 \delta^4(P_f - P_i) . \quad (3.33)$$

Note the cancellation of the factor of  $V$  for the initial state.

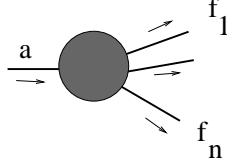


Figure 9: *Decay process*  $a \rightarrow f_1 + f_2 + \dots f_n$ .

Next consider the scattering process in Fig. 10. To obtain the cross section we need to divide the transition probability by the incident particle flux  $F$ ,

$$d\sigma_{fi} = \frac{dw_{fi}}{F} , \quad (3.34)$$

$$F = \frac{1}{V} |v_a - v_b| , \quad (3.35)$$

where  $|v_a - v_b|$  is the relative velocity of colliding particles. Thus

$$\begin{aligned} d\sigma_{fi} &= \frac{V}{|v_a - v_b|} \frac{1}{2E_a V 2E_b V} |\mathcal{M}_{fi}|^2 V \prod_f \left( \frac{d^3 p_f}{(2\pi)^3 2E_f} \right) (2\pi)^4 \delta^4(P_f - P_i) \\ &= \frac{1}{4E_a E_b |v_a - v_b|} |\mathcal{M}_{fi}|^2 \prod_f \left( \frac{d^3 p_f}{(2\pi)^3 2E_f} \right) (2\pi)^4 \delta^4(P_f - P_i) . \end{aligned} \quad (3.36)$$

Note again the cancellation of all  $V$  factors.

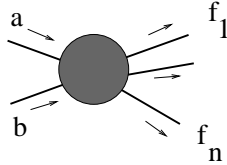


Figure 10: *Scattering process*  $a + b \rightarrow f_1 + f_2 + \dots f_n$ .

Therefore the scattering cross section has the form

$$d\sigma = \frac{1}{\mathcal{J}} |\mathcal{M}_{fi}|^2 d\Phi , \quad (3.37)$$

where each of the three factors is relativistically invariant. The invariant matrix element square  $|\mathcal{M}_{fi}|^2$  contains the dynamics of the process, while the factors  $\mathcal{J}$  and  $d\Phi$  are kinematic factors, giving respectively the invariant initial-state flux,

$$\mathcal{J} = 4E_a E_b |v_a - v_b| \quad , \quad (3.38)$$

and the invariant final-state phase space

$$d\Phi = \prod_f \left( \frac{d^3 p_f}{(2\pi)^3 2E_f} \right) (2\pi)^4 \delta^4(P_f - P_i) \quad . \quad (3.39)$$

The invariant flux  $\mathcal{J}$  can also be rewritten in equivalent forms as

$$\begin{aligned} \mathcal{J} &= 4E_a E_b |v_a - v_b| \\ &= 4|p_i^{(c.m.)}| \sqrt{s} \\ &= 4\sqrt{(p_a \cdot p_b)^2 - m_a^2 m_b^2} \quad , \end{aligned} \quad (3.40)$$

where  $s = (p_a + p_b)^2$ , and  $p_i^{(c.m.)}$  is the initial three-momentum in the center of mass frame.

## 4 Coulomb scattering

In this section we analyze Coulomb scattering in QED using the formalism developed in Sec. 3 for  $S$ -matrix calculations in perturbation theory. We begin in Subsec. 4.1 by recalling Coulomb scattering in the nonrelativistic case. In Subsecs. 4.2-4.4 we calculate elastic electron-muon scattering to lowest order in the QED coupling. Then in Subsec. 4.5 we obtain the cross section for the scattering of a relativistic particle from an external Coulomb potential. In Subsec. 4.6 we consider the annihilation of electron pairs into muon pairs, related to  $e\mu$  scattering by crossing symmetry.

### 4.1 Nonrelativistic case

The cross section in nonrelativistic quantum mechanics for the scattering of a particle of mass  $m$  from potential  $V$  is given in the first-order Born approximation by

$$\frac{d\sigma}{d\Omega} = \frac{m^2}{4\pi^2} |\tilde{V}(\mathbf{q})|^2 , \quad (4.1)$$

where  $\tilde{V}$  is the Fourier transform of the potential,

$$\tilde{V}(\mathbf{q}) = \int d^3x e^{-i\mathbf{q}\cdot\mathbf{x}} V(\mathbf{x}) , \quad (4.2)$$

$\mathbf{q}$  is the momentum transferred in the scattering (Fig. 11), and  $d\Omega$  is the solid angle element.

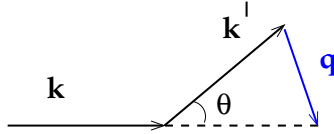


Figure 11: *Scattering through angle  $\theta$ , with  $\mathbf{q} = \mathbf{k} - \mathbf{k}'$ .*

Let us take a potential of the form

$$V(\mathbf{x}) = C \frac{e^{-\mu|\mathbf{x}|}}{|\mathbf{x}|} , \quad \mu > 0 . \quad (4.3)$$

We can apply Eq. (4.1), and we can obtain the nonrelativistic cross section for Coulomb scattering by letting

$$C \rightarrow e^2 , \quad \mu \rightarrow 0 \quad (4.4)$$

in the result.

By inserting Eq. (4.3) into Eq. (4.2), we get

$$\tilde{V}(\mathbf{q}) = C \frac{4\pi}{\mu^2 + \mathbf{q}^2} . \quad (4.5)$$

Thus

$$\frac{d\sigma}{d\Omega} = \frac{4C^2 m^2}{(\mu^2 + \mathbf{q}^2)^2} . \quad (4.6)$$



Substituting Eq. (4.4) into Eq. (4.6), we obtain that the Coulomb scattering cross section in the nonrelativistic case is given by

$$\begin{aligned} \left( \frac{d\sigma}{d\Omega} \right)_{\text{Coul.}} &= \frac{4m^2 e^4}{\mathbf{q}^4} \\ &= \frac{\alpha^2}{4 \mathbf{k}^2 \mathbf{v}^2 \sin^4(\theta/2)} \equiv \left( \frac{d\sigma}{d\Omega} \right)_R, \end{aligned} \quad (4.7)$$

where in the last line we have used  $\mathbf{q}^2 = 4\mathbf{k}^2 \sin^2(\theta/2)$ ,  $\mathbf{k} = m\mathbf{v}$ . The result is given by the classical Rutherford scattering cross section  $(d\sigma/d\Omega)_R$ .

In the next few sections we analyze elastic electron-muon scattering in the fully relativistic quantum theory. From this analysis we will also obtain, in Subsec. 4.5, the relativistic correction to the result (4.7) for scattering from an external Coulomb potential.

## 4.2 The $e\mu$ scattering matrix element in QED

Consider elastic electron-muon scattering  $e(p) + \mu(k) \rightarrow e(p') + \mu(k')$  (Fig. 12). Let  $m$  be the electron mass and  $M$  the muon mass.

Using the Feynman rules for perturbation theory in Sec. 3, the scattering matrix element  $\mathcal{M}_{fi}$  is given by

$$\mathcal{M}_{fi} = ie^2 \bar{u}_{r'}(k') \gamma^\mu u_r(k) \frac{g_{\mu\nu}}{q^2} \bar{u}_{s'}(p') \gamma^\nu u_s(p) \quad , \quad (4.8)$$

where the momentum and spin labels are given in Fig. 12, and  $q^2 = (k - k')^2$  is the invariant momentum transfer.

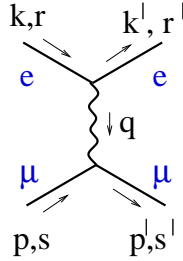


Figure 12: *Electron-muon scattering at lowest order in  $e$ .*

To compute the unpolarized cross section, we need the squared matrix element, averaged over initial spins and summed over final spins:

$$\begin{aligned} \overline{|\mathcal{M}_{fi}|^2} &= \frac{1}{2} \sum_{r=1}^2 \frac{1}{2} \sum_{s=1}^2 \sum_{r'=1}^2 \sum_{s'=1}^2 |\mathcal{M}_{fi}|^2 \\ &= \frac{1}{4} \frac{e^4}{(q^2)^2} \sum_{\text{spins}} |\bar{u}_{r'}(k') \gamma^\mu u_r(k)|^2 |\bar{u}_{s'}(p') \gamma_\mu u_s(p)|^2 \quad . \end{aligned} \quad (4.9)$$

In the next subsection we give the basic result that is needed to evaluate such spin sums.

### 4.3 Fermionic spin sums

For any matrix  $\Gamma$  given by a product of Dirac  $\gamma$  matrices, it can be shown that

$$\sum_{\alpha=1}^2 \sum_{\beta=1}^2 |\bar{u}_\alpha(p') \Gamma u_\beta(p)|^2 = \text{Tr} \left[ \Gamma (\not{p}' + m) \gamma^0 \Gamma^\dagger \gamma^0 (\not{p} + m) \right] . \quad (4.10)$$

To see this, write the square as

$$\sum_{\alpha=1}^2 \sum_{\beta=1}^2 |\bar{u}_\alpha(p') \Gamma u_\beta(p)|^2 = \sum_{\alpha=1}^2 \sum_{\beta=1}^2 [\bar{u}_\alpha(p') \Gamma u_\beta(p)] [\bar{u}_\alpha(p') \Gamma u_\beta(p)]^* \quad (4.11)$$

and evaluate the complex conjugate factor:

$$\begin{aligned} [\bar{u}_\alpha(p') \Gamma u_\beta(p)]^* &= u_\beta^\dagger(p) \Gamma^\dagger (u_\alpha^\dagger(p') \gamma^0)^\dagger \\ &= \bar{u}_\beta(p) \underbrace{\gamma^0 \Gamma^\dagger \gamma^0}_{\tilde{\Gamma}} u_\alpha(p') . \end{aligned} \quad (4.12)$$

Now write out all products of spinors and  $\gamma$  matrices in Eq. (4.11) in components:

$$\sum_{\alpha=1}^2 \sum_{\beta=1}^2 |\bar{u}_\alpha(p') \Gamma u_\beta(p)|^2 = \sum_{\alpha=1}^2 \sum_{\beta=1}^2 \bar{u}_{\alpha a}(p') \Gamma_{ab} u_{\beta b}(p) \bar{u}_{\beta c}(p) \tilde{\Gamma}_{cd} u_{\alpha d}(p') \quad (4.13)$$

Next use the completeness relation for  $u$  spinors:

$$\sum_{\alpha=1}^2 u_{\alpha j}(p) \bar{u}_{\alpha k}(p) = (\not{p} + m)_{jk} . \quad (4.14)$$

Then from Eq. (4.13) we have

$$\begin{aligned} \sum_{\alpha=1}^2 \sum_{\beta=1}^2 |\bar{u}_\alpha(p') \Gamma u_\beta(p)|^2 &= \Gamma_{ab} (\not{p}' + m)_{bc} \tilde{\Gamma}_{cd} (\not{p} + m)_{da} \\ &= [\Gamma (\not{p}' + m) \tilde{\Gamma} (\not{p} + m)]_{aa} \\ &= \text{Tr} [\Gamma (\not{p}' + m) \gamma^0 \Gamma^\dagger \gamma^0 (\not{p} + m)] , \end{aligned} \quad (4.15)$$

which is the result in Eq. (4.10).

Analogous results hold for spin sums involving  $v$  spinors. For instance,

$$\sum_{\alpha=1}^2 \sum_{\beta=1}^2 |\bar{u}_\alpha(p') \Gamma v_\beta(p)|^2 = \text{Tr} \left[ \Gamma (\not{p}' - m) \gamma^0 \Gamma^\dagger \gamma^0 (\not{p} + m) \right] . \quad (4.16)$$

### 4.4 Elastic $e\mu$ scattering cross section

By using the general result (4.10), the matrix element (4.9) can be written as

$$|\overline{\mathcal{M}}_{fi}|^2 = \frac{1}{4} \frac{e^4}{(q^2)^2} \text{Tr} [\gamma^\alpha (\not{k}' + m) \gamma^\lambda (\not{k} + m)] \text{Tr} [\gamma^\beta (\not{p}' + M) \gamma^\rho (\not{p} + M)] g_{\alpha\beta} g_{\lambda\rho} . \quad (4.17)$$

We can in general evaluate traces of products of  $\gamma$  matrices by using the anticommutation relations (1.34) and (2.43). To do the calculation in Eq. (4.17) we need the following traces,

$$\text{Tr}(\text{odd number of } \gamma \text{ matrices}) = 0 \quad , \quad (4.18)$$

$$\text{Tr}(\gamma^\mu \gamma^\nu) = 4g^{\mu\nu} \quad , \quad (4.19)$$

$$\text{Tr}(\gamma^\mu \gamma^\nu \gamma^\rho \gamma^\sigma) = 4 (g^{\mu\nu} g^{\rho\sigma} - g^{\mu\rho} g^{\nu\sigma} + g^{\mu\sigma} g^{\nu\rho}) \quad , \quad (4.20)$$

which can be obtained using Eqs. (1.34),(2.43). By then carrying out the algebra in Eq. (4.17), we get

$$\overline{|\mathcal{M}_{fi}|^2} = \frac{2e^4}{(q^2)^2} \left[ 2 (m^2 + M^2) q^2 + (s - m^2 - M^2)^2 + (s + q^2 - m^2 - M^2)^2 \right] \quad , \quad (4.21)$$

where  $s$  is the invariant center-of-mass energy square  $s = (k + p)^2$ .

We are now in a position to compute the cross section. This is given in terms of the scattering matrix element via Eq. (3.37),

$$d\sigma = \frac{1}{\mathcal{J}} |\mathcal{M}_{fi}|^2 d\Phi \quad , \quad (4.22)$$

where  $\mathcal{J}$  is the invariant initial-state flux and  $d\Phi$  is the invariant final-state phase space. We can compute the cross section by plugging Eq. (4.21) into Eq. (4.22), choosing a reference frame, and evaluating the flux factor  $\mathcal{J}$  and the phase space  $d\Phi$  integration in this frame.

Consider the center-of-mass reference frame,  $\mathbf{k} + \mathbf{p} = 0$  (Fig. 13). From Eq. (3.40) we have

$$\mathcal{J} = 4|\mathbf{p}|\sqrt{s} \quad . \quad (4.23)$$

To carry out the integration over the final state phase space in Eq. (3.39),

$$d\Phi = \frac{d^3k'}{(2\pi)^3 2E'_k} \frac{d^3p'}{(2\pi)^3 2E'_p} (2\pi)^4 \delta^4(p' + k' - p - k) \quad , \quad (4.24)$$

we can first use the three-momentum  $\delta$  function to do the integral in  $d^3k'$ , so that the cross section differential in the final-state solid angle  $d\Omega = \sin\theta d\theta d\varphi$  can be written

$$\frac{d\sigma}{d\Omega} = \frac{1}{4|\mathbf{p}|\sqrt{s}} \frac{1}{(2\pi)^2} \int \mathbf{p}'^2 d|\mathbf{p}'| \frac{1}{4E'_p E'_k} \overline{|\mathcal{M}_{fi}|^2} \delta(E'_p + E'_k - E_p - E_k) \quad . \quad (4.25)$$

Next it is convenient to make the change of integration variable

$$\begin{aligned} |\mathbf{p}'| \rightarrow E' &= \sqrt{\mathbf{p}'^2 + M^2} + \sqrt{\mathbf{p}'^2 + m^2} \\ &= E'_p + E'_k \quad , \end{aligned} \quad (4.26)$$

with jacobian

$$\frac{\partial E'}{d|\mathbf{p}'|} = \frac{E'|\mathbf{p}'|}{E'_p E'_k} \quad , \quad (4.27)$$

by which Eq. (4.25) can be rewritten as

$$\frac{d\sigma}{d\Omega} = \frac{1}{4|\mathbf{p}|\sqrt{s}} \frac{1}{(2\pi)^2} \int dE' \frac{|\mathbf{p}'|}{4E'} \overline{|\mathcal{M}_{fi}|^2} \delta(E' - \sqrt{s}) . \quad (4.28)$$

Performing the  $E'$  integral with the  $\delta$  function and substituting the explicit expression (4.21) of  $\overline{|\mathcal{M}_{fi}|^2}$ , we obtain ( $e^2 = 4\pi\alpha$ )

$$\frac{d\sigma}{d\Omega} = \frac{\alpha^2}{2 s q^4} \left[ 2 (m^2 + M^2) q^2 + (s - m^2 - M^2)^2 + (s + q^2 - m^2 - M^2)^2 \right] . \quad (4.29)$$

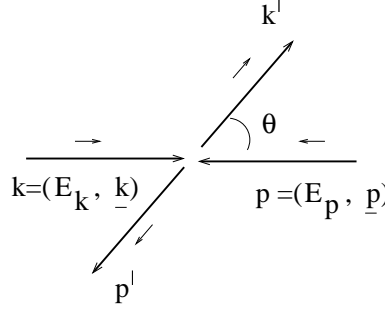


Figure 13: *Center-of-mass reference frame.*

The result (4.29) takes a simpler form in the high energy limit  $s \gg M^2, m^2$ . In this case we have  $s \rightarrow 4\mathbf{p}^2$ ,  $q^2 \rightarrow -4\mathbf{p}^2 \sin^2(\theta/2)$ , and the cross section becomes

$$\frac{d\sigma}{d\Omega} \simeq \frac{\alpha^2}{2 s \sin^4(\theta/2)} \left( 1 + \cos^4 \theta/2 \right) \quad \text{for } s \gg M^2, m^2 . \quad (4.30)$$

The leading behavior of the cross section (4.30) at small angle is given by

$$\frac{d\sigma}{d\Omega} \propto \frac{1}{\theta^4} \quad \text{for } \theta \ll 1 , \quad (4.31)$$

where the  $\theta^{-4}$  singularity is characteristic of the Coulomb interaction. It comes from the factor  $1/(q^2)^2$ , and reflects the long range of the interaction.

## 4.5 Scattering by an external Coulomb potential

The cross section for the scattering of a relativistic particle from an external Coulomb potential (Fig. 14) can be obtained as a particular case of the result of the previous subsection for  $e\mu$  scattering, by working in the rest frame of  $\mu$  and letting  $M \rightarrow \infty$ .

To this end, first express the invariant flux  $\mathcal{J}$  in terms of the electron's three-momentum  $\mathbf{k}$  in the rest frame of  $\mu$  (Fig. 14),

$$\mathcal{J} = 4|\mathbf{k}|M . \quad (4.32)$$

Next, carry through the final-state phase space integration in terms of rest-frame variables. This yields

$$\frac{d\sigma}{d\Omega} = \frac{1}{4|\mathbf{k}|M} \frac{|\mathbf{k}'|}{16\pi^2 M} \overline{|\mathcal{M}_{fi}|^2} . \quad (4.33)$$

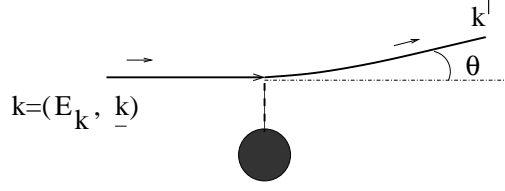


Figure 14: *Scattering by external Coulomb potential.*

Finally, let  $M \rightarrow \infty$  in the invariant matrix element (4.21). In this limit  $|\mathbf{k}'| \simeq |\mathbf{k}|$ ,  $q^2 \simeq -4\mathbf{k}^2 \sin^2(\theta/2)$ , and the square bracket in Eq. (4.21) becomes

$$\begin{aligned} & \left[ 2 (m^2 + M^2) q^2 + (s - m^2 - M^2)^2 + (s + q^2 - m^2 - M^2)^2 \right] \\ & \simeq [2M^2 q^2 + 2(2ME_k)^2 + \dots] \\ & \simeq 8M^2 E_k^2 \left[ 1 - (|\mathbf{k}|/E_k)^2 \sin^2(\theta/2) \right] . \end{aligned} \quad (4.34)$$

Substituting Eq. (4.34) into Eq. (4.33), we obtain

$$\frac{d\sigma}{d\Omega} = \frac{\alpha^2}{4 \mathbf{k}^2 \mathbf{v}^2 \sin^4(\theta/2)} \left[ 1 - \mathbf{v}^2 \sin^2(\theta/2) \right] , \quad (4.35)$$

where  $\mathbf{v} = |\mathbf{k}|/E_k$ .

Eq. (4.35) can be compared with the nonrelativistic result in Eq. (4.7). Observe that Eq. (4.35) has the form

$$\frac{d\sigma}{d\Omega} = \left( \frac{d\sigma}{d\Omega} \right)_R \left[ 1 - \mathbf{v}^2 \sin^2(\theta/2) \right] , \quad (4.36)$$

where

$$\left( \frac{d\sigma}{d\Omega} \right)_R = \frac{\alpha^2}{4 \mathbf{k}^2 \mathbf{v}^2 \sin^4(\theta/2)} \quad (4.37)$$

is the Rutherford cross section, and the factor in the square bracket is the relativistic correction.

The relativistic correction  $[1 - \mathbf{v}^2 \sin^2(\theta/2)]$  characterizes Coulomb scattering for spin 1/2. Computing Coulomb potential scattering of spinless charges, one finds

$$\left( \frac{d\sigma}{d\Omega} \right)_{\text{spin}=0} = \left( \frac{d\sigma}{d\Omega} \right)_R , \quad (4.38)$$

that is, in the case of spinless particles the result does not differ from the nonrelativistic result. Eq. (4.36) shows that for  $|\mathbf{v}| \rightarrow 1$  the angular distribution of a spin-1/2 particle differs from the nonrelativistic result as diffusion in the backward direction is strongly suppressed.

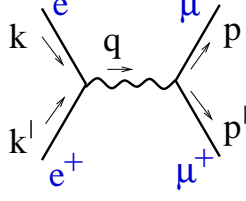


Figure 15: *Annihilation of electron pairs into muon pairs.*

#### 4.6 Crossing symmetry: $e^+e^- \rightarrow \mu^+\mu^-$ annihilation

The  $e\mu$  scattering process computed earlier is related by crossing symmetry to the annihilation process  $e^+(k')e^-(k) \rightarrow \mu^+(p')\mu^-(p)$  (Fig. 15). Let us compute this in the approximation of massless electrons. The matrix element square, averaged over initial spins and summed over final spins, is given by

$$\overline{|\mathcal{M}_{fi}|^2} = \frac{1}{4} \frac{e^4}{(q^2)^2} \text{Tr}[\gamma^\rho (\not{p}' + M) \gamma^\sigma (-\not{p} + M)] \text{Tr}[\gamma^\tau \not{k}' \gamma^\lambda (-\not{k})] g_{\lambda\rho} g_{\sigma\tau} \quad (4.39)$$

where  $q^2 = s$ , and we have set the electron mass to zero. Computing the traces yields

$$\overline{|\mathcal{M}_{fi}|^2} = \frac{8e^4}{s^2} [(p \cdot k)^2 + (p \cdot k')^2 + M^2 k \cdot k'] \quad (4.40)$$

Let us work in the center-of-mass reference system, and denote by  $\theta$  the center-of-mass scattering angle. In this system the matrix element square (4.40) takes the form

$$\overline{|\mathcal{M}_{fi}|^2} = e^4 \left[ 1 + \frac{4M^2}{s} + \left( 1 - \frac{4M^2}{s} \right) \cos^2 \theta \right] \quad (4.41)$$

The annihilation cross section can be computed via the general formula (3.37),

$$d\sigma = \frac{1}{\mathcal{J}} |\mathcal{M}_{fi}|^2 d\Phi \quad (4.42)$$

Note that for massless electrons

$$\mathcal{J} = 2s \quad (4.43)$$

and that the final-state phase space can be written as

$$d\Phi = \frac{|\mathbf{p}|}{16\pi^2 \sqrt{s}} d\Omega \quad (4.44)$$

where  $d\Omega = \sin \theta d\theta d\varphi$ , and

$$|\mathbf{p}| = \frac{\sqrt{s}}{2} \sqrt{1 - \frac{4M^2}{s}} \quad (4.45)$$

Then the differential cross section  $d\sigma/d\Omega$  is given by

$$\left( \frac{d\sigma}{d\Omega} \right)_{e^+e^- \rightarrow \mu^+\mu^-} = \frac{\alpha^2}{4s} \sqrt{1 - \frac{4M^2}{s}} \left[ 1 + \frac{4M^2}{s} + \left( 1 - \frac{4M^2}{s} \right) \cos^2 \theta \right] \quad (4.46)$$

In the high energy limit  $4M^2/s \rightarrow 0$ , from Eq. (4.46) we get

$$\left(\frac{d\sigma}{d\Omega}\right)_{e^+e^- \rightarrow \mu^+\mu^-} = \frac{\alpha^2}{4s} (1 + \cos^2 \theta) \quad \text{for } s \gg M^2. \quad (4.47)$$

The total cross section is obtained by integrating Eq. (4.46) over angles,

$$\begin{aligned} \sigma_{\text{tot}} &= \int \frac{d\sigma}{d\Omega} d\Omega \\ &= \frac{\alpha^2}{4s} \sqrt{1 - \frac{4M^2}{s}} 2\pi \left[ \left(1 + \frac{4M^2}{s}\right) \int_0^\pi \sin \theta d\theta + \left(1 - \frac{4M^2}{s}\right) \int_0^\pi \sin \theta \cos^2 \theta d\theta \right] \\ &= \frac{4\pi\alpha^2}{3s} \sqrt{1 - \frac{4M^2}{s}} \left(1 + \frac{2M^2}{s}\right). \end{aligned} \quad (4.48)$$

In the high energy limit,

$$\sigma_{\text{tot}} \simeq \frac{4\pi\alpha^2}{3s}. \quad (4.49)$$

*Remark.* In addition to the annihilation into muons and other leptons, experiments at high-energy  $e^+e^-$  accelerators measure the cross section for the annihilation of  $e^+e^-$  into hadrons. The cross section for  $e^+e^- \rightarrow \text{hadrons}$  at large  $s$  differs from the expression (4.49) for  $e^+e^- \rightarrow \mu^+\mu^-$  by a factor of the squared electric charge of the hadron constituents (quarks), summed over the possible  $N_c$  quark “colors” and  $N_f$  quark “flavors”, and by effects of higher order in the strong interaction:

$$\sigma(e^+e^- \rightarrow \text{hadrons}) = \frac{4\pi\alpha^2}{3s} N_c \sum_{i=1}^{N_f} Q_i^2 [1 + \mathcal{O}(\alpha_{\text{strong}})] \quad (4.50)$$

## 5 Compton scattering

Let us analyze electron-photon Compton scattering at lowest order in  $e$ . This receives contribution from the graphs in Fig. 16.

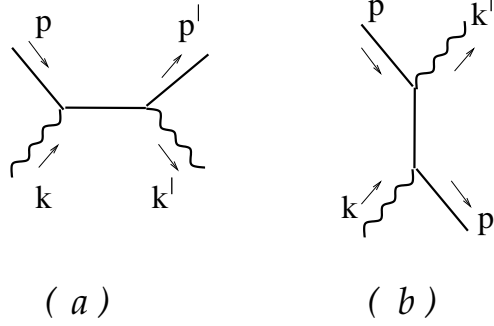


Figure 16: *Electron-photon scattering at lowest order in  $e$ .*

The scattering matrix element  $\mathcal{M}_{fi}$  is given by

$$\mathcal{M}_{fi} = -ie^2 \varepsilon'^{\mu}(k') \varepsilon^{\nu}(k) \bar{u}(p') \left[ \gamma_{\mu} \frac{(\not{p} + \not{k} + m)}{(p+k)^2 - m^2} \gamma_{\nu} + \gamma_{\nu} \frac{(\not{p} - \not{k}' + m)}{(p-k')^2 - m^2} \gamma_{\mu} \right] u(p), \quad (5.1)$$

where  $\varepsilon(k)$  and  $\varepsilon'(k')$  are the incoming and outgoing photon polarization vectors. The two terms in the square bracket in Eq. (5.1) correspond respectively to graphs (a) and (b) in Fig. 16.

The sum of graphs (a) and (b) is gauge invariant, namely, with  $\mathcal{M}_{fi} = M_{\mu\nu} \varepsilon'^{\mu}(k') \varepsilon^{\nu}(k)$ , we have

$$M_{\mu\nu} k'^{\mu} = M_{\mu\nu} k^{\nu} = 0. \quad (5.2)$$

This can be seen by writing

$$\begin{aligned} M_{\mu\nu} k^{\nu} &= -ie^2 \bar{u}(p') \left[ \gamma_{\mu} \frac{1}{\not{p} + \not{k} - m} \not{k} + \not{k} \frac{1}{\not{p}' - \not{k} - m} \gamma_{\mu} \right] u(p) \\ &= -ie^2 \bar{u}(p') \left\{ \gamma_{\mu} \frac{1}{\not{p} + \not{k} - m} [(\not{p} + \not{k} - m) - (\not{p} - m)] \right. \\ &\quad \left. + [-(\not{p}' - \not{k} - m) + (\not{p}' - m)] \frac{1}{\not{p}' - \not{k} - m} \gamma_{\mu} \right\} u(p). \end{aligned} \quad (5.3)$$

Then, from each of the square brackets in the last two lines, the contributions of the first terms cancel each other, while the contributions of the second terms vanish separately because of the Dirac equation. Thus

$$\begin{aligned} M_{\mu\nu} k^{\nu} &= -ie^2 \bar{u}(p') \left[ \gamma_{\mu} \frac{1}{\not{p} + \not{k} - m} (\not{p} - m) + (\not{p}' - m) \frac{1}{\not{p}' - \not{k} - m} \gamma_{\mu} \right] u(p) \\ &= 0. \end{aligned} \quad (5.4)$$

Similarly for the dot product of  $M_{\mu\nu}$  with  $k'^{\mu}$ .



To compute the unpolarized cross section, we need the squared matrix element, averaged over the initial electron and photon polarizations, and summed over the final electron and photon polarizations,

$$\overline{|\mathcal{M}_{fi}|^2} = \frac{1}{4} \sum_{\text{polarizations}} |\mathcal{M}_{fi}|^2 . \quad (5.5)$$

The electron sums can be dealt with using the general result in Subsec. 4.3. The photon sums are discussed in the next subsection.

## 5.1 Photon polarization sums

The sum over photon polarizations can be performed by replacing the sum with  $-g^{\mu\nu}$ ,

$$\sum_{\alpha=1}^2 \varepsilon_\mu^\alpha(k) \varepsilon_\nu^\alpha(k) \rightarrow -g_{\mu\nu} , \quad (5.6)$$

because the amplitude into which  $\varepsilon$  is dotted is conserved, Eq. (5.2).

To see this, consider a matrix element of the form

$$A^\mu \varepsilon_\mu(k) \quad (5.7)$$

for  $A^\mu$  such that

$$A^\mu k_\mu = 0 , \quad (5.8)$$

and sum the matrix element square over polarizations,

$$\sum_{\alpha=1}^2 |A^\mu \varepsilon_\mu^\alpha(k)|^2 = \sum_{\alpha=1}^2 A^\mu A^\nu \varepsilon_\mu^\alpha(k) \varepsilon_\nu^\alpha(k) . \quad (5.9)$$

Now use that polarizations form an orthonormal set in the plane transverse to the momentum  $\mathbf{k}$ ,

$$\sum_{\alpha=1}^2 \varepsilon^{\alpha i}(k) \varepsilon^{\alpha j}(k) = \delta^{ij} - \hat{k}^i \hat{k}^j , \quad \text{where} \quad \hat{k}^i = k^i / |\mathbf{k}| = k^i / k^0 . \quad (5.10)$$

Then the sum (5.9) can be written

$$\begin{aligned} \sum_{\alpha=1}^2 |A^\mu \varepsilon_\mu^\alpha(k)|^2 &= \sum_{\alpha=1}^2 A^\mu A^\nu \varepsilon_\mu^\alpha(k) \varepsilon_\nu^\alpha(k) \\ &= A^i A^j (\delta^{ij} - \hat{k}^i \hat{k}^j) = A^i A^i - (A^i \hat{k}^i)(A^j \hat{k}^j) \\ &= A^i A^i - A^0 A^0 = -A^\mu A^\nu g_{\mu\nu} , \end{aligned} \quad (5.11)$$

where in the last line we have used that Eq. (5.8) implies

$$A^0 k^0 - A^i k^i = 0 , \quad i.e., \quad A^i \hat{k}^i = A^0 . \quad (5.12)$$

From Eqs. (5.9) and (5.11) we obtain that the sum over polarizations amounts to

$$\sum_{\alpha=1}^2 \varepsilon_\mu^\alpha(k) \varepsilon_\nu^\alpha(k) \rightarrow -g_{\mu\nu} , \quad (5.13)$$

as stated in Eq. (5.6).

## 5.2 The $e\gamma$ unpolarized cross section

The unpolarized matrix element square (5.5) can now be determined from Eq. (5.1) by using the result in Eq. (4.10) for the electron polarization sums and the result in Eq. (5.6) for the photon polarization sums.

To do this calculation, we need to evaluate the traces of  $\gamma$  matrices generated by the electron spin sums in Eq. (4.10), making use of the  $\gamma$  matrix identities

$$\gamma_\mu \gamma^\mu = 4 \quad , \quad (5.14)$$

$$\gamma_\mu \gamma^\rho \gamma^\mu = -2\gamma^\rho \quad , \quad (5.15)$$

which follow from the anticommutation relations (1.34). By working out the algebra, we obtain the result

$$\begin{aligned} \overline{|\mathcal{M}_{fi}|^2} &= \frac{1}{4} \sum_{\text{polarizations}} |\mathcal{M}_{fi}|^2 \\ &= 2e^4 \left[ \frac{p \cdot k}{p \cdot k'} + \frac{p \cdot k'}{p \cdot k} + 2m^2 \left( \frac{1}{p \cdot k} - \frac{1}{p \cdot k'} \right) + m^4 \left( \frac{1}{p \cdot k} - \frac{1}{p \cdot k'} \right)^2 \right] \end{aligned} \quad (5.16)$$

The  $e\gamma$  cross section is related to the scattering matrix element via the general formula (3.37),

$$d\sigma = \frac{1}{\mathcal{J}} |\mathcal{M}_{fi}|^2 d\Phi \quad . \quad (5.17)$$

We can compute it by choosing a reference frame, plugging Eq. (5.16) into Eq. (5.17) and evaluating the flux factor  $\mathcal{J}$  and phase space  $d\Phi$  integration.

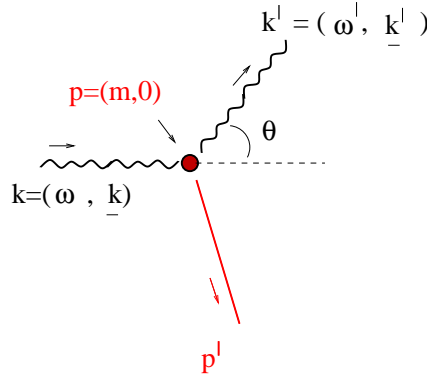


Figure 17: *Compton scattering in the laboratory frame.*

Consider the laboratory frame in which the electron is initially at rest,  $p^\mu = (m, \mathbf{0})$  (Fig. 17). In the notation of Fig. 17 we have

$$m^2 = p'^2 = (p + k - k')^2 = m^2 + 2m(\omega - \omega') - 2\omega\omega'(1 - \cos \theta) \quad , \quad (5.18)$$

which gives

$$\omega' = \frac{\omega}{1 + (\omega/m)(1 - \cos \theta)} \quad . \quad (5.19)$$

By evaluating the right hand side of Eq. (5.16) in the laboratory frame and using Eq. (5.19), we obtain

$$|\overline{\mathcal{M}}_{fi}|^2 = 2e^4 \left( \frac{\omega}{\omega'} + \frac{\omega'}{\omega} - \sin^2 \theta \right) . \quad (5.20)$$

From Eq. (3.40) for the flux factor we get

$$\mathcal{J} = 4E_a E_b |v_a - v_b| = 4m\omega . \quad (5.21)$$

Let us now carry out the integration over the final-state phase space (3.39),

$$d\Phi = \frac{d^3 k'}{(2\pi)^3 2\omega'} \frac{d^3 p'}{(2\pi)^3 2E'} (2\pi)^4 \delta^4(p' + k' - p - k) . \quad (5.22)$$

By using the three-momentum  $\delta$  function to perform the integral in  $d^3 p'$ , and inserting the results (5.20) and (5.21) into Eq. (5.17), the differential cross section in the solid angle  $\Omega$  of the final photon momentum is given by

$$\frac{d\sigma}{d\Omega} = \frac{2e^4}{4m\omega} \int d\omega' \frac{\omega'}{16\pi^2 E'} \delta(E' + \omega' - m - \omega) \left[ \frac{\omega}{\omega'} + \frac{\omega'}{\omega} - \sin^2 \theta \right] , \quad (5.23)$$

where

$$E' = \sqrt{\omega^2 + \omega'^2 - 2\omega\omega' \cos \theta + m^2} . \quad (5.24)$$

Performing the integral in  $d\omega'$ , we arrive at the unpolarized electron-photon cross section

$$\frac{d\sigma}{d\Omega} = \frac{\alpha^2}{2m^2} \left( \frac{\omega'}{\omega} \right)^2 \left[ \frac{\omega}{\omega'} + \frac{\omega'}{\omega} - \sin^2 \theta \right] , \quad (5.25)$$

where  $\alpha = e^2/4\pi$ .

In the low energy limit  $\omega \ll m$ , from Eq. (5.19) we have  $\omega' \approx \omega$ , and Eq. (5.25) reduces to the Thomson cross section,

$$\frac{d\sigma}{d\Omega} \longrightarrow \frac{\alpha^2}{2m^2} (1 + \cos^2 \theta) \quad \text{for } \omega \ll m , \quad (5.26)$$

describing the scattering of classical electromagnetic radiation by a free electron.

In the high energy limit  $\omega \gg m$ , Eq. (5.25) gives rise to a logarithmic behavior in the total cross section, arising from the emission of photons at small angles. This is because for  $\omega \gg m$  from Eq. (5.19) we have

$$\omega' \simeq \frac{m}{1 - \cos \theta} \quad \text{for } \frac{\omega}{m} (1 - \cos \theta) \gg 1 , \quad (5.27)$$

which means that in the region

$$1 \gg \theta^2 \gg \frac{2m}{\omega} \quad (5.28)$$

the cross section is strongly peaked,

$$\begin{aligned} \frac{d\sigma}{d\Omega} &\simeq \frac{\alpha^2}{2m^2} \left( \frac{m}{\omega} \right)^2 \frac{1}{(1 - \cos \theta)^2} \left[ \frac{\omega}{m} (1 - \cos \theta) - \sin^2 \theta \right] \\ &\simeq \frac{\alpha^2}{2m\omega} \frac{1}{1 - \cos \theta} . \end{aligned} \quad (5.29)$$

Integrating over angles gives

$$\begin{aligned}\sigma &\simeq 2\pi \int d\cos\theta \frac{\alpha^2}{2m\omega} \frac{1}{1-\cos\theta} \\ &\simeq 2\pi \int_{2m/\omega}^1 \frac{d\theta^2}{\theta^2} \frac{\alpha^2}{m\omega} \simeq \frac{2\pi\alpha^2}{m\omega} \ln \frac{\omega}{2m} .\end{aligned}\quad (5.30)$$

The total cross section  $\sigma$  falls like  $\omega^{-1}$ , but with a logarithmic enhancement from the integration over the small-angle, or collinear, region. The collinear region is cut off by the mass  $m$ . The occurrence of collinear logarithms illustrated by this example is a general feature associated with the massless limit of the theory.

### 5.3 Photon polarization dependence

The calculation performed above can be redone for fixed  $\varepsilon(k)$  and  $\varepsilon'(k')$  to obtain the dependence of the cross section on the initial and final photon polarizations. The result for the cross section including the polarization dependence is

$$\left(\frac{d\sigma}{d\Omega}\right)_{\text{pol.}} = \frac{\alpha^2}{4m^2} \left(\frac{\omega'}{\omega}\right)^2 \left[ \frac{\omega}{\omega'} + \frac{\omega'}{\omega} + 4(\varepsilon \cdot \varepsilon')^2 - 2 \right] . \quad (5.31)$$

From Eq. (5.31) we recover Eq. (5.25) through averaging over  $\varepsilon$  and summing over  $\varepsilon'$  by using Eq. (5.10), i.e., that the sum over polarizations gives the transverse projector with respect to the momentum,

$$\sum_{\alpha=1}^2 \varepsilon_i^\alpha(k) \varepsilon_j^\alpha(k) = \delta_{ij} - \hat{k}_i \hat{k}_j , \quad (5.32)$$

$$\sum_{\beta=1}^2 \varepsilon_i'^\beta(k') \varepsilon_j'^\beta(k') = \delta_{ij} - \hat{k}'_i \hat{k}'_j . \quad (5.33)$$

We thus have

$$\begin{aligned}& \frac{1}{2} \sum_{\alpha=1}^2 \sum_{\beta=1}^2 \left(\frac{d\sigma}{d\Omega}\right)_{\text{pol.}} \\ &= \frac{\alpha^2}{4m^2} \left(\frac{\omega'}{\omega}\right)^2 \left\{ 2 \left[ \frac{\omega}{\omega'} + \frac{\omega'}{\omega} - 2 \right] + 4 \frac{1}{2} \sum_{\alpha=1}^2 \sum_{\beta=1}^2 [\varepsilon^\alpha(k) \cdot \varepsilon'^\beta(k')]^2 \right\} ,\end{aligned}\quad (5.34)$$

where

$$\begin{aligned}\frac{1}{2} \sum_{\alpha=1}^2 \sum_{\beta=1}^2 [\varepsilon^\alpha(k) \cdot \varepsilon'^\beta(k')]^2 &= \frac{1}{2} \sum_{\alpha=1}^2 \sum_{\beta=1}^2 \varepsilon_i^\alpha(k) \varepsilon_j^\alpha(k) \varepsilon_i'^\beta(k') \varepsilon_j'^\beta(k') \\ &= \frac{1}{2} (\delta_{ij} - \hat{k}_i \hat{k}_j) (\delta_{ij} - \hat{k}'_i \hat{k}'_j) = \frac{1}{2} [1 + (\hat{\mathbf{k}} \cdot \hat{\mathbf{k}}')^2] \\ &= \frac{1}{2} (1 + \cos^2 \theta) = \frac{1}{2} (2 - \sin^2 \theta) .\end{aligned}\quad (5.35)$$

Substituting Eq. (5.35) into Eq. (5.34) we re-obtain the unpolarized result (5.25).

## 6 Strong interactions

In this section we extend the discussion given in the previous sections to the case of strong interactions. The theory of strong interactions, Quantum Chromodynamics (QCD), is treated systematically in the Standard Model course. Here we give a brief introduction building on material presented for QED. In Subsec. 6.1 we introduce the gauge symmetry of the strong interaction as a generalization of that of QED and examine the couplings that follow from it. In Subsec. 6.2 we contrast features of photon and gluon polarization degrees of freedom and discuss physical implications. In Subsec. 6.3 we give basic results on the algebra of QCD charges that serve in practical calculations.

We will use the results presented here to further discuss strong interactions in Sec. 8.

### 6.1 Basic structure

We can think of QCD as a theory similar to QED but with

- $N = 3$  charged spin-1/2 particles  $\psi_i$  (quarks, replicated in six families — the so-called quark “flavors”),
- $N^2 - 1 = 8$  gauge bosons  $A_\mu^a$  (gluons),

with different couplings to different charges. The couplings are to be thought of as matrices

$$T^a, \quad a = 1, \dots, N^2 - 1 \quad (6.1)$$

obeying well-prescribed commutation relations

$$[T^a, T^b] = if^{abc}T^c, \quad (6.2)$$

where  $f^{abc}$  are “structure constants”, antisymmetric in all indices. The quantum number specifying the charge of QCD is called “color”, and  $T^a$  are the color-charge matrices. Thus QCD contains multiple vector particles and its charges are non-commuting, or “non-abelian”.

Eq. (6.2) defines an algebra of color-charge operators whose formal properties can usefully be thought of along similar lines to the discussion given in Sec. 2 for the algebra (2.1) of angular momentum operators  $J^i$ .  $J^i$  are the generators of the rotation group.  $T^a$  are the generators of the color symmetry group ( $SU(N)$  with  $N = 3$ ), and have matrix representations for different dimensionalities  $n$ . The fundamental representation is the representation with dimensionality  $n = N$  to which quarks belong,  $\psi_i, i = 1, 2, 3$ . The matrix representation of the generators is given by

$$T^a \rightarrow \frac{1}{2} \lambda^a, \quad (6.3)$$

where  $\lambda^a$  are the eight Gell-Mann  $3 \times 3$  matrices. The adjoint representation is the representation with dimensionality  $n = N^2 - 1$  to which gluons belong,  $A_\mu^a, a = 1, \dots, 8$ . The matrix representation of the generators in the adjoint is given by the structure constants themselves,

$$(T^a)^{bc} \rightarrow -if^{abc}. \quad (6.4)$$

As in QED, the spin-1/2 charged particles satisfy equations of motion of Dirac type,

$$(i\not{D} - m)\psi = 0 \quad , \quad (6.5)$$

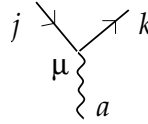
and we can write down their coupling to the vector particles, the gluons, based on similar reasoning as in QED. While in QED we write the electron-photon interaction by replacing

$$\partial_\mu \rightarrow D_\mu = \partial_\mu + ieA_\mu \quad (\text{QED}) \quad (6.6)$$

in the equations of motion, in QCD it is not just one term by which we modify  $\partial^\mu$  but a sum of terms, one for each of the gluons, and each term is proportional not just to a number like the electric charge but to a color-charge matrix:

$$\partial_\mu \rightarrow D_\mu = \partial_\mu + ig_s A_\mu^a T^a \quad (\text{QCD}) \quad , \quad (6.7)$$

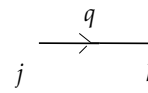
where  $g_s$  is the strong-interaction coupling constant. With this interaction term, by going through the analogous perturbation analysis as for QED, we can extract the Feynman rule for the quark-quark-gluon coupling. This is given in Fig. 18. It has a similar structure to the QED vertex of Fig. 6, with the difference being in the color matrix.

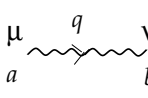


$$ig_s \gamma^\mu (T^a)_{jk}$$

Figure 18: *QCD Feynman rule for quark-quark-gluon vertex.*

For internal lines we have the Feynman rules for propagators (Fig. 19), similar to those of QED except for the additional dependence on color indices.



$$\delta^{jk} \frac{i (\not{q} + m)}{q^2 - m^2 + i\epsilon}$$
  


$$\delta^{ab} \frac{-ig^{\mu\nu}}{q^2 + i\epsilon} \quad (\text{Feynman gauge})$$

Figure 19: *QCD Feynman rules for quark and gluon propagators.*

The quark-gluon coupling above does not exhaust QCD interactions, though. In a theory of multiple vector particles such as QCD the vector particles turn out to necessarily be self-interacting. The reason for this lies with the non-abelian nature of the color

charges, i.e., with the nonzero commutator (6.2). The origin and precise form of the gluon self-couplings can specifically be traced back to the form of the gauge transformations in QCD and relationship between potentials and fields.

Electromagnetism is invariant under gauge transformations given by changes of the four-potential  $A_\mu$  by an arbitrary four-gradient,

$$A_\mu \rightarrow A_\mu + \partial_\mu \lambda \quad (\text{QED}) \quad . \quad (6.8)$$

In QCD the gauge freedom involves an additional contribution, namely we can change  $A_\mu$  by a four-gradient and/or by a pure rotation of its color indices,

$$A_\mu^a \rightarrow A_\mu^a + \partial_\mu \lambda^a - g_s f^{abc} \lambda^b A_\mu^c \quad (\text{QCD}) \quad , \quad (6.9)$$

leaving physics invariant. Eq. (6.9) specifies the form of the gauge transformations in QCD. Because of the nonvanishing structure constants  $f^{abc}$ , while the field strength tensor  $F_{\mu\nu}$  in QED is given by

$$F_{\mu\nu} = \partial_\mu A_\nu - \partial_\nu A_\mu \quad (\text{QED}) \quad , \quad (6.10)$$

in QCD this acquires an extra term,

$$F_{\mu\nu}^a = \partial_\mu A_\nu^a - \partial_\nu A_\mu^a + g_s f^{abc} A_\mu^b A_\nu^c \quad (\text{QCD}) \quad . \quad (6.11)$$

It is precisely the extra term in  $F_{\mu\nu}^a$  in Eq. (6.11) which is responsible for producing gluon self-interactions when one constructs a gauge-invariant kinetic energy term for gluons by taking the square of  $F_{\mu\nu}^a$ , analogously to the case of photons. The square of  $F_{\mu\nu}^a$  in Eq. (6.11) gives rise to both cubic and quartic gluon self-interaction terms. The cubic term is proportional to  $g_s \times f$  and contains derivative couplings, while the quartic term is proportional to  $g_s^2 \times f^2$ , with no derivatives. Their precise form is given in Fig. 20.

$$\begin{aligned}
& \text{Cubic vertex: } g_s f^{abc} [g^{\mu\nu} (k-p)^\rho + g^{\nu\rho} (p-q)^\mu + g^{\rho\mu} (q-k)^\nu] \\
& \text{Quartic vertex: } -i g_s^2 f^{abc} f^{abc} (g^{\mu\rho} g^{\nu\sigma} - g^{\mu\sigma} g^{\nu\rho}) + \text{permutations}
\end{aligned}$$

Figure 20: *QCD Feynman rules for cubic and quartic gluon vertices.*

The construction above implies in particular that the coupling constant  $g_s$  in the gauge boson self-interaction vertices is one and the same as the coupling constant  $g_s$  in the quark-gluon interaction vertex. Later in the section we see a specific example showing that this equality of couplings is necessary for non-abelian gauge invariance to be satisfied.

## 6.2 Physical polarization states and ghosts

In this subsection we discuss implications of the non-abelian gauge symmetry by comparing features of photon and gluon polarization degrees of freedom. We start from examining gauge invariance in a simple example, the QCD analogue of Compton scattering, and contrast the case of QCD with the case of QED seen in Sec. 5.

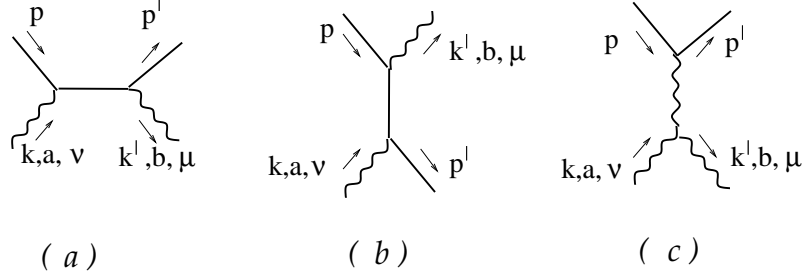


Figure 21: *Quark-gluon Compton scattering at lowest order in  $g_s$ .*

The QCD analogue of Compton scattering is the quark-gluon scattering depicted in Fig. 21 at lowest order in the coupling  $g_s$ . The graphs in Fig. 21(a) and (b) are analogous to the QED graphs of Fig. 16, while the three-gluon coupling graph in Fig. 21(c) is non-abelian. The scattering matrix element  $\mathcal{M}_{fi}$  can be written as

$$\mathcal{M}_{fi} = M_{\mu\nu} \varepsilon'^{\mu}(k') \varepsilon^{\nu}(k) . \quad (6.12)$$

From graphs (a) and (b) in Fig. 21 we have

$$M_{\mu\nu}^{(a)+(b)} = -ig_s^2 \bar{u}(p') \left[ \gamma_{\mu} T^b \frac{1}{\not{p} + \not{k} - m} \gamma_{\nu} T^a + \gamma_{\nu} T^a \frac{1}{\not{p} - \not{k}' - m} \gamma_{\mu} T^b \right] u(p) . \quad (6.13)$$

The sum of graphs (a) and (b) is not by itself gauge-invariant, because by dotting Eq. (6.13) into  $k^{\nu}$  we get

$$M_{\mu\nu}^{(a)+(b)} k^{\nu} = ig_s^2 [T^a, T^b] \bar{u}(p') \gamma_{\mu} u(p) , \quad (6.14)$$

which is nonvanishing due to the nonzero commutator of color charges.

From graph (c) in Fig. 21 we have

$$M_{\mu\nu}^{(c)} = g_s^2 \bar{u}(p') \gamma^{\rho} T^c u(p) \frac{1}{(k - k')^2} f^{abc} [g_{\nu\mu}(k + k')_{\rho} + g_{\mu\rho}(k - 2k')_{\nu} + g_{\rho\nu}(k' - 2k)_{\mu}] . \quad (6.15)$$

By dotting Eq. (6.15) into  $k^{\nu}$  we get

$$\begin{aligned} M_{\mu\nu}^{(c)} k^{\nu} &= g_s^2 f^{abc} T^c \bar{u}(p') \gamma_{\mu} u(p) + \{ \dots \} k'_{\mu} \\ &= -ig_s^2 [T^a, T^b] \bar{u}(p') \gamma_{\mu} u(p) + \{ \dots \} k'_{\mu} \end{aligned} \quad (6.16)$$

where in the last line we have used Eq. (6.2) to rewrite  $f^{abc} T^c$  in terms of the commutator. The second term in the right hand side of Eq. (6.16) is a term proportional to  $k'_{\mu}$ , which



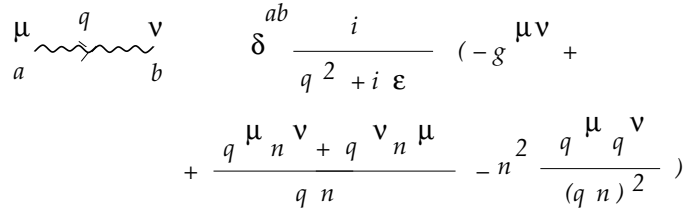


tive coupling in Fig. 22. Ghosts are a non-abelian effect. Their coupling is proportional to  $f^{abc}$ . We could introduce ghosts in electrodynamics, but they will just decouple.

It is possible to exploit the gauge freedom in order to devise a gauge-fixing condition such that the unphysical gluon polarizations are automatically eliminated, and thus no need arises for ghosts. Such gauges without ghosts are referred to as physical gauges, and are the gauges in which the non-abelian theory looks the most like its abelian counterpart. They are distinct from the covariant gauges based on the Lorentz gauge-fixing condition (3.12) in which we have worked so far. The gauge-fixing relation for physical gauges is given by assigning a four-vector  $n^\mu$  and setting

$$A_\mu^a n^\mu = 0 . \quad (6.18)$$

Physical gauges (6.18) present certain advantages, as they do not contain unphysical degrees of freedom. However, the form of the gluon propagator becomes rather more complicated in these gauges. This is given in Fig. 23.



$$\begin{aligned} & \delta^{ab} \frac{i}{q^2 + i\epsilon} \left( -g^{\mu\nu} + \right. \\ & \left. + \frac{q^\mu n^\nu + q^\nu n^\mu}{q \cdot n} - n^2 \frac{q^\mu q^\nu}{(q \cdot n)^2} \right) \end{aligned}$$

Figure 23: *Gluon propagator in physical gauge  $A \cdot n = 0$ .*

### 6.3 Color algebra

QCD calculations involve charge factors based on the color algebra in Eq. (6.2). We here introduce basic invariants of the algebra which occur in practical applications, the Casimir invariants  $C_R$  and the trace invariants  $T_R$ . The subscript  $R$  specifies the representation of the algebra (6.2).

The Casimir invariant can be defined from the square operator  $T^2 = T^a T^a$ . This operator commutes with all generators of the algebra (6.2),

$$\begin{aligned} [T^a T^a, T^b] &= T^a [T^a, T^b] + [T^a, T^b] T^a \\ &= i f^{abc} (T^a T^c + T^c T^a) = 0 \end{aligned} \quad (6.19)$$

where the last line vanishes due to  $f^{abc}$  being antisymmetric. This is analogous to the case of the algebra of angular momentum operators, where  $[J^2, J^i] = 0$ , and the eigenvalue of the square operator  $J^2$  is used to label different representations. In the case of the color charge operators, Eq. (6.19) implies that  $T^2$  takes a constant value on each representation, and the matrix representation of  $T^2$  is given by a constant  $C_R$  times the identity matrix,

$$T^a T^a = C_R \mathbf{1} . \quad (6.20)$$

Here  $\mathbf{1}$  is the identity matrix in  $n$  dimensions, where  $n$  is the dimensionality of the representation. The constant  $C_R$  is the Casimir invariant, and characterizes the specific representation.

The trace invariant can be defined from the trace of two generators,  $\text{Tr}(T^a T^b)$ , based on the fact that one can choose a basis such that this trace is proportional to  $\delta^{ab}$ ,

$$\text{Tr}(T^a T^b) = T_R \delta^{ab} . \quad (6.21)$$

The constant  $T_R$  is the trace invariant, specific to any given representation. Conventionally we normalize the color generators so that in the fundamental representation  $R = F$ , specified by the generator matrices (6.3), we have

$$T_F = \frac{1}{2} . \quad (6.22)$$

Once this is fixed, all other Casimir and trace invariants are determined in all representations. The normalization (6.22) for the color generators is analogous to that of the angular momentum generators in the spin-1/2 representation (2.3),  $J^i \rightarrow \sigma^i/2$ , for which

$$\text{Tr}(J^i J^j) = \frac{1}{2} \delta^{ij} . \quad (6.23)$$

The Casimir invariant  $C_R$  and the trace invariant  $T_R$  are related to each other, because if we multiply Eq. (6.21) by  $\delta^{ab}$  we get

$$\delta^{ab} \text{Tr}(T^a T^b) = T_R \delta^{ab} \delta^{ab} = T_R d , \quad (6.24)$$

where  $d = N^2 - 1$  is the number of generators, and therefore, using Eq. (6.20) to evaluate the left hand side of Eq. (6.24), we have

$$C_R n = T_R d . \quad (6.25)$$

Eq. (6.25) implies that the Casimir invariant for the fundamental representation  $R = F$ , for which  $n = N = 3$ , is given by

$$C_F = T_F \frac{d}{n} = \frac{N^2 - 1}{2N} = \frac{4}{3} , \quad (6.26)$$

where we have used Eq. (6.22). In the adjoint representation  $R = A$  specified by the generator matrices (6.4), for which  $n = N^2 - 1$ , Eq. (6.25) implies that the Casimir invariant and trace invariant are equal,  $C_A = T_A$ . By performing the explicit calculation we get

$$C_A = T_A = N = 3 . \quad (6.27)$$

We will see examples of QCD calculations involving the color factors above in Sec. 8.

## 7 Renormalization

So far we have considered tree-level effects, that is, Feynman graphs that do not contain loops. Loop corrections to processes described in earlier sections arise at higher orders of perturbation theory. For instance, the graph in Fig. 24 is an example of a loop correction to fermion pair production.

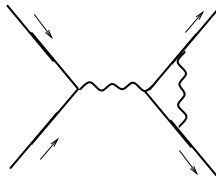


Figure 24: *Loop correction to fermion pair production.*

In this section we address loop effects. The part of the theory that deals with these effects is renormalization. We give an introduction to the idea of renormalization and its physical implications, discussing two specific examples: i) the renormalization of the electric charge; ii) the electron’s anomalous magnetic moment. In Sec. 8 we continue the discussion by introducing further concepts and including both electromagnetic and strong interactions.

### 7.1 General principles

While the treatment given so far specifies interaction processes at tree level, the method of renormalization is required to treat processes including loops.

A symptom that renormalization is required is that Feynman graphs with loops may give rise to integrals containing divergences from high-momentum regions. Renormalization allows one to give meaning to the occurrence of these ultraviolet divergences.

Ultraviolet power counting provides the basic approach to renormalization. For a Feynman graph involving a loop integral of the form

$$\int d^4k \frac{N(k)}{M(k)} , \quad (7.1)$$

consider the superficial degree of divergence defined as

$$D = \frac{\text{powers of } k \text{ in } N}{\text{powers of } k \text{ in } M} . \quad (7.2)$$

If  $D \geq 0$ , the integral is ultraviolet divergent. A first way of characterizing a theory as “renormalizable” is that the number of ultraviolet divergent amplitudes is finite. This is the case for instance with QED. There are 3 ultraviolet divergent amplitudes in QED, depicted in Fig. 25. QCD has a few more, due to the more complex structure of interactions seen in Sec. 6, but still a finite number. In a renormalizable theory there can of course be infinitely many Feynman graphs that are ultraviolet divergent, but they are so because they contain one of the few primitively divergent amplitudes as a subgraph.

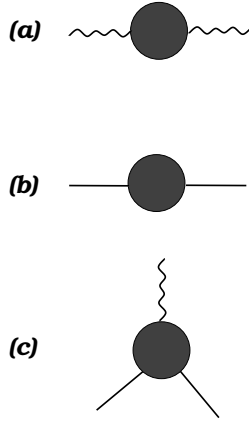


Figure 25: *Ultraviolet divergent amplitudes in QED: (a) photon self-energy; (b) electron self-energy; (c) electron-photon vertex.*

The main point about renormalizability is that it implies that all the ultraviolet divergences can be absorbed, according to a well-prescribed procedure specified below, into rescalings of the parameters and wave functions in the theory. For a given quantity  $\phi$ , the rescaling is of the form

$$\phi \rightarrow \phi_0 = Z \phi , \quad (7.3)$$

where  $\phi_0$  and  $\phi$  are respectively the unrenormalized and renormalized quantities, and  $Z$  is a calculable constant, into which the divergence can be absorbed. Here  $Z$  is the renormalization constant, possibly divergent but unobservable. Once the rescalings are done and the predictions of the theory are expressed in terms of renormalized quantities, all physical observables are finite and free of divergences.

This leads to a characterization of the renormalization program which we can formulate as a sequence of steps as follows.

- Compute the divergent amplitudes, by prescribing a “regularization method”. Examples of regularization methods are a cut-off  $\Lambda$  on the ultraviolet integration region, where the result diverges as we let  $\Lambda \rightarrow \infty$ , or, as we will see in explicit calculations later, dimensional regularization.
- Assign parameter and wave-function rescalings to eliminate divergences. In the case of QED, these involve the electromagnetic potential  $A$ , the electron wave function  $\psi$  and mass  $m$ , and the coupling  $e$ . Using traditional notation for the QED renormalization constants  $Z_i$ , the rescalings can be written as

$$\begin{aligned} A \rightarrow A_0 &= \sqrt{Z_3} A , \\ \psi \rightarrow \psi_0 &= \sqrt{Z_2} \psi , \\ m \rightarrow m_0 &= \frac{Z_m}{Z_2} m , \\ e \rightarrow e_0 &= \frac{Z_1}{Z_2 \sqrt{Z_3}} e . \end{aligned} \quad (7.4)$$

Here  $Z_3$  and  $Z_2$  are the respectively the renormalization constants for the photon and electron wave function,  $Z_1$  is the vertex renormalization constant and  $Z_m$  is the electron mass renormalization constant.

- Once the rescalings are done, all physical observables are calculable, i.e., unambiguously defined in terms of renormalized quantities, and free of divergences.

Theories for which this program succeeds in giving finite predictions for physical quantities are renormalizable theories. Non-renormalizable theories are theories in which one cannot absorb all divergences in a finite number of  $Z$ : for instance, as we go to higher orders new divergences appear and an infinite number of  $Z$  is needed.

The above program, while it appears quite abstract at first, gives in fact testable, measurable effects. In the next few subsections we see specific examples of this.

A further, general point is that gauge invariance places strong constraints on renormalization, implying relations among the divergent amplitudes of the theory, and thus among the renormalization constants. Here is an example for the case of QED. Gauge invariance establishes the following relation between the electron-photon vertex  $\Gamma_\mu$  dotted into the photon momentum  $q^\mu$  and the electron propagators  $S$ ,

$$q^\mu \Gamma_\mu = S^{-1}(p+q) - S^{-1}(p) . \quad (7.5)$$

Eq. (7.5), pictured in Fig. 26, is referred to as the Ward identity and is valid to all orders. Using the renormalization constants  $Z_1$  and  $Z_2$  defined by the rescalings in Eq. (7.4),

$$\Gamma^\mu = \frac{1}{Z_1} \gamma^\mu + \dots , \quad S(p) = \frac{Z_2}{\not{p} - m} + \dots , \quad (7.6)$$

we have

$$\frac{1}{Z_1} \not{q} = \frac{1}{Z_2} [(\not{p} + \not{q} - m) - (\not{p} - m)] . \quad (7.7)$$

Thus in the abelian case

$$Z_1 = Z_2 \quad (\text{QED}) . \quad (7.8)$$

As a result, the rescaling relation in Eq. (7.4) defining the renormalized coupling in QED becomes

$$e^2 = Z_3 e_0^2 . \quad (7.9)$$

That is, the renormalization of the electric charge is entirely determined by the renormalization constant  $Z_3$ , associated with the photon wave function, and does not depend on any other quantity related to the electron.

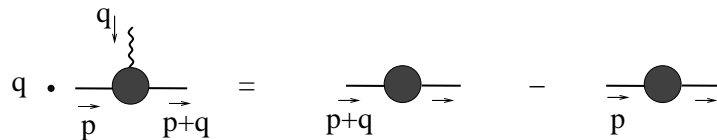


Figure 26: *Relation between electron-photon vertex and electron propagators.*

In the non-abelian case the relation (7.8) does not apply. However, it is still valid that non-abelian gauge invariance sets constraints on renormalization, leading to other, more complex relations among the renormalization constants. We will see examples of this in Sec. 8.3.

In the rest of this section we describe specific calculations of renormalization at one loop.

## 7.2 The gauge boson self-energy

Let us consider the gauge boson self-energy. This is one of the divergent amplitudes shown in Fig. 25. The Feynman graphs contributing to the self-energy through one loop are given in Fig. 27 for the photon and gluon cases. In the photon case one has the fermion loop graph only, while in the gluon case one has in addition gluon loop and ghost loop graphs.

Because of the relations (7.8),(7.9), in the QED case the calculation of the gauge boson self-energy is all that is needed to determine the renormalization of the coupling. So the result of this subsection will be used in Subsec. 7.3 to discuss the renormalized electric charge.

$$\begin{aligned}
 \text{QED:} \quad & \text{wavy line with a solid black circle} = \text{wavy line} + \text{wavy line with a white circle} + \dots \\
 \text{QCD:} \quad & \text{wavy line with a solid black circle} = \text{wavy line} + \left( \text{wavy line with a white circle} + \text{gluon loop} + \text{ghost loop} + \text{ghost loop} \right) + \dots
 \end{aligned}$$

Figure 27: (top) Photon and (bottom) gluon self-energy through one loop.

We now compute the fermion loop graph in Fig. 28. As shown in Fig. 27, in the QED case the fermion loop is all that contributes to the self-energy, while in the QCD case this gives one of the required contributions.

$$\begin{array}{c}
 \begin{array}{ccc}
 \mu, a & & \nu, b \\
 \text{wavy line} & \text{Feynman diagram: a circle with a fermion loop, incoming wavy line from left with momentum q and index \mu, a; outgoing wavy line to right with momentum q+k and index \nu, b; internal fermion lines with momenta k and q+k} & \\
 \xrightarrow{q} & & \xrightarrow{q+k}
 \end{array}
 \end{array} = i \pi \frac{a b}{\mu \nu} (q)$$

Figure 28: Fermion loop contribution to the gauge boson self-energy.

The graph in Fig. 28 is given by

$$i\pi_{\mu\nu}^{ab}(q) = -g^2 \text{Tr}(T^a T^b) \int \frac{d^4 k}{(2\pi)^4} \frac{\text{Tr}[\gamma_\mu(\not{k} + \not{q} + m)\gamma_\nu(\not{k} + m)]}{(k^2 - m^2 + i0^+)((k+q)^2 - m^2 + i0^+)} . \quad (7.10)$$

This expression is written in general for the non-abelian case. In this case the color-charge factor is evaluated from Eqs. (6.21),(6.22) and equals

$$\text{Tr}(T^a T^b) = \frac{1}{2} \delta^{ab} . \quad (7.11)$$

The QED case is obtained from Eq. (7.10) by taking

$$\begin{aligned} g^2 &\longrightarrow e^2 = 4\pi\alpha , \\ \text{Tr}(T^a T^b) &\longrightarrow 1 . \end{aligned} \quad (7.12)$$

The integral in Eq. (7.10) is ultraviolet divergent. By superficial power counting in the loop momentum  $k$ , the divergence is quadratic. Gauge invariance however requires that  $\pi_{\mu\nu}$  be proportional to the transverse projector  $g_{\mu\nu}q^2 - q_\mu q_\nu$ , that is,

$$\pi_{\mu\nu} = (g_{\mu\nu}q^2 - q_\mu q_\nu) \Pi(q^2) . \quad (7.13)$$

This reduces the degree of divergence by two powers of momentum. As a result, the divergence in Eq. (7.10) is not quadratic but logarithmic.

We need a regularization method to calculate the integral (7.10) and parameterize the divergence. We take the method of dimensional regularization. This consists of continuing the integral from 4 to  $d = 4 - 2\varepsilon$  dimensions by introducing the dimensionful mass-scale parameter  $\mu$  so that

$$g^2 \frac{d^4 k}{(2\pi)^4} \longrightarrow g^2(\mu^2)^\varepsilon \frac{d^{4-2\varepsilon} k}{(2\pi)^{4-2\varepsilon}} . \quad (7.14)$$

In dimensional regularization a logarithmic divergence  $d^4 k/k^4$  appears as a pole at  $\varepsilon = 0$  (i.e.,  $d = 4$ ). We thus identify ultraviolet divergences in the integral (7.10) by identifying poles in  $1/\varepsilon$ .

By carrying out the calculation in dimensional regularization, the result for  $\pi_{\mu\nu}$  is

$$\begin{aligned} \pi_{\mu\nu}^{ab}(q) &= - (g_{\mu\nu}q^2 - q_\mu q_\nu) \text{Tr}(T^a T^b) \frac{g^2}{4\pi^2} \Gamma(\varepsilon) \int_0^1 dx \left( \frac{4\pi\mu^2}{m^2 - x(1-x)q^2} \right)^\varepsilon 2x(1-x) \\ &\equiv (g_{\mu\nu}q^2 - q_\mu q_\nu) \Pi(q^2) . \end{aligned} \quad (7.15)$$

We can interpret the different factors in this result. As mentioned above, the first factor on the right hand side, consistent with the gauge-invariance requirement (7.13), implies that the gauge boson self-energy is purely transverse,

$$(g_{\mu\nu}q^2 - q_\mu q_\nu) q^\mu = (g_{\mu\nu}q^2 - q_\mu q_\nu) q^\nu = 0 . \quad (7.16)$$

Owing to the transversality of the self-energy, loop corrections do not give mass to gauge bosons in QED and QCD. The factor  $\text{Tr}(T^a T^b)$  in Eq. (7.15) is the non-abelian charge



factor, which just reduces to 1 in the QED case according to Eq. (7.12). Next,  $g^2/(4\pi^2)$  is the coupling factor, which becomes  $e^2/(4\pi^2) = \alpha/\pi$  in the QED case (7.12). The Euler gamma function  $\Gamma(\varepsilon)$  contains the logarithmic divergence, i.e., the pole at  $\varepsilon = 0$  ( $d = 4$ ) in dimensional regularization:

$$\Gamma(\varepsilon) = \frac{1}{\varepsilon} - C_E + \mathcal{O}(\varepsilon) \quad , \quad C_E \simeq .5772 \quad . \quad (7.17)$$

The first factor in the integrand of Eq. (7.15) results from the regularization method, depending on the ratio between the dimensional-regularization scale  $\mu^2$  and a linear combination of the physical mass scales  $m^2$  and  $q^2$ . The last factor in the integrand,  $2x(1-x)$ , depends on the details of the calculated Feynman graph.

We can extract the ultraviolet divergent part of the self-energy by computing the integral in Eq. (7.15) at  $q^2 = 0$ . Higher  $q^2$  powers in the expansion of  $\Pi(q^2)$  give finite contributions. We have

$$\begin{aligned} \Pi(0) &= -\text{Tr}(T^a T^b) \frac{g^2}{4\pi^2} \Gamma(\varepsilon) \int_0^1 dx \left( \frac{4\pi\mu^2}{m^2} \right)^\varepsilon 2x(1-x) \\ &\simeq -\text{Tr}(T^a T^b) \frac{g^2}{4\pi} \frac{1}{3\pi} \frac{1}{\varepsilon} + \dots \quad , \end{aligned} \quad (7.18)$$

where in the last line we have used the expansion (7.17) of the gamma function and computed the integral in  $dx$ . Specializing to the QED case according to Eq. (7.12) gives

$$\Pi(0) \simeq -\frac{\alpha}{3\pi} \frac{1}{\varepsilon} + \dots \quad (\text{QED}) \quad . \quad (7.19)$$

We will next use the results in Eqs. (7.15),(7.19) to discuss the renormalization of the electromagnetic coupling.

### 7.3 Renormalization of the electromagnetic coupling

Suppose we consider a physical process occurring via photon exchange, and ask what the effect is of the renormalization on the photon propagator. Fig. 29 illustrates this effect by multiple insertions of the photon self-energy,

$$D_0 \rightarrow D = D_0 + D_0 \pi D_0 + D_0 \pi D_0 \pi D_0 + \dots \quad , \quad (7.20)$$

where  $D_0$  is the photon propagator given in Fig. 8 and  $\pi$  is the photon self-energy computed in Eq. (7.15). We can sum the series in Eq. (7.20) by applying repeatedly the transverse projector in  $\pi$  and using that longitudinal contributions vanish by gauge invariance, and we get

$$D_0 \rightarrow D = D_0 \frac{1}{1 + \Pi(q^2)} \quad . \quad (7.21)$$

Then the effect of renormalization in the photon exchange process amounts to

$$\frac{e_0^2}{q^2} \longrightarrow \frac{e_0^2}{q^2} \frac{1}{1 - \Pi(q^2)} \quad , \quad (7.22)$$

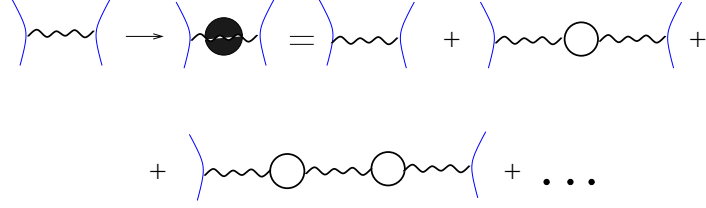


Figure 29: *Effect of renormalization in a photon exchange process.*

where  $q$  is the photon momentum.

Let us now rewrite the denominator on the right hand side of Eq. (7.22) by separating the divergent part and the finite part in  $\Pi$ . According to the discussion around Eq. (7.18), this can be achieved by

$$1 - \Pi(q^2) = [1 - \Pi(0)] \left[ 1 - (\Pi(q^2) - \Pi(0)) \right] + \mathcal{O}(\alpha^2) . \quad (7.23)$$

Therefore Eq. (7.22) gives

$$\begin{aligned} \frac{e_0^2}{q^2} &\longrightarrow \frac{e_0^2}{q^2} \frac{1}{1 - \Pi(q^2)} \\ &\simeq \underbrace{\frac{1}{q^2} \frac{e_0^2}{1 - \Pi(0)}}_{e^2 \equiv Z_3 e_0^2} \underbrace{\frac{1}{1 - [\Pi(q^2) - \Pi(0)]}}_{q^2\text{-dependence}} . \end{aligned} \quad (7.24)$$

In the last line of Eq. (7.24) we have underlined two distinct effects in the result we obtain from renormalization. The first is that the strength of the coupling is modified to

$$\frac{e_0^2}{1 - \Pi(0)} \equiv e^2 , \quad (7.25)$$

from which, by comparison with Eq. (7.9), we identify the renormalization constant  $Z_3$ :

$$\begin{aligned} Z_3 &\simeq 1 + \Pi(0) \\ &= 1 - \frac{\alpha}{3\pi} \frac{1}{\varepsilon} + \dots , \end{aligned} \quad (7.26)$$

where in the last line we have used the explicit result for  $\Pi(0)$  in Eq. (7.19). The coupling  $e$  in Eq. (7.25) is the physical coupling, that is, the renormalized coupling. This is obtained from the unrenormalized one,  $e_0$ , via a divergent, but unobservable, rescaling, according to the general procedure outlined below Eq. (7.3).

The second effect in Eq. (7.24) is that the coupling acquires a dependence on the momentum transfer  $q^2$ , controlled by the finite part of the self-energy,  $\Pi(q^2) - \Pi(0)$ . This dependence is free of divergences and observable. The  $q^2$ -dependence of the electromagnetic coupling is a new physical effect due to loop corrections. Using the explicit expression for  $\Pi$  in Eq. (7.15), we obtain that for low  $q^2$

$$\Pi(q^2) - \Pi(0) \rightarrow 0 \quad \text{for} \quad q^2 \rightarrow 0 , \quad (7.27)$$

and for high  $q^2$

$$\Pi(q^2) - \Pi(0) \simeq \frac{\alpha}{3\pi} \ln \frac{q^2}{m^2} \quad \text{for } q^2 \gg m^2 . \quad (7.28)$$

Thus  $e^2$  in Eq. (7.25) is the value of the coupling at  $q^2 = 0$ ; the coupling increases as  $q^2$  increases. Substituting Eqs. (7.25),(7.28) into Eq. (7.24) and rewriting it in terms of the fine structure, we have for large momenta

$$\alpha(q^2) = \frac{\alpha}{1 - (\alpha/(3\pi)) \ln(q^2/m^2)} . \quad (7.29)$$

The  $q^2$ -dependence of the coupling is referred to as running coupling. We will discuss this topic further in Sec. 8.

The result for the electromagnetic coupling that we have just found can be viewed as summing a series of perturbative large logarithms for  $q^2 \gg m^2$ . By expanding Eq. (7.29) in powers of  $\alpha$ , we have

$$\begin{aligned} \alpha(q^2) &= \frac{\alpha}{1 - (\alpha/(3\pi)) \ln(q^2/m^2)} \\ &= \alpha \left( 1 + \frac{\alpha}{3\pi} \ln \frac{q^2}{m^2} + \dots + \frac{\alpha^n}{(3\pi)^n} \ln^n \frac{q^2}{m^2} + \dots \right) . \end{aligned} \quad (7.30)$$

This is the simplest example of a conceptual framework referred to as resummation in QED and QCD. The point is that if the result (7.24) for the physical process is expressed in terms of an expansion in powers of  $\alpha$ , as in Eq. (7.30), perturbative coefficients to higher orders are affected by large logarithmic corrections. On the other hand, one obtains a well-behaved perturbation series, without large higher-order coefficients, if the result is expressed in terms of the effective charge  $\alpha(q^2)$ .

## 7.4 Vertex correction and anomalous magnetic moment

In this section we study the one-loop vertex correction of Fig. 30. In particular we compute its contribution to the electron's magnetic moment,

$$\boldsymbol{\mu} = g \frac{e}{2m} \mathbf{S} , \quad (7.31)$$

where  $\mathbf{S}$  is the spin operator and  $g$  is the gyromagnetic ratio. This computation gives

$$g = g_{\text{Dirac}} + \frac{\alpha}{\pi} + \mathcal{O}(\alpha^2) , \quad g_{\text{Dirac}} = 2 , \quad (7.32)$$

where  $g_{\text{Dirac}} = 2$  is the prediction from the Dirac equation and  $\alpha/\pi$  is the correction from the graph in Fig. 30. Higher order corrections arise from multi-loop graphs. The deviations from the Dirac value are referred to as the electron's anomalous magnetic moment.

Let us consider first the Dirac equation coupled to electromagnetism, Eq. (3.20), and write the magnetic interaction term explicitly. We can recast Eq. (3.20) in the two-component notation of Subsec. 2.4, including the electromagnetic coupling, as

$$E \begin{pmatrix} \chi \\ \phi \end{pmatrix} = \begin{pmatrix} m & \boldsymbol{\sigma} \cdot (\mathbf{p} - e\mathbf{A}) \\ \boldsymbol{\sigma} \cdot (\mathbf{p} - e\mathbf{A}) & -m \end{pmatrix} \begin{pmatrix} \chi \\ \phi \end{pmatrix} . \quad (7.33)$$

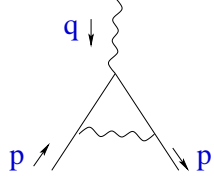


Figure 30: *One-loop vertex correction in QED.*

Now substitute the bottom equation in (7.33) into the top equation, use the Pauli  $\sigma$  matrix relation

$$\boldsymbol{\sigma} \cdot \mathbf{a} \boldsymbol{\sigma} \cdot \mathbf{b} = \mathbf{a} \cdot \mathbf{b} + i \boldsymbol{\sigma} \cdot \mathbf{a} \wedge \mathbf{b} , \quad (7.34)$$

and take the nonrelativistic limit  $E \simeq m$ , in which  $\phi \ll \chi$ . We then obtain that the action of the hamiltonian on the spinor  $\psi$  can be written as

$$H\psi \simeq \left( (\mathbf{p} - e\mathbf{A})^2 - \frac{e}{2m} \mathbf{B} \cdot 2\mathbf{S} \right) \psi , \quad (7.35)$$

where  $\mathbf{B} = \nabla \wedge \mathbf{A}$  is the magnetic field and  $\mathbf{S}$  is the spin operator given in terms of the  $\sigma$  matrices in Eq. (2.57). We recognize that the second term in the right hand side of Eq. (7.35) is the magnetic interaction

$$-\boldsymbol{\mu} \cdot \mathbf{B} , \quad \text{with } \boldsymbol{\mu} = \frac{e}{2m} 2\mathbf{S} . \quad (7.36)$$

That is, the Dirac equation prediction for the gyromagnetic ratio  $g$  in Eq. (7.31) is

$$g_{\text{Dirac}} = 2 . \quad (7.37)$$

Let us consider now the vertex function  $\Gamma^\nu(p, p')$  represented at one loop in Fig. 30. We can determine the general structure of the vertex function based on relativistic invariance and gauge invariance. Because  $\Gamma^\nu(p, p')$  transforms like a Lorentz vector, we can write it as a linear combination of  $\gamma^\nu$ ,  $p^\nu$ ,  $p'^\nu$ , or equivalently

$$\Gamma^\nu(p, p') = A \gamma^\nu + B(p + p')^\nu + C(p - p')^\nu , \quad (7.38)$$

where  $A$ ,  $B$  and  $C$  are scalar functions of  $q^2$  only ( $q = p' - p$ ).

Gauge invariance requires

$$q_\nu \Gamma^\nu = 0 . \quad (7.39)$$

By dotting  $q_\nu$  into Eq. (7.38), the term in  $B$  gives zero, and the term in  $A$  gives zero once it is sandwiched between  $\bar{u}(p')$  and  $u(p)$ . Thus  $C = 0$ . We can further show that the following identity holds,

$$\bar{u}(p') \gamma^\nu u(p) = \frac{1}{2m} \bar{u}(p') (p + p')^\nu u(p) + \frac{i}{m} \bar{u}(p') \Sigma^{\nu\rho} q_\rho u(p) , \quad (7.40)$$

where  $\Sigma$  is given in Eq. (2.28),  $\Sigma^{\nu\rho} \equiv (i/4) [\gamma^\nu, \gamma^\rho]$ . This implies that the term in  $(p + p')^\nu$  in Eq. (7.38) can be traded for a linear combination of a term in  $\gamma^\nu$  and a term in  $\Sigma^{\nu\rho} q_\rho$ . Therefore the vertex function can be decomposed in general as

$$\Gamma^\nu(p, p') = F_1(q^2) \gamma^\nu + \frac{i}{m} F_2(q^2) \Sigma^{\nu\rho} q_\rho , \quad (7.41)$$

where the scalar functions  $F_1(q^2)$  and  $F_2(q^2)$  are the electron's electric and magnetic form factors. At tree level,  $\Gamma^\nu = \gamma^\nu$ , thus  $F_1 = 1$  and  $F_2 = 0$ . In general,  $F_1$  and  $F_2$  receive radiative corrections from loop graphs and are related to the electron's charge and magnetic moment,

$$F_1(0) = Q \quad , \quad (7.42)$$

$$F_2(0) = \frac{g-2}{2} \quad , \quad (7.43)$$

where  $Q$  is the electron's charge in units of  $e$  and  $g$  is the electron's magnetic moment in units of  $(e/(2m))S$  where  $S$  is the electron spin.  $F_1(0)$  is 1 to all orders, that is, radiative corrections to  $F_1$  vanish at  $q^2 = 0$ . We next compute the correction to  $F_2(0)$  at one loop.

To this end, consider the one-loop graph in Fig. 30. This is given by

$$\bar{u}(p')ie\Gamma^\nu u(p) = e^3 \int \frac{d^4k}{(2\pi)^4} \frac{\bar{u}(p') \gamma^\lambda (\not{k} + \not{q} + m) \gamma^\nu (\not{k} + m) \gamma_\lambda u(p)}{[(k+q)^2 - m^2 + i\varepsilon] [k^2 - m^2 + i\varepsilon] [(p-k)^2 + i\varepsilon]} . \quad (7.44)$$

The integral in Eq. (7.44) can be handled starting with the following Feynman's parameterization of the three denominators in the integrand,

$$\begin{aligned} & \frac{1}{[(k+q)^2 - m^2 + i\varepsilon] [k^2 - m^2 + i\varepsilon] [(p-k)^2 + i\varepsilon]} \\ &= \int_0^1 dx_1 \int_0^1 dx_2 \int_0^1 dx_3 \frac{2 \delta(x_1 + x_2 + x_3 - 1)}{[x_1 ((k+q)^2 - m^2) + x_2 (k^2 - m^2) + x_3 (p-k)^2 + i\varepsilon]^3} \\ &= \int_0^1 dx_1 \int_0^1 dx_2 \int_0^1 dx_3 \frac{2 \delta(x_1 + x_2 + x_3 - 1)}{(\tilde{k}^2 - K + i\varepsilon)^3} , \end{aligned} \quad (7.45)$$

where in the last line we have set  $\tilde{k} = k + x_1 q - x_3 p$ ,  $K = m^2(1 - x_3)^2 - q^2 x_1 x_2$ .

Next change integration variable  $k \rightarrow \tilde{k}$  in Eq. (7.44), and note that the numerator in the integrand can be rewritten according to

$$\begin{aligned} & \gamma^\lambda (\not{k} + \not{q} + m) \gamma^\nu (\not{k} + m) \gamma_\lambda \\ &= \gamma^\nu [\tilde{k}^2 - 2q^2(1 - x_1)(1 - x_2) + 2m^2(4x_3 - 1 - x_3^2)] - 4mi\Sigma^{\nu\rho} q_\rho x_3(1 - x_3) . \end{aligned} \quad (7.46)$$

Then Eq. (7.44) can be recast in the form

$$\begin{aligned} \bar{u}(p')\Gamma^\nu u(p) &= -ie^2 \bar{u}(p') \int_0^1 dx_1 \int_0^1 dx_2 \int_0^1 dx_3 \frac{2 \delta(x_1 + x_2 + x_3 - 1)}{[\tilde{k}^2 - K]^3} \\ &\quad \times \int \frac{d^4\tilde{k}}{(2\pi)^4} \left[ \gamma^\nu \frac{\tilde{k}^2 - 2q^2(1 - x_1)(1 - x_2) - 2m^2(1 - 4x_3 + x_3^2)}{[\tilde{k}^2 - K]^3} \right. \\ &\quad \left. + \frac{i}{m} \Sigma^{\nu\rho} q_\rho \frac{-4m^2 x_3(1 - x_3)}{[\tilde{k}^2 - K]^3} \right] u(p) . \end{aligned} \quad (7.47)$$

Comparing Eq. (7.47) with the general decomposition in Eq. (7.41), we see that the two terms in the second and third line of Eq. (7.47) give one-loop integral representations for,

respectively, the form factors  $F_1(q^2)$  and  $F_2(q^2)$ . Let us concentrate on the calculation of  $F_2$ :

$$F_2(q^2) = -ie^2 \int_0^1 dx_1 \int_0^1 dx_2 \int_0^1 dx_3 \, 2 \, \delta(x_1 + x_2 + x_3 - 1) \\ \times \int \frac{d^4 \tilde{k}}{(2\pi)^4} \frac{-4m^2 x_3 (1 - x_3)}{[\tilde{k}^2 - K]^3} . \quad (7.48)$$

While the integral for  $F_1$  in Eq. (7.47) has divergences that need regularization, the integral (7.48) for  $F_2$  is finite. Let us compute the result for  $q^2 = 0$ .

The integration over the four-momentum  $\tilde{k}$  in Eq. (7.48) can be done by using the transformation of variables  $\tilde{k}^0 \rightarrow -e^{i\pi/2} \tilde{k}^0$  in the integral over the time component of the momentum. This yields the result

$$\int \frac{d^4 \tilde{k}}{(2\pi)^4} \frac{1}{[\tilde{k}^2 - K]^3} = -\frac{i}{32\pi^2 K} . \quad (7.49)$$

Then we have ( $e^2 = 4\pi\alpha$ )

$$F_2(0) = \frac{\alpha}{\pi} \int_0^1 dx_1 \int_0^1 dx_2 \int_0^1 dx_3 \, \delta(x_1 + x_2 + x_3 - 1) \frac{m^2 x_3 (1 - x_3)}{(1 - x_3)^2 m^2} \\ = \frac{\alpha}{\pi} \int_0^1 dx_3 \int_0^{1-x_3} dx_2 \frac{x_3}{1 - x_3} \\ = \frac{\alpha}{\pi} \int_0^1 dx_3 (1 - x_3) \frac{x_3}{1 - x_3} = \frac{\alpha}{2\pi} . \quad (7.50)$$

We thus obtain that the one-loop contribution to the electron's anomalous magnetic moment  $g - 2 = 2F_2(0)$  is given by

$$g - 2 = 2F_2(0) = \frac{\alpha}{\pi} . \quad (7.51)$$

## 8 Renormalization group

Let us discuss renormalization from the standpoint of the renormalization group. We have seen that renormalization introduces dependence on a renormalization scale  $\mu$  in loop calculations. As the value of  $\mu$  is arbitrary, physics must be invariant under changes in this scale. This invariance is expressed in a precise manner by the renormalization group. We will see that by studying the dependence on the renormalization scale  $\mu$  we gain insight into the asymptotic behavior of the theory at short distances.

### 8.1 Renormalization scale dependence and evolution equations

In this section we illustrate how the relation between renormalized and unrenormalized quantities, applied to a given physical quantity  $G$ , can be used to study the dependence on the renormalization scale  $\mu$  and to obtain renormalization group evolution equations.

Renormalizability implies that the divergent dependence in the unrenormalized quantity  $G_0$  can be factored out in the renormalization constant  $Z$ , provided we re-express renormalized  $G$  in terms of the renormalized coupling and renormalization scale  $\mu$ ,

$$G_0(p_i, \alpha_0) = ZG(p_i, \alpha, \mu) . \quad (8.1)$$

Here  $p_i$  is the set of physical momenta on which  $G$  depends,  $\alpha$  is the renormalized coupling and  $\alpha_0$  is the unrenormalized coupling. Because the left hand side in Eq. (8.1) does not depend on  $\mu$ ,

$$\frac{d}{d \ln \mu^2} G_0 = 0 , \quad (8.2)$$

we have

$$\frac{d}{d \ln \mu^2} (ZG) = 0 \implies \frac{\partial G}{\partial \ln \mu^2} + \frac{\partial G}{\partial \alpha} \frac{\partial \alpha}{\partial \ln \mu^2} + \frac{\partial \ln Z}{\partial \ln \mu^2} G = 0 . \quad (8.3)$$

By defining

$$\beta(\alpha) = \frac{\partial \alpha}{\partial \ln \mu^2} , \quad (8.4)$$

$$\gamma(\alpha) = \frac{\partial \ln Z}{\partial \ln \mu^2} , \quad (8.5)$$

we can rewrite Eq. (8.3) as

$$\left[ \frac{\partial}{\partial \ln \mu^2} + \beta(\alpha) \frac{\partial}{\partial \alpha} + \gamma(\alpha) \right] G(p_i, \alpha, \mu) = 0 , \quad (8.6)$$

where  $\beta(\alpha)$  and  $\gamma(\alpha)$  are calculable functions of  $\alpha$ .

Suppose we measure  $G$  at a physical mass-scale  $Q$ . Let us rescale by  $Q$  the arguments in  $G$  and set

$$G(p_i, \alpha, \mu) = F(x_i, t, \alpha) , \quad (8.7)$$

where

$$x_i = \frac{p_i}{Q} , \quad t = \ln \frac{Q^2}{\mu^2} . \quad (8.8)$$

In this notation Eq. (8.6) can be written as

$$\left[ -\frac{\partial}{\partial t} + \beta(\alpha) \frac{\partial}{\partial \alpha} + \gamma(\alpha) \right] F(t, \alpha) = 0 \quad , \quad (8.9)$$

where from now on we will not write explicitly the dependence on the rescaled physical momenta  $x_i$  in  $F$ .

Eq. (8.9) is the renormalization group evolution equation, which we can solve with boundary condition  $F(0, \alpha)$  at  $t = 0$ , i.e.,  $\mu = Q$ . To do this, we first write the solution for the case  $\gamma = 0$  and then generalize this solution to any  $\gamma$ .

For  $\gamma = 0$  we have

$$\left[ -\frac{\partial}{\partial t} + \beta(\alpha) \frac{\partial}{\partial \alpha} \right] F(t, \alpha) = 0 \quad (\gamma = 0) \quad . \quad (8.10)$$

Now observe that if we construct  $\alpha(t)$  such that

$$t = \int_{\alpha}^{\alpha(t)} \frac{d\alpha'}{\beta(\alpha')} \quad , \quad (8.11)$$

then any  $F$  of the form

$$F(t, \alpha) = F(0, \alpha(t)) \quad (8.12)$$

satisfies the equation and the boundary condition.

Eq. (8.11) defines  $\alpha(t)$  as an implicit function. To verify that Eq. (8.12) is solution, note first that the boundary condition at  $t = 0$  is

$$t = 0 \quad , \quad \alpha(0) = \alpha \quad \implies \quad F = F(0, \alpha) \quad . \quad (8.13)$$

Next evaluate the derivative of Eq. (8.11) with respect to  $t$ ,

$$1 = \frac{1}{\beta(\alpha(t))} \frac{\partial \alpha(t)}{\partial t} \quad , \quad (8.14)$$

and with respect to  $\alpha$ ,

$$0 = \frac{1}{\beta(\alpha(t))} \frac{\partial \alpha(t)}{\partial \alpha} - \frac{1}{\beta(\alpha)} \quad . \quad (8.15)$$

Then the differential operator in Eq. (8.10) applied to  $F(0, \alpha(t))$  gives

$$\begin{aligned} & \left[ -\frac{\partial}{\partial t} + \beta(\alpha) \frac{\partial}{\partial \alpha} \right] F(0, \alpha(t)) \\ &= -\frac{\partial F}{\partial \alpha(t)} \left[ \underbrace{\frac{\partial \alpha(t)}{\partial t}}_{\beta(\alpha(t))} - \beta(\alpha) \underbrace{\frac{\partial \alpha(t)}{\partial \alpha}}_{\beta(\alpha(t))/\beta(\alpha)} \right] = 0 \quad , \end{aligned} \quad (8.16)$$

where in the last line we have used Eqs. (8.14),(8.15).



In the general case  $\gamma \neq 0$ , the solution to Eq. (8.9) is obtained from the  $\gamma = 0$  answer (8.12) by multiplication by the exponential of a  $\gamma$  integral, as follows

$$\begin{aligned} F(t, \alpha) &= F(0, \alpha(t)) \exp \left[ \int_{\alpha}^{\alpha(t)} d\alpha' \frac{\gamma(\alpha')}{\beta(\alpha')} \right] \\ &= F(0, \alpha(t)) \exp \left[ \int_0^t dt' \gamma(\alpha(t')) \right] . \end{aligned} \quad (8.17)$$

In the second line in Eq. (8.17) we have made the integration variable transformation using Eq. (8.11). We can verify that Eq. (8.17) is solution by a method similar to that employed above for the case  $\gamma = 0$ .

Eq. (8.17) indicates that once ultraviolet divergences are removed through renormalization, all effects of varying the scale in  $F$  from  $\mu$  to  $Q$  can be taken into account by i) replacing  $\alpha$  by  $\alpha(t)$ , and ii) including the  $t$ -dependence given by the exponential factor in  $\gamma$ . The latter factor breaks scaling in  $t$ , modifying the “engineering” dimensions of  $F$  by  $\gamma$ -dependent terms. For this reason  $\gamma$  is referred to as anomalous dimension. By expanding the exponential factor in powers of the coupling, we see that this factor sums terms of the type  $(\alpha t)^n$  to all orders in perturbation theory. Eq. (8.17) thus provides a second example, besides that seen in Eq. (7.30) for the electric charge, of perturbative resummation of logarithmic corrections to all orders in the coupling, giving rise to an improved perturbation expansion, in which coefficients of higher order are free of large logarithms.

In QCD the  $e^+e^-$  annihilation cross section  $\sigma(e^+e^- \rightarrow \text{hadrons})$  is an example of the  $\gamma = 0$  case in Eq. (8.12), while deep-inelastic scattering structure functions are an example of the  $\gamma \neq 0$  case in Eq. (8.17).

## 8.2 RG interpretation of the photon self-energy

Let us revisit the analysis of the photon self-energy in Sec. 7 from the standpoint of the renormalization group. The divergent part of the renormalization constant  $Z_3$  computed in Eq. (7.26) determines the QED  $\beta$  function at one loop.

According to Eq. (8.4), the variation of the coupling  $\alpha$  with the energy scale  $\mu$  is governed by the  $\beta$  function, calculable as a function of  $\alpha$ . In dimensional regularization, from

$$\alpha(\mu^2)^\varepsilon = Z_3 \alpha_0 , \quad (8.18)$$

by using Eq. (7.26) we have

$$\begin{aligned} \frac{\partial \alpha}{\partial \ln \mu^2} &= -\varepsilon \left( 1 - \frac{\alpha}{3\pi} \frac{1}{\varepsilon} \right) \alpha_0 (\mu^2)^{-\varepsilon} \\ &= \frac{1}{3\pi} \alpha^2 . \end{aligned} \quad (8.19)$$

The leading term of the QED  $\beta$  function at small coupling is given by (Fig. 31),

$$\begin{aligned} \beta(\alpha) &= b\alpha^2 + \mathcal{O}(\alpha^3) , \\ b &= \frac{1}{3\pi} . \end{aligned} \quad (8.20)$$

Inserting the result (8.20) into Eq. (8.4) gives the differential equation

$$\frac{\partial \alpha}{\partial \ln \mu^2} = b \alpha^2 . \quad (8.21)$$

This can be solved by

$$\frac{d\alpha}{\alpha^2} = b \frac{d\mu^2}{\mu^2} \implies -\frac{1}{\alpha(q^2)} + \frac{1}{\alpha} = b \ln \frac{q^2}{q_0^2} , \quad (8.22)$$

which gives

$$\alpha(q^2) = \frac{\alpha}{1 - b\alpha \ln(q^2/q_0^2)} , \quad b = 1/(3\pi) , \quad (8.23)$$

that is, the result (7.29) derived directly in Subsec. 7.3.

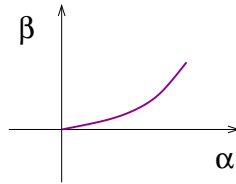


Figure 31: *Small-coupling approximation to the  $\beta$  function in QED.*

To sum up, we have found from the analysis of electric charge renormalization in Sec. 7.3 and in this section that as a result of loop graphs the electromagnetic coupling is energy-dependent. We can regard this result as illustrating the breaking of scale invariance as an effect of the quantum corrections taken into account by renormalization. We start at tree level with a coupling that is scale invariant. Then we include loops. This implies introducing an unphysical mass scale, such as the renormalization scale  $\mu$ , to treat quantum fluctuations at short distances, or high momenta. At the end of the calculation in the renormalized theory, the unphysical mass scale disappears from physical quantities. But an observable, physical effect from including loop corrections remains in the fact that scale invariance is broken. The physical coupling depends on the energy scale at which we probe the interaction. The renormalization group provides the appropriate framework to describe this phenomenon, in which the rescalings (7.4) of the couplings and wave functions, necessary to compensate variations in the arbitrary renormalization scale, are governed by universal functions, respectively the  $\beta$  and  $\gamma$  functions (8.4),(8.5) of the theory.

### 8.3 QCD $\beta$ function at one loop

We now extend the discussion to the case of renormalization in QCD at one loop, and determine the one-loop  $\beta$  function.

In the QCD case we assign rescaling relations analogous to those in Eq. (7.4) for the abelian theory. For wave function and mass renormalization we set

$$A \rightarrow A_0 = \sqrt{Z_3} A ,$$

$$\begin{aligned}
\psi \rightarrow \psi_0 &= \sqrt{Z_2} \psi , \\
c \rightarrow c_0 &= \sqrt{\tilde{Z}_3} c , \\
m \rightarrow m_0 &= \frac{Z_m}{Z_2} m .
\end{aligned} \tag{8.24}$$

where, in addition to the renormalization constants of the abelian case, we introduce  $\tilde{Z}_3$  for ghost renormalization. For renormalization of quark-gluon, ghost-gluon and gluon self-coupling vertices we set

$$\begin{aligned}
Z_2 \sqrt{Z_3} g_0 &= Z_1 g , \\
\tilde{Z}_3 \sqrt{Z_3} g_0 &= \tilde{Z}_1 g , \\
Z_3^{3/2} g_0 &= Z_{1,3} g , \\
Z_3^2 g_0^2 &= Z_{1,4} g .
\end{aligned} \tag{8.25}$$

As noted in Sec. 6.2, non-abelian gauge invariance requires that the vertices have equal couplings. This implies relations among the different  $Z$  in Eq. (8.25), as follows

$$\frac{\tilde{Z}_1}{\tilde{Z}_3} = \frac{Z_1}{Z_2} = \frac{Z_{1,3}}{Z_3} = \sqrt{\frac{Z_{1,4}}{Z_3}} . \tag{8.26}$$

In the non-abelian theory, unlike QED, in general one has  $Z_1 \neq Z_2$ . The relations in Eq. (8.26) can be seen as non-abelian generalizations of the QED result  $Z_1 = Z_2$  given in Eq. (7.8).

We can define the renormalized coupling from the quark-gluon vertex. The analogue of Eq. (8.18) for the QCD case is

$$\alpha_s (\mu^2)^\varepsilon = \frac{Z_2^2}{Z_1^2} Z_3 \alpha_{s0} . \tag{8.27}$$

Each of the renormalization constants  $Z_i$  has a perturbation series expansion, with the coefficients of the expansion being ultraviolet divergent. In dimensional regularization the ultraviolet divergences appear as poles at  $\varepsilon = 0$ , so that the  $Z_i$  have the form

$$Z_i = 1 + \alpha_s \frac{1}{\varepsilon} c_i + \text{finite} , \tag{8.28}$$

where the coefficients  $c_i$  of the divergent terms are to be calculated. By using Eqs. (8.27) and (8.28), the  $\beta$  function is given by

$$\begin{aligned}
\beta(\alpha_s) &= \frac{\partial \alpha_s}{\partial \ln \mu^2} \\
&= -\varepsilon \alpha_B (\mu^2)^{-\varepsilon} [1 - 2(Z_1 - 1) + 2(Z_2 - 1) + (Z_3 - 1)] \\
&= 2\alpha_s^2 (c_1 - c_2 - \frac{1}{2} c_3) .
\end{aligned} \tag{8.29}$$

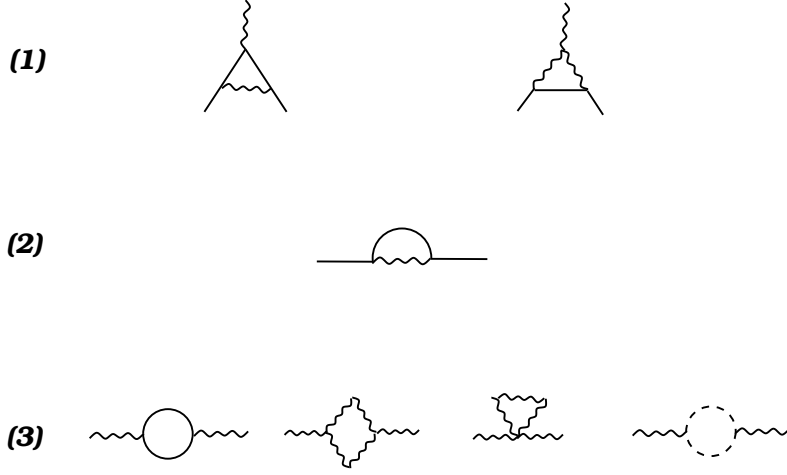


Figure 32: *One-loop corrections to (1) quark-gluon vertex; (2) quark self-energy; (3) gluon self-energy.*

The Feynman graphs contributing to  $c_1$ ,  $c_2$  and  $c_3$  are the one-loop graphs for, respectively, the quark-gluon vertex renormalization, quark self-energy renormalization, and gluon self-energy renormalization, and they are shown in Fig. 32. The calculation of these graphs proceeds similarly to the calculation done in Sec. 7.2 for the fermion loop contribution. By computing these graphs, working in Feynman gauge  $\xi = 1$  (as in Fig. 19), we obtain the results for the renormalization constants  $Z_i$ ,

$$Z_1 = 1 - \frac{\alpha_s}{4\pi} \frac{1}{\varepsilon} (C_F + C_A) , \quad (8.30)$$

$$Z_2 = 1 - \frac{\alpha_s}{4\pi} \frac{1}{\varepsilon} C_F , \quad (8.31)$$

$$Z_3 = 1 + \frac{\alpha_s}{4\pi} \frac{1}{\varepsilon} \left( \frac{5}{3} C_A - \frac{4}{3} N_f T_F \right) , \quad (8.32)$$

where  $N_f$  is the number of quark flavors (Sec. 6.1), and the color charge factors are given in Sec. 6.3,

$$C_A = N = 3 , \quad C_F = \frac{N^2 - 1}{2N} = \frac{4}{3} , \quad T_F = \frac{1}{2} . \quad (8.33)$$

Note from the expression for  $Z_3$  that the second term in the bracket in Eq. (8.32) is the term computed in Sec. 7.2 from the fermion loop graph, which, in the abelian limit  $N_f T_F \rightarrow 1$ , gives the QED contribution  $-\alpha/(3\pi\varepsilon)$  of Eq. (7.26).

From Eqs. (8.30)-(8.32) we read the coefficients  $c_i$  to be put into Eq. (8.29) to determine the  $\beta$  function. We obtain

$$\begin{aligned} \beta(\alpha_s) &= 2\alpha_s^2 \left( c_1 - c_2 - \frac{1}{2} c_3 \right) = 2 \frac{\alpha_s^2}{4\pi} \left( -C_F - C_A + C_F - \frac{1}{2} \frac{5}{3} C_A + \frac{1}{2} \frac{4}{3} N_f T_F \right) \\ &= \frac{\alpha_s^2}{4\pi} \left( -\frac{11}{3} C_A + \frac{4}{3} N_f T_F \right) = -\frac{\alpha_s^2}{12\pi} (11N - 2N_f) . \end{aligned} \quad (8.34)$$

Eq. (8.34) shows that for  $N_f < 11N/2$  the  $\beta$  function in the non-abelian case has negative sign at small coupling (Fig. 33),

$$\beta(\alpha_s) = -\beta_0 \alpha_s^2 + \mathcal{O}(\alpha_s^3) , \quad (8.35)$$

where

$$\beta_0 = \frac{1}{12\pi}(11N - 2N_f) . \quad (8.36)$$

This behavior of the  $\beta$  function is opposite to the behavior of the  $\beta$  function in QED, Eq. (8.20) (Fig. 31).

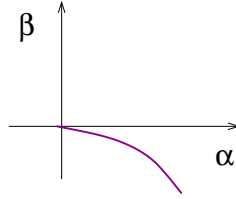


Figure 33: *Small-coupling approximation to the  $\beta$  function in QCD.*

The behavior of the  $\beta$  function in Eqs. (8.35),(8.36) implies that QCD is asymptotically free, i.e., weakly coupled at short distances. By inserting Eq. (8.35) into the renormalization group evolution equation,

$$\frac{\partial \alpha_s}{\partial \ln \mu^2} = \beta(\alpha_s) \simeq -\beta_0 \alpha_s^2 , \quad (8.37)$$

and solving Eq. (8.37), we obtain

$$\alpha_s(q^2) = \frac{\alpha_s(\mu^2)}{1 + \beta_0 \alpha_s(\mu^2) \ln q^2/\mu^2} , \quad (8.38)$$

where  $\beta_0$  is given in Eq. (8.36). Eq. (8.38) expresses the  $q^2$ -dependence of the QCD running coupling at one loop. The QCD coupling decreases logarithmically as the momentum scale  $q^2$  increases. This property is the basis for the perturbative calculability of scattering processes due to strong interactions at large momentum transfers.

## 8.4 The QCD scale $\Lambda$

From Eq. (8.38) we also see that QCD becomes strongly coupled in the infrared, low-momentum region. This behavior is opposite to that in QED. In the QED case, taking  $q_0 \sim m$  in Eq. (8.23), with  $m$  the electron mass, we have strong coupling in the ultraviolet region for

$$q^2 \sim m^2 e^{3\pi/\alpha} , \quad (8.39)$$

corresponding to enormously high energies.

In the QCD case, calling  $\Lambda$  the mass scale at which the denominator in Eq. (8.38) vanishes, we have

$$1 + \beta_0 \alpha_s(\mu^2) \ln \frac{\Lambda^2}{\mu^2} = 0 \implies \Lambda^2 = \mu^2 e^{-1/(\beta_0 \alpha_s(\mu^2))} . \quad (8.40)$$

In QED and QCD we thus get the different pictures in Fig. 34 for the scale, referred to as the Landau pole, at which the coupling becomes strong.

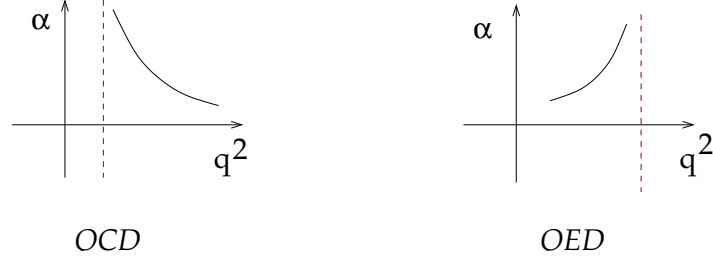


Figure 34: *Landau pole pictures in QCD and in QED.*

The scale  $\Lambda$  in Eq. (8.40) is renormalization-group invariant, i.e., it is independent of  $\mu$ . Under transformations

$$\begin{aligned}\mu^2 &\longrightarrow \mu'^2 = \mu^2 e^t, \\ \alpha_s(\mu^2) &\longrightarrow \alpha_s(\mu'^2) = \frac{\alpha_s(\mu^2)}{1 + \beta_0 \alpha_s(\mu^2) t},\end{aligned}\quad (8.41)$$

we have

$$\begin{aligned}\Lambda^2 &\longrightarrow \mu'^2 e^{-1/(\beta_0 \alpha_s(\mu'^2))}, \\ &= \mu^2 e^t e^{-(1+\beta_0 \alpha_s(\mu^2)t)/(\beta_0 \alpha_s(\mu^2))} = \mu^2 e^t e^{-1/(\beta_0 \alpha_s(\mu^2))} e^{-t} = \Lambda^2.\end{aligned}\quad (8.42)$$

The scale  $\Lambda$  is a physical mass scale of the theory of strong interaction. Its measured value is about 200 MeV.

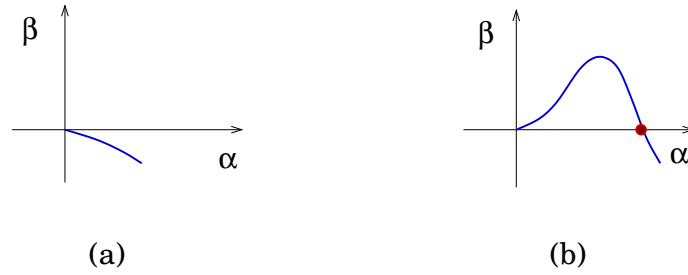


Figure 35: *(a) Trivial and (b) nontrivial ultraviolet fixed points of the  $\beta$  function.*

The running coupling (8.38) can be equivalently expressed in terms of  $\Lambda$ ,

$$\begin{aligned}\alpha_s(q^2) &= \frac{\alpha_s(\mu^2)}{1 + \beta_0 \alpha_s(\mu^2) [\ln(q^2/\Lambda^2) - 1/(\beta_0 \alpha_s(\mu^2))]} \\ &= \frac{1}{\beta_0 \ln(q^2/\Lambda^2)}.\end{aligned}\quad (8.43)$$

The rewriting (8.43) of Eq. (8.38) makes it manifest that the running coupling  $\alpha_s$  does not depend on the choice of the renormalization scale  $\mu$ .

*Remark.* The zero of the QCD  $\beta$  function at the origin, sketched in Fig. 35a, is responsible for the theory being weakly coupled at short distances. This behavior is referred to as a trivial ultraviolet fixed point. A behavior such as that in Fig. 35b (nontrivial ultraviolet fixed point), leading to strong coupling at short distances, is in principle possible but not realized in nature as far as we know. This is the reason why renormalization can be understood perturbatively and Feynman graphs provide a very effective method to investigate physical theories of fundamental interactions.

## Acknowledgments

I thank the School Director, Mark Thomson, and the School Administrators, Gill Birch and Jacqui Graham, for the excellent organization and for making this School a very pleasant event. I am grateful to the other members of the teaching staff and to the students for the nice atmosphere at the School and for interesting conversations. Many thanks to Nick Evans for providing teaching material from past editions of the School and for advice on the content of this course.



## References

- [1] J D Bjorken and S D Drell, *Relativistic Quantum Mechanics*, McGraw-Hill 1964  
I J R Aitchison and A J G Hey, *Gauge theories in particle physics*, 2nd edition Adam Hilger 1989  
F Halzen and A D Martin, *Quarks and Leptons*, Wiley 1984
- [2] M E Peskin and D V Schroeder, *An Introduction to Quantum Field Theory*, Addison Wesley 1995  
F Mandl and G Shaw, *Quantum Field Theory*, Wiley 1984  
C Itzykson and J-B Zuber, *Quantum Field Theory*, McGraw-Hill 1987



# THE STANDARD MODEL

**Chris Maxwell**

Institute for Particle Physics Phenomenology, Durham University, Durham DH1 3LE, U.K.

Lectures presented at the School for Young High Energy Physicists,  
Somerville College, Oxford, September 2010.



## Contents

<b>1</b>	<b>Abelian and non-Abelian local gauge theories.....</b>	<b>121</b>
1.1	QED Lagrangian from local gauge invariance .....	121
1.2	The Non-Abelian Recipe Book.....	122
1.3	The Lagrangian of QCD.....	125
<b>2</b>	<b>Glashow's Model <math>SU(2)_L \times U(1)_Y</math>.....</b>	<b>126</b>
2.1	Kinetic Energy Terms for Glashow's Model.....	130
<b>3</b>	<b>The Higgs Mechanism for <math>SU(2)_L \times U(1)_Y</math>.....</b>	<b>132</b>
3.1	Yukawa terms for lepton masses.....	135
3.2	Electroweak quark sector.....	136
3.3	SM Lagrangian and independent parameter count.....	138
	<b>Acknowledgements .....</b>	<b>139</b>
<b>4</b>	<b>Appendix of Feynman rules .....</b>	<b>140</b>



# 1 Abelian and non-Abelian local gauge theories

The Standard Model is based on a product of groups  $SU(3)_c \times SU(2)_L \times U(1)_Y$ , describing QCD, the chiral  $SU(2)_L$  electroweak sector and the hypercharge  $U(1)_Y$  sector in which QED is embedded. The first two of these groups are non-abelian, and are based on non-commuting group generators. The final group is abelian. We shall review in what follows how such gauge theories can be constructed from the principle of local gauge invariance, beginning with the simplest case of QED, and generalising this recipe to the construction of the non-abelian  $SU(N)$  theories.

## 1.1 QED Lagrangian from local gauge invariance

The QED Lagrangian can be defined more fundamentally by demanding **local gauge invariance**. The Dirac Lagrangian

$$\mathcal{L}_{Dirac} = i\bar{\psi}\gamma^\mu\partial_\mu\psi - m\bar{\psi}\psi, \quad (1.1)$$

has an obvious invariance under the **global** gauge transformation

$$\psi(x) \rightarrow \psi'(x) = e^{i\alpha}\psi(x), \quad \bar{\psi}(x) \rightarrow \bar{\psi}'(x) = e^{-i\alpha}\bar{\psi}(x), \quad (1.2)$$

where the phase  $i\alpha$  is independent of spacetime position  $x$ . Each term is simply multiplied by  $e^{i\alpha}e^{-i\alpha} = 1$ . **Local** gauge invariance corresponds to demanding invariance with phases  $i\alpha(x)$  which are chosen independently at each spacetime point.

$$\psi(x) \rightarrow \psi'(x) = e^{i\alpha(x)}\psi(x), \quad \bar{\psi}(x) \rightarrow \bar{\psi}'(x) = e^{-i\alpha(x)}\bar{\psi}(x). \quad (1.3)$$

One now finds that local gauge invariance does not hold since

$$\begin{aligned} i\bar{\psi}(x)\gamma^\mu\partial_\mu\psi(x) &\rightarrow i\bar{\psi}(x)e^{-i\alpha(x)}\gamma^\mu\partial_\mu[e^{i\alpha(x)}\psi(x)] \\ &= i\bar{\psi}(x)\gamma^\mu\partial_\mu\psi(x) - \bar{\psi}(x)\gamma^\mu\psi(x)[\partial_\mu\alpha(x)]. \end{aligned} \quad (1.4)$$

The  $\partial_\mu\alpha(x)$  term violates the local gauge invariance. The resolution is that one needs to replace the ordinary derivative  $\partial_\mu$  by the **covariant derivative**  $D_\mu$ . To ensure local gauge invariance one needs to ensure that under a gauge transformation  $D_\mu\psi(x)$  transforms in exactly the same way as  $\psi(x)$  itself. It is in this sense that one has a “covariant derivative”.

$$D_\mu \psi(x) \rightarrow D'_\mu \psi'(x) = e^{i\alpha(x)}(D_\mu \psi(x)) . \quad (1.5)$$

This transformation rule holds if we define the covariant derivative

$$D_\mu \equiv \partial_\mu + ieA_\mu , \quad (1.6)$$

where under a local gauge transformation the **gauge field**  $A_\mu$  transforms as

$$A_\mu \rightarrow A'_\mu = A_\mu - \frac{1}{e} \partial_\mu \alpha(x) . \quad (1.7)$$

The gauge transformation of  $A_\mu$  is exactly the same as the classical EM transformation, but the idea will be that the covariant derivative  $D_\mu$  and gauge fields  $A_\mu$  can provide a general recipe for constructing general non-abelian gauge theories. Having changed  $\partial_\mu$  to  $D_\mu$ , and adding in the “kinetic energy” term  $-\frac{1}{4}F_{\mu\nu}F^{\mu\nu}$  one has the QED Lagrangian

$$\begin{aligned} \mathcal{L}_{QED} &= \frac{1}{4}F_{\mu\nu}F^{\mu\nu} + i\bar{\psi}\gamma^\mu D_\mu \psi - m\bar{\psi}\psi \\ &= \frac{1}{4}F_{\mu\nu}F^{\mu\nu} + i\bar{\psi}\gamma^\mu \partial_\mu \psi - e\bar{\psi}\gamma^\mu \psi A_\mu - m\bar{\psi}\psi . \end{aligned} \quad (1.8)$$

Crucially  $F_{\mu\nu}$  can be defined in terms of the commutator of covariant derivatives,  $D_\mu$ . This involves introducing a “gauge comparator” and is analogous to parallel transport in General Relativity. The definition is

$$[D_\mu, D_\nu]\psi \equiv ieF_{\mu\nu}\psi . \quad (1.9)$$

In the case of abelian QED one finds the classical EM result

$$F_{\mu\nu} = \partial_\mu A_\nu - \partial_\nu A_\mu . \quad (1.10)$$

How does this generalise to non-Abelian gauge groups ?

## 1.2 The Non-Abelian Recipe Book

Local gauge transformations will be of the form

$$\psi(x) \rightarrow \psi'(x) = U(x)\psi(x) \quad , \quad \bar{\psi}(x) \rightarrow \bar{\psi}'(x) = \bar{\psi}(x)U^{-1}(x) . \quad (1.11)$$

Here  $U(x)$  denotes an element of the gauge group  $\mathcal{G}$  chosen independently at each spacetime point. In the case of QED  $\mathcal{G} = U(1)$  the group of  $1 \times 1$  unitary ( $MM^\dagger = I$ ) matrices (complex phases). We shall be interested in the non-Abelian Lie groups  $SU(N)$  of  $N \times N$  unitary matrices with  $\det U = 1$ . An element of such a Lie Group will have the form



$$U(x) = \exp(i \sum_{j=1}^{N^2-1} \alpha_j(x) T_j) . \quad (1.12)$$

Here the sum is over the  $N^2 - 1$  **generators** of the Lie group. These satisfy the **Lie Algebra**

$$[T_i, T_j] = i c_{ijk} T_k . \quad (1.13)$$

Here the  $c_{ijk}$  are the real **structure constants** of the group. Abelian groups have commuting generators and so for the U(1) of QED  $c_{ijk} = 0$ . For SU(2) the generators involve the three Pauli matrices  $T_i = \sigma_i/2$  and the structure constants are  $c_{ijk} = \epsilon_{ijk}$ , whilst for SU(3) the generators involve the eight Gell-Mann  $\lambda$  matrices  $T_i = \lambda_i/2$ . The spin- $\frac{1}{2}$  matter fields are  $N$ -plets in the **fundamental** representation of the gauge group, For instance (chiral) leptonic doublets of neutrinos and electrons in electroweak SU(2)<sub>L</sub>

$$\begin{pmatrix} \nu_e \\ e \end{pmatrix} , \quad (1.14)$$

or quark colour triplets (red, green and blue, RGB) in SU(3) QCD.

$$\psi(x) = \begin{pmatrix} \psi_R(x) \\ \psi_G(x) \\ \psi_B(x) \end{pmatrix} . \quad (1.15)$$

The gauge fields are linear combinations of the generators of the gauge group

$$A_\mu = \sum_{i=1}^{N^2-1} A_\mu^i T_i . \quad (1.16)$$

One defines the covariant derivative

$$D^\mu = (\partial_\mu + ig A_\mu) . \quad (1.17)$$

Here  $g$  is the gauge coupling. For local gauge invariance one requires that

$$D^\mu \psi(x) \rightarrow D'^\mu \psi'(x) = U(x) [D^\mu \psi(x)] , \quad (1.18)$$

and hence  $A_\mu$  transforms as

$$A_\mu \rightarrow A'_\mu = U(x) A_\mu U^{-1}(x) - \frac{i}{g} U(x) [\partial_\mu U^{-1}(x)] . \quad (1.19)$$

The locally gauge invariant Lagrangian is then obtained by replacing  $\partial_\mu \rightarrow D_\mu$  in the free Dirac Lagrangian

$$\mathcal{L} = i\bar{\psi}\gamma^\mu D_\mu\psi - m\bar{\psi}\psi$$

The non-Abelian expression for  $F_{\mu\nu}$  follows from

$$[D_\mu, D_\nu]\psi(x) = igF_{\mu\nu}\psi(x) \quad (1.20)$$

which yields

$$\begin{aligned} F_{\mu\nu} &= \partial_\mu A_\nu - \partial_\nu A_\mu + ig[A_\mu, A_\nu] \\ &= \partial_\mu A_\nu - \partial_\nu A_\mu + igA_\mu^i A_\nu^j [T_i, T_j] \\ &= \partial_\mu A_\nu - \partial_\nu A_\mu - gA_\mu^i A_\nu^j c_{ijk} T_k . \end{aligned}$$

One can easily check that under a local gauge transformation

$$F_{\mu\nu} \rightarrow F'_{\mu\nu} = U(x)F_{\mu\nu}U^{-1}(x) , \quad (1.21)$$

and so the kinetic energy term

$$-\frac{1}{4}\text{Tr}[F_{\mu\nu}F^{\mu\nu}] , \quad (1.22)$$

is locally gauge invariant since the trace is cyclic.

$$\text{Tr}[F'_{\mu\nu}F'^{\mu\nu}] = \text{Tr}[UF_{\mu\nu}U^{-1}UF^{\mu\nu}U^{-1}] = \text{Tr}[F_{\mu\nu}F^{\mu\nu}] \quad (1.23)$$

$$-\frac{1}{4}\text{Tr}[F_{\mu\nu}F^{\mu\nu}] = -\frac{1}{4}F_{\mu\nu}^i F^{j\mu\nu} \text{Tr}[T_i T_j] . \quad (1.24)$$

Defining the generators so that  $\text{Tr}[T_i T_j] = \frac{1}{2}\delta_{ij}$  one arrives at the kinetic energy term

$$-\frac{1}{8}F_{\mu\nu}^i F^{i\mu\nu} . \quad (1.25)$$

### 1.3 The Lagrangian of QCD

Quantum Chromodynamics (QCD) is a non-abelian gauge theory of interacting quarks and gluons. The gauge group is  $SU(N_c)$ , and there are  $N_c^2 - 1$  gluons. Experimental indications are that  $N_c = 3$ . The Lagrangian density is

$$\mathcal{L}_{QCD} = \bar{\psi}(i\gamma^\mu \partial_\mu - m)\psi - g_s(\bar{\psi}\gamma^\mu T_a \psi)G_\mu^a - \frac{1}{8}G_{\mu\nu}^a G_a^{\mu\nu}. \quad (1.26)$$

Here  $a = 1, 2, 3, \dots, 8$ , and  $T_a$  are the generators of  $SU(3)$ ,  $T_a = \lambda_a/2$ , where  $\lambda_a$  ( $a = 1, 2, \dots, 8$ ) are the Gell-Mann  $\lambda$ -matrices. They satisfy the Lie algebra

$$[T_a, T_b] = if_{abc}T_c \quad (1.27)$$

The quark fields carry colour, R, G, B, and transform as a triplet in the fundamental representation

$$\psi(x) = \begin{pmatrix} \psi_R(x) \\ \psi_G(x) \\ \psi_B(x) \end{pmatrix} \quad (1.28)$$

$\mathcal{L}_{QCD}$  is invariant under local  $SU(3)$  gauge transformations

$$\psi(x) \rightarrow U(x)\psi = e^{iT^a\alpha_a(x)}\psi(x). \quad (1.29)$$

The field strength tensor  $G_{\mu\nu}^a$  contains the abelian (QED) result and an extra term proportional to the structure constants  $f^{abc}$  which are responsible for three and four-point self-interactions of gluons, not present for photons in QED.

$$G_{\mu\nu}^a = \partial_\mu G_\nu^a - \partial_\nu G_\mu^a + g_s f^{abc} G_\mu^b G_\nu^c. \quad (1.30)$$

For QCD (but not QED) one also needs to include unphysical *ghost* particles. These are scalar Grassmann (anti-commuting) fields needed to cancel unphysical polarization states for the gluons. The required Fadeev-Popov extra term in  $\mathcal{L}_{QCD}$  is

$$\mathcal{L}_{\text{ghost}} = \bar{\eta}^a(-\partial^2\delta^{ac} - g_s\partial^\mu f^{abc}G_\mu^b)\eta^c. \quad (1.31)$$

In both QED and QCD one needs also to include a gauge fixing term if inverse propagators are to be defined.

$$\mathcal{L}_{\text{gauge-fixing}} = \frac{1}{2\xi}(\partial^\mu G_\mu^a)^2 \quad (1.32)$$

There is only one other gauge-invariant structure that we could add involving the *dual* field strength tensor  $\tilde{G}_{\mu\nu}^a$ ,

$$\mathcal{L}_\theta = \frac{\theta g_s^2}{64\pi^2} \tilde{G}^{a,\mu\nu} G_a^{\rho\sigma} \quad (1.33)$$

This is a total derivative and so produces no effects at the perturbative level. However, if  $\theta \neq 0$  non-perturbative effects would induce a CP-violating electric dipole moment for the neutron, experimental constraints on this provide a bound  $|\theta| < 3.10^{-10}$ .

## 2 Glashow's Model $SU(2)_L \times U(1)_Y$

We begin by defining a weak isospin doublet containing a left-handed electron and electron neutrino

$$\chi_L = \begin{pmatrix} \nu_L \\ e_L \end{pmatrix} \equiv \begin{pmatrix} \nu \\ e \end{pmatrix}_L. \quad (2.1)$$

With an adjoint

$$\bar{\chi}_L = \begin{pmatrix} \nu_L \\ e_L \end{pmatrix}. \quad (2.2)$$

We shall introduce a weak isospin quantum number  $T^3$ . The upper and lower members of the doublet have  $T^3 = \pm \frac{1}{2}$ , respectively.

These row and column matrices are acted on by isospin generators in the form of  $2 \times 2$  Pauli matrices

$$\tau^1 = \begin{pmatrix} 0 & 1 \\ 1 & 0 \end{pmatrix}, \tau^2 = \begin{pmatrix} 0 & -i \\ i & 0 \end{pmatrix}, \tau^3 = \begin{pmatrix} 1 & 0 \\ 0 & -1 \end{pmatrix}. \quad (2.3)$$

The generators  $\frac{1}{2}\tau^i$  satisfy the  $SU(2)$  Lie Algebra

$$[\frac{1}{2}\tau^i, \frac{1}{2}\tau^j] = i\epsilon_{ijk}\frac{1}{2}\tau^k. \quad (2.4)$$

The isospin raising and lowering operators are  $\tau^\pm = \frac{1}{2}(\tau^1 \pm i\tau^2)$ .

One can then write an isospin triplet of weak currents

$$J_\mu^i = \bar{\chi}_L \gamma_\mu \frac{1}{2} \tau^i \chi_L \quad (i = 1, 2, 3). \quad (2.5)$$

Putting in row vectors, column vectors and matrices, we have explicitly on multiplying out

$$\begin{aligned} J_\mu^1 &= \frac{1}{2}(\bar{e}_L \gamma_\mu \nu_L + \bar{\nu}_L \gamma_\mu e_L) \\ J_\mu^2 &= \frac{i}{2}(\bar{e}_L \gamma_\mu \nu_L - \bar{\nu}_L \gamma_\mu e_L) \\ J_\mu^3 &= \frac{1}{2}(\bar{\nu}_L \gamma_\mu \nu_L - \bar{e}_L \gamma_\mu e_L). \end{aligned} \quad (2.6)$$

The charge raising and lowering V-A currents can be written in terms of  $J_\mu^1$  and  $J_\mu^2$

$$J_\mu^\pm = \bar{\chi}_L \gamma_\mu \tau^\pm \chi_L = J_\mu^1 \pm i J_\mu^2 . \quad (2.7)$$

The isospin triplet of currents have corresponding charges

$$T^i = \int d^3x J_0^i(x) , \quad (2.8)$$

and these satisfy an SU(2) algebra

$$[T^i, T^j] = i \epsilon_{ijk} T^k . \quad (2.9)$$

To construct a combined weak and electromagnetic theory we will also require the electromagnetic current

$$J_\mu^{em} = Q(\bar{e}_L \gamma_\mu e_L + \bar{e}_R \gamma_\mu e_R) , \quad (2.10)$$

where  $Q$  denotes the charge of the particle (in this case an electron) in units of  $e \approx 0.303$  ( $\alpha = e^2/4\pi$  is the fine structure constant). So  $Q = -1$  for  $e^-$ . In terms of the net charge of interacting particles  $J_\mu^3$  and  $J_\mu^{em}$  are neutral currents, whereas  $J_\mu^1$  and  $J_\mu^2$  are charged currents.  $J_\mu^3$  does not involve  $e_R$  whereas electromagnetism does, and so to have a gauge theory involving both weak and electromagnetic interactions we must add an extra current  $J_\mu^Y$  to  $J_\mu^3$ . The simplest approach is to write

$$J_\mu^{em} = J_\mu^3 + \frac{1}{2} J_\mu^Y , \quad (2.11)$$

then putting in the expressions for  $J_\mu^{em}$  and  $J_\mu^3$  we have

$$\begin{aligned} J_\mu^Y &= -\bar{\chi}_L \gamma_\mu \chi_L - 2\bar{e}_R \gamma_\mu e_R \\ &= -\bar{\nu}_L \gamma_\mu \nu_L - \bar{e}_L \gamma_\mu e_L - 2\bar{e}_R \gamma_\mu e_R . \end{aligned} \quad (2.12)$$

In virtue of the above identity between  $J_\mu^{em}$ ,  $J_\mu^3$  and  $J_\mu^Y$  the corresponding charges,  $Q$  (electric charge in units of  $e$ ),  $T^3$  (third component of weak isospin) and  $Y$  (termed hypercharge) satisfy

$$Q = T^3 + \frac{Y}{2} . \quad (2.13)$$

This is identical to the Gell-Mann Nishijima relation obtained in the quark model of hadrons. The  $\frac{1}{2}$  coefficient in front of  $J_\mu^Y$  is purely conventional.  $T^3$ ,  $Q$  and  $Y$  may be read off from the coefficients of the  $\bar{\nu}_L \gamma_\mu \nu_L$ ,  $\bar{e}_L \gamma_\mu e_L$  and  $\bar{e}_R \gamma_\mu e_R$  terms in  $J_\mu^3$ ,  $J_\mu^{em}$  and  $J_\mu^Y$  above. The charge assignments  $(T, T^3, Q, Y)$  for the particles in the model are

$$\begin{aligned} \nu_L &= \left( \frac{1}{2}, \frac{1}{2}, 0, -1 \right) \\ e_L &= \left( \frac{1}{2}, -\frac{1}{2}, -1, -1 \right) \\ e_R &= (0, 0, -1, -2) \end{aligned} \quad (2.14)$$

Each generation of leptons will have a similar weak isospin doublet with the same quantum numbers,

$$\begin{pmatrix} \nu_e \\ e^- \end{pmatrix}_L, \begin{pmatrix} \nu_\mu \\ \mu^- \end{pmatrix}_L, \begin{pmatrix} \nu_\tau \\ \tau^- \end{pmatrix}_L. \quad (2.15)$$

We have an  $SU(2)_L \times U(1)_Y$  structure where the generators of  $U(1)_Y$  commute with those of  $SU(2)_L$ . This implies that members of an isospin doublet must have the same hypercharge.

We have the following commutation relations for the generators  $T^i, Q, Y$  ( $i = 1, 2, 3$ )

$$[T^i, Y] = 0, [Q, Y] = 0, [Q, T^i] = i\epsilon_{3ij}T^j, \quad (2.16)$$

so  $Q, T^3, Y$ , form a mutually commuting set of generators, but only **two** are independent because of the relation  $Q = T^3 + \frac{Y}{2}$ . The maximum number of independent mutually commuting generators defines the **rank** of the group.  $SU(2)_L \times U(1)_Y$  has rank 2.

Notice that  $U(1)_Y$  is chiral since  $e_L^-$  and  $e_R^-$  have **different** hypercharges whereas the electromagnetic charges are the same. To complete the specification of an  $SU(2)_L \times U(1)_Y$  gauge theory invariant under local gauge transformations, we need to introduce suitable vector fields to couple to these currents.

QED is based on the interaction  $-eJ_\mu^{em}A_\mu$  of the electromagnetic current  $Q\bar{\psi}\gamma^\mu\psi$  with the photon field  $A_\mu$ . This leads to a term in the Lagrangian  $\bar{\psi}\gamma^\mu(i\partial_\mu + eA_\mu)\psi$ . Analogously we introduce an isotriplet of vector gauge bosons  $W_\mu^i$ , ( $i = 1, 2, 3$ ), to gauge the  $SU(2)_L$  symmetry with coupling  $g$  and a vector boson  $B_\mu$  to gauge the  $U(1)_Y$  symmetry with coupling  $g'/2$ . The interaction (analogous to QED) will be  $-gJ^\mu W_\mu^i - \frac{g'}{2}J^\mu B_\mu$ , leading to the lepton-gauge boson portion of  $\mathcal{L}$ ,

$$\bar{\chi}_L\gamma^\mu[i\partial_\mu - g\left(\frac{1}{2}\right)\vec{\tau} \cdot \vec{W}_\mu - \frac{g'}{2}(-1)B_\mu]\chi_L + \bar{e}_R[i\partial_\mu - \frac{g'}{2}(-2)B_\mu]e_R. \quad (2.17)$$

The  $(\frac{1}{2}), (-1), (-2)$  in brackets are, respectively, the weak isospin of the doublet  $\chi_L$ ,  $Y(e_L)$ , and  $Y(e_R)$ . The notation  $\vec{\tau} \cdot \vec{W}_\mu$  is shorthand for  $\tau^i W_\mu^i = \tau^1 W_\mu^1 + \tau^2 W_\mu^2 + \tau^3 W_\mu^3$ . The full lepton-gauge boson Lagrangian will contain  $\sum_{l=e,\mu,\tau} \mathcal{L}(l)$ , a sum over the three generations.

The  $SU(2)_L$  and  $U(1)_Y$  gauge transformations under which  $\mathcal{L}(l)$  is invariant are

$$\begin{aligned} \chi_L &\rightarrow \chi'_L = \exp[-ig\frac{\vec{\tau}}{2} \cdot \vec{\Delta} + i\frac{1}{2}g'\Lambda]\chi_L \\ e_R &\rightarrow e'_R = \exp(ig'\Lambda)e_R \end{aligned}$$

$$\begin{aligned}\vec{W}_\mu \rightarrow \vec{W}'_\mu &= W_\mu + g\vec{\Delta} \times \vec{W}_\mu + \partial_\mu \vec{\Delta} \\ B_\mu \rightarrow B'_\mu &= B_\mu + \partial_\mu \Lambda.\end{aligned}\tag{2.18}$$

Here  $\Lambda(x)$  specifies the local  $U(1)_Y$  gauge transformations and  $\vec{\Delta}(x) = (\Delta^1(x), \Delta^2(x), \Delta^3(x))$  the local  $SU(2)_L$  gauge transformations. Explicitly  $W_\mu^{i'} = W_\mu^i + g\epsilon_{ijk}\Delta^j W_\mu^k + \partial_\mu \Delta^i$

Separating off the interaction piece of  $\mathcal{L}(l)$  we have

$$\mathcal{L}_I = \bar{\chi}_L \gamma^\mu [-g \frac{1}{2} \vec{\tau} \cdot \vec{W}_\mu + \frac{1}{2} g' B_\mu] \chi_L + \bar{e}_R \gamma^\mu g' B_\mu e_R.\tag{2.19}$$

We want to decompose this into a charged current (exchange of electrically charged  $W^\pm$ ) and a neutral current (exchange of electrically neutral  $Z^0$ .)

$$\mathcal{L}_I = \mathcal{L}_{CC} + \mathcal{L}_{NC}.\tag{2.20}$$

Consider the  $\vec{\tau} \cdot \vec{W}_\mu$  term in  $\mathcal{L}_I$ . We have

$$\begin{aligned}\frac{1}{2}(\vec{\tau} \cdot \vec{W}_\mu) &= \frac{\tau^1}{2} W_\mu^1 + \frac{\tau^2}{2} W_\mu^2 + \frac{\tau^3}{2} W_\mu^3 \\ &= \frac{1}{\sqrt{2}}(\tau^+ W_\mu^+ + \tau^- W_\mu^-) + \frac{\tau^3}{2} W_\mu^3.\end{aligned}\tag{2.21}$$

Here we have defined the charged vector fields  $W_\mu^\pm = \frac{1}{\sqrt{2}}(W_\mu^1 \mp W_\mu^2)$ . The  $W_\mu^3$  term is neutral and so belongs in  $\mathcal{L}_{NC}$ . We therefore have

$$\begin{aligned}\mathcal{L}_{CC} &= \bar{\chi}_L \gamma^\mu [-\frac{g}{\sqrt{2}}(\tau^+ W_\mu^+ + \tau^- W_\mu^-)] \chi_L \\ &= -\frac{g}{\sqrt{2}}[J_\mu^+ W^{+\mu} + J_\mu^- W^{-\mu}].\end{aligned}\tag{2.22}$$

So the  $V - A$  charge raising and lowering currents of Eq.(2.7) couple to the charged  $W_\mu^\pm$  fields. The rest of  $\mathcal{L}_I$  gives us

$$\begin{aligned}\mathcal{L}_{NC} &= \bar{\chi}_L \gamma^\mu [-\frac{g}{2}\tau^3 W_\mu^3 + g' B_\mu] \chi_L + \bar{e}_R \gamma^\mu g' B_\mu e_R \\ &= -g J_\mu^3 W^{3\mu} - \frac{g'}{2} J_\mu^Y B^\mu.\end{aligned}\tag{2.23}$$

The next step is to identify the physical neutral vector fields  $Z_\mu$  and  $A_\mu$ . We therefore write  $W_\mu^3$  and  $B_\mu$  as an orthogonal mixture of  $Z_\mu$  and  $A_\mu$ .

$$\begin{pmatrix} W_\mu^3 \\ B_\mu \end{pmatrix} = \begin{pmatrix} \cos \theta_w & \sin \theta_w \\ -\sin \theta_w & \cos \theta_w \end{pmatrix} \begin{pmatrix} Z_\mu \\ A_\mu \end{pmatrix}\tag{2.24}$$

The angle  $\theta_w$  is the **weak mixing angle**. So in terms of  $Z_\mu$  and  $A_\mu$

$$\mathcal{L}_{NC} = -g J_\mu^3 [\cos \theta_w Z^\mu + \sin \theta_w A^\mu] - \frac{g'}{2} J_\mu^Y [-\sin \theta_w Z^\mu + \cos \theta_w A^\mu].\tag{2.25}$$

We must have that  $J_\mu^{em} = J_\mu^3 + \frac{1}{2}J_\mu^Y$  is coupled to  $A_\mu$  with strength  $e$ , so we need

$$\mathcal{L}_{NC} = -eA^\mu(J_\mu^3 + \frac{1}{2}J_\mu^Y) + \dots \quad (2.26)$$

So both  $J_\mu^3 A^\mu$  and  $\frac{1}{2}J_\mu^Y A^\mu$  terms must have coefficient  $-e$  implying that

$$g \sin \theta_w = g' \cos \theta_w = e, \quad (2.27)$$

or equivalently

$$\frac{1}{g^2} + \frac{1}{g'^2} = \frac{1}{e^2}. \quad (2.28)$$

We then have

$$\mathcal{L} = -eJ_\mu^{em} A^\mu + Z^\mu [-g \cos \theta_w J_\mu^3 g' \sin \theta_w J_\mu^3 + g' \sin \theta_w J_\mu^{em}], \quad (2.29)$$

where  $J_\mu^Y$  has been eliminated using  $J_\mu^Y = 2(J_\mu^{em} - J_\mu^3)$ . The terms in the square bracket coefficient of  $Z^\mu$  can then be written as

$$\left[ -g \frac{\cos^2 \theta_w}{\cos \theta_w} J_\mu^3 - g \frac{\sin^2 \theta_w}{\cos \theta_w} J_\mu^3 + g \frac{\sin^2 \theta_w}{\cos \theta_w} J_\mu^{em} \right] \quad (2.30)$$

where  $g' = g \sin \theta_w / \cos \theta_w$  has been used. Then setting  $\sin^2 + \cos^2 = 1$  we get

$$\mathcal{L}_{NC} = -eJ_\mu^{em} A^\mu - \frac{g}{\cos \theta_w} [J_\mu^3 - \sin^2 \theta_w J_\mu^{em}]. \quad (2.31)$$

So finally assembling all this we have

$$\mathcal{L}_I = -\frac{g}{\sqrt{2}} [J_\mu^+ W^{+\mu} + J_\mu^- W^{-\mu}] - eJ_\mu^{em} A^\mu - \frac{g}{\cos \theta_w} [J_\mu^3 - \sin^2 \theta_w J_\mu^{em}] Z^\mu. \quad (2.32)$$

Expressing the currents in terms of the full fermion fields  $\nu, e$  we obtain

$$\begin{aligned} \mathcal{L}_I = & -\frac{g}{\sqrt{2}} [\bar{\nu} \gamma_\mu \frac{1}{2} (1 - \gamma_5) e W^{+\mu} + \bar{e} \gamma_\mu \frac{1}{2} (1 - \gamma_5) \nu W^{-\mu}] + e (\bar{e} \gamma_\mu e A^\mu) \\ & - \frac{g}{2 \cos \theta_w} \left[ \bar{\nu} \gamma_\mu \frac{1}{2} (1 - \gamma_5) \nu - \bar{e} \gamma_\mu \frac{1}{2} (1 - \gamma_5) e + 2 \sin^2 \theta_w \bar{e} \gamma_\mu e \right] Z^\mu. \end{aligned} \quad (2.33)$$

From the coefficients of the  $\bar{l}lV$  terms ( $l = e, \nu, V = A(\gamma), W^\pm, Z$ ) multiplied by  $i$  we obtain the fermion-gauge boson vertex factors given in the Appendix.

## 2.1 Kinetic Energy Terms for Glashow's Model

To complete the Glashow model Lagrangian we need  $SU(2)_L \times U(1)_Y$  gauge invariant the kinetic energy terms for the vector boson fields. In QED we have the kinetic energy term



$-\frac{1}{4}F_{\mu\nu}F^{\mu\nu}$  with  $F_{\mu\nu} = \partial_\mu A_\nu - \partial_\nu A_\mu$ . The relevant terms for the  $W_\mu^i$  fields ( $\mathcal{L}_W$ ) and  $B_\mu$  ( $\mathcal{L}_B$ ) are

$$\mathcal{L}_W = -\frac{1}{4}\vec{W}_{\mu\nu} \cdot \vec{W}^{\mu\nu} = -\frac{1}{4}\sum_i (\vec{W}_{\mu\nu})^i (\vec{W}^{\mu\nu})^i, \quad (2.34)$$

where

$$\vec{W}_{\mu\nu} = \partial_\mu \vec{W}_\nu - \partial_\nu \vec{W}_\mu - g\vec{W}_\nu \times \vec{W}_\mu, \quad (2.35)$$

and

$$(\vec{W}_{\mu\nu})^i = \partial_\mu W_\nu^i - \partial_\nu W_\mu^i - gW_\mu^k W_\nu^l \epsilon_{ikl}. \quad (2.36)$$

Explicitly in terms of the fields  $W_\mu^i$  ( $i = 1, 2, 3$ ) which gauge  $SU(2)_L$ . For the  $U(1)_Y$  field  $B_\mu$  one has the Abelian field strength tensor  $B_{\mu\nu} = \partial_\mu B_\nu - \partial_\nu B_\mu$ , and the kinetic energy term

$$\mathcal{L}_B = -\frac{1}{4}B_{\mu\nu}B^{\mu\nu}. \quad (2.37)$$

These terms can of course be rewritten in terms of the physical fields  $W^+, W^-, Z_\mu, A_\mu$ .

$$\begin{aligned} W_\mu^1 &= \frac{1}{\sqrt{2}}(W_\mu^+ + W_\mu^-) \\ W_\mu^2 &= \frac{i}{\sqrt{2}}(W_\mu^- - W_\mu^+) \\ W_\mu^3 &= \cos\theta_w Z_\mu + \sin\theta_w A_\mu \\ B_\mu &= \cos\theta_w A_\mu - \sin\theta_w Z_\mu. \end{aligned} \quad (2.38)$$

Having so rewritten  $\mathcal{L}_W$  and  $\mathcal{L}_B$  we can pick out the  $(\partial_\mu V)VV$  and  $VVVV$  cross terms in the physical fields. The Feynman Rules are in momentum space so  $i\partial_\mu V$  should be replaced by  $p_\mu V$ , where  $p_\mu$  is the momentum of the vector boson  $V$ . We have therefore generated the three and four-point self-interactions of  $W^\pm$ ,  $Z$  and  $\gamma$ . The relevant Feynman Rules are given in the Appendix.

We now have all the Feynman rules for the Glashow model Lagrangian

$$\mathcal{L} = \sum_{l=e,\mu,\tau} \mathcal{L}(l) + \mathcal{L}_W + \mathcal{L}_B. \quad (2.39)$$

Notice that there are no mass terms. If we want to have an  $SU(2)_L \times U(1)_Y$  gauge invariant theory we cannot have them! For instance a mass term for the field  $B_\mu$  would be  $\frac{1}{2}M_B^2 B_\mu B^\mu$ . Under the local gauge transformation in Eq.(2.18)  $B_\mu \rightarrow B'_\mu = B_\mu + \partial_\mu \Lambda$  it is obvious that  $\frac{1}{2}M_B^2 B_\mu B^\mu \neq \frac{1}{2}M_B^2 B'_\mu B'^\mu$ . Similarly for a term involving  $M_W^2 = M_W^2 \vec{W}_\mu \vec{W}^\mu$  under an  $SU(2)_L$  gauge transformation. This comment would apply in QED and forbid the photon mass term  $\frac{1}{2}M_\gamma^2 A_\mu A^\mu$ , of course this is not a problem since we know experimentally that  $M_\gamma = 0$  and that photons are massless particles. A Dirac mass term for the leptons is also

disallowed since  $m\bar{\psi}\psi = m(\bar{\psi}_R\psi_L + \bar{\psi}_L\psi_R)$ , written in terms of chiral L and R components. This is gauge invariant in QED which is  $L/R$  symmetric, but in the chiral  $SU(2)_L \times U(1)_Y$  theory  $\psi_R$  and  $\psi_L$  have **different** gauge transformations in Eq.(2.18). Simply adding mass terms by brute force would lead to a sick theory. For massless vector bosons, e.g a photon in QED, one only has transverse polarization degrees of freedom, gauge invariance implies the absence of the longitudinal ( $L$ ) modes. For massive  $W$  bosons one could consider the scattering of longitudinally polarized  $W$  pairs,  $W_L^+W_L^- \rightarrow W_L^+W_L^-$ . The propagator for a massive vector boson of virtuality  $q^2$  involves  $(g_{\mu\nu} - q_\mu q_\nu / M_W^2) / (q^2 - M_W^2)$ . The longitudinally polarized  $W$  bosons are described by polarization vectors with  $\epsilon_\mu^L \rightarrow \frac{q_\mu}{M_W}$  as  $q^2 \rightarrow \infty$ , so the propagator approaches a constant at large  $q^2$ . This implies that the longitudinally polarized  $W$  scattering grows like the square of the c.m. energy and unitarity is violated since at most a logarithmic growth is required. We therefore need to generate mass more subtly. One possibility is to exploit the so-called Higgs mechanism suggested by Peter Higgs in 1964 and motivated by the generation of Cooper pairs in superconductivity, involving the concept of spontaneous symmetry breaking.

### 3 The Higgs Mechanism for $SU(2)_L \times U(1)_Y$

We begin by defining the  $SU(2)_L \times U(1)_Y$  covariant derivative

$$D_\mu = \partial_\mu + \frac{i}{2}g\vec{\tau} \cdot \vec{W}_\mu + ig' \frac{Y}{2}B_\mu . \quad (3.1)$$

We introduce an  $SU(2)_L$  doublet of complex scalar Higgs fields

$$\Phi = \begin{pmatrix} \phi^+ \\ \phi^0 \end{pmatrix} . \quad (3.2)$$

The doublet has weak isospin  $T = \frac{1}{2}$  and hypercharge  $Y = 1$  leading to electromagnetic charges  $+1, 0$ , for the  $T^3 = \pm\frac{1}{2}$  upper and lower members of the doublet (recall  $Q = T^3 + Y/2$ ).

In terms of real scalar fields  $\phi_i$  one has

$$\phi^+ = \frac{\phi_1 + i\phi_2}{\sqrt{2}} , \phi^0 = \frac{\phi_3 + i\phi_4}{\sqrt{2}} . \quad (3.3)$$

We then add to the massless Glashow model Lagrangian of Eq.(2.39) the scalar contribution

$$\mathcal{L}_\Phi = (D_\mu \Phi)^\dagger D^\mu \Phi - V(\Phi) . \quad (3.4)$$

The conjugate  $\Phi^\dagger$  contains the antiparticles  $(\phi^-, \bar{\phi}^0)$ .

The most general  $SU(2)_L \times U(1)_Y$  invariant and renormalisable scalar potential  $V(\Phi)$  is

$$V(\Phi) = -\mu^2(\Phi^\dagger\Phi) + \lambda(\Phi^\dagger\Phi)^2 . \quad (3.5)$$

We arrange that  $\mathcal{L}_\Phi$  contains a  $+\mu^2\Phi^\dagger\Phi$  term. Notice that an ordinary scalar mass term would be  $-\mu^2\Phi^\dagger\Phi$ , but we want  $V(\Phi)$  to be bounded below so there will be an  $SU(2)_L \times U(1)_Y$  invariant manifold of minima lying below  $V(\Phi) = 0$ , and we obtain the “wine-bottle” or “mexican hat” potential.  $\mathcal{L}_\Phi$  is invariant under the  $SU(2)_L \times U(1)_Y$  gauge transformations

$$\Phi \rightarrow \Phi' = \exp[-ig\frac{\vec{\tau}}{2} \cdot \Delta - ig'\frac{1}{2}\Lambda] \Phi . \quad (3.6)$$

$V(\Phi)$  has minima specified by

$$\frac{dV}{d(\Phi^\dagger\Phi)} = 0 \Rightarrow -\mu^2 + 2\lambda(\Phi^\dagger\Phi) = 0 \quad (3.7)$$

so that the degenerate minima are specified by

$$\Phi^\dagger\Phi|_{min} = \frac{\mu^2}{2\lambda} , \quad (3.8)$$

or in terms of real scalar fields  $\phi_i$

$$\frac{1}{2}(\phi_1^2 + \phi_2^2 + \phi_3^2) = \frac{\mu^2}{2\lambda} . \quad (3.9)$$

We need to spontaneously break  $SU(2)_L \times U(1)_Y$  by picking the vacuum from the set of minima of the potential  $V$ . We shall choose the vacuum expectation values (vev's) of the fields  $\phi_1$ ,  $\phi_2$  and  $\phi_4$  to be zero

$$\langle 0|\phi_1|0\rangle = \langle 0|\phi_2|0\rangle = \langle 0|\phi_4|0\rangle = 0 . \quad (3.10)$$

We assign a non-zero vev  $v$  to the field  $\phi_3$

$$\langle 0|\phi_3|0\rangle^2 = v^2 = \frac{\mu^2}{\lambda} . \quad (3.11)$$

Of course, we should be able to pick the vacuum direction completely arbitrarily, but in order for the photon to remain massless, as it must do after the spontaneous symmetry breaking we need to give a non-zero vev to a neutral field. To do things generally we should only assign charges and other quantum numbers after performing the symmetry breaking. We shall proceed with these particular choices.

We now expand  $\Phi$  around this chosen vacuum, setting  $\phi_3 = H + v$ , where  $H$  is the neutral scalar Higgs field. It is possible to choose a special gauge, the *unitary gauge*, in which

$$\Phi = \frac{1}{\sqrt{2}} \begin{pmatrix} 0 \\ H + v \end{pmatrix} . \quad (3.12)$$

That is the “Goldstone” fields with **zero vevs**,  $\phi_1, \phi_2, \phi_4$  can be eliminated. To see this we can apply the local gauge transformation  $\exp(i\vec{\tau} \cdot \vec{\theta}(x)/v)$  to this unitary gauge form to obtain

$$\Phi' = \frac{1}{\sqrt{2}} \exp \left[ \frac{i\vec{\tau} \cdot \vec{\theta}(x)}{v} \right] \begin{pmatrix} 0 \\ H + v \end{pmatrix}. \quad (3.13)$$

Expanding the exponential to  $O(\theta)$  we find

$$\begin{aligned} \Phi' &= \frac{1}{\sqrt{2}} \begin{pmatrix} 1 + i\theta_3/v & i(\theta_1 - i\theta_2)/v \\ i(\theta_1 + i\theta_2)/v & 1 - i\theta_3/v \end{pmatrix} \\ &= \frac{1}{\sqrt{2}} \begin{pmatrix} \theta_2 + i\theta_1 \\ v + H - i\theta_3 \end{pmatrix}. \end{aligned} \quad (3.14)$$

So we see that the unitary gauge field of Eq.(3.12) is a gauge transformation of a general  $\Phi$  with four independent scalar fields. The idea is that the three originally massless gauge fields  $W^\pm, Z^0$  will become massive and acquire three extra longitudinal polarization degrees of freedom by “eating” the three unphysical Goldstone bosons. Notice that the above gauge transformation accordingly uses only three of the four possible  $SU(2)_L \times U(1)_Y$  gauge transformation parameters.  $\lambda = 0, \vec{\Delta} = -\frac{2\vec{\theta}}{v}$ . In practice the unitary gauge is unsuited for calculations. One will need to add extra Feynman rules for the Goldstone bosons, analogous to the extra Feynman rules for Fadeev Popov ghost particles in QCD.

We can now evaluate  $\mathcal{L}_\Phi$  in unitary gauge explicitly and exhibit the spontaneously generated mass terms for  $W^\pm$  and  $Z^0$ . From Eq.(3.1) we find

$$\begin{aligned} D_\mu \Phi &= \begin{pmatrix} \partial_\mu + i\frac{g}{2}W_\mu^3 + i\frac{g'}{2}B_\mu & i\frac{g}{2}(W_\mu^1 - iW_\mu^2) \\ i\frac{g}{2}(W_\mu^1 + iW_\mu^2) & \partial_\mu - i\frac{g}{2}W_\mu^3 + i\frac{g'}{2}B_\mu \end{pmatrix} \begin{pmatrix} 0 \\ H + v \end{pmatrix} \\ &= \begin{pmatrix} i\frac{g}{2}(W_\mu^1 - iW_\mu^2)(H + v) \\ (\partial_\mu - i\frac{g}{2}W_\mu^3 + i\frac{g'}{2}B_\mu)(H + v) \end{pmatrix} \\ &= \begin{pmatrix} i\frac{g}{\sqrt{2}}W_\mu^+(H + v) \\ (\partial_\mu - \frac{i}{2}(g \cos \theta_w + g' \sin \theta_w)Z_\mu)(H + v) \end{pmatrix}. \end{aligned} \quad (3.15)$$

Notice that the photon field  $A_\mu$  is no longer involved, only  $W_\mu^\pm$  and  $Z_\mu$ . The photon will therefore not acquire a  $\frac{1}{2}M^2 A_\mu A^\mu$  mass term. The masslessness of the photon is guaranteed by the  $U(1)_{em}$  gauge invariance of the Lagrangian.  $U(1)_{em}$  is a residual symmetry.  $SU(2)_L \times U(1)_Y$  has been spontaneously broken to  $U(1)_{em}$ , and the originally massless  $W^\pm, Z^0$  gauge bosons have acquired masses in the process.

We finally obtain in the unitary gauge

$$\mathcal{L}_\Phi = (D_\mu \Phi)^\dagger D^\mu \Phi + \mu^2 \Phi^\dagger \Phi - \lambda (\Phi^\dagger \Phi)^2$$

$$\begin{aligned}
&= \frac{1}{2}\partial_\mu H \partial^\mu H + \frac{1}{4}g^2(H^2 + 2vH + v^2)W_\mu^+ W^{-\mu} \\
&+ \frac{1}{8}(g^2 + g'^2)(H^2 + 2vH + v^2)Z_\mu Z^\mu \\
&- \mu^2 H^2 - \frac{\lambda}{4}(H^4 + 4vH^3) .
\end{aligned} \tag{3.16}$$

We have used the relation  $(g \cos \theta_w + g' \sin \theta_w)^2 = g^2 + g'^2$ . The masses of  $W^\pm$  and  $Z$  can now be read off by identifying the terms  $M_W^2 W_\mu^+ W^{-\mu}$  and  $\frac{1}{2}M_Z^2 Z_\mu Z^\mu$  in Eq.(3.16). We find

$$M_W = \frac{1}{2}gv \tag{3.17}$$

$$M_Z = \frac{1}{2}(g^2 + g'^2)^{1/2}v = \frac{1}{2}\frac{gv}{\cos \theta_w} . \tag{3.18}$$

For the Higgs scalar we identify the overall  $H^2$  term  $(\frac{1}{2}\mu^2 - \frac{3}{2}\lambda v^2)H^2$  coming from  $\frac{\mu^2}{2}(H + v)^2 - \frac{\lambda}{4}(H + v)^4$ , and recalling that  $\mu^2 = \lambda v^2$  we obtain the  $H^2$  coefficient  $-\frac{1}{2}M_H^2 = -\mu^2$  so that  $M_H = \sqrt{2}\mu$ . There are also VVH, VVHH and HHH, HHHH Higgs self-interactions. The corresponding Feynman rules and vertex factors are contained in the Appendix.

An immediate consequence of the above vector boson masses is that

$$\frac{M_W}{M_Z} = \cos \theta_w . \tag{3.19}$$

This is often referred to as the “weak  $\Delta I = \frac{1}{2}$  rule” and is connected with our choice of a Higgs doublet to perform the spontaneous symmetry breaking.

Notice that from the measured fine structure constant  $\alpha = e^2/4\pi$  and the vector boson masses  $M_W$  and  $M_Z$  we can determine  $\sin^2 \theta_w$ ,  $v$  and  $g$ , but **not**  $\mu$ . This means that the Higgs mass  $M_H$  is not determined directly by other experimentally measured parameters. We shall return a little later to a discussion of the number of independent Standard Model parameters.

### 3.1 Yukawa terms for lepton masses

To give charged leptons a mass one adds a so-called Yukawa term to the Lagrangian,  $\mathcal{L}_Y(l)$ , where  $l = e, \mu, \tau$  labels the lepton. We have for instance for an electron

$$\mathcal{L}_Y(e) = -G_e[\bar{\chi}_L \Phi e_R + \bar{e}_R \Phi^\dagger \chi_L] . \tag{3.20}$$

This is  $SU(2)_L \times U(1)_Y$  invariant.  $G_e$  is the Yukawa coupling. On spontaneous symmetry breaking we have in the unitary gauge

$$\Phi = \frac{1}{\sqrt{2}} \begin{pmatrix} 0 \\ H + v \end{pmatrix}, \quad (3.21)$$

substituting this into  $\mathcal{L}_Y(e)$  one has

$$\begin{aligned} \mathcal{L}_Y(e) &= -\frac{G_e}{\sqrt{2}}(v + H)(\bar{e}_L e_R + \bar{e}_R e_L) \\ &= -\frac{G_e}{\sqrt{2}}(H + v)\bar{e}e = -\frac{G_e v}{\sqrt{2}}(\bar{e}) - \frac{G_e}{\sqrt{2}}(\bar{e}eH). \end{aligned} \quad (3.22)$$

From which we can identify the electron mass  $m_e = G_e v / \sqrt{2}$ , and the lepton-Higgs coupling  $g(H\bar{e}e) = m_e/v = g m_e / (2M_W)$ . Notice that the  $\nu_L$  upper element of the doublet does not appear since in unitary gauge the upper entry in  $\Phi$  is zero, and so as required we do not generate a neutrino mass term or interaction with the Higgs. We see that the coupling between leptons and the Higgs is proportional to the lepton mass, so  $\tau$  signatures involving the heaviest mass lepton will be important for Higgs searches at colliders. Similarly for quarks  $b\bar{b}$ , and  $t\bar{t}$  signatures will be important. The vertex factor and Feynman rule for the Yukawa term is contained in the Appendix.

### 3.2 Electroweak quark sector

So far we have just considered the lepton sector. We also need to include a Lagrangian  $\mathcal{L}(q)$  to describe electroweak quark interactions. We have six quarks (three generations)  $u, d, s, c, b, t$ .  $Q_u = Q_c = Q_t = \frac{2}{3}$ , and  $Q_d = Q_s = Q_b = -\frac{1}{3}$ . We can construct  $SU(2)_L$  isospin doublets analogous to the leptonic case

$$\chi_L^f = \begin{pmatrix} U_f \\ D_f \end{pmatrix} \quad f = 1, 2, 3 \quad (3.23)$$

Here  $U_1 = u, U_2 = c, U_3 = t$  and  $D_1 = d, D_2 = s, D_3 = b$ . However experimentally one observes  $n \rightarrow pe^- \bar{\nu}_e$  and also  $\Lambda \rightarrow pe^- \bar{\nu}_e$  decays, corresponding to  $d \rightarrow u$  and  $s \rightarrow u$  transitions. This implies that the weak interaction eigenstates are mixtures of flavour eigenstates. We therefore replace the above  $\chi_L^f$  by

$$\chi_L^f = \begin{pmatrix} U_f \\ D'_f \end{pmatrix}, \quad f = 1, 2, 3, \quad (3.24)$$

where  $D'_f$  is a flavour rotated mixture

$$D'_f = \sum_{f'=1,2,3} V_{ff'} D_{f'}. \quad (3.25)$$

Here  $V$  is a  $3 \times 3$  unitary matrix ( $VV^\dagger = 1$ ) called the Cabibbo-Kobayashi-Maskawa **CKM** matrix. For two generations we have the Cabibbo model

$$\begin{aligned} D'_1 &= \cos \theta_c d + \sin \theta_c s \\ D'_2 &= -\sin \theta_c d + \cos \theta_c s . \end{aligned} \quad (3.26)$$

Here  $\theta_c$  is the Cabibbo angle, and experimentally one finds  $\theta_c \approx 13$  degrees or  $\cos \theta_c \approx 0.97$ . The full three generation CKM matrix has the following  $|V_{ij}|$  structure for the magnitudes of the elements

$$V = \begin{pmatrix} |V_{ud}| = 0.97 & |V_{us}| = .23 & |V_{ub}| \approx 0 \\ |V_{cd}| = 0.24 & |V_{cs}| = 0.97 & |V_{cb}| = 0.06 \\ |V_{td}| \approx 0 & |V_{ts}| \approx 0 & |V_{tb}| \approx 1 \end{pmatrix} . \quad (3.27)$$

The matrix involves 4 parameters- 3 angles and 1 complex phase. The presence of this complex phase enables CP violation to occur.

In analogy with the leptonic isotriplet of currents one then defines the quark isotriplet

$$J_\mu^{fi} = \bar{\chi}_L^f \gamma_\mu \frac{1}{2} \tau_i \chi_L^f \quad (i = 1, 2, 3) . \quad (3.28)$$

As before  $i = 1, 2$  are charged currents, and  $J_\mu^{f3}$  is a neutral current.

$$\begin{aligned} J_\mu^{f3} &= \frac{1}{2} (\bar{U}_{fL} \gamma_\mu U_{fL} - \bar{D}'_{fL} \gamma_\mu D'_{fL}) \\ &= \frac{1}{2} (\bar{U}_{fL} - \bar{D}_{fL} \gamma_\mu D_{fL}) . \end{aligned} \quad (3.29)$$

Notice that  $D'_{fL}$  the rotated flavour mixture has been replaced by  $D_{fL}$  in the final line. This follows from the unitarity property  $VV^\dagger = 1$ . It has the important consequence that flavour changing neutral current processes are forbidden. We can now determine the electromagnetic quark currents

$$J_\mu^{f(em)} = \left(\frac{2}{3}\right) \bar{U}_{fR} \gamma_\mu U_{fR} + \left(\frac{2}{3}\right) \bar{U}_{fL} \gamma_\mu U_{fL} + \left(\frac{-1}{3}\right) \bar{D}_{fR} \gamma_\mu U_{fR} + \left(\frac{-1}{3}\right) \bar{D}_{fL} \gamma_\mu U_{fL} . \quad (3.30)$$

Here the  $(\frac{2}{3})$ ,  $(-\frac{1}{3})$  in brackets denote the electric charges of the quarks. If we define the hypecharge current  $J_\mu^{fY}$  in the same way as for the leptons, so that  $J_\mu^{f(em)} = J_\mu^{f3} + \frac{1}{2} J_\mu^{fY}$ , then we can infer that

$$J_\mu^{fY} = \left(\frac{1}{3}\right) (\bar{U}_{fL} \gamma_\mu U_{fL} + \bar{D}_{fL} \gamma_\mu U_{fL}) + \left(\frac{4}{3}\right) \bar{U}_{fR} \gamma_\mu U_{fR} + \left(\frac{-2}{3}\right) \bar{D}_{fR} \gamma_\mu U_{fR} . \quad (3.31)$$

Again the  $(\frac{1}{3})$  etc. numbers in brackets refer to the hypercharges of the particles. One can then read off for each generation  $U_f$ ,  $D_f$  the charges  $(T, T^3, Q, Y)$

$$U_L = \left(\frac{1}{2}, \frac{1}{2}, \frac{2}{3}, \frac{1}{3}\right)$$

$$\begin{aligned}
D_L &= \left(\frac{1}{2}, -\frac{1}{2}, -\frac{1}{3}, \frac{1}{3}\right) \\
U_R &= \left(0, 0, \frac{2}{3}, \frac{4}{3}\right) \\
D_R &= \left(0, 0, -\frac{1}{3}, -\frac{2}{3}\right)
\end{aligned} \tag{3.32}$$

So analogous to  $\mathcal{L}(l)$  for leptons one obtains the quark electroweak lagrangian  $\mathcal{L}(\Pi)$

$$\begin{aligned}
\mathcal{L}(q) &= \sum_{f=1,2,3} (\bar{\chi}_L^f \gamma^\mu \left[ i\partial_\mu - \frac{1}{2} \vec{\tau} \cdot \vec{W}_\mu - \left(\frac{1}{3}\right) B_\mu \right] \chi_L^f \\
&= +\bar{U}_{fR} \gamma^\mu \left[ i\partial_\mu - \frac{g'}{2} \left(\frac{4}{3}\right) B_\mu \right] U_{fR} + \bar{D}_{fR} \gamma^\mu \left[ i\partial_\mu - \frac{g'}{2} \left(\frac{-2}{3}\right) B_\mu \right] D_{fR} .
\end{aligned} \tag{3.33}$$

To give masses to the quarks we shall require a corresponding quark Yukawa term  $\mathcal{L}_Y(q)$ .

$$\mathcal{L}_Y(q) = \sum_{f=1,2,3} -[\bar{\chi}_L^f G_{ff'}^D \Phi D_{f'R} + \bar{\chi}_L^f G_{ff'}^U \Phi^c U_{f'R} + \text{h.c.}] . \tag{3.34}$$

Here the  $G_{ff'}^U$  and  $G_{ff'}^D$  are the matrix of quark Yukawa couplings. To give a mass to the upper  $U_{fL}$  members of the chiral doublet one needs to use the conjugate scalar field

$$\Phi^c = \begin{pmatrix} \bar{\phi}^0 \\ -\phi^- \end{pmatrix} . \tag{3.35}$$

After spontaneous symmetry breaking one has in unitary gauge

$$\Phi^c = \begin{pmatrix} H + v \\ 0 \end{pmatrix} . \tag{3.36}$$

In this way one generates a quark mass matrix and  $q\bar{q}H$  interactions. We shall not pursue the details any further.

### 3.3 SM Lagrangian and independent parameter count

Assembling all the pieces we have discussed we can now arrive at the Glashow-Weinberg-Salam Standard Model Lagrangian

$$\mathcal{L}_{SM} = \mathcal{L}_W + \mathcal{L}_B + \sum_{l=e,\mu,\tau} \mathcal{L}(l) + \sum_{l=e,\mu,\tau} \mathcal{L}_Y(l) + \mathcal{L}(q) + \mathcal{L}_Y(q) + \mathcal{L}_\Phi + \mathcal{L}_{QCD} + \dots . \tag{3.37}$$

The ellipsis denotes further gauge-fixing and ghost contributions. The Standard Model as specified by this Lagrangian has been shown to be renormalisable by 't Hooft and Veltman. The unitarity problem for  $W_L^+ W_L^- \rightarrow W_L^+ W_L^-$  scattering is also cured. It is solved by extra diagrams involving virtual Higgs exchange which now appear due to the  $WWH$  interaction



terms.

It is interesting to count how many of the parameters in the Standard Model are independent. There are fifteen parameters overall if we ignore the quark sector, which may be divided into couplings:  $e(\alpha), g, g', G_e, G_\mu, G_\tau$ . Masses:  $M_W, M_Z, M_H, m_e, m_\mu, m_\tau$ . Higgs sector parameters  $\mu^2, \lambda$  ( $v^2 = \frac{\mu^2}{\lambda^2}$ ), and last but not least the weak mixing angle  $\sin^2 \theta_w$ . There are clearly many relations between the parameters, such as  $M_W = \frac{1}{2}gv$  or  $e = g \sin \theta_w$  for instance. It turns out that there are in fact **seven** independent parameters which if specified can then predict all fifteen. One can choose for instance the set  $g, g', G_e, G_\mu, G_\tau, \mu^2, \lambda$ . Alternatively  $\alpha, M_W, M_Z, M_H, m_e, m_\mu, m_\tau$  or  $\alpha, \sin^2 \theta_w, M_H, v, G_e, G_\mu, G_\tau$  are possible sets.

Including the electroweak quark sector adds the CKM matrix  $V$  (three angles and one complex phase) and mass matrices  $m(U), M(D), (m_u, m_c, m_t, m_d, m_s, m_b)$  making  $4 + 3 + 3 = 10$  extra parameters. Including QCD we have in addition  $\Lambda_{QCD}$  and the QCD  $\theta$ -parameter involved in the strong CP problem. So overall there are 19 independent free parameters in  $SU(3)_c \times SU(2)_L \times U(1)_Y$ .

A model with at least 19 undetermined parameters, in which the particular representations containing fermions and scalars are not compellingly motivated, and with a mysterious replication of three generations, does not seem a likely candidate for a complete theory of everything, even though it has proved consistent with experiment in essentially every detail checked. The remaining ingredient to be discovered is of course the Higgs, experimental evidence for which is keenly anticipated at the LHC.

## Acknowledgements

It is a pleasure to thank Mark Thomson, ably assisted by the administrative team of Gill Birch and Jacqui Graham, for organizing a very enjoyable and productive school. The students were keen and motivated and the atmosphere made for a perfect learning environment. The staff of Somerville College are also thanked for their helpfulness and hospitality.

## 4 Appendix of Feynman rules

The following pages summarize the Feynman Rules in unitary gauge for one generation of leptons. All the Lagrangian terms needed to derive the vertex factors for the different interactions are contained in these lecture notes.

# Feynman Rules in the Unitary Gauge (for one Generation of Leptons)

## Propagators:

All propagators carry momentum  $p$ .

$$\mu \overset{\text{W}}{\sim} \nu \qquad -i (g_{\mu\nu} - p_\mu p_\nu / M_W^2) / (p^2 - M_W^2)$$

$$\mu \overset{\text{Z}}{\sim} \nu \qquad -i (g_{\mu\nu} - p_\mu p_\nu / M_Z^2) / (p^2 - M_Z^2)$$

$$\mu \overset{\text{A}}{\sim} \nu \qquad -i g_{\mu\nu} / p^2$$

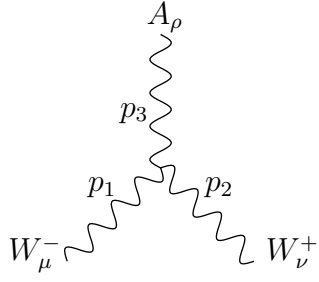
$$\overset{\text{e}}{\longrightarrow} \qquad i (\gamma \cdot p + m_e) / (p^2 - m_e^2)$$

$$\overset{\nu}{\longrightarrow} \qquad i \gamma \cdot p / p^2$$

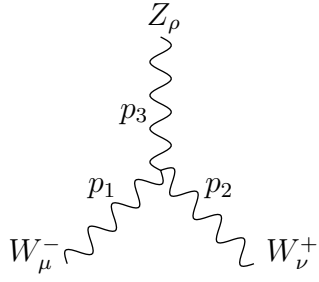
$$\overset{\text{H}}{---} \qquad i / (p^2 - m_H^2)$$

### Three-point gauge-boson couplings:

All momenta are incoming

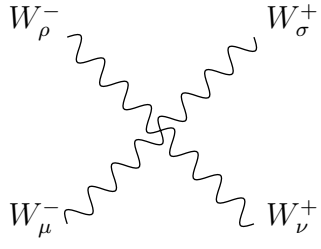


$$i g \sin \theta_W \left( (p_1 - p_2)_\rho g_{\mu\nu} + (p_2 - p_3)_\mu g_{\nu\rho} + (p_3 - p_1)_\nu g_{\rho\mu} \right)$$

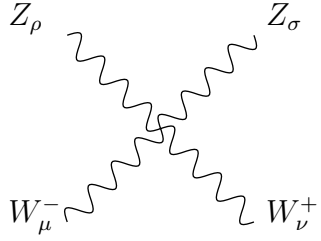


$$i g \cos \theta_W \left( (p_1 - p_2)_\rho g_{\mu\nu} + (p_2 - p_3)_\mu g_{\nu\rho} + (p_3 - p_1)_\nu g_{\rho\mu} \right)$$

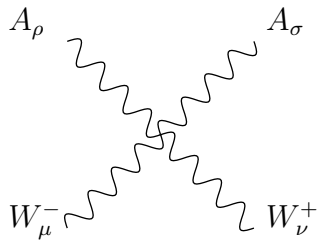
**Four-point gauge-boson couplings:**



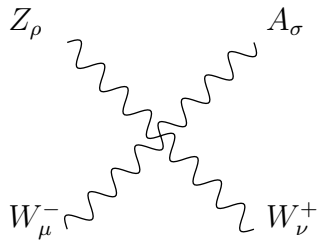
$$i g^2 (2g_{\mu\rho} g_{\nu\sigma} - g_{\mu\nu} g_{\rho\sigma} - g_{\mu\sigma} g_{\nu\rho})$$



$$i g^2 \cos^2 \theta_W (2g_{\mu\nu} g_{\rho\sigma} - g_{\mu\rho} g_{\nu\sigma} - g_{\mu\sigma} g_{\nu\rho})$$

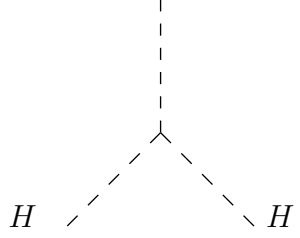


$$i g^2 \sin^2 \theta_W (2g_{\mu\nu} g_{\rho\sigma} - g_{\mu\rho} g_{\nu\sigma} - g_{\mu\sigma} g_{\nu\rho})$$



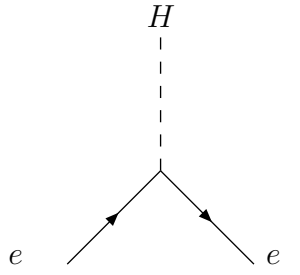
$$i g^2 \cos \theta_W \sin \theta_W (2g_{\mu\nu} g_{\rho\sigma} - g_{\mu\rho} g_{\nu\sigma} - g_{\mu\sigma} g_{\nu\rho})$$

Three-point couplings with Higgs scalars:



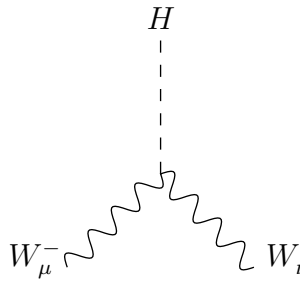
A Feynman diagram representing the Higgs trilinear coupling. It consists of a central vertex from which three dashed lines emerge. One dashed line extends vertically upwards, while the other two extend downwards and outwards at approximately 45-degree angles. Each of the two lower dashed lines is labeled with the letter  $H$ .

$$-\frac{3}{2} i g m_H^2 / M_W$$



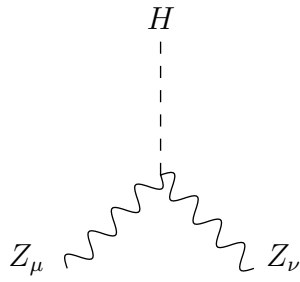
A Feynman diagram representing the Higgs-electron coupling. It features a central vertex. A dashed line labeled  $H$  extends vertically upwards from the vertex. Two solid lines extend downwards and outwards from the vertex at approximately 45-degree angles. Each solid line has an arrow pointing away from the vertex and is labeled with the letter  $e$ .

$$-\frac{1}{2} i g m_e / M_W$$



A Feynman diagram representing the Higgs-WW coupling. A dashed line labeled  $H$  extends vertically upwards from a central vertex. From this vertex, two wavy lines extend downwards and outwards at approximately 45-degree angles. The left wavy line is labeled  $W_\mu^-$  and the right wavy line is labeled  $W_\nu^+$ .

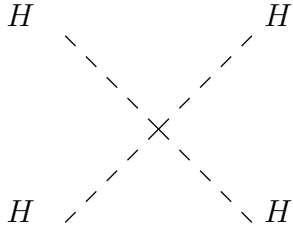
$$i g M_W g_{\mu\nu}$$



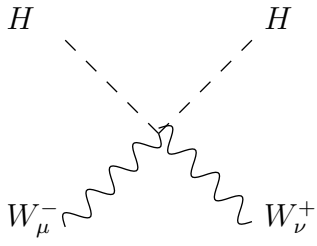
A Feynman diagram representing the Higgs-ZZ coupling. A dashed line labeled  $H$  extends vertically upwards from a central vertex. From this vertex, two wavy lines extend downwards and outwards at approximately 45-degree angles. The left wavy line is labeled  $Z_\mu$  and the right wavy line is labeled  $Z_\nu$ .

$$i (g / \cos^2 \theta_W) M_W g_{\mu\nu}$$

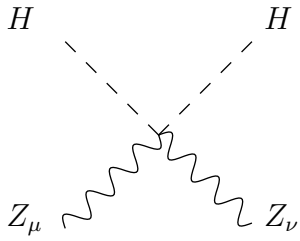
Four-point couplings with Higgs scalars:



$$-\frac{3}{4} i g (m_H^2/M_W^2)$$

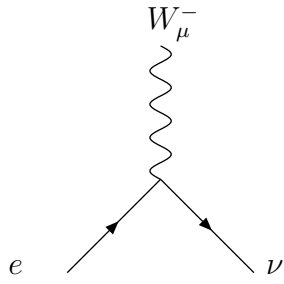


$$\frac{1}{2} i g^2 g_{\mu\nu}$$

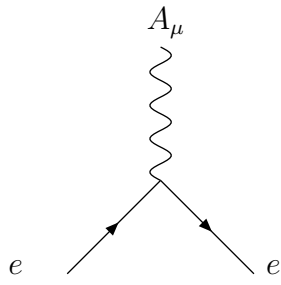


$$\frac{1}{2} i (g^2/\cos^2 \theta_W) g_{\mu\nu}$$

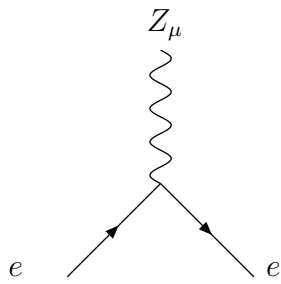
**Fermion interactions with gauge bosons:**



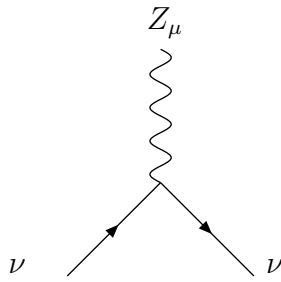
$$-i \left( g/2\sqrt{2} \right) \gamma_\mu (1 - \gamma^5)$$



$$+i g \sin \theta_W \gamma_\mu$$



$$+ \frac{1}{4} i \left( g/\cos \theta_W \right) \gamma_\mu \left( 1 - 4 \sin^2 \theta_W - \gamma^5 \right)$$



$$- \frac{1}{4} i \left( g/\cos \theta_W \right) \gamma_\mu (1 - \gamma^5)$$



# **Phenomenology**

Dr P. Richardson

IPPP, Durham University

Lecture presented at the School for Experimental High Energy Physics Students  
Somerville College, Oxford, September 2010



# Contents

<b>1</b>	<b>Introduction .....</b>	<b>151</b>
<b>2</b>	<b><math>e^+e^-</math> Annihilation.....</b>	<b>152</b>
2.1	Leading Order .....	152
2.2	Higher Order Corrections.....	153
2.2.1	Real Emission.....	154
2.2.2	Virtual Corrections.....	157
<b>3</b>	<b>Running Coupling.....</b>	<b>158</b>
3.1	Event Shapes.....	158
<b>4</b>	<b>Deep Inelastic Scattering.....</b>	<b>163</b>
<b>5</b>	<b>Hadron Collisions.....</b>	<b>166</b>
<b>6</b>	<b>Jets.....</b>	<b>168</b>
6.1	Cone Algorithms.....	170
6.2	Sequential Recombination Algorithms.....	171
6.3	Jet Cross Sections .....	172
6.4	Jet Properties.....	173
<b>7</b>	<b>Electroweak Physics .....</b>	<b>177</b>
7.1	Quantum Corrections to Masses .....	179
7.2	Electroweak Observables.....	180
7.2.1	$W$ mass measurements .....	181
7.2.2	$\rho$ parameter .....	182
<b>8</b>	<b>Higgs Boson .....</b>	<b>182</b>
8.1	Unitarity .....	184
8.2	Higgs Searches .....	185
8.3	Extended Higgs Sectors .....	188
8.3.1	The Two Higgs Doublet Model.....	188
<b>9</b>	<b>Beyond the Standard Model Physics .....</b>	<b>189</b>
9.1	Models .....	190
9.1.1	Grand Unified Theories.....	190
9.1.2	Hierarchy Problem.....	192
9.1.3	Technicolor.....	192
9.1.4	Supersymmetry .....	193
9.1.5	Extra Dimensions .....	199
9.1.6	Little Higgs Models.....	201
9.1.7	Unparticles .....	201
9.2	Beyond the Standard Model Signatures.....	202
9.2.1	Deviations from the Standard Model.....	202
9.2.2	Monojets .....	203
9.2.3	New Particle Production.....	203
9.2.4	Resonance Production .....	204
9.2.5	SUSY-like models.....	205

<b>A</b>	<b>Kinematics and Cross Sections .....</b>	<b>208</b>
A.1	Kinematics.....	208
A.2	Cross Sections .....	209
A.3	Cross Sections in Hadron Collisions .....	210
A.3.1	Resonance production ( $2 \rightarrow 1$ processes).....	211
A.3.2	$2 \rightarrow 2$ Scattering Processes .....	211
<b>B</b>	<b>Flavour Physics.....</b>	<b>212</b>
	<b>References.....</b>	<b>216</b>

# Phenomenology

August 10, 2011

P. Richardson,  
IPPP, Durham University.

## 1 Introduction

Historically the lecture notes for the phenomenology course have consisted of the slides presented in the lectures. These notes are intended to provide additional information, and more mathematical detail, on the more theoretical aspects of the course which don't change from year to year. The recent experimental results, which as the LHC experiments take more and more data change from day-to-day, will continue to be presented solely on the slides used in the lectures.

The course will focus primarily, and unapologetically, on hadron collider, and specifically LHC, phenomenology. In order to study hadron collisions we need to understand the basics of cross section calculations, Quantum Chromodynamics (QCD) and jets which we will first consider in the simpler environment of  $e^+e^-$  and lepton-hadron collisions before we go on to study hadron-hadron collisions. This occupies the first three lectures of the course. The next two lectures consider the electroweak and Higgs sector of the Standard Model. Lectures six and seven consider possible physics beyond the Standard Model. The final lecture looks at the physics of Monte Carlo event generators which are now an essential tool in all aspects of modern collider physics.

Unfortunately there is no single good book on modern phenomenology. Two old classics but now a bit dated are:

- *Quarks and Leptons* Halzen and Martin [1];
- *Collider Physics* Barger and Phillips [2].

Two good books, although mainly focused on QCD and probably at a bit too high a level for this course, are:

- *QCD and Collider Physics* Ellis, Stirling and Webber [3];
- *Quantum Chromodynamics* Dissertori, Knowles and Schmelling [4];

and of course the classic on Higgs physics

- *The Higgs Hunter's Guide* Gunion, Haber, Kane and Dawson [5].

In addition the recent reviews:

- *Towards Jetography* [6] which provides a good primer on jet physics;
- *General-purpose event generators for LHC physics* [7] which gives a detailed description of the physics of Monte Carlo event generators;

are good sources of additional information.

## 2 $e^+e^-$ Annihilation

Historically this course would spend a significant amount of time looking at  $e^+e^-$  annihilation. It is less relevant for current experiments but the results from LEP are still important and it is worth discussing as the simplest type of collisions. If we consider what happens when electrons and positrons collide, then the most likely thing is that some hadrons are produced. However, none of the Lagrangians or Feynman rules you've learnt involve hadrons. This is the key issue in most collider physics, we can calculate things for quarks and gluons but we observe hadrons.

### 2.1 Leading Order

We will start by studying one of the simplest possible processes,  $e^+e^-$  annihilation via the exchange of a photon or  $Z^0$  boson, as shown in Fig. 1. This process can produce either



Figure 1: Feynman diagrams for  $e^+e^-$  annihilation into leptons and quarks.

quarks or leptons. Unfortunately due to quark confinement we cannot observe free quarks directly, instead quarks and antiquarks will produce hadrons with unit probability. Much of what we will study in this course will be concerned with the question, given we observe hadrons how do we infer what was going on in the fundamental process involving quarks?

We will start with the simplest example, given quarks and antiquarks produce quarks with unit probability we can measure the cross section for the process  $e^+e^- \rightarrow q\bar{q}$ , which we can calculate perturbatively, by measuring the cross section for  $e^+e^- \rightarrow \text{hadrons}$ . This is the basis of most collider phenomenology, we want to measure things using hadrons that we can calculate using quarks. The total cross section for  $e^+e^-$  annihilation into hadrons is the simplest such observable.

Using the techniques you have learnt in the other courses you can now calculate the total cross section for  $e^+e^-$  annihilation. In reality it is more common to study the ratio

$$R \equiv \frac{\sigma(e^+e^- \rightarrow \text{hadrons})}{\sigma(e^+e^- \rightarrow \mu^+\mu^-)}, \quad (1)$$

as this reduces experimental uncertainties. At low energies this process is dominated by photon exchange so we can neglect the  $Z^0$  boson. In this limit

$$\sigma(e^+e^- \rightarrow \mu^+\mu^-) = \frac{4\pi\alpha^2}{3s}, \quad (2)$$

where  $s$  is the centre-of-mass energy of the collision squared. The cross section for the production of quarks is

$$\sigma(e^+e^- \rightarrow \text{hadrons}) = \frac{4\pi\alpha^2}{3s} \sum_q e_q^2 N_C, \quad (3)$$

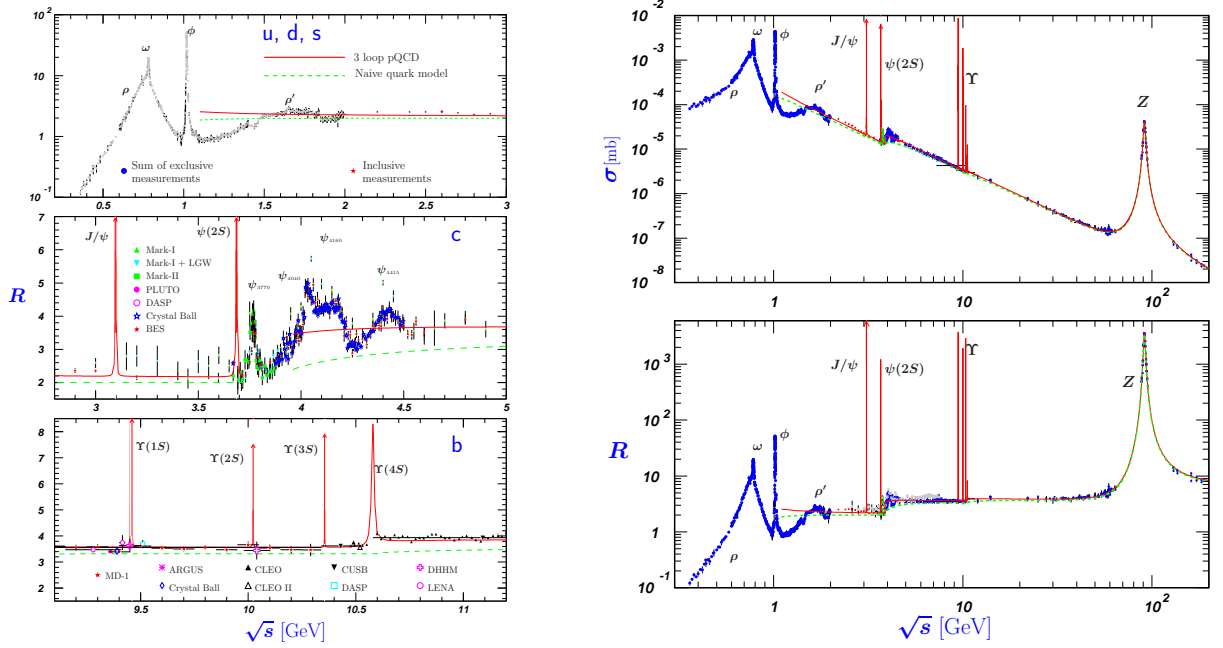


Figure 2: The ratio  $R \equiv \frac{\sigma(e^+e^- \rightarrow \text{hadrons})}{\sigma(e^+e^- \rightarrow \mu^+\mu^-)}$  as a function of energy taken from Ref. [8].

where  $e_q$  is the charge of the quark in units of the positron charge and the sum runs over all quarks for which the centre-of-mass energy  $\sqrt{s} > 2m_q$ , where  $m_q$  is the mass of the quark. Remember we must sum over all the quantum numbers of the quarks so the cross section is multiplied by number of colours,  $N_c$ . Therefore for centre-of-mass energies much less than the mass of the  $Z^0$  boson,  $\sqrt{s} \ll M_z$ ,

$$R = \sum_q e_q^2 N_c. \quad (4)$$

The experimental measurement of this ratio is shown in Fig.2 as a function of energy showing the thresholds for the production of the charm and bottom quarks. Below the charm threshold there are three active quarks down ( $e_d = -\frac{1}{3}$ ), up ( $e_u = \frac{2}{3}$ ) and strange ( $e_s = -\frac{1}{3}$ ) giving  $R = 2$ . Above the charm ( $e_c = \frac{2}{3}$ ) threshold  $R = \frac{10}{3}$  while above the bottom ( $e_b = -\frac{1}{3}$ ) threshold  $R = \frac{11}{3}$ .

## 2.2 Higher Order Corrections

When we draw Feynman diagrams we are performing a perturbative expansion in the (hopefully) small coupling constant. Unfortunately the strong coupling often isn't very small, at the  $Z^0$  mass,  $\alpha_s(M_Z) = 0.118$ . We therefore need to consider higher orders in the perturbative expansion. There are always two types of correction:

- real gluon emission;
- virtual gluon loops.

### 2.2.1 Real Emission

There are two possible diagrams for gluon emission, see Fig. 3. The matrix element, only



Figure 3: Feynman diagrams for  $e^+e^- \rightarrow q\bar{q}g$ .

considering photon exchange for simplicity, is

$$\begin{aligned} \mathcal{M} = & e^2 e_q g_s t_{ij}^a \bar{v}(p_b) \gamma_\mu u(p_a) \frac{-g^{\mu\nu}}{q^2} \\ & \bar{u}_i(p_1) \left[ \gamma_\sigma \frac{\not{p}_1 + \not{p}_3}{(p_1 + p_3)^2} \gamma_\nu - \gamma_\nu \frac{\not{p}_2 + \not{p}_3}{(p_2 + p_3)^2} \gamma_\sigma \right] v_j(p_2) \epsilon_a^\sigma(p_3), \end{aligned} \quad (5)$$

where  $p_{a,b}$  are the 4-momenta of the incoming electron and positron, respectively. The outgoing quark, antiquark and gluon have 4-momenta  $p_{1,2,3}$ , respectively. The total momentum of the system  $q = p_a + p_b = p_1 + p_2 + p_3$ . The gluon has colour index  $a = 1, \dots, N_C^2 - 1$  whereas the quark/antiquark have colour indices  $i, j = 1, \dots, N_C$ .

Summing/averaging over spins and colours

$$|\overline{\mathcal{M}}|^2 = \frac{4e^2 e_q^2 g_s^2 N_c}{s} C_F \frac{(p_1 \cdot p_a)^2 + (p_1 \cdot p_b)^2 + (p_2 \cdot p_a)^2 + (p_2 \cdot p_b)^2}{p_1 \cdot p_3 p_2 \cdot p_3}. \quad (6)$$

The colour algebra gives a colour factor

$$\sum_a^{N_C^2-1} t_{ij}^a (t_{ij}^a)^* = t_{ij}^a t_{ji}^a = \frac{1}{2} \delta^{aa} = \frac{1}{2} (N_C^2 - 1) = N_C C_F, \quad (7)$$

where the colour charges in the fundamental (quarks and antiquarks) and adjoint (gluons) representations are

$$C_F \equiv \frac{1}{2N_C} (N_C^2 - 1) \quad \text{and} \quad C_A \equiv N_C, \quad (8)$$

respectively.

The three-body phase space is

$$\begin{aligned} d\Phi_n(p_a + p_b; p_1, p_2, p_3) &= \delta^4(p_a + p_b - p_1 - p_2 - p_3) \frac{d^3 p_1}{(2\pi)^3 2E_1} \frac{d^3 p_2}{(2\pi)^3 2E_2} \frac{d^3 p_3}{(2\pi)^3 2E_3} \\ &= \frac{1}{8(2\pi)^9} p_1 dp_1 d\cos\theta d\phi p_2 dp_2 d\cos\beta d\alpha \frac{1}{p_3} \delta(\sqrt{s} - p_1 - p_2 - p_3), \end{aligned}$$

where  $\theta$  and  $\phi$  are the polar and azimuthal angles, respectively, of the outgoing quark with respect to the beam direction. The polar and azimuthal angles of the antiquark with



respect to the quark direction are  $\beta$  and  $\alpha$ , respectively. We have integrated over  $p_3$  using the  $\delta$ -function and assumed that the outgoing particles are massless.

Using momentum conservation

$$|\vec{p}_3| = |\vec{p}_1 + \vec{p}_2| = \sqrt{p_1^2 + p_2^2 + 2p_1p_2 \cos \beta}. \quad (9)$$

Therefore the integral over the remaining  $\delta$ -function is

$$\int d\cos \beta \delta(\sqrt{s} - p_1 - p_2 - p_3) = \frac{p_3}{p_1 p_2}, \quad (10)$$

so

$$\begin{aligned} d\Phi_n(p_a + p_b; p_1, p_2, p_3) &= \frac{1}{8(2\pi)^9} dp_1 d\cos \theta d\phi dp_2 d\alpha \\ &= \frac{s}{16(2\pi)^7} dx_1 dx_2 \frac{d\cos \theta d\phi d\alpha}{2(2\pi)^2}, \end{aligned} \quad (11)$$

where  $x_i \equiv 2p_i/\sqrt{s}$ . Momentum and energy conservation requires that  $x_1 + x_2 + x_3 = 2$ .

The total cross section is

$$\begin{aligned} \sigma &= \frac{1}{2s} \frac{s}{16(2\pi)^3} \int dx_1 dx_2 \frac{d\cos \theta d\phi d\alpha}{2(2\pi)^2} |\overline{M}|^2, \\ &= \frac{4\pi\alpha^2 e_q^2 N_c}{3s} C_F \frac{\alpha_S}{2\pi} \int dx_1 dx_2 \frac{x_1^2 + x_2^2}{(1-x_1)(1-x_2)}. \end{aligned} \quad (12)$$

The contribution from the  $Z^0$  boson is the same except for  $\sigma_0$ . This is divergent at the edge of phase space as  $x_{1,2} \rightarrow 1$  so that the total cross section is  $\sigma = \infty$ !

This is a common feature of all perturbative QCD calculations. Configurations which are indistinguishable from the leading-order result are divergent. Physically there are two regions where this happens.

1. *Collinear limit:* If we take  $x_1 \rightarrow 1$  at fixed  $x_2$  or  $x_2 \rightarrow 1$  at fixed  $x_1$ . We can see what happens physically by considering the dot product of the antiquark and gluon 4-momenta, *i.e.*

$$2p_2 \cdot p_3 = \frac{s x_2 x_3}{2} (1 - \cos \theta_{23}) = s(1 - x_1) \Rightarrow (1 - \cos \theta_{23}) = \frac{2(1 - x_1)}{x_2 x_3} \rightarrow 0. \quad (13)$$

So the limit  $x_1 \rightarrow 1$ , where the matrix element diverges, corresponds to the angle between the antiquark and gluon  $\theta_{23} \rightarrow 0$ , *i.e.* collinear emission of the gluon from the antiquark. Similarly the limit  $x_2 \rightarrow 1$  corresponds to collinear emission of the gluon from the quark.

2. *Soft limit:*  $x_{1,2} \rightarrow 1$  at fixed  $\frac{1-x_1}{1-x_2}$ . We can consider what happens in this limit by considering the energy of the gluon

$$E_g = \frac{\sqrt{s}}{2} x_3 = \frac{\sqrt{s}}{2} (1 - x_1 + 1 - x_2) \rightarrow 0, \quad (14)$$

*i.e.* the matrix element diverges in the soft limit, when the energy of the gluon is small.

These are both universal features of QCD matrix elements. In these limits QCD matrix elements *factorize*, *i.e.* the matrix element including the emission of a soft or collinear gluon can be written as the convolution of the matrix element before the emission and a universal term describing collinear or soft emission.

**Collinear Limit** If we first consider collinear emission we take the momentum of the gluon  $p_3$  parallel to  $p_2$  ( $\theta_{23} = 0$ ). We can therefore define

$$p_2 = (1 - z)\bar{p}_2, \quad p_3 = z\bar{p}_2, \quad \text{with } \bar{p}_2^2 = 0, \quad (15)$$

where  $\bar{p}_2$  is the momentum of the antiquark before the gluon radiation and  $z$  is the fraction of the original antiquark's momentum carried by the gluon. In this limit the matrix element factorizes

$$|\mathcal{M}_{q\bar{q}g}|^2 = |\mathcal{M}_{q\bar{q}}|^2 \times \frac{g_s^2}{p_2 \cdot p_3} \times C_F \frac{1 + (1 - z)^2}{z}. \quad (16)$$

As does the phase space

$$dx_1 dx_2 \longrightarrow \frac{1}{4} z(1 - z) dz d\theta_{23}^2. \quad (17)$$

Putting this together

$$\sigma = \sigma_0 \int \frac{d\theta_{23}^2}{\theta_{23}^2} dz C_F \frac{\alpha_S}{2\pi} \frac{1 + (1 - z)^2}{z} = \sigma_0 \int \frac{d\theta_{23}^2}{\theta_{23}^2} dz \frac{\alpha_S}{2\pi} \hat{P}_{q \rightarrow gq}(z). \quad (18)$$

The Dokshitzer-Gribov-Lipatov-Altarelli-Parisi (DGLAP) splitting function is a universal probability distribution for the radiation of a collinear gluon in any processes producing a quark. The splitting functions are:

$$\begin{aligned} \hat{P}_{g \rightarrow gg}(z) &= C_A \left[ \frac{1 - z}{z} + \frac{z}{1 - z} + z(1 - z) \right]; & \hat{P}_{q \rightarrow qg}(z) &= C_F \frac{1 + z^2}{1 - z}; \\ p_{g \rightarrow q\bar{q}}(z) &= T_R [z^2 + (1 - z)^2]; & \hat{P}_{q \rightarrow gq}(z) &= C_F \frac{1 + (1 - z)^2}{z}; \end{aligned} \quad (19)$$

where  $z$  is the fraction of the momenta carried by the first outgoing particle and  $T_R = \frac{1}{2}$ .

**Soft Limit** In the limit that  $E_g \rightarrow 0$  the matrix element for the process factorizes

$$\mathcal{M}_{q\bar{q}g} = \mathcal{M}_{q\bar{q}} g_s t_{ij}^a \left( \frac{p_1}{p_1 \cdot p_3} - \frac{p_2}{p_2 \cdot p_3} \right) \cdot \epsilon_A(p_3), \quad (20)$$

the *eikonal current*. The matrix element squared therefore factorizes in this case

$$|\mathcal{M}_{q\bar{q}g}|^2 = |\mathcal{M}_{q\bar{q}}|^2 g_s^2 C_F \frac{2p_1 \cdot p_2}{p_1 \cdot p_3 p_2 \cdot p_3}. \quad (21)$$

The phase space is

$$dx_1 dx_2 \longrightarrow \frac{2}{s} E_g dE_g d\cos\theta. \quad (22)$$

So in the soft limit

$$\sigma = \sigma_0 \int C_F \frac{\alpha_S}{2\pi} \frac{dE_g}{E_g} d\cos\theta \frac{2(1 - \cos\theta_{qq})}{(1 - \cos\theta_{qg})(1 - \cos\theta_{\bar{q}g})}, \quad (23)$$

the *dipole radiation pattern* a universal probability distribution for the emission of a soft gluon from any colour-connected pair of partons.<sup>1</sup>

### 2.2.2 Virtual Corrections

There are three diagrams involving virtual gluon loops, see Fig. 4. This contribution is

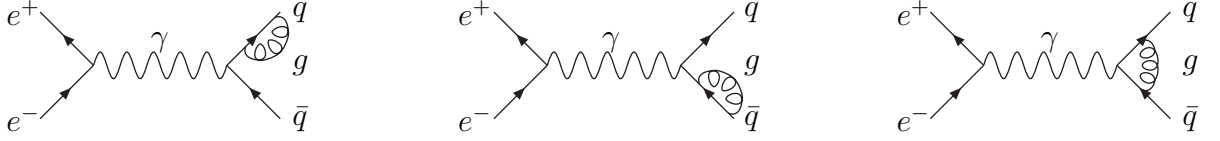


Figure 4: Virtual loop corrections to  $e^+e^- \rightarrow q\bar{q}$ .

also divergent, but negative. This will cancel the real divergence to give a finite answer. To show this we need to regularize both the real and virtual cross sections and add them together. The result should be finite when we remove the regularization. The standard way of doing this is to work in  $d = 4 - 2\epsilon$  dimensions where to regularize these infrared divergences  $\epsilon < 0$ . In this case

$$\begin{aligned} \sigma_{\text{real}} &= \sigma_0 C_F \frac{\alpha_S}{2\pi} H(\epsilon) \left( \frac{4}{\epsilon^2} + \frac{3}{\epsilon} + \frac{19}{2} - \pi^2 + \mathcal{O}(\epsilon) \right), \\ \sigma_{\text{virtual}} &= \sigma_0 C_F \frac{\alpha_S}{2\pi} H(\epsilon) \left( -\frac{4}{\epsilon^2} - \frac{3}{\epsilon} - 8 + \pi^2 + \mathcal{O}(\epsilon) \right), \end{aligned}$$

where  $H(0) = 1$ . The sum

$$\sigma_{\text{total}} = \sigma_{\text{real}} + \sigma_{\text{virtual}} = \sigma_0 C_F \frac{3\alpha_S}{4\pi}, \quad (24)$$

is finite as  $\epsilon \rightarrow 0$ . So finally combining this correction with the leading-order result

$$R(e^+e^-) = R_0(e^+e^-) \left( 1 + \frac{\alpha_s}{\pi} \right). \quad (25)$$

Measuring  $R(e^+e^-)$  is one way of measuring the strong coupling giving<sup>2</sup>

$$\alpha_S(m_Z) = 0.1226 \pm 0.0038. \quad (26)$$

The second and third order corrections, and the results for the next-to-leading-order corrections including quark masses are also known.

This is the simplest example of an observable which we can calculate using perturbation theory involving quarks and gluons, but measure experimentally using hadrons. We now need to go on and consider more complicated observables.

<sup>1</sup>Strictly this is only universal at the amplitude level, not as a probability distribution.

<sup>2</sup>Taken from the Ref. [8].

### 3 Running Coupling



Figure 5: Example virtual corrections contributing to the evolution of the strong coupling constant.

In addition to the infrared, soft and collinear, divergences we saw in the calculation of  $\sigma(e^+e^- \rightarrow \text{hadrons})$  it is possible to have ultraviolet divergences. The virtual corrections shown in Fig. 5 are divergent in the ultraviolet. These, and other similar corrections, lead to the strong coupling being *renormalized* to absorb the ultraviolet singularities. The renormalisation procedure introduces an unphysical renormalisation scale  $\mu$ .

The leads to:

1. diagrams are dependent on  $\mu$ ;
2.  $\alpha_S$  is replaced by the running coupling  $\alpha_S(\mu)$ ;
3. although we can't calculate the coupling we can calculate how it changes with scale:

$$\mu^2 \frac{d\alpha_S}{d\mu^2} \equiv \beta(\alpha_S) = -\beta_0 \alpha_S^2 + \dots \quad \beta_0 = \frac{11N_c - 4T_R n_f}{12\pi}, \quad (27)$$

where  $n_f$  is the number of active quark flavours.

For  $\beta_0 > 0$  the coupling displays *asymptotic freedom*, i.e.  $\alpha_S(\mu) \rightarrow 0$  as  $\mu \rightarrow \infty$  which allows us to perform perturbative calculations at high energies where the coupling is small.

It is standard to quote the value of  $\alpha_S(M_Z)$ . The value at other scales can be found by solving the evolution equation. Recent experimental measurements of the strong coupling evolved to the  $Z^0$  mass and the running of coupling are shown in Fig. 6.

It is common to define a scale  $\Lambda_{\text{QCD}}$  so that

$$\alpha_s(\mu) = \frac{4\pi}{\beta_0 \ln \left( \frac{\mu^2}{\Lambda_{\text{QCD}}^2} \right)} [1 + \dots]. \quad (28)$$

In general there is a choice of precisely how we perform the renormalisation, which leads to both *renormalisation scale* and *scheme* dependence. Physical observables don't depend on  $\mu_F$  or the renormalisation scheme, but fixed order perturbative calculations do.

#### 3.1 Event Shapes

If we consider the  $e^+e^-$  annihilation events shown in Fig. 7 we see a collimated bunch of hadrons travelling in roughly the same direction as the original quarks or gluons. Often you can “see” the jets without some fancy mathematical definition. We will come back

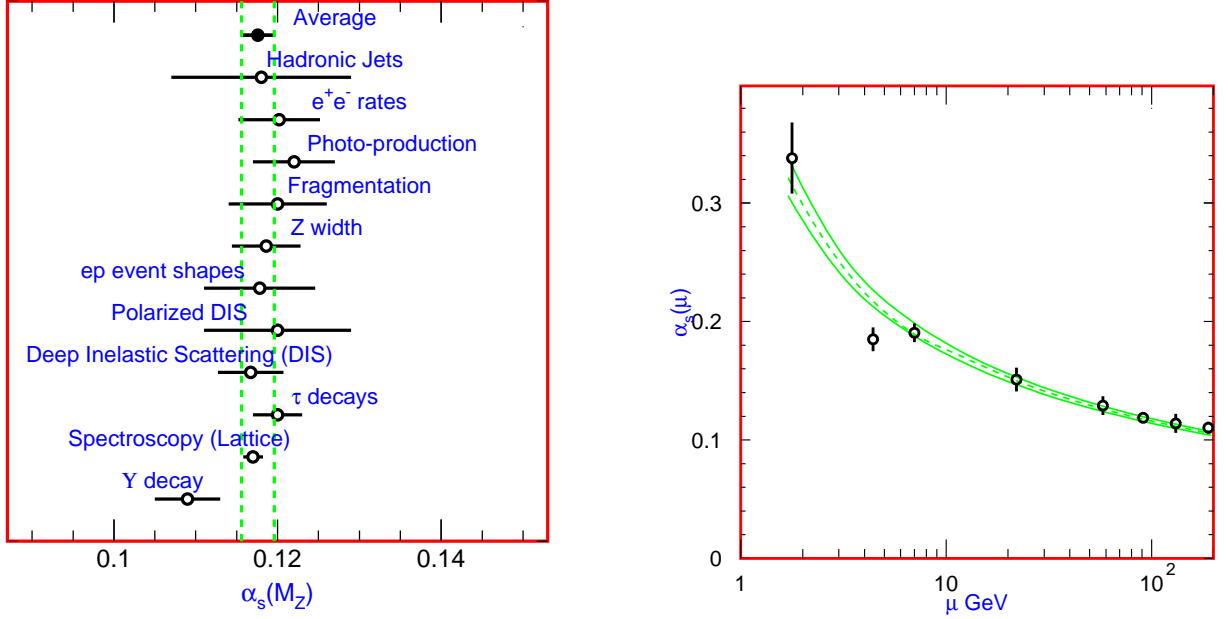


Figure 6: Measurements of the strong coupling at the  $Z^0$  mass and the running of the coupling taken from Ref. [8].

and consider jets in more detail when we consider hadron–hadron collisions later in the course, in Section 6.

An alternative to defining jets is to define a more global measure of the event which is sensitive to the structure of the event. We need a number of properties to achieve this, the most important of which is *infrared safety*, *i.e.* if there is soft or collinear emission the answer doesn’t change. Formally if a parton splits into two collinear partons

$$p \rightarrow zp + (1 - z)p, \quad (29)$$

or if a soft parton is emitted with momentum

$$p \rightarrow 0, \quad (30)$$

the result should not change.

After the total cross section, the simplest infrared safe observable is the thrust

$$T = \max_{\vec{n}} \frac{\sum_i |\vec{p}_i \cdot \vec{n}|}{\sum_i |\vec{p}_i|}, \quad (31)$$

where the sum is over all the final-state particles and the direction of the unit vector  $\vec{n}$ , the thrust axis, is chosen to maximize the projection of the momenta of the final-state particles along that direction.

For a two-jet *pencil-like* event all the particles lie along the thrust axis giving  $T = 1$ . For a totally *spherical* event the thrust can be calculated by taking a spherical distribution of particles in the limit of an infinite number of particles giving  $T = \frac{1}{2}$ . For three partons

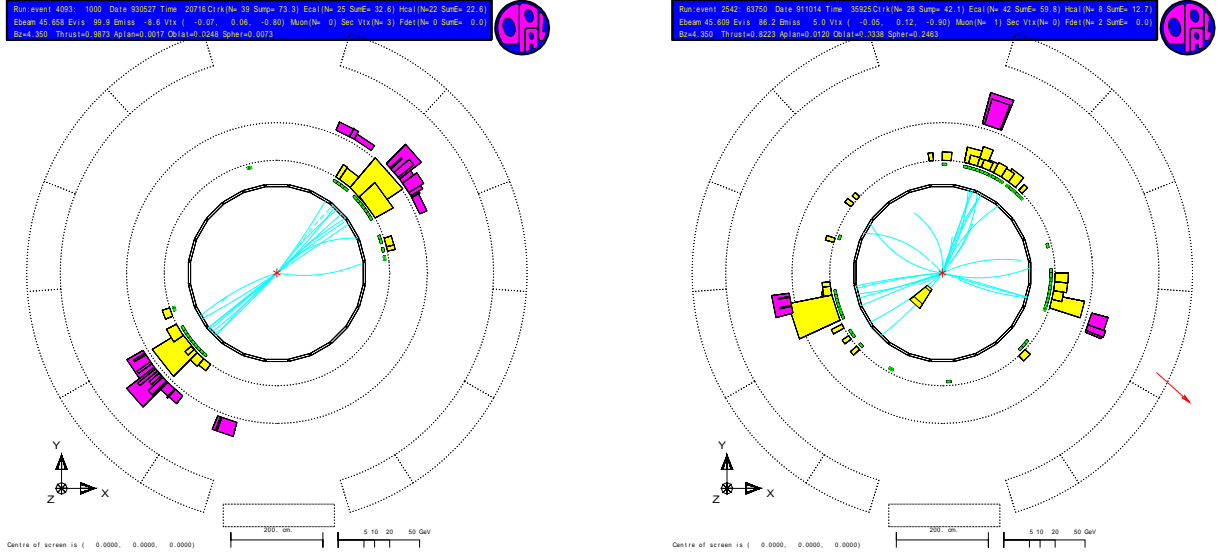


Figure 7: Example two and three jet  $e^+e^-$  events.

the thrust axis will lie along the direction of the most energetic parton, by momentum conservation there is an equal contribution to the thrust from the other partons giving  $T = \max\{x_1, x_2, x_3\}$ .

In order to calculate the differential cross section with respect to the thrust for  $e^+e^- \rightarrow q\bar{q}g$  we can start from the differential cross section in Eqn.12. In many cases when we wish to introduce a new quantity into a differential cross section it is easier to insert the definition using a  $\delta$ -function rather than performing a Jacobian transform, in this case we use

$$1 = \int dT \delta(T - \max\{x_1, x_2, x_3\}), \quad (32)$$

to give

$$\frac{d\sigma}{dT} = \sigma_0 C_F \frac{\alpha_S}{2\pi} \int dx_1 dx_2 \frac{x_1^2 + x_2^2}{(1-x_1)(1-x_2)} \delta(T - \max\{x_1, x_2, x_3\}), \quad (33)$$

where  $\sigma_0$  is the leading-order cross section for  $e^+e^- \rightarrow q\bar{q}$ . This expression can be evaluated in each of the three phase-space regions shown in Fig.8. First in the region where  $x_1 > x_{2,3}$

$$\begin{aligned} \left. \frac{d\sigma}{dT} \right|_{x_1 > x_{2,3}} &= \sigma_0 C_F \frac{\alpha_S}{2\pi} \int_{2(1-T)}^T dx_2 \frac{T^2 + x_2^2}{(1-T)(1-x_2)} \\ &= \sigma_0 C_F \frac{\alpha_S}{2\pi} \frac{1}{1-T} \int_{2(1-T)}^T dx_2 \frac{T^2 + 1}{(1-x_2)} - (1+x_2), \end{aligned} \quad (34)$$

where we have used the  $\delta$ -function to integrate over  $x_1$  and the limits on  $x_2$  are given by  $x_2 = x_1 = T$  for the upper limit and  $T = x_1 = x_3 = 2 - x_1 - x_2 = 2 - T - x_2$  for the lower limit. Performing the integral gives

$$\left. \frac{d\sigma}{dT} \right|_{x_1 > x_{2,3}} = \sigma_0 C_F \frac{\alpha_S}{2\pi} \frac{1}{1-T} \left[ (T^2 + 1) \ln \left( \frac{2T-1}{1-T} \right) + 4 - 7T + \frac{3}{2}T^2 \right]. \quad (35)$$

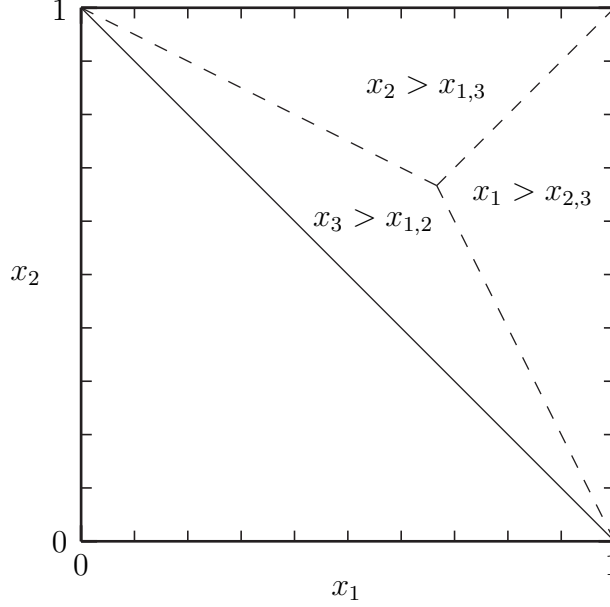


Figure 8: Phase space for  $e^+e^- \rightarrow q\bar{q}g$ . The requirement that  $x_3 \leq 1$  ensures that  $x_1 + x_2 \geq 1$  by momentum conservation so that physical phase space is the upper half plane.

The same result is obtained in the region  $x_2 > x_{1,3}$  due to the symmetry of the formulae under  $x_1 \leftrightarrow x_2$ .

In the final region we can take the integrals to be over  $x_{2,3}$  and use the  $\delta$ -function to eliminate the integral over  $x_3$  giving

$$\begin{aligned}
\left. \frac{d\sigma}{dT} \right|_{x_3 > x_{1,2}} &= \sigma_0 C_F \frac{\alpha_S}{2\pi} \int_{2(1-T)}^T dx_2 \frac{(2-T-x_2)^2 + x_2^2}{(T+x_2-1)(1-x_2)}, \\
&= \sigma_0 C_F \frac{\alpha_S}{2\pi} \int_{2(1-T)}^T dx_2 \frac{1}{T} [(2-T-x_2)^2 + x_2^2] \left[ \frac{1}{T+x_2-1} + \frac{1}{1-x_2} \right], \\
&= \sigma_0 C_F \frac{\alpha_S}{2\pi} \frac{2}{T} \left[ (2-2T+T^2) \ln \left( \frac{2T-1}{1-T} \right) + 2T-3T^2 \right],
\end{aligned} \tag{36}$$

where after the integral over  $x_3$ ,  $x_1 = 2 - x_2 - T$  and the limits are calculated in the same way as before.

Putting the results from the three regions together gives

$$\frac{d\sigma}{dT} = \sigma_0 C_F \frac{\alpha_S}{2\pi} \left[ \frac{2}{T(1-T)} (3T(T-1) + 2) \ln \left( \frac{2T-1}{1-T} \right) + \frac{3(3T-2)(T-2)}{1-T} \right]. \tag{37}$$

This result clearly diverges as  $T \rightarrow 1$ , indeed in this limit

$$\frac{1}{\sigma_0} \frac{d\sigma}{dT} \xrightarrow{T \rightarrow 1} -C_F \frac{\alpha_S}{2\pi} \left[ \frac{4}{(1-T)} \ln(1-T) + \frac{3}{1-T} \right]. \tag{38}$$

We can use this result to define a two- and three-jet rate so that the three jet rate is

$$R_3(\tau) = \int_{\frac{1}{2}}^{1-\tau} \frac{1}{\sigma_0} \frac{d\sigma}{dT} \xrightarrow{\tau \rightarrow 0} C_F \frac{\alpha_S}{2\pi} 2 \ln^2 \tau, \tag{39}$$

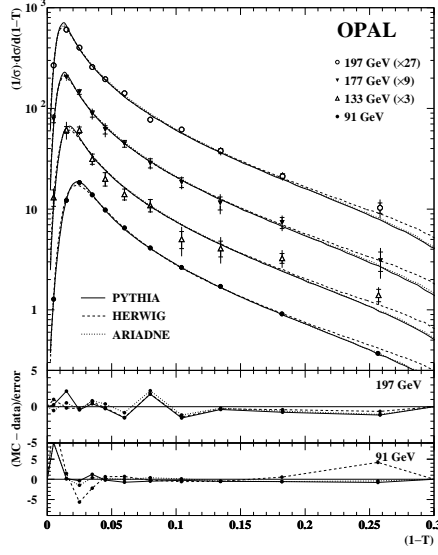


Figure 9: Thrust distribution at various centre-of-mass energies compared with Monte Carlo simulations, taken from Ref. [9].

and the two jet rate

$$R_2(\tau) = 1 - R_3(\tau) \xrightarrow{\tau \rightarrow 0} 1 - C_F \frac{\alpha_S}{2\pi} 2 \ln^2 \tau. \quad (40)$$

Similar logarithmically enhanced terms appear at all orders in the perturbative expansion giving an extra  $\ln^2 \tau$  at every order in  $\alpha_S$ , *i.e.*

$$R_2(\tau) \equiv \int_{1-\tau}^1 dT \frac{1}{\sigma} \frac{d\sigma}{dT} \xrightarrow{\tau \rightarrow 0} 1 - C_F \frac{\alpha_S}{2\pi} 2 \ln^2 \tau + \left( C_F \frac{\alpha_S}{2\pi} \right)^2 2 \ln^4 \tau + \dots \quad (41)$$

Although  $\alpha_S$  is small,  $\ln^2 \tau$  is large so the perturbative expansion breaks down. The solution is to resum the large  $\alpha_S^n \ln^{2n} \tau$  terms to all orders giving the *Sudakov Form Factor*

$$R_2(\tau) \xrightarrow{\tau \rightarrow 0} \exp \left[ -C_F \frac{\alpha_S}{2\pi} 2 \ln^2 \tau \right]. \quad (42)$$

This is finite (zero) at  $\tau = 0$ , *i.e.* the probability for no gluon radiation is zero. In general the Sudakov form factor gives the probability of no radiation

$$P(\text{no emission}) = \exp \left[ -\hat{P}_{\text{naive}}(\text{emission}) \right]. \quad (43)$$

An example of the experimental measurement of the thrust distribution is shown in Fig. 9 compared to various Monte Carlo simulations which include resummation of these large logarithmic contributions..



## 4 Deep Inelastic Scattering

Historically measurements of deep inelastic scattering were very important for establishing the nature of QCD. Nowadays they are mainly important for the measurement of the parton distribution functions we need to calculate all cross sections for processes with incoming hadrons. As the proton isn't fundamental at sufficiently high energies the scattering is from the constituent quarks and gluons.

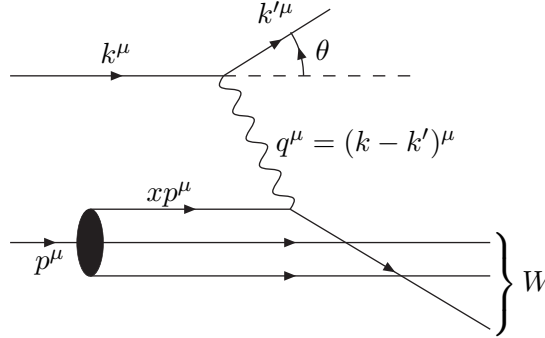


Figure 10: Deep inelastic scattering kinematics.

In deep inelastic scattering processes it is conventional to use the kinematic variables shown in Fig.10. The struck parton carries a fraction  $x$  of the four-momentum of the incoming hadron. The four-momentum of the exchanged boson is  $q$  and the virtuality of the boson  $Q^2 = -q^2$ . Using momentum conservation

$$xp + q = p', \quad (44)$$

where  $p'$  is the 4-momentum of the scattered quark. Therefore  $(xp + q)^2 = 0$  giving  $x = \frac{Q^2}{2p \cdot q}$ . Similarly the mass of the hadronic system is  $W^2 = (p + q)^2$ . By definition  $(k + p)^2 = 2k \cdot p = s$  and therefore  $y = \frac{p \cdot q}{p \cdot k} = \frac{Q^2}{xs}$ .

Deep inelastic scattering has  $Q^2 \gg M^2$  (deep) and  $W^2 \gg M^2$  (inelastic), where  $M$  is the proton mass. Historically the observation and understanding of DIS was one of the key pieces of evidence for quarks. On general grounds the cross section has the form

$$\frac{d^2\sigma}{dx dQ^2} = \frac{4\pi\alpha^2}{xQ^4} [y^2 x F_1(x, Q^2) + (1 - y) F_2(x, Q^2)], \quad (45)$$

which parameterizes the cross section in terms of two unknown structure functions,  $F_{1,2}(x, Q^2)$ . If we consider that the proton is a bound state of partons we can calculate these structure functions.

Suppose that the probability of a given type of quark carrying a fraction  $\eta$  of the proton's momentum is  $f_q(\eta)$  the cross section for hadron scattering can be written in terms of those for partonic scattering

$$\frac{d^2\sigma(e + \text{proton})}{dx dQ^2} = \sum_q \int_0^1 d\eta f_q(\eta) \frac{d^2\sigma(e + q(\eta p))}{dx dQ^2}. \quad (46)$$

## H1 and ZEUS

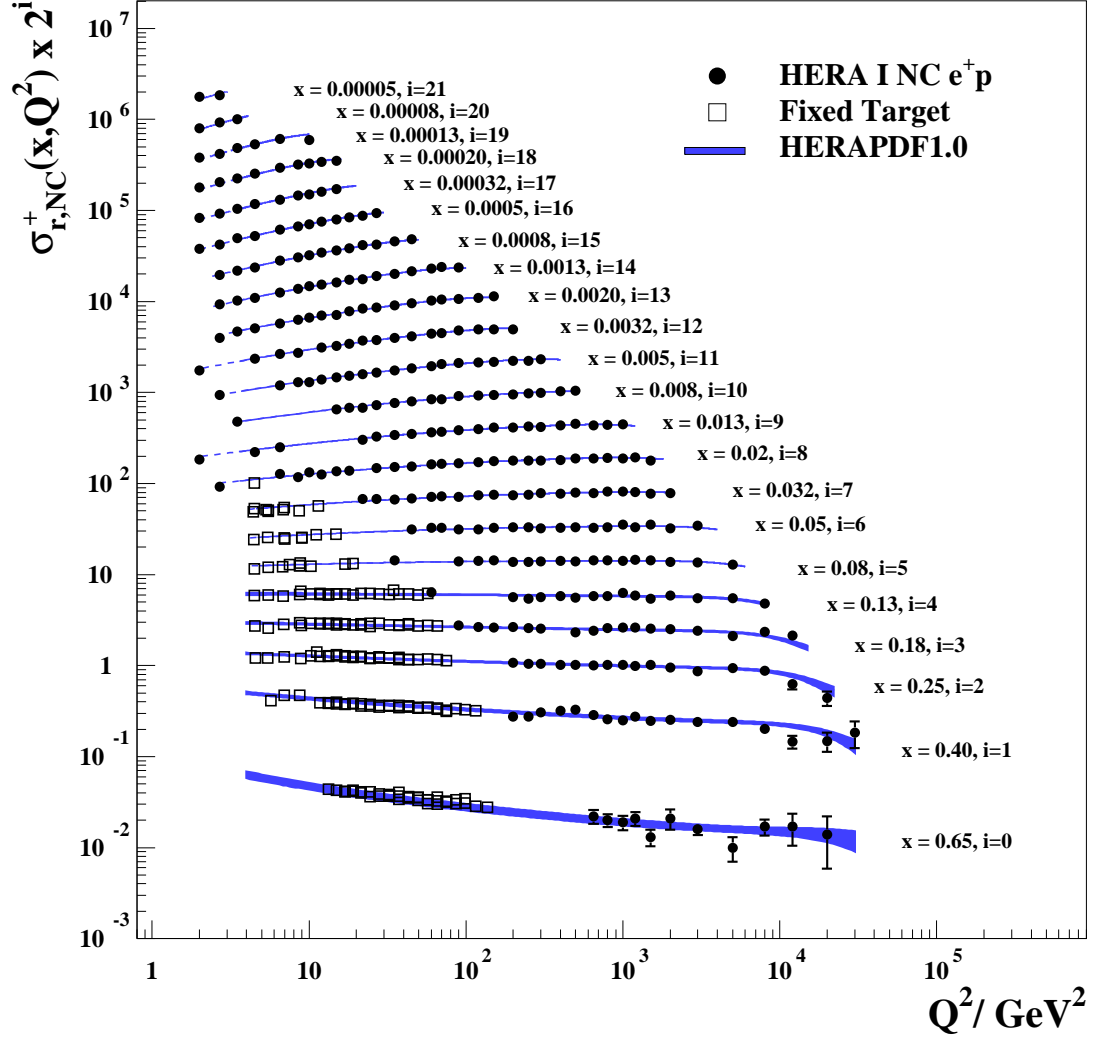


Figure 11: The reduced cross section, which is equivalent to  $F_2$  up to some small corrections, measured by the H1 and ZEUS experiments from Ref. [10].

Taking the outgoing parton to be on-shell:

$$(q + \eta p)^2 = 2\eta p \cdot q - Q^2 = 0 \quad \Rightarrow \quad \eta = x.$$

Therefore

$$\frac{d^2\sigma(e + \text{proton})}{dx dQ^2} = \sum_q f_q(x) \frac{d^2\sigma(e + q(xp))}{dQ^2}. \quad (47)$$

The differential cross section for  $e^\pm(k) + q(p) \rightarrow e^\pm(k') + q(p')$  via photon exchange which

dominates at low  $Q^2$  for neutral current scattering is

$$\frac{d^2\sigma(e + q(xp))}{dQ^2} = \frac{2\pi\alpha^2 e_q^2}{Q^4} [1 + (1 - y)^2], \quad (48)$$

where  $e_q$  is the charge of the quark.

So in the naive parton model

$$\begin{aligned} 2xF_1(x) &= F_2(x), \\ F_2(x) &= x \sum_q e_q^2 f_q(x), \end{aligned} \quad (49)$$

are functions of  $x$  only, *Bjorken scaling*. Bjorken scaling works reasonably well, see Fig. 11, but the quantum corrections, lead to *scaling violations*.

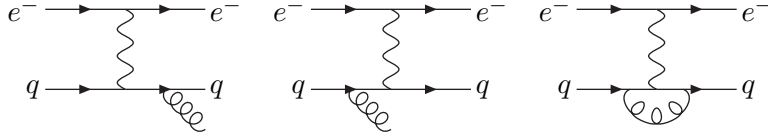


Figure 12: Real and virtual corrections to DIS.

If we consider the  $\mathcal{O}(\alpha_S)$  corrections we have the following divergent contributions:

1. soft gluon,  $E_g \rightarrow 0$ ;
2. gluon collinear to the final-state quark;
3. gluon collinear to the initial-state quark;
4. the virtual matrix element has a negative divergence;

corresponding to the diagrams shown in Fig. 12.

The contributions from (1), (2) and (4) are indistinguishable from the tree-level configuration and the divergences cancel between the real and virtual corrections. However (3) has momentum fraction  $\eta > x$  and (4)  $\eta = x$  so the initial-state divergences don't cancel.

Just as with final-state radiation in the collinear limit it can be shown that

$$d\sigma_{q \rightarrow qg} \rightarrow d\sigma_{q \rightarrow q} \times \frac{\alpha_S}{2\pi} C_F \frac{1 + z^2}{1 - z} \frac{dt}{t} \frac{dz}{z}. \quad (50)$$

Here we have the unregularized DGLAP splitting function  $\hat{P}_{q \rightarrow qg}$ , it is singular as  $z \rightarrow 1$ . The virtual contribution contains a compensating singularity at exactly  $z = 1$ . The

regularized splitting function is defined to be the sum of real and virtual contributions<sup>3</sup>

$$\begin{aligned} P_{qq}(z) &= C_F \frac{1+z^2}{1-z} + C_F \delta(1-z) \left\{ \frac{3}{2} - \int_0^1 dz' \frac{2}{1-z'} \right\}, \\ &\equiv C_F \left( \frac{1+z^2}{(1-z)_+} + \frac{3}{2} \delta(1-z) \right). \end{aligned} \quad (51)$$

The total contribution is

$$\begin{aligned} F_2(x, Q^2) &= x \sum_q e_q^2 \int_x^1 \frac{d\eta}{\eta} f_q(\eta) \left[ \delta \left( 1 - \frac{x}{\eta} \right) \right. \\ &\quad \left. + \frac{\alpha_S}{2\pi} P_{qq} \left( \frac{x}{\eta} \right) \int_0^1 \frac{dt}{t} + \bar{R}_{qq} \left( \frac{x}{\eta} \right) \right], \end{aligned} \quad (52)$$

where  $\bar{R}_{qq} \left( \frac{x}{\eta} \right)$  is a calculable finite correction.

The integral over  $t$  is infrared divergent, comes from long timescales and should be part of the hadronic wavefunction. We therefore introduce a factorization scale  $\mu_F$  and absorb contributions with  $t < \mu_F$  into the parton distribution function so that  $f_q(\eta)$  becomes  $f_q(\eta, \mu_F^2)$ .

$$\begin{aligned} F_2(x, Q^2) &= x \sum_q e_q^2 \int_x^1 \frac{d\eta}{\eta} f_q(\eta, \mu_F^2) \left[ \delta \left( 1 - \frac{x}{\eta} \right) \right. \\ &\quad \left. + \frac{\alpha_S}{2\pi} P_{qq} \left( \frac{x}{\eta} \right) \ln \frac{Q^2}{\mu_F^2} + R_{qq} \left( \frac{x}{\eta} \right) \right]. \end{aligned} \quad (53)$$

The finite piece is dependent on exactly how we define the parton distribution function, the factorization scheme dependence. Physical cross sections are independent of  $\mu_F$ , however at any finite order in perturbation theory they do depend on the factorization scale.

Recall that in perturbation theory we cannot predict  $\alpha_S(M_Z)$  but we can predict its evolution, Eqn. 27. Similarly for the PDFs

$$\mu_F^2 \frac{\partial f_q(x, \mu_F^2)}{\partial \mu_F^2} = \frac{\alpha_S(\mu_F^2)}{2\pi} \int_x^1 \frac{dy}{y} f_q(y, \mu_F^2) P_{qq} \left( \frac{x}{y} \right) + \dots \quad (54)$$

## 5 Hadron Collisions

In hadron collisions QCD processes dominate due to strength of the strong coupling. The cross sections for electroweak processes,  $W^\pm$ ,  $Z^0$  and Higgs production are much smaller. The values of  $x$  and  $Q^2$  probed in hadron collisions and examples of the cross sections for various processes are shown in Fig. 13. In this section we will look at some of the basics

---

<sup>3</sup>The  $+$ -prescription is defined by convolution with a well defined function,  $g(z)$ , such that

$$\int_0^1 dz [f(z)]_+ g(z) = \int_0^1 dz f(z) [(g(z) - g(1))].$$

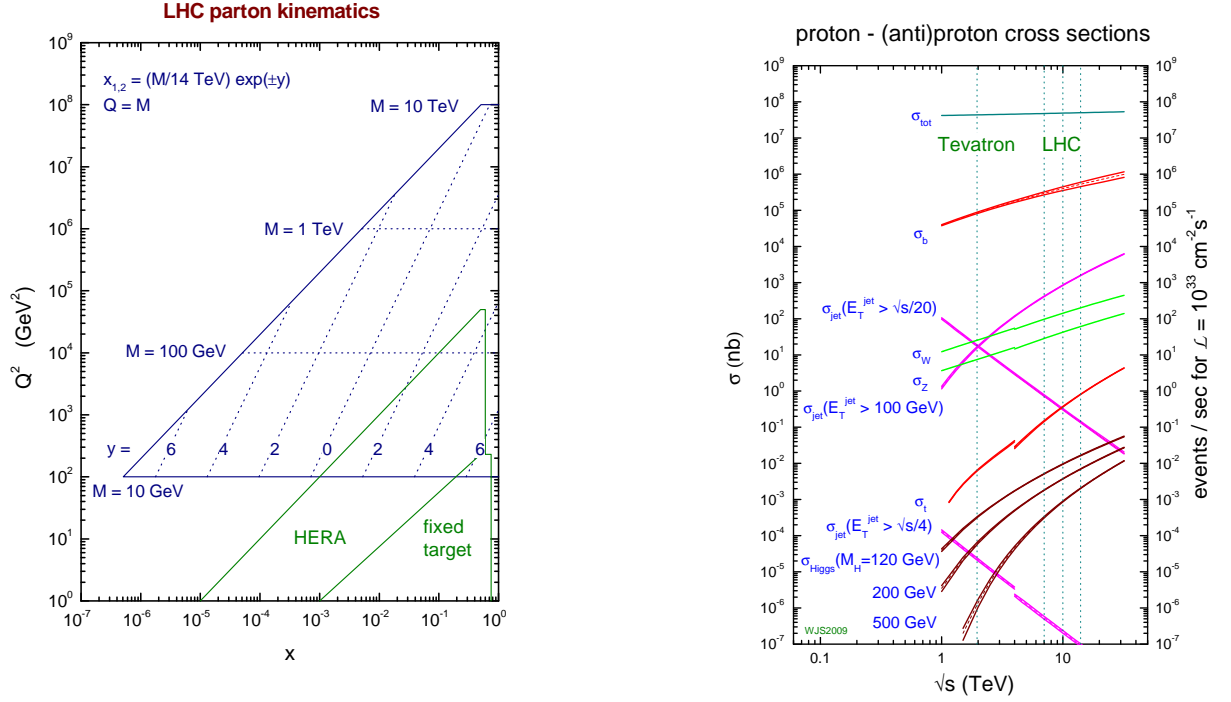


Figure 13: The values of  $x$  and  $Q^2$  probed in hadron collisions and examples of the cross sections for various processes taken from Ref. [11].

of the production of the  $Z^0$  boson, as a simple example of a hadron–hadron process, in the next section we will go on and study the physics of jets.

The calculation of the cross section for the production of an  $s$ -channel resonance in hadron–hadron collisions is described in more detail in Appendix A.3.1 where the cross section is given in Eqn. 126. The only dependence of the cross section on the rapidity of the  $Z^0$  boson is via the PDFs, *i.e.* the rapidity distribution of  $Z^0$  contains information on the PDFs of the partons  $a$  and  $b$ . The higher the mass of the produced system the more central it is, see Fig. 13. The  $Z^0$  boson is centrally produced in both  $p\bar{p}$  and  $pp$  collisions. The experimental results, for example those from the Tevatron shown in Fig. 14, are in good agreement with the theoretical predictions.

At leading order the transverse momentum of the gauge boson is zero. As before we have include real and virtual corrections, as shown in Fig. 15. In the same way as DIS the initial-state singularities must be factorized into the PDFs. At low transverse momentum we need to resum the multiple soft emissions whereas, as with the  $e^+e^-$  event shapes, at large  $p_\perp$  the fixed-order approach is more reliable. The transverse momentum of the  $Z^0$  boson at the Tevatron is shown in Fig. 16.

In hadron-hadron collisions we would like at least next-to-leading order (NLO) calculations. This is the first order at which we have a reliable calculation of the cross section. If possible we would like next-to-next-to-leading order (NNLO) calculations but

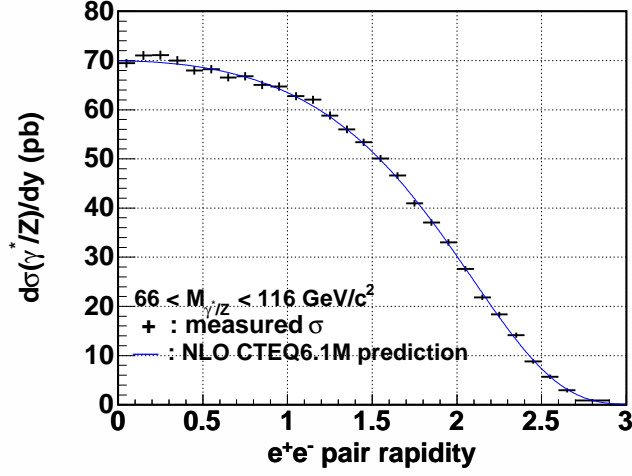


Figure 14: Rapidity of the  $Z^0$  boson measured by the CDF experiment, taken from Ref. [12].

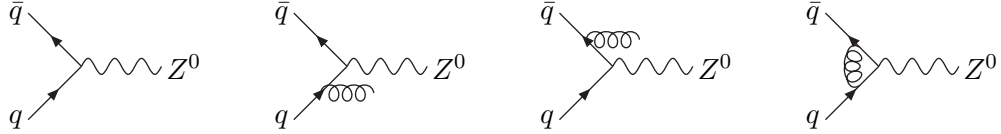


Figure 15: Real and virtual corrections to the production of the  $Z^0$  boson.

that is much harder and takes a long time, *e.g.*  $e^+e^- \rightarrow 3\text{jets}$  was calculated at: LO in 1974 [15]; NLO in 1980 [16]; NNLO in 2007 [17]. Calculating NNLO corrections is still extremely challenging in hadron collisions, only the Drell-Yan process and  $gg \rightarrow H$  are known. However, we need higher order calculations because while the factorization scale uncertainty is significantly less at NLO when compared to leading order it can still be significant, see for example the scale uncertainty on the rapidity of the  $Z^0$  boson shown in Fig. 17.

## 6 Jets

While we can often see the jets in an event when we look at an event display we need a precise definition to perform quantitative analyzes.<sup>4</sup> Jets are normally related to the underlying perturbative dynamics, *i.e.* quarks and gluons. The purpose of a *jet algorithm* is to reduce the complexity of the final state, combining a large number of final-state particles to a few jets, *i.e.*

$$\{p_i\} \xrightarrow{\text{jet algorithm}} \{j_l\}. \quad (55)$$

We need a number of properties to achieve this (Snowmass accord):

<sup>4</sup>This section is based on the excellent review *Towards Jetography* [6].

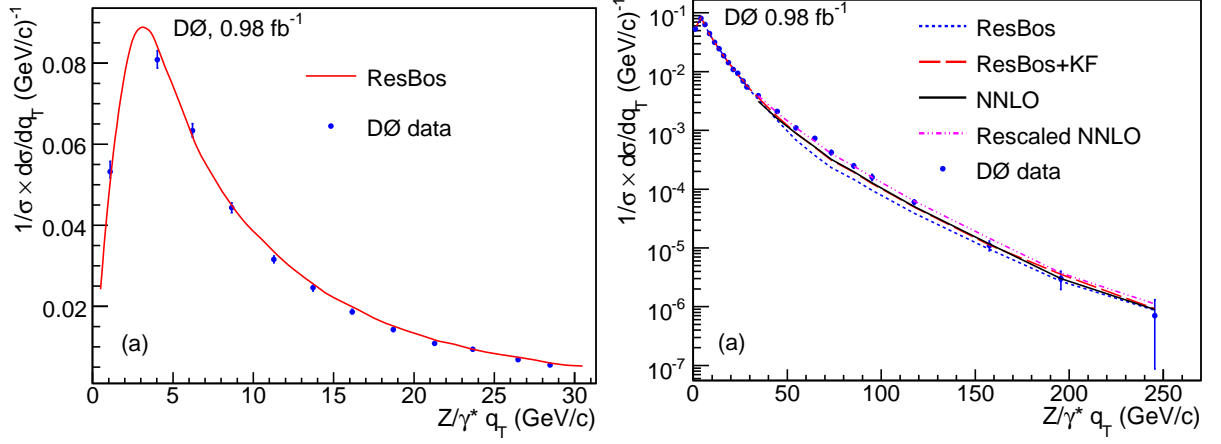


Figure 16: Transverse momentum of the  $Z^0$  boson measured by the D0 experiment at the Tevatron, taken from Ref. [13].

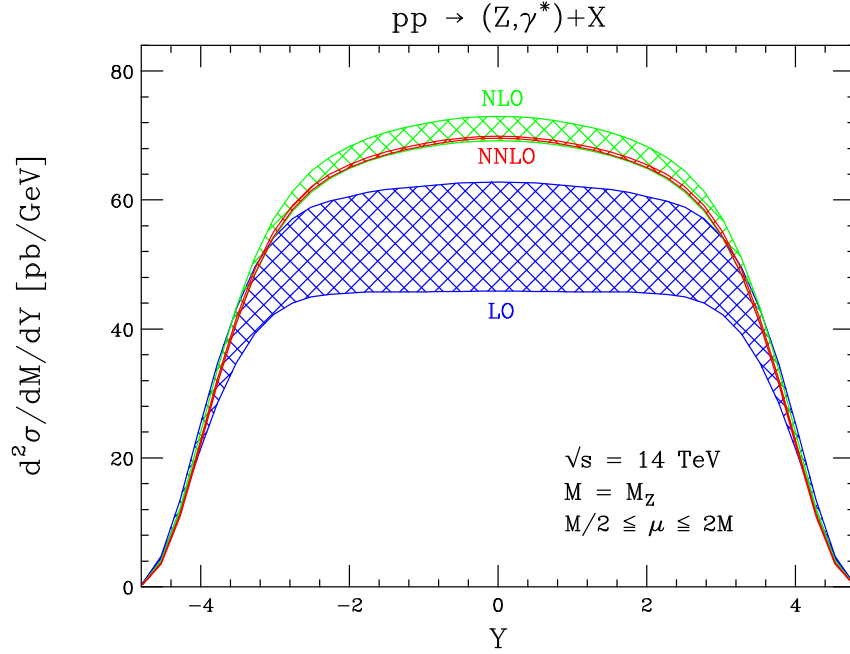


Figure 17: Rapidity distribution of the  $Z^0$  boson for the LHC at  $\sqrt{s} = 14$  TeV, taken from Ref. [14].

- simple to implement in experimental analyzes and theoretical calculations;
- defined at any order in perturbation theory and gives finite cross sections at any order in perturbation theory (*i.e.* infrared safe);
- insensitive to hadronization effects.

The most important of these properties is *infrared safety*, as with the event shapes we considered earlier. Provided the jet algorithm is infrared safe there are a range of different approaches.

The two main types of jet algorithm are:

1. cone algorithms;
2. sequential recombination algorithms.

There is a long history to this subject with: theorists and  $e^+e^-$  experimentalists generally preferring recombination algorithms for their better theoretical properties; hadron collider experimentalists preferring cone algorithms for their more intuitive picture and because applying many experimental corrections was easier. However, with the start of the LHC we have converged on a specific recombination algorithm.

## 6.1 Cone Algorithms

The simplest, oldest, and most intuitively appealing idea is a cone algorithm. The most widely used algorithms are *iterative cone* algorithms where the initial direction of the cone is determined by a seed particle,  $i$ . The sum of the momentum of all the particles with a cone of radius  $R$ , the jet radius, in the azimuthal angle  $\phi$  and rapidity<sup>5</sup>  $y$  is then used as a new seed direction and the procedure iterated until the direction of the resulting cone is stable. In this approach the momenta of all the particles  $j$  such that

$$\Delta R_{ij}^2 = (y_i - y_j)^2 + (\phi_i - \phi_j)^2 < R^2, \quad (56)$$

are summed. As these algorithms are almost exclusively used in hadron–hadron collisions it is normal to use the kinematical variables defined in Appendix A.1.

While this may seem simple there are a lot of complications in the details of the algorithm in particular: what should be used as the seeds; what happens when the cones obtained from two different seeds share particles, *overlap*. The details of the treatment of these issues can lead to problems with infrared safety, which can often be very subtle.

Consider a simple approach where we take all the particles to be seeds. If we have two partons separated in  $(y, \phi)$  by twice the cone radius then two jets, with the direction



Figure 18: Example of cone jets.

---

<sup>5</sup>Or sometimes pseudorapidity  $\eta$ .



given by that of the original partons, are formed as shown in Fig. 18. However if there is an additional soft gluon emission between the two jets, as shown in Fig. 19, depending on the approach we can get only one jet, *i.e.* the algorithm is unsafe. A simple solution was

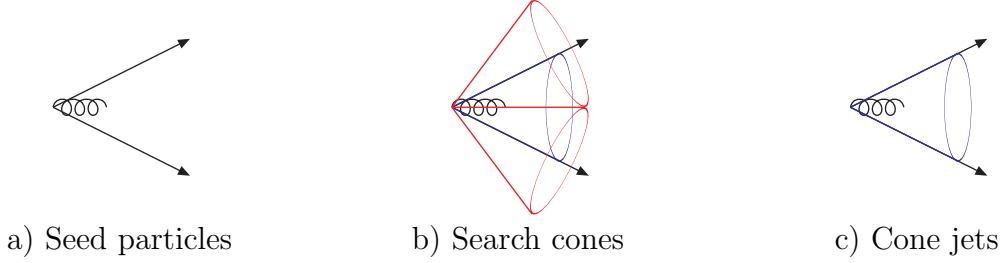


Figure 19: Example of cone jets with additional soft radiation.

to use the midpoint between all the seeds as a seed, the *midpoint algorithm*. This solves the problem at this level but similar problems appear for higher multiplicities. The final solution, for the only known infrared safe cone algorithm, SIScone, is to avoid the use of seeds and treat overlapping jets carefully.

## 6.2 Sequential Recombination Algorithms

In this approach jets are constructed by sequential recombination. We define a distance measure between two objects  $d_{ij}$ , in hadron collisions we must also define a distance measure  $d_{iB}$  with respect to the beam direction. There are two variants of the algorithm the *inclusive* where all jets are retained and *exclusive* where only jets above the cut-off value of the jet measure  $d_{\text{cut}}$ , the jet resolution scale, are kept. The algorithm proceeds as follows:

1. the distance measure is computed for each pair of particles, and with the beam direction in hadronic collisions, and the minimum found;
2. if the minimum value is for a final-state merging in the exclusive approach the particles  $i$  and  $j$  are recombined into a pseudoparticle if  $d_{ij} \leq d_{\text{cut}}$ , while in the inclusive algorithm they are always recombined;
3. otherwise if a beam merging is selected in the inclusive approach the particle is declared to be a jet, while in the exclusive approach it is discarded if  $d_{iB} \leq d_{\text{cut}}$ ;
4. in the inclusive approach we continue until no particles remain, while in the exclusive approach we stop when the selected merging has  $\min\{d_{iB}, d_{ij}\} \geq d_{\text{cut}}$ .

In the inclusive approach the jets are all those selected from merging with the beam, whereas in the exclusive approach the jets are all the remaining particles when the iteration is terminated.

The choice of the distance measure, and to a lesser extent the recombination procedure,<sup>6</sup> defines the algorithm.

The earliest JADE algorithm for  $e^+e^-$  collisions uses the distance measure

$$d_{ij} = 2E_i E_j (1 - \cos \theta_{ij}), \quad (57)$$

where  $E_{i,j}$  are the energies of the particles and  $\theta_{ij}$  the angle between them. In  $e^+e^-$  collisions we have to use the exclusive algorithm and it is conventional to use a dimensionless measure  $y_{ij} = d_{ij}/Q^2$ , where  $Q$  is the total energy in the event. While this choice can easily be proved to be safe in the soft and collinear limits there are problems with the calculation of higher order corrections.

Therefore a class of  $k_T$  algorithms was developed in which the distance measure was chosen to be the relative transverse momentum of the two particles in the collinear limit, *i.e.*

$$d_{ij} = \min\{E_i^2, E_j^2\} \theta_{ij}^2 \simeq k_{\perp ij}^2 \quad \text{for } \theta_{ij} \rightarrow 0. \quad (58)$$

In  $e^+e^-$  collisions the conventional choice is

$$d_{ij} = 2 \min\{E_i^2, E_j^2\} (1 - \cos \theta_{ij}). \quad (59)$$

In hadron collisions it is best to use a choice which is invariant under longitudinal boosts along the beam direction. The standard choice is

$$d_{ij} = \min\{p_{i,\perp}^2, p_{j,\perp}^2\} \frac{\Delta R_{ij}^2}{R^2}, \quad (60)$$

where  $R$  is the “cone-size” and  $p_{i,\perp}$  is the transverse momentum of particle  $i$  with respect to the beam direction. The standard choice for the beam distance is  $d_{iB} = p_{i,\perp}^2$ . There are other definitions, particularly of the distance  $d_{ij}$ , which are invariant under longitudinal boosts but that in Eqn. 60 is the most common choice.

In general there is a whole class of measures defined by

$$d_{ij} = \min\{p_{i,\perp}^{2p}, p_{j,\perp}^{2p}\} \frac{\Delta R_{ij}^2}{R}, \quad (61)$$

and  $d_{iB} = p_{i,\perp}^{2p}$ .

The parameter  $p = 1$  for the  $k_T$  algorithm and 0 for the Cambridge/Aachen algorithm.

Recently a new approach, the anti- $k_T$  algorithm, with  $p = -1$ , was proposed which favours clustering with hard collinear particles rather than clusterings of soft particles, as in the  $k_T$  and Cambridge/Aachen algorithms. The anti- $k_T$  algorithm is still infrared safe and gives “conical” jets due to the angular part of the distance measure and is the algorithm preferred by both general-purpose LHC experiments.

### 6.3 Jet Cross Sections

All cone jet algorithms, except from SISCone, are not infrared safe. The best ones typically fail in processes where we consider extra radiation from three-parton configurations

Process	Last meaningful order		Known at
	JetClu Atlas cone	MidPoint CMS cone	
inclusive jet cross section	LO	NLO	NLO ( $\rightarrow$ NNLO)
$W^\pm/Z^0 + 1$ -jet cross section	LO	NLO	NLO
3-jet cross section	none	LO	NLO
$W^\pm/Z^0 + 2$ -jet cross section	none	LO	NLO
jet masses in 3-jet and $W^\pm/Z^0 + 2$ -jet events	none	none	LO

Table 1: Comparisons of various cone algorithms for hadron–hadron processes. Adapted from Ref. [6].

while some already fail when we consider radiation from two-parton configurations, see the summary in Table 1.

Examples of the jets, and their areas, formed using different algorithms on a sample parton-level event are shown in Fig. 20. As can be seen the  $k_T$  and Cambridge/Aachen algorithms tend to cluster many soft particles giving jets with an irregular area whereas the jets produced by the cone and anti- $k_T$  algorithms are more regular making applying corrections for pile-up and underlying event contamination easier.

In order to study jet production in hadron collisions we need to understand both the jet algorithm and the production of the partons which give rise to the jets. The spin/colour summed/average matrix elements are given in Table 2. Many of these matrix elements have  $t$ -channel dominance, typically  $t \rightarrow 0 \iff p_\perp^2 \rightarrow 0$ . As a consequence the parton–parton scattering cross section grows quickly as  $p_\perp \rightarrow 0$  an effect which is further enhanced by the running of  $\alpha_s$  when using  $\mu_R = p_\perp$  as the renormalisation scale. An example of the  $p_\perp$  spectrum of jets for different rapidities measured using the midpoint cone-algorithm is shown in Fig. 21.

## 6.4 Jet Properties

In general the computation of jet properties in hadron–hadron collisions is extremely complicated, however for some quantities we can get estimates of various effects. The simplest of these is to estimate the change in the  $p_\perp$  between a parton and the jet it forms.

We can start by considering the change due to perturbative QCD radiation. Suppose we have a quark with transverse momentum  $p_\perp$  which radiates a gluon such that the quark carries a fraction  $z$  of its original momentum and the gluon a fraction  $1 - z$ , as shown in Fig. 22. In this case after the radiation the centre of the jet will be the parton with the highest transverse momentum after the branching, *i.e.* the quark if  $z > 1 - z$  or the gluon if  $z < 1 - z$ . If the other parton is at an angular distance greater  $\theta > R$  it will

---

<sup>6</sup>In practice the so-called “E-scheme” where the four-momenta of the particles are added to give the pseudoparticle’s four-momentum is almost always used.

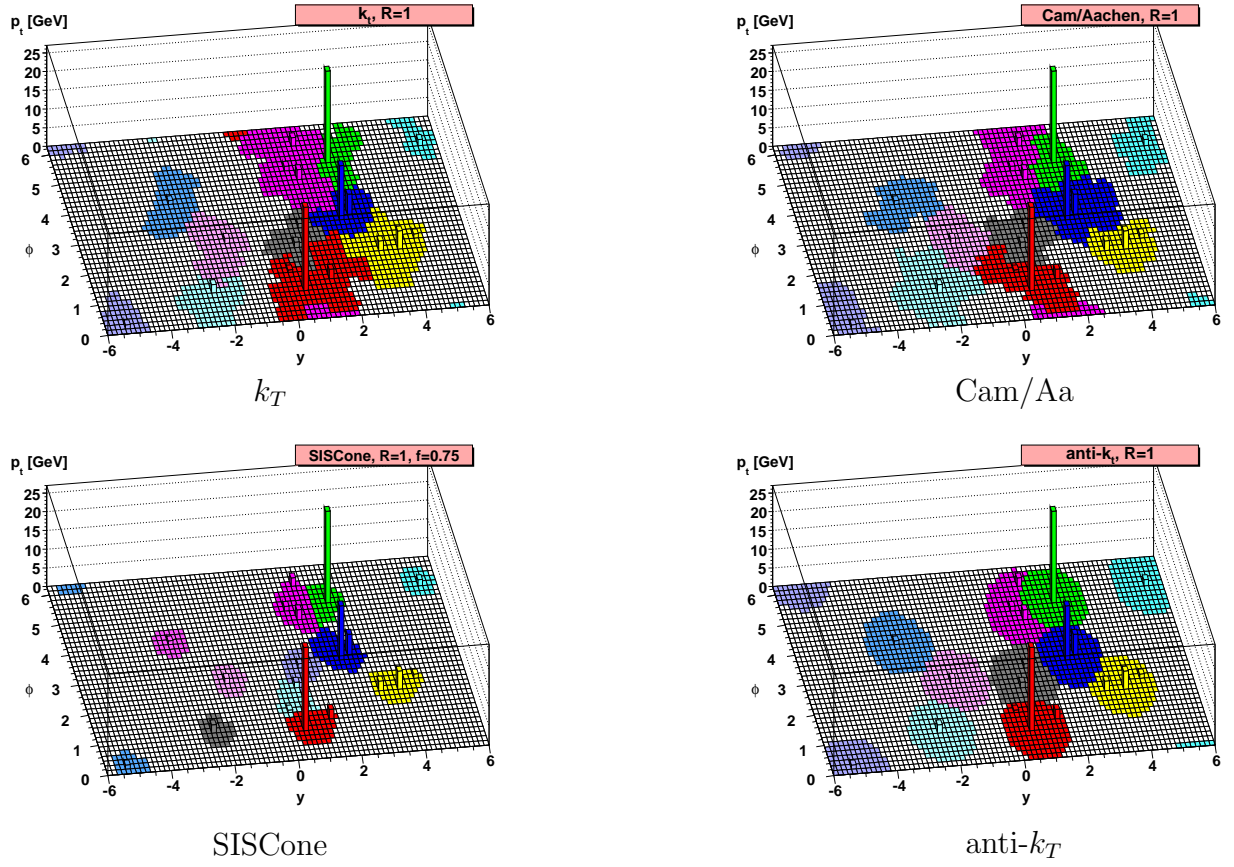


Figure 20: Examples of jets formed by different jet algorithms, taken from Ref. [6].

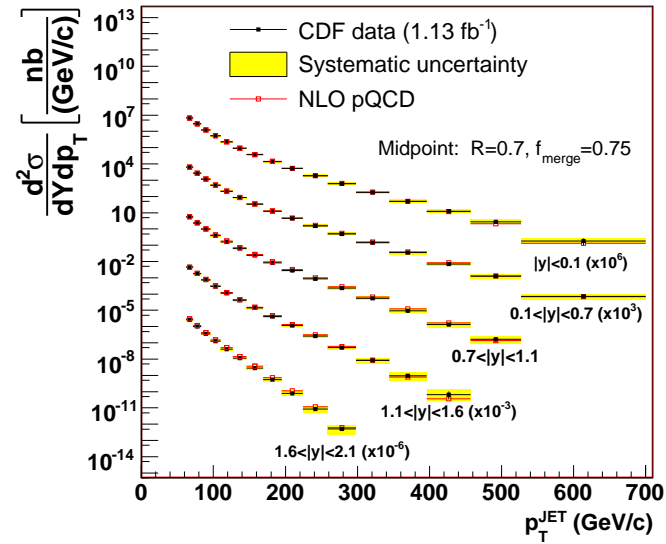


Figure 21: Transverse momentum spectrum of jets measured by the CDF experiment at the Tevatron, taken from Ref. [18].

$qq' \rightarrow qq'$	$\frac{4}{9} \frac{\hat{s}^2 + \hat{u}^2}{\hat{t}^2}$
$q\bar{q} \rightarrow q'\bar{q}'$	$\frac{4}{9} \frac{\hat{t}^2 + \hat{u}^2}{\hat{s}^2}$
$q\bar{q} \rightarrow gg$	$\frac{32}{27} \frac{\hat{t}^2 + \hat{u}^2}{\hat{t}\hat{u}} - \frac{8}{3} \frac{\hat{t}^2 + \hat{u}^2}{\hat{s}^2}$
$qg \rightarrow qg$	$\frac{\hat{s}^2 + \hat{u}^2}{\hat{t}^2} - \frac{4}{9} \frac{\hat{s}^2 + \hat{u}^2}{\hat{s}\hat{u}}$
$gg \rightarrow q\bar{q}$	$\frac{1}{6} \frac{\hat{t}^2 + \hat{u}^2}{\hat{t}\hat{u}} - \frac{3}{8} \frac{\hat{t}^2 + \hat{u}^2}{\hat{s}^2}$
$gg \rightarrow gg$	$\frac{9}{2} \left( 3 - \frac{\hat{t}\hat{u}}{\hat{s}^2} - \frac{\hat{s}\hat{u}}{\hat{t}^2} - \frac{\hat{s}\hat{t}}{\hat{u}^2} \right)$
$q\bar{q} \rightarrow g\gamma$	$\frac{8}{9} \frac{\hat{t}^2 + \hat{u}^2 + 2\hat{s}(\hat{s} + \hat{t} + \hat{u})}{\hat{t}\hat{u}}$
$qg \rightarrow q\gamma$	$-\frac{1}{3} \frac{\hat{s}^2 + \hat{u}^2 + 2\hat{t}(\hat{s} + \hat{t} + \hat{u})}{\hat{s}\hat{u}}$

Table 2: Spin and colour summed/averaged matrix elements for  $2 \rightarrow 2$  parton scattering processes with massless partons taken from Ref. [3]. A common factor of  $g^4 = (4\pi\alpha_s)^2$  (QCD),  $g^2e^2e_q^2$  (photon production) has been removed.

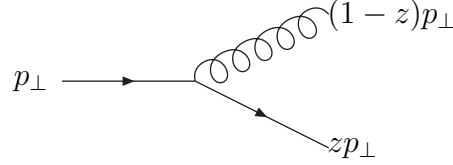


Figure 22: Kinematics of jet branching

no longer be in the jet and the jet will have a smaller transverse momentum

$$\begin{aligned}
\delta p_\perp &= (1-z)p_\perp - p_\perp &= -zp_\perp & 1-z > z \\
\delta p_\perp &= zp_\perp - p_\perp &= -(1-z)p_\perp & z > 1-z
\end{aligned} \tag{62}$$

than the original parton.

We can use the splitting probabilities given in Eqn. 18 to compute the average transverse momentum loss

$$\begin{aligned}
\langle p_\perp \rangle_q &= -\frac{C_F\alpha_S}{2\pi} p_\perp \int_{R^2} \frac{d\theta^2}{\theta^2} \int_0^1 dz \frac{1+z^2}{1-z} \min\{1-z, z\}, \\
&= -\frac{C_F\alpha_S}{2\pi} p_\perp \ln\left(\frac{1}{R^2}\right) \left[ \int_0^{\frac{1}{2}} \frac{1+z^2}{1-z} z + \int_{\frac{1}{2}}^1 \frac{1+z^2}{1-z} 1-z \right], \\
&= -\frac{C_F\alpha_S}{\pi} p_\perp \ln\left(\frac{1}{R}\right) \left[ 2\ln 2 - \frac{3}{8} \right].
\end{aligned} \tag{63}$$

The loss of transverse momentum can be calculated for gluon jets in the same way using the gluon splitting functions giving

$$\langle p_\perp \rangle_g = -\frac{\alpha_S}{\pi} p_\perp \ln\left(\frac{1}{R}\right) \left[ C_A \left( 2\ln 2 - \frac{43}{96} \right) + T_R n_f \frac{7}{48} \right]. \tag{64}$$

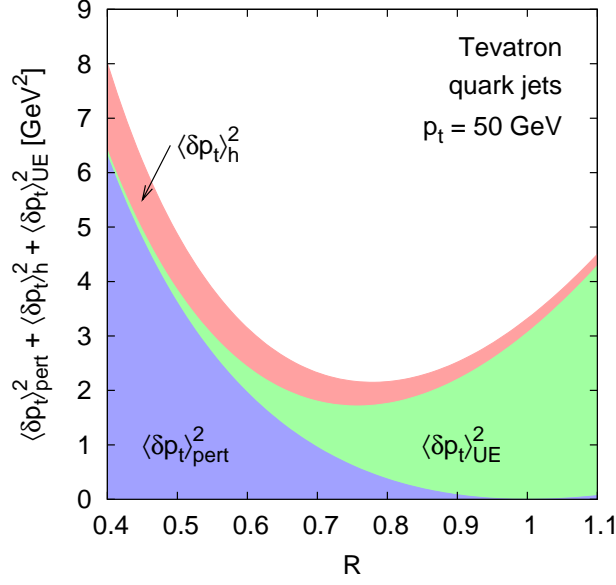


Figure 23: Example of various contributions to the shift of the transverse momentum, taken from Ref. [6].

These calculations give

$$\frac{\langle p_{\perp} \rangle_q}{p_{\perp}} = -0.43\alpha_S \ln \frac{1}{R}, \quad \frac{\langle p_{\perp} \rangle_g}{p_{\perp}} = -1.02\alpha_S \ln \frac{1}{R}.$$

So for a jet with  $R = 0.4$  quark and gluon jets will have 5% and 11% less transverse momentum than the parent parton, respectively. These results are subject to significant finite  $R$  and higher order corrections. The result will also depend on the precise details of the recombination scheme, for example SISCONE has a different recombination scheme where the centre of the cone is the direction of the sum of the partons and we require one parton to fall outside the cone.

While this gives the perturbative energy loss by the jet there are other effects which can change the transverse momentum of the jet. In particular the jet can also lose energy in the hadronization process and can gain energy from the underlying event.

While these effects cannot be calculated from first principles we can use some simple models to gauge the size of the effects.

One model for the effect of hadronization on event shapes in  $e^+e^-$  collisions, due to Dokshitzer and Webber, is to perform a perturbative calculation and instead of stopping the calculation at some small energy scale  $\mu_I$  because the strong coupling becomes non-perturbative continue the calculation into the infrared regime with a model of the strong coupling in this regime which does not diverge. They define

$$\mathcal{A}(\mu_I) = \frac{1}{\pi} \int_0^{\mu_I} dk_{\perp} \alpha_S(k_{\perp}). \quad (65)$$

This model can also be used to assess the size of the hadronization corrections for the jet transverse momentum. The hadronization is modelled by soft gluons with  $k_{\perp} \sim \Lambda_{\text{QCD}}$ .

In this case the transverse momentum loss is

$$\delta p_{\perp} = zp_{\perp} - p_{\perp} = -(1-z)p_{\perp}. \quad (66)$$

As before the transverse momentum loss is

$$\langle p_{\perp} \rangle_q = -\frac{C_F}{2\pi} p_{\perp} \int \frac{d\theta^2}{\theta^2} \int dz \alpha_S \frac{1+z^2}{1-z} (1-z). \quad (67)$$

As we are dealing with soft gluons  $z \sim 1$  so  $1+z^2 \simeq 2$ . In this case we will not use a fixed value of  $\alpha_S$  but need to evaluate it at the scale of the transverse momentum of the gluon with respect to the quark  $k_{\perp} = p_{\perp}(1-z)\theta$ . We also transform the integration variables to use  $k_{\perp}$  and  $\theta$  giving

$$\langle p_{\perp} \rangle_q = -\frac{2C_F}{\pi} \int_R^1 \frac{d\theta}{\theta^2} \int_0^{\mu_I} dk_{\perp} \alpha_S(k_{\perp}) = -\frac{2C_F \mathcal{A}}{R}. \quad (68)$$

Using the coefficients from fits to the  $e^+e^-$  thrust distribution

$$\langle \delta p_{\perp} \rangle_q \sim -\frac{0.5 \text{ GeV}}{R}, \quad \langle \delta p_{\perp} \rangle_g \sim -\frac{1 \text{ GeV}}{R}. \quad (69)$$

The hadronization correction has a  $\frac{1}{R}$  dependence on the size of the jet, unlike the  $\ln \frac{1}{R}$  dependence of the perturbative radiation.

We can estimate the underlying event contribution by assuming there is  $\Lambda_{\text{UE}}$  energy per unit rapidity due to soft particles from the underlying event giving a correction to the transverse momentum of

$$\langle \delta p_{\perp} \rangle = \Lambda_{\text{UE}} \int_{\eta^2 + \phi^2 < R^2} d\eta \frac{d\phi}{2\pi} = \Lambda_{\text{UE}} \frac{R^2}{2}. \quad (70)$$

This is a useful estimate although strictly the area of the jet is only  $\pi R^2$  for the anti- $k_T$  algorithm.

An example of the various contributions to the shift between the partonic and jet transverse momentum is shown in Fig. 23.

## 7 Electroweak Physics

The Standard Model has 18 parameters (assuming massless neutrinos):

- 6 quark and 3 charged lepton masses;
- 3 quark mixing angles and 1 phase;
- 1 strong coupling;
- 1 electromagnetic coupling and 3 boson masses,  $m_W$ ,  $m_Z$ ,  $m_h$ .

All observables are a function of these 18 parameters. In principle we could choose 18 well-measured observables and define them to be the fundamental parameters of the theory, *e.g.*

$$\alpha, \quad G_F, \quad \alpha_S, \quad M_Z, \quad M_h, \quad m_f,$$

and calculate everything else in terms of them.

For the electroweak part of the theory we need  $m_t$ ,  $m_h$  and three other parameters to specify everything, neglecting the masses of the other Standard Model fermions. Everything else can then be calculated from these parameters, *e.g.*

$$\cos \theta_W = \frac{m_W}{m_Z}, \quad e = g \sin \theta_W.$$

The current values of the electroweak parameters are

$$\begin{aligned} m_W &= 80.41 \text{ GeV}, & m_Z &= 91.188 \text{ GeV}, & \sin^2 \theta_W &= 0.231, \\ \alpha(m_Z) &= \frac{1}{128.89}, & G_F &= 1.16639 \times 10^{-5} \text{ GeV}^{-2}. \end{aligned}$$

It is common to include the Fermi constant,  $G_F = \frac{\sqrt{2}g^2}{8m_W^2}$ , from the effective theory of weak interactions at low energies as a parameter.

Different choices for the input parameters give different values for the calculated parameters.

1. input:  $\alpha(m_Z)$ ,  $G_F$ ,  $\sin^2 \theta_W$ , extracted:

$$g = \frac{4\pi\alpha(m_Z)}{\sin^2 \theta_W} = 0.6497, \quad m_W = \frac{g}{\sqrt{4\sqrt{2}G_F}} = 79.98 \text{ GeV}, \quad m_Z = \frac{m_W}{\cos \theta_W} = 91.20 \text{ GeV};$$

2. input:  $m_W$ ,  $G_F$ ,  $\sin^2 \theta_W$  extracted:

$$m_Z = \frac{m_W}{\cos \theta_W} = 91.695 \text{ GeV}, \quad g = \sqrt{4\sqrt{2}G_F m_W} = 0.653, \quad \alpha(m_Z) = \frac{g^2 \sin^2 \theta_W}{4\pi} = 1/127.51;$$

3. input:  $m_Z$ ,  $\alpha(m_Z)$ ,  $\sin^2 \theta_W$  extracted:

$$m_W = \frac{m_Z}{\cos \theta_W} = 79.97 \text{ GeV}, \quad g = \frac{4\pi\alpha(m_Z)}{\sin \theta_W} = 0.6497;$$

4. input:  $m_Z$ ,  $m_W$ ,  $G_F$  extracted:

$$\sin^2 \theta_W = 1 \left( \frac{m_W}{m_Z} \right)^2 = 0.2224, \quad g = \sqrt{4\sqrt{2}G_F m_W} = 0.653, \quad \alpha(m_Z) = \frac{g^2 \sin^2 \theta_W}{4\pi} = 1/132.42.$$

This is due to the quantum corrections.

It was the great triumph of the LEP/SLD and Tevatron physics programmes that the quantum corrections to the theory were probed. The normal choice of input parameters is:



1.  $\alpha = 1/137.035999679(94)$  the fine-structure constant at  $q^2 = 0$  is accurately measured, however the error on its evolution to  $q^2 = m_Z^2$  has greater uncertainty due to hadronic corrections;
2.  $G_F = 1.166367(5) \times 10^5 \text{ GeV}^{-2}$  is very accurately measured in muon decay  $\mu^- \rightarrow e^- \nu_\mu \bar{\nu}_e$ ;
3.  $m_Z = 91.1876 \pm 0.0021 \text{ GeV}$  from the LEP1 lineshape scan;

as these are the most accurately measured.

## 7.1 Quantum Corrections to Masses

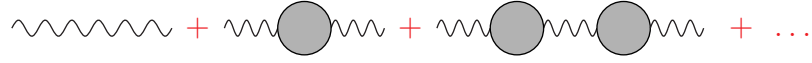


Figure 24: Example quantum corrections to the gauge boson propagator.

We have already considered the running of the coupling and corrections to cross sections and other observables. However masses are also renormalized in the Standard Model. If we consider the propagator for a massive gauge boson we get corrections of the form shown in Fig. 24. If we omit the Lorentz structures this gives a propagator

$$D(q^2) = \frac{i}{q^2 - m^2} + \frac{i}{q^2 - m^2} i\Pi(q^2) \frac{i}{q^2 - m^2} + \frac{i}{q^2 - m^2} i\Pi(q^2) \frac{i}{q^2 - m^2} i\Pi(q^2) \frac{i}{q^2 - m^2} + \dots,$$

where  $\Pi(q^2)$  is the gauge boson self energy. This is a geometric progression, summing the series gives

$$D(q^2) = \frac{i}{q^2 - m^2} \frac{1}{1 - \frac{\Pi(q^2)}{q^2 - m^2}} = \frac{i}{q^2 - m^2 - \Pi(q^2)}. \quad (71)$$

If the particle can decay to the particles in the loop there is an imaginary part of the self energy  $\Pi(q^2)$  which is related to the width of the particle

$$\text{Im } \Pi(q^2) = -iq\Gamma(q). \quad (72)$$

The real part of the self energy correction renormalizes the particle's mass giving

$$D(q^2) = \frac{i}{q^2 - m_R^2(q) + iq\Gamma(q)}. \quad (73)$$

As we have defined the mass of the  $Z^0$  boson to be a fundamental parameter  $\delta m_Z^2 = 0$ , by definition.

The dominant corrections to the  $W$  mass come from top-bottom and Higgs loop corrections, as shown in Fig. 25.

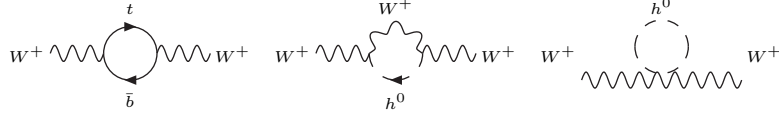


Figure 25: Quantum corrections to the  $W^\pm$  boson mass.

The correction to the  $W^\pm$  boson mass is

$$\delta m_W^2 \sim \frac{4s_W^2}{1-2s_W^2} \frac{G_F}{8\pi^2\sqrt{2}} m_W^2 \times \frac{c_W^2}{s_W^2} N_C (m_t^2 - m_b^2) - \frac{4s_W^2}{1-2s_W^2} \frac{G_F}{8\pi^2\sqrt{2}} m_W^2 \times m_W^2 \frac{11}{3} \left( \ln \frac{M_h^2}{m_W^2} - \frac{5}{6} \right).$$

## 7.2 Electroweak Observables

A number of observables are used in the electroweak fit performed by the LEP Electroweak Working Group (LEPEWWG):

1. the  $Z^0$  mass and width  $m_Z, \Gamma_Z$ ;
2. the hadronic cross section at the  $Z^0$  pole  $\sigma(\text{had}) \equiv \frac{12\pi\Gamma(e^+e^-)\Gamma(\text{had})}{m_Z^2\Gamma_Z^2}$ ;
3. the ratio of the hadronic to leptonic partial widths of the  $Z^0$ ,  $R_\ell \equiv \frac{\Gamma(\text{had})}{\Gamma_{\ell^+\ell^-}}$ , and the ratio of the bottom,  $R_b \equiv \Gamma(b\bar{b})/\Gamma(\text{had})$ , and charm,  $R_c \equiv \Gamma(c\bar{c})/\Gamma(\text{had})$ , quark partial widths to the hadronic partial width of the  $Z^0$ ;
4. the forward-backward asymmetry for  $e^+e^- \rightarrow f\bar{f}$

$$A_{fb}^{0,f} = \frac{\sigma_F - \sigma_B}{\sigma_F + \sigma_B}, \quad (74)$$

for charged leptons,  $A_{fb}^{0,\ell}$ , bottom  $A_{fb}^{0,b}$ , and charm  $A_{fb}^{0,c}$  quarks;

5. the couplings of the fermions to the  $Z^0$  can be extracted from the forward-backward asymmetry in polarized scattering at SLD

$$A_{LR}^{FB}(f) = \frac{\sigma_{LF}^f - \sigma_{LB}^f - \sigma_{RF}^f + \sigma_{RB}^f}{\sigma_{LF}^f + \sigma_{LB}^f + \sigma_{RF}^f + \sigma_{RB}^f} = \frac{3}{4} A_f. \quad (75)$$

The couplings for the bottom,  $A_b$ , and charm,  $A_c$ , quarks can be extracted from these measurements. There are a number of possible ways of extracting  $A_\ell$ ;

6.  $\sin^2 \theta_{\text{eff}}^{\text{lept}}(Q_{fb})$  is extracted from the hadronic charge asymmetry;
7. the  $W$  mass,  $m_W$ , and width,  $\Gamma_W$  are measured in a range of ways;
8. the top quark mass,  $m_t$ , is measured at the Tevatron.

The results of the precision electroweak fit are in good agreement with the experimental results, as shown in Fig. 26, and for example shows that there are 3 massless neutrinos which couple to the  $Z$  boson.

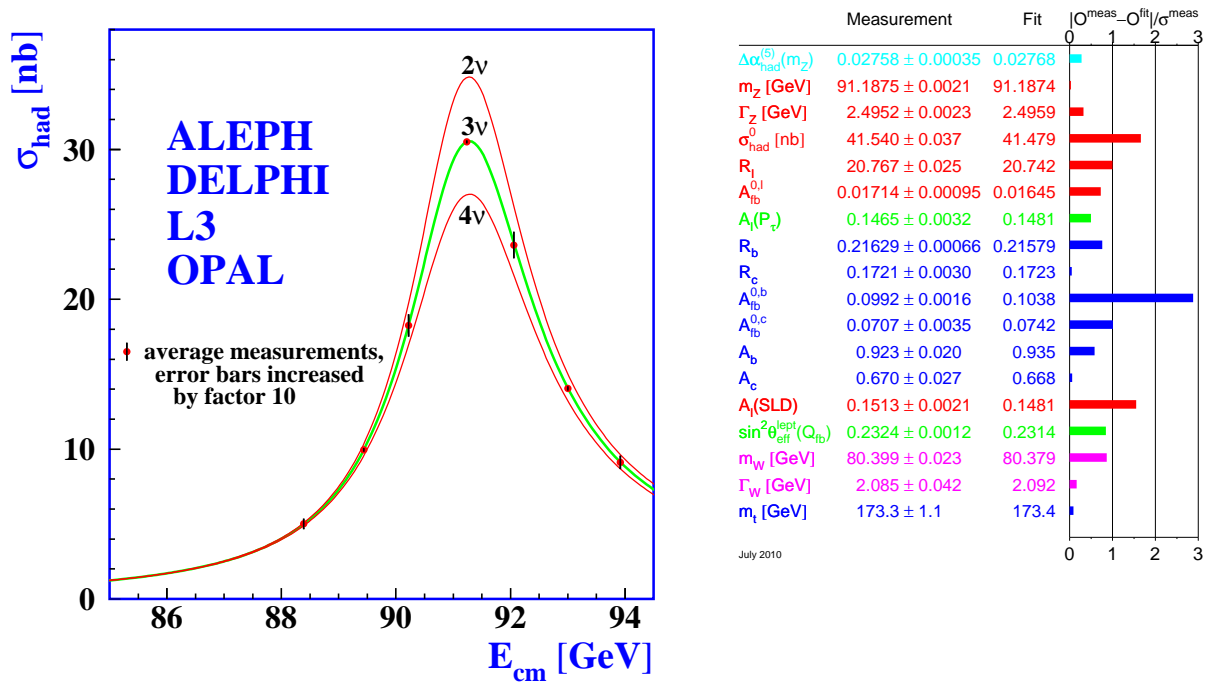


Figure 26: The lineshape of the  $Z$  boson and results of the precision electroweak fit taken from the LEPWWG.

### 7.2.1 $W$ mass measurements

One of the most important quantities in electroweak sector is the mass of the  $W^\pm$  boson. The first measurements of the  $W$  mass were in hadronic collisions. The QCD backgrounds and resolution means that the hadronic  $W^\pm$  decay mode cannot be used. The mass cannot be directly reconstructed using the leptonic mode due to the unobserved neutrino. Instead the transverse mass

$$M_{\perp}^{\ell\nu 2} = 2p_{\perp}^{\ell} E_{\perp} (1 - \cos \phi_{\ell, \text{miss}}), \quad (76)$$

where  $p_{\perp}^{\ell}$  is the transverse momentum of the observed lepton,  $E_{\perp}$  is the missing transverse energy and  $\phi_{\ell, \text{miss}}$  is the azimuthal angle between the lepton and the direction of the missing transverse energy, is used.

The maximum value of the transverse mass is  $M_{\perp}^{\ell\nu 2} \leq m_W^2$  and can be used to extract the  $W^\pm$  mass. This approach was used by the UA1 and UA2 experiments for the original  $W$  mass measurements and the recent results at the Tevatron, for example Fig. 27. The endpoint is smeared by the non-zero  $p_{\perp}$  and width of the  $W$  boson.

A major result of the LEP2 programme was the study of the production of pairs of electroweak gauge bosons,  $W^+W^-$  and  $Z^0Z^0$ . The mass of the  $W$  can be extracted in two ways:

1. measuring the cross section near the threshold

$$\sigma \sim \frac{G_F^2 m_W^2}{2\pi} \sqrt{1 - \frac{4m_W^2}{s}}, \quad (77)$$

which is clean theoretical but limited by statistics, see Fig. 28;

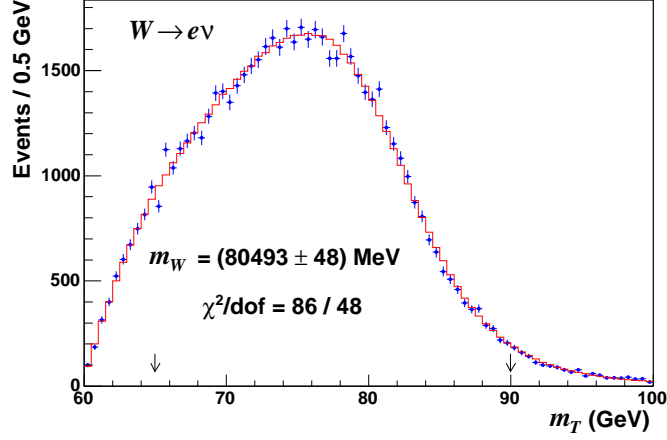


Figure 27: The transverse mass of the  $W$  at the Tevatron taken from Ref. [19].

2. reconstructing the mass from the  $W$  decay products above threshold.

### 7.2.2 $\rho$ parameter

In principle we should compare the full predictions of the Standard Model, or any model of new physics, with all the electroweak observables. However it is often useful, particularly in new physics models as corrections from new particles can lead to large corrections, to consider the  $\rho$  parameter. Naively

$$\rho = \frac{m_W^2}{m_Z^2 \cos^2 \theta_W} = 1, \quad (78)$$

connects the  $Z^0$  and  $W^\pm$  masses with the weak mixing angle. The dominant loop corrections to it from self energies give

$$\Delta\rho = \frac{3G_F m_W^2}{8\sqrt{2}\pi^2} \left[ \frac{m_t^2}{m_W^2} - \frac{\sin^2 \theta_W}{\cos^2 \theta_W} \left( \ln \frac{m_H^2}{m_W^2} - \frac{5}{6} \right) + \dots \right].$$

This relates  $m_W$ ,  $m_t$ , and  $m_H$ . For a long time,  $m_t$  was most significant uncertainty in this relation; by now,  $m_W$  has more than caught up.

## 8 Higgs Boson

So far we have concentrated on the particles from the Standard Model we have already seen, however there is one remaining SM particle which hasn't been discovered, the Higgs Boson.

The SM contains spin-1 gauge bosons and spin- $\frac{1}{2}$  fermions. Massless fields ensure gauge invariance under  $SU(2)_L \times U(1)_Y$  and renormalizability. While we could introduce

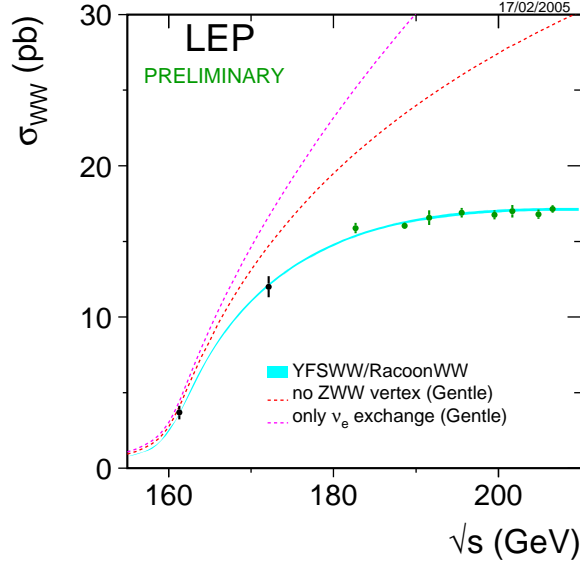


Figure 28: Cross section for the pair production of  $W^+W^-$  close to threshold from the LEPEWWG.

mass terms “by hand”, *i.e.*

$$\mathcal{L} \propto m_A^2 A^\mu A_\mu + m_f (\bar{\Psi}_R \Psi_L + \bar{\Psi}_L \Psi_R), \quad (79)$$

this violates gauge invariance. Under the gauge transformation,  $A^\mu \rightarrow A^\mu + \frac{1}{g} \partial^\mu \theta$ , the mass term  $A^\mu A_\mu$  gives terms proportional to the gauge transformation parameter  $\theta$ , *i.e.* the gauge boson mass term is not gauge invariant. As the fields  $\Psi_L$  and  $\Psi_R$  transform differently under  $SU(2)_L$  under the gauge transformation of the left-handed fermion field the fermion mass term is not gauge invariant.

Adding these mass terms by hand is obviously a bad idea. Instead we add a complex scalar doublet under the  $SU(2)_L$  gauge group which introduces an additional four degrees of freedom. This scalar field can be coupled gauge invariantly to the gauge bosons, *i.e.*

$$\mathcal{L}_{\Phi A} = (D^\mu \Phi)(D_\mu \Phi). \quad (80)$$

A gauge-invariant interaction term with fermions can also be included<sup>7</sup>

$$\mathcal{L}_{\Phi \Psi} = g_f \bar{\Psi}_L \Phi \Psi_R + \text{h.c.} \quad (81)$$

In addition we need the Higgs potential

$$\mathcal{V}(\Phi) = \lambda (\Phi^\dagger \Phi)^2 + \mu^2 \Phi^\dagger \Phi. \quad (82)$$

<sup>7</sup>While we can use  $\Phi$  to couple to the down-type fermions we need to use  $i\sigma_2 \Phi^*$  to couple to the up-type fermions in a gauge invariant manner.

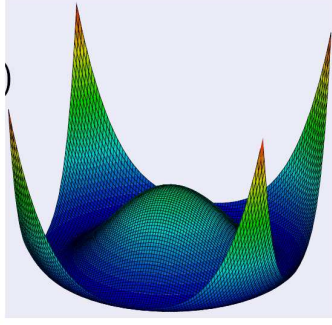


Figure 29: The Higgs boson potential.

For  $\mu^2 < 0$  this potential has an infinite number of equivalent minima,

$$|\Phi| = \sqrt{\frac{-\mu^2}{2\lambda}} \equiv \frac{v}{\sqrt{2}}, \quad (83)$$

as shown in Fig. 29. We expand around one of these minima giving one radial and three circular modes. The circular modes are “gauged away”  $\rightarrow$  “eaten” by gauge bosons to give them mass via the vacuum expectation value (vev) the minimum of the potential.

From the structure above:

$$\begin{aligned} (D_\mu \Phi)^2 &\longrightarrow \frac{g^2 v^2}{4} W_\mu W^\mu &\longrightarrow M_W^2 = \frac{g^2 v^2}{4}; \\ g_f \bar{\Psi}_L \Phi \Psi_R &\longrightarrow g_f \frac{v}{\sqrt{2}} \bar{\Psi}_L \Phi \Psi_R &\longrightarrow m_f = \frac{g_f v}{\sqrt{2}}; \\ \lambda(|\Phi|^2 - v^2/2)^2 &\longrightarrow \lambda v^2 H^2 &\longrightarrow M_H^2 = 2\lambda v^2. \end{aligned}$$

This gives a fixed relation between the mass of the particles and their coupling to (surviving) scalar Higgs boson.

## 8.1 Unitarity

While in the Standard Model introducing the Higgs boson is the only way to give mass to the particles in a gauge invariant manner there are other arguments for the existence of the Higgs boson and it is interesting to ask what would happen if the Higgs boson did not exist.

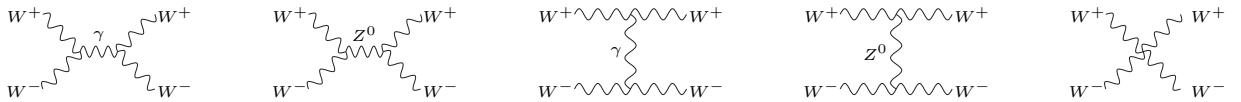


Figure 30: Feynman diagrams for  $WW$  scattering via gauge boson exchange.

If we consider  $W^+W^- \rightarrow W^+W^-$  scattering, via the Feynman diagrams shown in Fig. 30, in the high energy limit the matrix element is

$$\mathcal{M} = g^2 \frac{s}{8M_W^2} \left( 1 - \frac{4M_W^2}{s} \right) (1 + \cos \theta). \quad (84)$$

So without the Higgs boson the cross section

$$\sigma \sim \frac{s}{M_W^4}, \quad (85)$$

for  $s \gg M_W$ .



Figure 31: Higgs boson contributions to  $WW$  scattering.

This violates unitarity, so we need something to cancel the bad high energy behaviour of the cross section. We can arbitrarily invert a particle to cure this. This particle must be a scalar, suppose it has coupling,  $\lambda$ , to  $W^+W^-$ . This gives a contribution, via the Feynman diagrams in Fig. 31,

$$\mathcal{M} = \lambda^2 \left[ -\frac{s}{8M_W^4} (1 + \cos \theta) - \frac{M_H^2}{4M_W^4} \left\{ \frac{s}{s - M_H^2} + \frac{t}{t - M_H^2} \right\} \right]. \quad (86)$$

This cancels the bad high energy behaviour if  $\lambda = gM_W$ , *i.e.* the Higgs coupling to the  $W^\pm$  boson. If we repeat the same procedure for  $WW \rightarrow ZZ$  we need a coupling  $g_{ZZH} \propto gm_Z$  and for  $WW \rightarrow f\bar{f}$  we need a coupling  $g_{f\bar{f}H} \propto gm_f$ , *i.e.* the Higgs boson couplings to the  $Z^0$  boson and Standard Model fermions.

So even if there was no Higgs boson we are forced to introduce a scalar interaction that couples to all particles proportional to their mass. There must be something Higgslike in the theory!

## 8.2 Higgs Searches

As with all searches for Higgs searches we want:

- channels with a high signal rate;
- and a low background rate.

Unfortunately the channels with the highest signal rate often have the largest backgrounds. We need to be able to trigger on a given signal. Good mass resolution for the mass of the Higgs boson and its decay products can help to suppress backgrounds. We should also try and measure things that are well understood theoretically.

In order to consider the signals we need to understand how the Higgs boson is produced and then decays in hadron-hadron collisions.

The analytic results for the partial widths for various Higgs boson decay modes are given in Table 3 and the branching ratios are plotted as a function of the mass of the Higgs boson in Fig. 32. For  $m_H < 2m_W$  the Higgs boson is quite narrow,  $\Gamma_H = \mathcal{O}(\text{MeV})$ , while for  $m_H > 2m_W$  the Higgs boson becomes obese,  $\Gamma_H(m_H = 1\text{TeV}) \approx 0.5 \text{ TeV}$ . At large  $m_H$  the decay into vector boson pairs,  $W^+W^-$  and  $Z^0Z^0$ , is dominant with

Decay mode	Partial Width, $\Gamma$
$H \rightarrow f\bar{f}$	$\frac{G_F M_H}{8\pi\sqrt{2}} \cdot 2m_f^2 N_c \left(1 - \frac{4m_f^2}{m_H^2}\right)^{\frac{3}{2}}$
$H \rightarrow W^+W^-$	$\frac{G_F M_H}{8\pi\sqrt{2}} \cdot m_H^2 \left(1 - \frac{4m_W^2}{m_H^2} + \frac{12m_W^4}{m_H^4}\right) \left(1 - \frac{4m_W^2}{m_H^2}\right)^{\frac{1}{2}}$
$H \rightarrow ZZ$	$\frac{G_F M_H}{8\pi\sqrt{2}} \cdot m_H^2 \frac{m_W^2}{2m_Z^2} \left(1 - \frac{4m_Z^2}{m_H^2} + \frac{12m_Z^4}{m_H^4}\right) \left(1 - \frac{4m_Z^2}{m_H^2}\right)^{\frac{1}{2}}$
$H \rightarrow \gamma\gamma$	$\frac{G_F M_H}{8\pi\sqrt{2}} \cdot m_H^2 \left(\frac{\alpha}{4\pi}\right)^2 \cdot \left(\frac{4}{3}N_c Q_t^2\right)^2 (2m_t > m_H)$
$H \rightarrow gg$	$\frac{G_F M_H}{8\pi\sqrt{2}} \cdot m_H^2 \left(\frac{\alpha_s}{4\pi}\right)^2 \cdot \left(\frac{2}{3}\right)^2 (2m_t > m_H)$
$H \rightarrow VV^*$	more complicated, but important for $m_H \lesssim 2m_V$

Table 3: Partial widths for various Higgs decay modes.

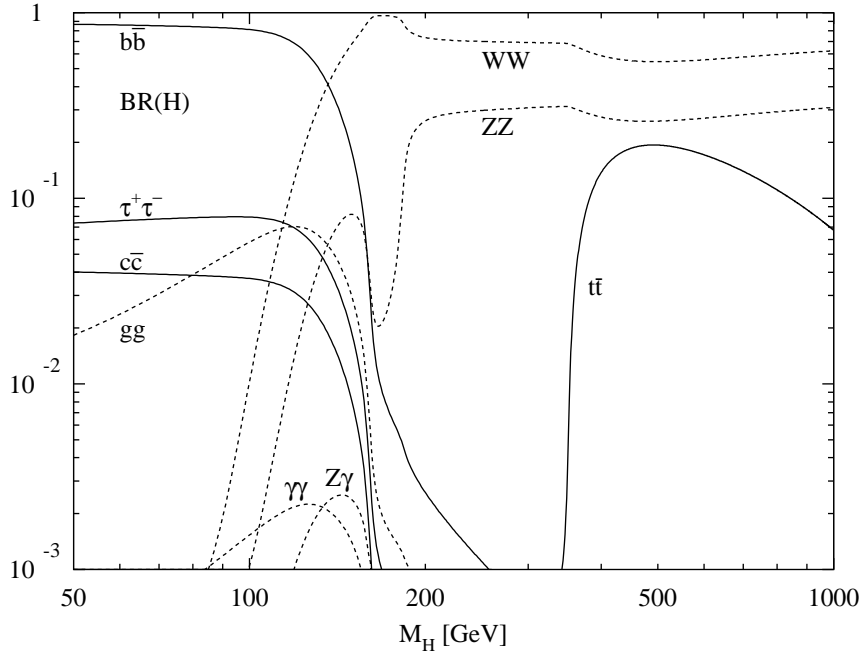


Figure 32: Branching ratios for the Higgs boson as a function of the Higgs boson mass, taken from Ref. [20], calculation by M. Spira.



$\Gamma_{H \rightarrow WW} : \Gamma_{H \rightarrow ZZ} \approx 2 : 1$ , while for small  $m_H$  the decay into bottom quark pairs is dominant,

As the Higgs boson likes to couple to heavy objects (top,  $W$ ,  $Z$ ) there are a range of important Higgs production processes where the Higgs boson couples to heavy particles. The Feynman diagrams for the important processes are shown in Fig. 33 while the cross

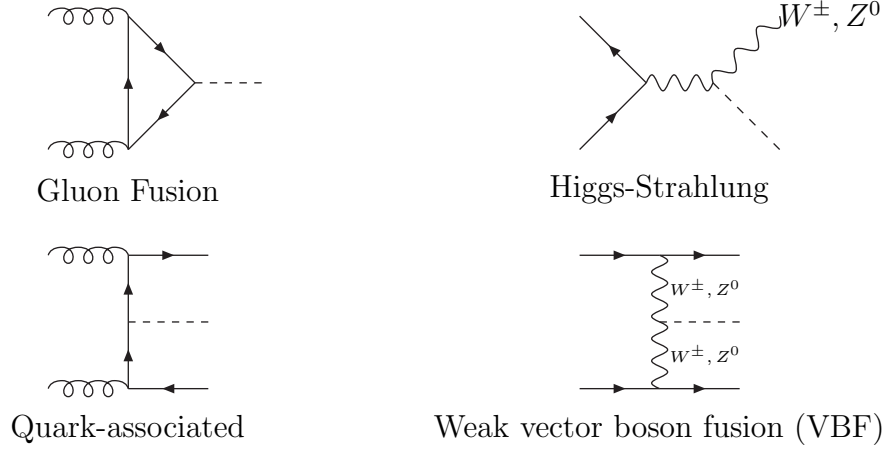


Figure 33: Feynman diagrams for important Higgs boson production processes.

sections for the important processes are shown in Fig. 34 as a function of the Higgs boson mass.

The important search channels depend on the collider energy. At the Tevatron typical channels include:

- $gg \rightarrow H \rightarrow W^+W^- \rightarrow \ell\ell' + \cancel{E}_\perp$  this is the “golden plated” channel because although there is no mass peak the background can be reduced by using quantities, such as the angle between the leptons, which differ in the signal and background due to the different  $W$  boson production mechanisms;
- $q\bar{q} \rightarrow ZH \rightarrow \ell\ell b\bar{b}$  the key ingredient for this process is the  $b$ -tagging efficiency and mass resolution for jets in order to suppress the QCD backgrounds;
- $q\bar{q}' \rightarrow WH \rightarrow \ell\nu b\bar{b}$  has similar features to  $q\bar{q} \rightarrow ZH \rightarrow \ell\ell b\bar{b}$ ;
- $q\bar{q}' \rightarrow ZH \rightarrow \cancel{E}_\perp + b\bar{b}$  the key feature is again the  $b$ -tagging efficiency and mass resolution for jets in order to suppress the QCD backgrounds;
- $q\bar{q}' \rightarrow W^\pm H \rightarrow W^\pm W^+W^-$  in this case there is the possibility of same sign lepton production which has a low background together with the decay of remaining  $W$  to hadrons in order to increase the cross section.

Typical channels at the LHC include:

- $gg \rightarrow H \rightarrow ZZ \rightarrow 4\mu, 2e2\mu$  which is the “Golden plated” channel for  $m_H > 140$  GeV, the key ingredient is the excellent resolution of the  $Z$  mass peak from the leptonic decay;

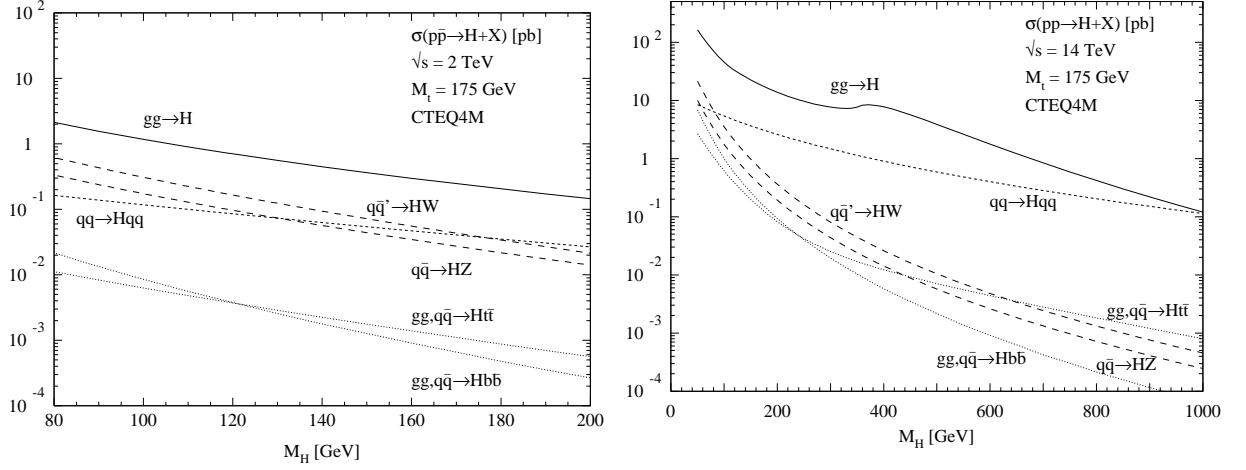


Figure 34: Higgs production cross sections at hadron colliders taken from Ref. [20], calculation by M. Spira.

- $gg \rightarrow H \rightarrow W^+W^- \rightarrow \ell\ell' + \cancel{E}_\perp$  is similar to the Tevatron analysis but with better statistics due to the larger production cross section;
- $gg \rightarrow H \rightarrow \gamma\gamma$  is good for low mass,  $m_H \lesssim 120$  GeV, Higgs bosons although the branching ratio is small, the key ingredient is the mass resolution for photon pairs and a veto on photons from  $\pi^0$  decays;
- $VBF \rightarrow H \rightarrow \tau\tau$  is a popular mode where the key ingredient is that QCD backgrounds are reduced by requiring a rapidity gap between the two tagging jets;
- $VBF \rightarrow H \rightarrow WW$  as for  $VBF \rightarrow H \rightarrow \tau\tau$ ;
- $VBF \rightarrow H \rightarrow b\bar{b}$  is in principle similar to the other VBF modes but it is hard to trigger on pure QCD-like objects (jets).

### 8.3 Extended Higgs Sectors

Adding a single Higgs doublet is the simplest choice for the Higgs sector. As we have yet to observe the Higgs boson it is possible to have a more complicated Higgs sector. There is some tension in the Standard Model between the value of the Higgs mass preferred by precision electroweak fits ( $M_H \sim 100$  GeV) and the experimental limit ( $M_H > 114$  GeV). Many theoretically attractive models like SUSY naturally have a larger Higgs sector. However, we need to be careful to respect constraints from flavour changing neutral currents (FCNC) and the electroweak precision data.

#### 8.3.1 The Two Higgs Doublet Model

The simplest extension to the Standard Model is the *Two Higgs Doublet Model* (THDM). In this model there are two Higgs doublets. There are a number of variants on the model depending on whether or not CP is conserved and how the Higgs bosons couple

to the fermions. The most interesting variant (called Type-II) is that which occurs (in a constrained variant) in SUSY models. In the general version of the Type-II model there are  $\sim 10$  new parameters, whereas in the constrained SUSY version there are only two  $m_{A^0}$  and  $\tan\beta$ . There are indirect constraints from rare processes, *e.g.* kaon and bottom mixing and decays, precision EW data and cosmology.

As there are two doublets there are two vevs:  $v_{1,2}$ . They are constrained by the requirement

$$v_1^2 + v_2^2 = v^2 \approx (246\text{GeV})^2, \quad (87)$$

in order to give the correct gauge boson masses as in the Standard Model. There is an additional parameter  $\tan\beta = v_2/v_1$ . In the Type-II mode the  $H_1$  doublet gives mass to up-type fermions while the  $H_2$  doublet gives mass to down-type fermions. Both doublets couple and give mass to the gauge bosons. After electroweak symmetry breaking there are five scalar boson mass eigenstates, two neutral scalars  $h^0, H^0$ , one neutral pseudoscalar  $A^0$ , and two charged scalars  $H^\pm$ . The coupling of all the Higgs bosons to the vector bosons are reduced. The couplings to the fermions are enhanced (up-type) and suppressed (down-type) as  $\tan\beta$  increases. At tree level the masses are related by

$$m_{H^\pm}^2 = m_{A^0}^2 + m_W^2, \quad m_{H^0}^2 + m_{h^0}^2 = m_{A^0}^2 + m_Z^2. \quad (88)$$

At tree level in SUSY  $m_{h^0} \leq M_Z$  however there are large quantum corrections ( $m_{h^0} \lesssim 140\text{GeV}$ ).

## 9 Beyond the Standard Model Physics

As discussed in Section 7 the Standard Model has 18 free parameters, although in principle we should also include the  $\Theta$  parameter of QCD. We now need more parameters to incorporate neutrino masses. Despite the excellent description of all current experimental data there are still a number of important questions the Standard Model does not answer.

- What are the values of these parameters?
- Why is the top quark so much heavier than the electron?
- Why is the  $\Theta$  parameter so small?
- Is there enough CP-violation to explain why we are here, *i.e.* the matter-antimatter asymmetry of the universe?
- What about gravity?

While these are all important questions there is no definite answer to any of them.

There are however a large number of models of Beyond the Standard Model (BSM) physics which motivated by trying to address problems in the Standard Model. Given the lack of any experimental evidence of BSM physics the field is driven by theoretical and ascetic arguments, and unfortunately fashion.

All models of BSM physics predict either new particles or differences from the Standard Model, otherwise they cannot be distinguished experimentally from the Standard Model. There are a number of ways of looking for BSM effects:

**Collider Experiments** if the theory contains new particles these should be produced in collider experiments and decay to give Standard Model particles, currently the searches at the energy frontier are at the LHC general-purpose detectors ATLAS and CMS;

**Precision Experiments** measure something predicted by the Standard Model to very high accuracy and compare the results with the theoretical prediction, examples include the LEP/SLD precision measurements at the  $Z^0$  pole and the anomalous magnetic moment,  $g - 2$ , of the muon;

**Rare Decays or Processes** measure the cross section or decay rate for some process which the Standard Model predicts to be small (or zero). Examples include: neutron electric dipole moment experiments, proton decay experiments, neutrino mixing experiments, rare B and kaon decay and CP-violation experiments (BELLE, BaBar, NA48/62, LHCb).

In many ways these approaches are complimentary. Some effects, *e.g.* CP-violation, are best studied by dedicated experiments but if the result of these experiments differs from the SM there should be new particles which are observable at collider experiments.

We will consider the collider signals of BSM physics in detail but only look at the constraints from low-energy physics as we look at various models. The most important low energy constraints are flavour changing neutral currents and proton decay. Often other constraints, *e.g.* from astrophysics and cosmology are also considered.

## 9.1 Models

We will briefly review some of the more promising models and then look at the implications of these models for collider physics taking a pragmatic view looking at the different possible signatures rather than the details of specific models.

There are a wide range of models: grand unified theories; Technicolor; supersymmetry; large extra dimensions; small extra dimensions; little Higgs models; unparticles .... Depending on which model builder you talk to they may be almost fanatical in their belief that one of these models is realized in nature.

### 9.1.1 Grand Unified Theories

The first attempts to answer the problems in the Standard Model were *Grand Unified Theories* (GUTs.) The basic idea is that the Standard Model gauge group  $SU(3)_c \times SU(2)_L \times U(1)_Y$  is the subgroup of some larger gauge symmetry. The simplest group is  $SU(5)$ , which we will consider here, other examples include  $SO(10)$ .  $SU(5)$  has  $5^2 - 1 = 24$  generators which means there are 24 gauge bosons. In the Standard Model there are 8 gluons and 4 electroweak gauge bosons ( $W^\pm$ ,  $W^0$ ,  $B^0 \Rightarrow W^\pm$ ,  $\gamma$ ,  $Z^0$ ). Therefore there are 12 new gauge bosons  $X^{\pm\frac{4}{3}}$  and  $Y^{\pm\frac{1}{3}}$ . The right-handed down type quarks and left

handed leptons form a  $\bar{5}$  representation of  $SU(5)$ . The rest of the particles form a 10 representation of the gauge group

$$\begin{array}{c} \text{gluons} \\ W^\pm \end{array} \begin{array}{c} \rightarrow \\ \rightarrow \\ \rightarrow \\ \rightarrow \end{array} \left( \begin{array}{c} d \\ d \\ d \\ e^c \\ \bar{\nu}_e \end{array} \right)_R \begin{array}{c} \leftarrow \\ \leftarrow \\ \leftarrow \\ \leftarrow \end{array} \begin{array}{c} X, Y \end{array} \quad \left( \begin{array}{ccccc} 0 & u^c & -u^c & -u & -d \\ u^c & 0 & u^c & -u & -d \\ u^c & -u^c & 0 & -u & -d \\ u & u & u & 0 & -e^c \\ d & d & d & e^c & 0 \end{array} \right)_L. \quad (89)$$

In this model there are two stages of symmetry breaking. At the GUT scale the  $SU(5)$  symmetry is broken and the  $X$  and  $Y$  bosons get masses. At the electroweak scale the  $SU(2) \times U(1)$  symmetry is broken as before. There are three problems with this theory: the couplings do not unify at the GUT scale; why is the GUT scale higher than the electroweak scale; and proton Decay. We will come back to the first two of these questions.

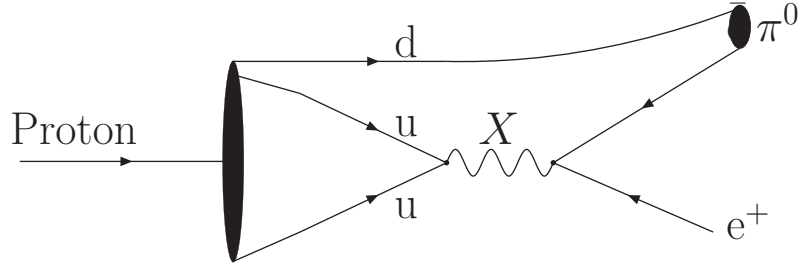


Figure 35: Proton Decay in a Grand Unified theory.

**Proton Decay** Grand unified theories predict the decay of the proton via the exchange of the  $X$  and  $Y$  bosons, as shown in Fig. 35. We would expect this decay rate to go like

$$\Gamma(p \rightarrow \pi^0 e^+) \sim \frac{M_p^5}{M_X^4}, \quad (90)$$

where  $M_X$  is the mass of the  $X$  boson and  $M_p$  the mass of the proton, on dimensional grounds.

There are limits on the proton lifetime from water Čerenkov experiments. The decay of the proton will produce an electron which is travelling faster than the speed of light in water. This will give Čerenkov radiation, just as the electron produced in the weak interaction of a neutrino does. This is used to search for proton decay. As there is no evidence of proton decay there is limit of

$$\tau_P \geq 1.6 \times 10^{32} \text{ years} \quad (91)$$

on the proton lifetime. This means  $M_X > 10^{16-17} \text{ GeV}$  which is larger than preferred by coupling unification. Proton decay gives important limits on other models.

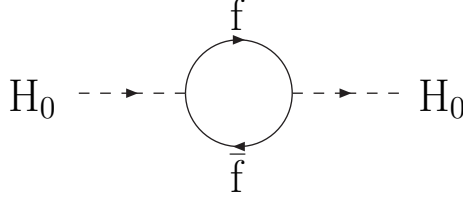


Figure 36: Quantum correction to the Higgs mass from a fermion loop.

### 9.1.2 Hierarchy Problem

The vast majority of new physics models are motivated by considering the hierarchy problem, *i.e.* why is the electroweak scale is so much less than the GUT or Planck (where gravity becomes strong) scales? It is more common to discuss the technical hierarchy problem which is related to the Higgs boson mass. If we look at the Higgs mass there are quantum corrections from fermion loops such as that shown in Fig.36. This gives a correction to the Higgs mass,

$$\delta M_{Hf}^2 = i \frac{|g_f|^2}{4} \int \frac{d^4 k}{(2\pi)^4} \frac{\text{tr} [(k + \not{p} + m_f)(k + m_f)]}{[(k + p)^2 - m_f^2] [k^2 - m_f^2]}, \quad (92)$$

where  $p$  is the four-momentum of the Higgs boson,  $k$  the four-momentum flowing in the loop,  $g_f$  the coupling of the Higgs boson to the fermion and  $m_f$  the fermion mass. We need to introduce an ultra-violet cut-off,  $\Lambda$ , to regularize the integral giving

$$\delta M_{Hf}^2 = \frac{|g_f|^2}{16\pi^2} [-2\Lambda^2 + 6m_f^2 \ln(\Lambda/m_f)]. \quad (93)$$

So either the Higgs mass is the GUT/Planck scale or there is a cancellation

$$M_H^2 = M_{H\text{bare}}^2 + \delta M_H^2, \quad (94)$$

of over 30 orders of magnitude to have a light Higgs boson.

This worries a lot of BSM theorists, however there are values of the Higgs boson mass for which the Standard Model could be correct up to the Planck scale. The Higgs boson mass is  $m_H^2 = \lambda v^2$ . There are two constraints on the mass: the coupling should be perturbative,  $\lambda \lesssim 1$ ; the vacuum must be non-trivial,  $\lambda \rightarrow 0$  is forbidden. As can be seen in Fig. 37 there is an island of stability in the middle where the Standard Model can be valid to the Planck scale.

Many solutions to the hierarchy problem have been proposed. They come in and out of fashion and occasionally new ones are proposed. Examples include: Technicolor; supersymmetry; extra dimensions; and little Higgs models.

### 9.1.3 Technicolor

Technicolor is one of the oldest solutions to the hierarchy problem. The main idea is that as the problems in the theory come from having a fundamental scalar particle they can be solved by not having one. The model postulates a new set of gauge interactions *Technicolor*, which acts on new technifermions. We think of this interaction like QCD,

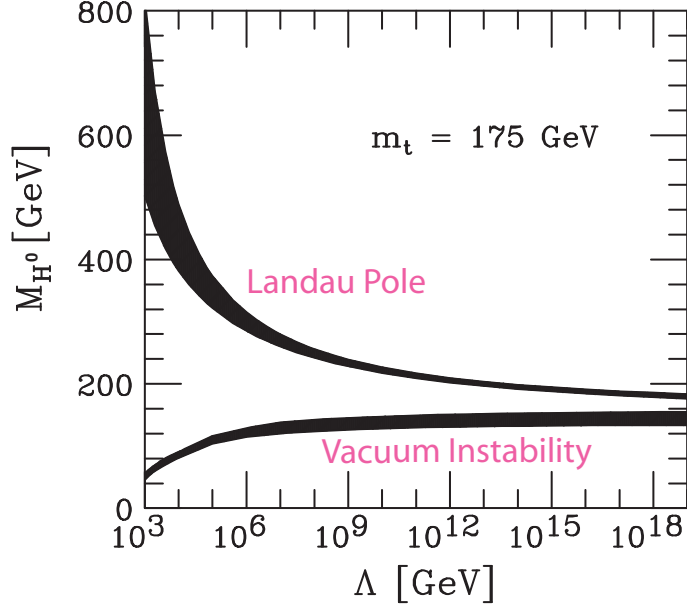


Figure 37: Region of stability for the Standard Model Higgs boson.

although different gauge groups have been considered. The technifermions form bound states, the lightest being technipions. Using the Higgs mechanism these technipions give the longitudinal components of the  $W^\pm$  and  $Z$  bosons, and hence generate the gauge boson masses. There must also be a way to generate the fermions masses, *Extended Technicolor*. It has proved hard to construct realistic models which are not already ruled out. For many years Technicolor fell out of fashion, however following the introduction of little Higgs models there has been a resurgence of interest and the new walking Technicolor models look more promising.

#### 9.1.4 Supersymmetry

If there is a scalar loop in the Higgs propagator, as shown in Fig.38. We get a new

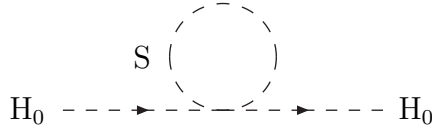


Figure 38: New scalar boson loop in the Higgs boson propagator.

contribution to the Higgs mass,

$$\delta M_{HS}^2 = \frac{\lambda_s}{16\pi^2} (\Lambda^2 - 2M_S^2 \ln(\Lambda/M_S)), \quad (95)$$

where  $M_S$  is the mass of the new scalar particle. If there are two scalars for every fermion, with the same mass and  $\lambda_s = |g_f|^2$  the quadratic dependence cancels. Theorists like to

SM particle	Spin	SUSY particle	Spin
Electron	1/2	Selectron	0
Neutrino	1/2	Sneutrino	0
Up	1/2	Sup	0
Down	1/2	Sdown	0
Gluon	1	Gluino	1/2
Photon	1	Photino	1/2
Z	1	Zino	1/2 Neutralinos
Higgs	0	Higgsino	1/2
W <sup>+</sup>	1	Wino	1/2 Charginos
H <sup>+</sup>	0	Higgsino	1/2

Table 4: Particle content of the Minimal Supersymmetric Standard Model.

have symmetries to explain cancellations like this, *Supersymmetry* (SUSY). For every fermionic degree of freedom there is a corresponding bosonic degree of freedom: all the SM fermions have two spin-0 partners; all the SM gauge bosons have a spin- $\frac{1}{2}$  partner. The full particle content of the theory is given in Table 4. In SUSY models we need to have two Higgs doublets to give mass to both the up- and down-type quarks in a way which is invariant under the supersymmetric transformations.

There are major two reasons, in addition to the solution of the hierarchy problem, to favour SUSY as an extension of the SM.

**Coleman-Mandula theorem** If we consider any extension to the Poincaré group any new generators which transform as bosons lead to a trivial S-matrix, *i.e.* scattering only through discrete angles. Later Haag, Lopuszanski and Sohnius showed that SUSY is the only possible extension of the Poincaré group which doesn't give a trivial S-matrix.

**SUSY coupling unification** In SUSY GUTS the additional SUSY particles change the running of the couplings and allow the couplings to truly unify at the GUT scale, as shown in Fig. 39. However, with increasingly accurate experimental measurements of the strong coupling this is no longer quite true.

In the modern view of particle physics we construct a theory by specifying the particle content and symmetries. All the terms allowed by the symmetries are then included in the Lagrangian. If we do this in supersymmetric models we naturally get terms which do not conserve lepton and baryon number. This leads to proton decay as shown in Fig. 40. Proton decay requires that both lepton and baryon number conservation are violated. The limits on the proton lifetime lead to very stringent limits on the product of the couplings leading to proton decay.

$$\lambda'_{11k} \cdot \lambda''_{11k} \lesssim 2 \cdot 10^{-27}. \quad (96)$$

Only natural way for this to happen is if some symmetry requires that one or both couplings are zero. Normally a multiplicatively conserved symmetry *R-parity*

$$R_p = (-1)^{3B+L+2S}, \quad (97)$$



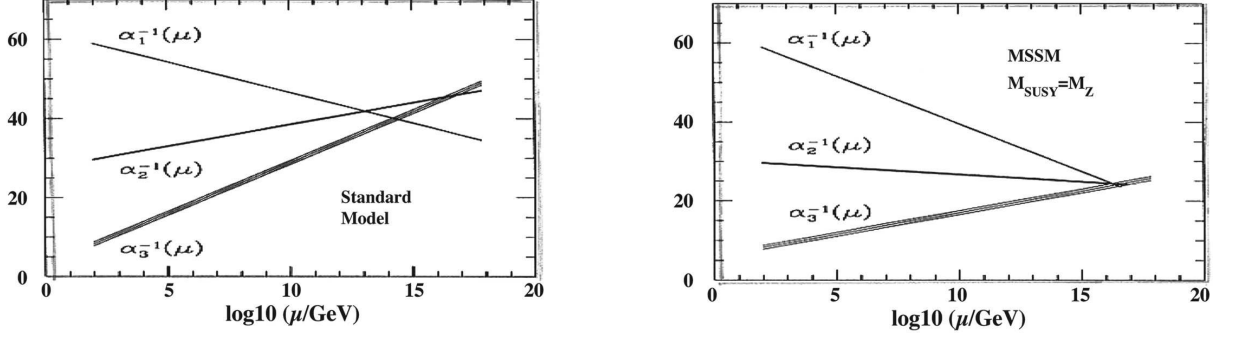


Figure 39: Coupling constant unification in the Standard and Minimal Supersymmetric Standard Models.

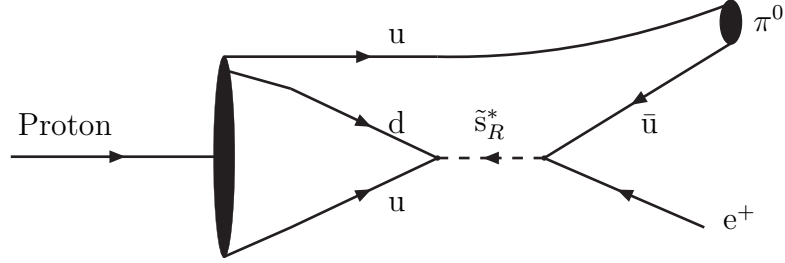


Figure 40: Proton decay in supersymmetric models.

such that Standard Model Particles have  $R_p = +1$  and SUSY particles have  $R_p = -1$ , is introduced which forbids both terms.

Alternatively symmetries can be imposed which only forbid the lepton or baryon number violating terms. The simplest SUSY extension of the Standard Model has  $R_p$  conservation and is called the Minimal Supersymmetric Standard Model (MSSM). The multiplicative conservation of R-parity has two important consequences: SUSY particles are only pair produced; the lightest SUSY particle is stable, and therefore must be neutral on cosmological grounds. It is therefore a good dark matter candidate.

So far we haven't dealt with the biggest problem in SUSY. Supersymmetry requires that the SUSY particles have the same mass as their Standard Model partner and the SUSY partners have not been observed. SUSY must therefore be a broken symmetry in such a way that the Higgs mass does not depend quadratically on the ultraviolet cut-off, called *soft SUSY breaking*. This introduces over 120 parameters into the model. Many of these parameters involve either flavour changing or CP-violating couplings and are constrained by limits on flavour changing neutral currents.

**Flavour Changing Neutral Currents** In the Standard Model the only interactions which change the quark flavour are those with the  $W^\pm$  boson. So any processes which change the flavour of the quarks, but not the charge, *Flavour Changing Neutral Currents* (FCNCs), must be loop mediated.

There are two important types: those which change the quark flavour with the emission of a photon, *i.e.*  $b \rightarrow s\gamma$ ; those which give meson-antimeson mixing, *e.g.*  $B - \bar{B}$  mixing.

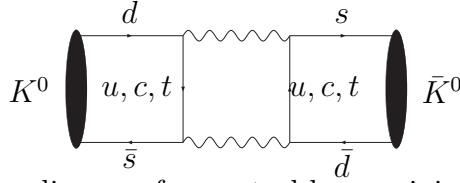


Figure 41: Feynman diagram for neutral kaon mixing in the Standard Model.

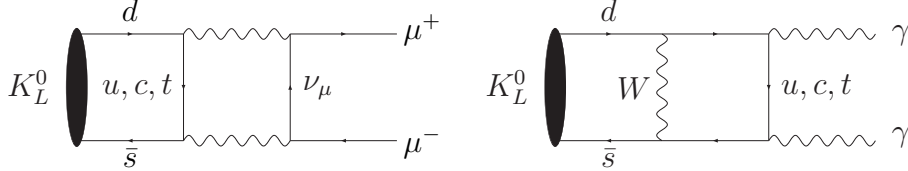


Figure 42: Feynman diagrams for the decay of the neutral kaon to  $\mu^+\mu^-$  and  $\gamma\gamma$  in the Standard Model.

Both are important in the Standard Model and in constraining possible new physics models.

In the Standard Model flavour changing neutral currents are suppressed by the Glashow-Iliopoulos-Maiani (GIM) mechanism. If we consider neutral Kaon mixing, as shown in Fig. 41, and the rare Kaon decays  $K_L^0 \rightarrow \mu^+\mu^-$  and  $K_L^0 \rightarrow \gamma\gamma$ , as shown in Fig. 42.

Considering only two generations for simplicity all these diagrams go like

$$\frac{1}{M_W^2} \frac{m_u^2 - m_c^2}{M^2}, \quad (98)$$

times a factor due to the Cabibbo mixing angle where  $M$  is the largest mass left after the removal of one  $W$  propagator, *i.e.*  $M_W$  for  $K^0 - \bar{K}^0$  mixing and  $K_L^0 \rightarrow \mu^+\mu^-$ , and  $m_c$  for  $K_L^0 \rightarrow \gamma\gamma$ . This suppression is called the GIM mechanism and explains why  $\Gamma(K_L^0 \rightarrow \mu^+\mu^-) \sim 2 \times 10^{-5} \Gamma(K_L^0 \rightarrow \gamma\gamma)$ . The current experimental results are in good agreement with the SM. This often proves a problem in BSM physics as there are often new sources of FCNCs.

In SUSY theories the SUSY partners also give contributions to FCNCs, as shown in Fig. 43. In this case the diagrams proportional to the mass difference of the squarks.

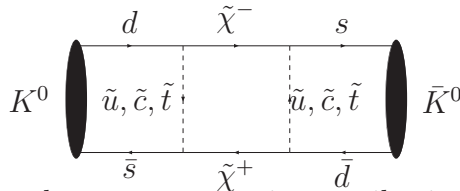


Figure 43: An example supersymmetric contribution to neutral kaon mixing.

Provide the SUSY breaking masses are flavour independent this is not a problem, as the mass differences are the same as the SM. It is also not a problem if there is no flavour mixing in the model. In general both these things are possible and must be considered.

**SUSY Breaking** What are the 120 SUSY breaking parameters? In general there are: SUSY breaking masses for the scalars; SUSY breaking masses for the gauginos;  $A$  terms which mix three scalars; mixing angles and CP-violating phases. We need a model of

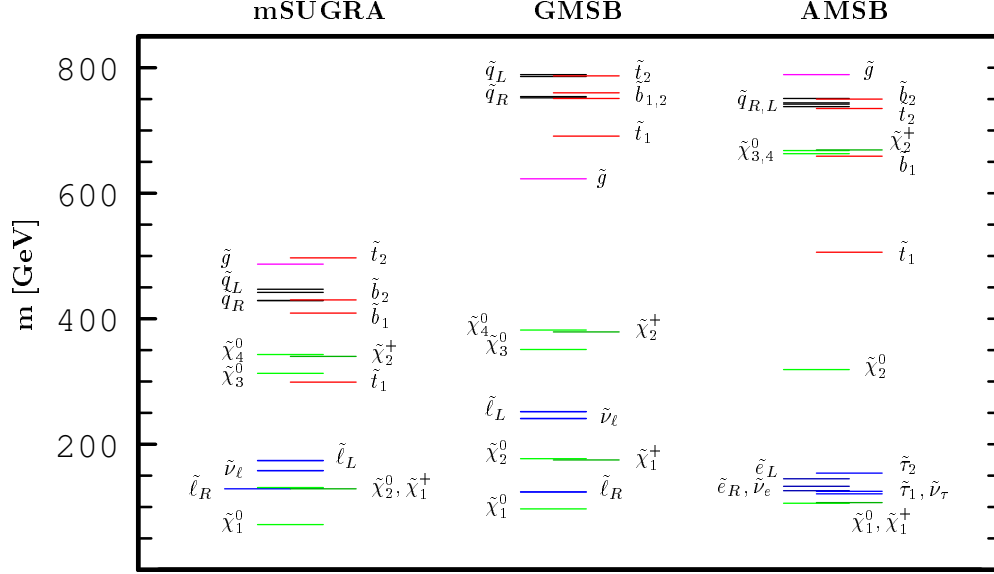


Figure 44: Examples of the mass spectra in different SUSY breaking models.

where these parameters come from in order to do any phenomenological or experimental studies. We therefore use models which predict these parameters from physics at higher energy scales, *i.e.* the GUT or Planck scale. In all these models SUSY is broken in a hidden sector, *i.e.* the MSSM particles.

**SUGRA** SUSY breaking is transmitted via gravity. All the scalar ( $M_0$ ) and gaugino ( $M_{1/2}$ ) masses are unified at the GUT scale. The  $A$  and  $B$  terms are also universal. The known value of  $M_Z$  is used to constrain the  $\mu$  and  $B$  parameters leaving  $\tan \beta = v_1/v_2$  as a free parameter. There are five parameters which give the mass spectrum:  $M_0$ ,  $M_{1/2}$ ,  $\tan \beta$ ,  $\text{sgn } \mu$ ,  $A$ . The gluino mass is correlated with  $M_{1/2}$  and slepton mass with  $M_0$ .

**GMSB** In gauge mediated SUSY breaking (GMSB) the flavour-changing neutral current problem is solved by using gauge fields instead to gravity to transmit the SUSY breaking. The messenger particles,  $X$ , transmit the SUSY breaking. The simplest choice is a complete  $SU(5)$  **5** or **10** of particles transmitting the SUSY breaking to preserve the GUT symmetry. The fundamental SUSY breaking scale  $\lesssim 10^{10}$  GeV is lower than in gravity mediated models. The gaugino masses occur at one-loop,  $M_{\tilde{g}} \sim \alpha_s N_X \Lambda$  while the scalar masses occur at two-loop,  $M_{\tilde{q}} \sim \alpha_s^2 \sqrt{N_X} \Lambda$ , where  $\Lambda$  is the breaking scale and  $N_X$  the number of messenger fields. The true LSP is the almost massless gravitino. The lightest superpartner is unstable and decays to gravitino and can be neutral, *e.g.*  $\tilde{\chi}_1^0$ , or charged, *e.g.*  $\tilde{\tau}_1$ .

**AMSB** The superconformal anomaly is always present and can give anomaly mediated SUSY breaking (AMSB). This predicts the sparticle masses in terms of the gravitino mass,  $M_{3/2}$ . The simplest version of the model predicts tachyonic particles so another SUSY breaking mechanism is required to get a realistic spectrum, *e.g.* adding universal scalar masses ( $M_0$ ). The model has four parameters  $M_0$ ,  $M_{3/2}$ ,  $\tan \beta$  and  $\text{sgn } \mu$ . In this model the lightest chargino is almost degenerate with the lightest neutralino.

The mass spectrum in the models is different, as shown in Fig. 44. The main differences are: the mass splitting between gluino and electroweak gauginos; the mass splitting of the squarks and sleptons; and the nature of the LSP.

**Muon g-2** Another important low energy constraint on BSM physics is the anomalous magnetic moment of the muon. The magnetic moment of any fundamental fermion is

$$\mu = g \left( \frac{e}{2m} \right) \mathbf{S}, \quad (99)$$

where  $g$  is the  $g$ -factor,  $m$  the mass and  $\mathbf{S}$  the spin of the particle. The Dirac equation predicts  $g = 2$ . However there are quantum corrections, as shown in Fig. 45, which lead to an anomalous magnetic moment,  $g - 2$ .

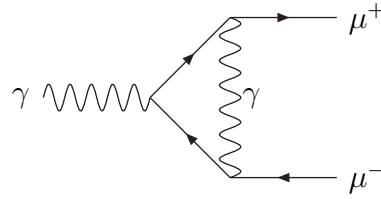


Figure 45: Vertex correction contributing to the anomalous muon magnetic moment in the Standard Model.

There are also quark loops in the photon propagator, as shown in Fig. 46. This is a low energy process so we can not use perturbative QCD. Instead we must use the measured  $e^+e^-$  total cross section and the optical theorem to obtain the corrections which leads to an experimental error on the theoretical prediction. In many BSM theories, for example

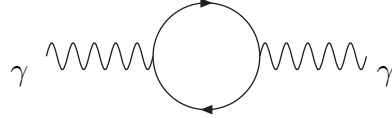


Figure 46: Quark loop in the photon propagator which contributes to the anomalous muon magnetic moment in the Standard Model.

in SUSY, there are additional corrections from diagrams, such as that shown in Fig. 47.

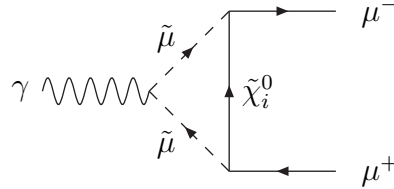


Figure 47: Example of a SUSY correction to the muon magnetic moment.

The original experimental result disagreed with the SM at  $2.6\sigma$ , but there was an error in the sign in one of the terms in the theoretical calculation reducing the significance to about  $1.4\sigma$ . However if you measure enough quantities some of them should disagree with the prediction by more the 1 sigma (about 1/3), and some by 2 sigma (4.6%) or 3 sigma (0.3%). This is why we define a discovery to be 5 sigma ( $6 \times 10^{-50}\%$ ), so this is nothing to worry about.

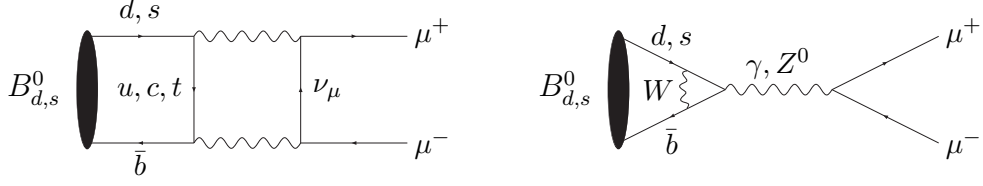


Figure 48: Standard Model Feynman diagrams for  $B_s \rightarrow \mu^+ \mu^-$ .

**Rare  $B$  decays** There is an amazing consistency of the current flavour physics measurements. However, many new physics models can have a similar pattern in their flavour sector, the new physics model must have this otherwise it is experimentally excluded. However, there can still be new physics in rare processes (like  $B^+ \rightarrow \tau^+ \nu_\tau$ ) and CP-asymmetries. One promising examples is the decay  $B_s \rightarrow \mu^+ \mu^-$ . There are two Standard Model contributions from box and penguin diagrams as shown in Fig. 48. Both of these are suppressed by  $V_{tb} V_{ts}^*$  giving a Standard Model branching ratio

$$\text{BR}_{B_s, d \rightarrow \mu\mu}^{(\text{SM})} \approx 10^{-9}. \quad (100)$$

This gives a simple leptonic final state with minor theoretical uncertainties but a huge background so the mass resolution is paramount, the expected mass resolution for the LHC experiments is given in Table 5.

Exp.	ATLAS	CMS	LHCb
$\sigma_m$ (MeV)	77	36	18

Table 5: Expected mass resolution for  $B_s \rightarrow \mu^+ \mu^-$ .

In the MSSM, however, the amplitude involves three powers of  $\tan^2 \beta$ , so that

$$\text{BR}_{B_s \rightarrow \mu\mu}^{(\text{MSSM})} \propto \tan^6 \beta, \quad (101)$$

which leads to an enhancement over the SM value by up to three orders of magnitude.

### 9.1.5 Extra Dimensions

Many theorists believe there are more than 4 dimensions, for example string theories can only exist in 10/11 dimensions. The hierarchy problem can be solved (redefined?) in these models in one of two ways.

1. There is a large extra dimension with size  $\sim 1\text{mm}$ . In this case

$$M_{\text{Planck}}^2 \sim M^{n+2} R^n, \quad (102)$$

where  $M_{\text{Planck}}$  is the observed Planck mass,  $M$  is the extra-dimensional Planck mass and  $R$  the radius of the additional  $n$  dimensions. In this case the Planck mass is of order 1 TeV so there is no hierarchy problem. However the hierarchy in the sizes of the dimensions must be explained.

2. Small extra dimensions in which case the extra dimension is warped. The model has two branes, we live on one and the other is at the Planck scale. The Higgs VEV is suppressed by a warp factor,  $\exp(-kr_c\pi)$ , where  $r_c$  is the compactification radius of the extra dimension, and  $k$  a scale of the order of the Planck scale.

We can consider what happens in extra-dimensional models by studying a scalar field in 5-dimensions. In this case the equation of motion for the scalar field is

$$\left(\frac{\partial^2}{\partial t^2} - \nabla_5^2 + m^2\right) \Phi(x, y, z, x_5, t) = 0, \quad (103)$$

where

$$\nabla_5^2 = \frac{\partial^2}{\partial x^2} + \frac{\partial^2}{\partial y^2} + \frac{\partial^2}{\partial z^2} + \frac{\partial^2}{\partial x_5^2} \quad (104)$$

is the 5-dimensional Laplace operator. If the 5-th dimension is circular we can Fourier decompose the field,

$$\Phi(x, y, z, x_5, t) = \sum_n \Phi_n(x, y, z, t) \exp(inx_5/R). \quad (105)$$

The equation of motion therefore becomes,

$$\sum_n \left(\frac{\partial^2}{\partial t^2} - \nabla_4^2 + m^2 + \frac{n^2}{R^2}\right) \Phi_n(x, y, z, t). \quad (106)$$

This gives a Kaluza-Klein (KK) tower of states with mass splitting  $\sim 1/R$ . There are a number of different models.

**Large Extra Dimensions** Only gravity propagates in the bulk, *i.e.* in the extra dimensions. We therefore only get Kaluza-Klein excitations of the graviton. In large extra dimensional models the mass splitting between the KK excitations is small and all the gravitons contribute to a given process. Phenomenologically there are deviations from the SM prediction for SM processes.

**Small Extra Dimensions** Again only gravity propagates in the bulk so there are only KK excitations of the graviton. In this case the mass splitting is large leading to resonant graviton production.

**Universal Extra Dimensions** Another alternative is to let all the Standard Model fields propagate in the bulk, *Universal Extra Dimensions* (UED). All the particles have Kaluza-Klein excitations. It is possible to have a Kaluza-Klein parity, like R-parity in SUSY. The most studied model has one extra dimension and a similar particle content to SUSY, apart from the spins. There are also some 6-dimensional models.

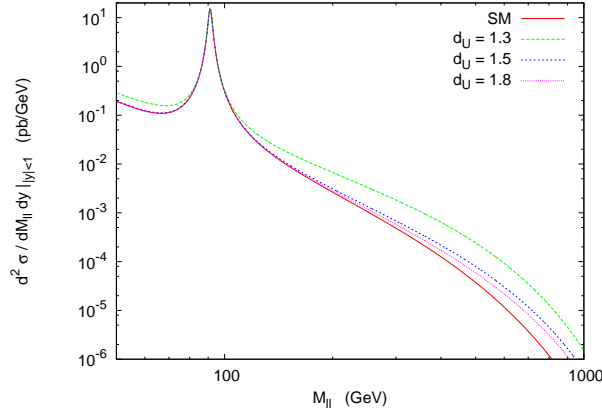


Figure 49: Drell-Yan mass spectrum including unparticle exchange taken from Ref. [21].

### 9.1.6 Little Higgs Models

In little Higgs models the Higgs fields are Goldstone bosons associated with breaking a global symmetry at a high scale,  $\Lambda_S$ . The Higgs fields acquire a mass and become pseudo-Goldstone bosons via symmetry breaking at the electroweak scale. The Higgs fields remain light as they are protected by the approximate global symmetry. The model has heavy partners for the photon,  $Z^0$ ,  $W^\pm$  bosons and the top quark as well as extra Higgs bosons. The non-linear  $\sigma$ -model used for the high energy theory is similar to the low energy effective theory of pions which can be used to describe QCD, or in Technicolor models. This similarity with Technicolor models is one of the reasons for the resurgence of Technicolor models in recent years.

The original Little Higgs models had problems with electroweak constraints. The solution is to introduce a discrete symmetry called T-parity, analogous to R-parity in SUSY models. This solves the problems with the precision electroweak data and provides a possible dark matter candidate. This model has a much larger particle content than the original Little Higgs model and is more SUSY-like with a partner for each Standard Model particle.

### 9.1.7 Unparticles

In these models a new sector at a high energy scale with a non-trivial infrared (IR) fixed point is introduced. This sector interacts with the Standard Model via the exchange of particles with a large mass scale leading to an effective theory

$$\frac{C_U \Lambda_U^{d_{BZ} - d_U}}{M_U^k} O_{SM} O_U, \quad (107)$$

where:  $d_U$  is the scaling dimension of the unparticle operator  $O_U$ ;  $M_U$  is the mass scale for the exchanged particles;  $O_{SM}$  is the Standard Model operator;  $d_{BZ}$  is the dimension of the operator in the high energy theory;  $k$  gives the correct overall dimension of the interaction term. This leads to new operators which give deviations from the Standard Model predictions for various observables.

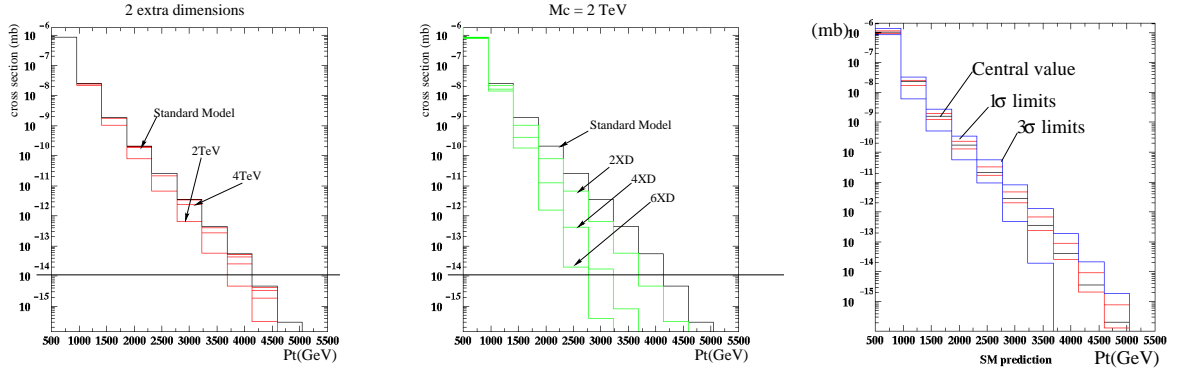


Figure 50: Jet  $p_{\perp}$  spectrum for various numbers of extra dimensions in the ADD model taken from Ref. [22].

## 9.2 Beyond the Standard Model Signatures

Before we go on and consider the signals of models of new physics in great detail it is worthwhile considering what we expect to see in general. Most models of new physics predict either the existence of more particles than the Standard Model or new operators which give deviations from the Standard Model predictions. The signatures of the model depend on either how these particles are produced and decay or the type of deviations expected. In any study of BSM physics the most important thing is to understand the Standard Model backgrounds. Often the signal is at the tail of some distribution and the limits of our ability to calculate or simulate it.

### 9.2.1 Deviations from the Standard Model

There can be deviations from what is expected in the Standard Model due to: compositeness; exchanging towers of Kaluza-Klein gravitons in large extra dimension models; unparticle exchange; .... This tends to give changes in the shapes of spectra. Therefore in order to see a difference you need to know the shape of the Standard Model prediction.

**Example I: High  $p_{\perp}$  jets** One possible signal of compositeness is the production of high  $p_{\perp}$  jets. At one point there was a disagreement between theory and experiment at the Tevatron. However, this was not due to new physics but too little high- $x$  gluon in the PDFs. Now as well as looking in the  $p_{\perp}$  spectra at central rapidities where we expect to see a signal of BSM physics we also look at high rapidity as a disagreement at both central and high rapidities is more likely to be due to the parton distribution functions. An example of the jet  $p_{\perp}$  spectrum at a range of rapidities is shown in Fig. 21.

**Example II: Unparticles** Many models predict deviations in the Drell-Yan mass spectra, for example in an unparticle model with the exchange of virtual spin-1 unparticles, see Fig. 49. However, we need to be careful as higher order weak corrections which can also change the shape are often neglected.



Background	Expected Events
$Z \rightarrow \nu\nu$	$130 \pm 14$
$W \rightarrow \tau\nu$	$60 \pm 7$
$W \rightarrow \mu\nu$	$36 \pm 4$
$W \rightarrow e\nu$	$17 \pm 2$
$Z \rightarrow ll$	$3 \pm 1$
QCD	$15 \pm 10$
Non-Collision	$4 \pm 4$
<b>Total Predicted</b>	<b><math>265 \pm 30</math></b>
<b>Data Observed</b>	<b>263</b>

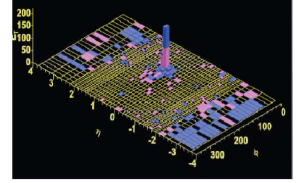
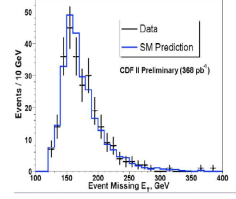


Figure 51: CDF results for monojet production taken from Fermilab wine and cheese seminar by K. Burkett.

**Example III: PDF uncertainty or new physics** In the ADD model of large extra dimensions there are changes in the shape of the jet  $p_{\perp}$  and dijet mass spectra due to the exchange of KK towers of gravitons and their destructive interference with SM, as shown in Fig. 50.

### 9.2.2 Monojets

There are a range of models which predict monojet signals with the production of a quark or gluon which is recoiling against either: a stable neutral particle; a tower of KK gravitons in large extra dimension models; unparticles; ....

**Example IV: Mono-jets at the SppS** In Ref. [23] the UA1 collaboration reported: 5 events with  $E_{\perp, \text{miss}} > 40$  GeV and a narrow jet; 2 events with  $E_{\perp, \text{miss}} > 40$  GeV and a neutral EM cluster. They could “not find a Standard Model explanation”, and compared their findings with a calculation of SUSY pair-production [24]. They deduced a gluino mass larger than around 40 GeV. In Ref. [25], the UA2 collaboration describes similar events, also after  $113 \text{ nb}^{-1}$ , without indicating any interpretation as strongly as UA1. In Ref. [26] S. Ellis, R. Kleiss, and J. Stirling calculated the backgrounds to that process more carefully, and showed agreement with the Standard Model.

There are many different Standard Model electroweak backgrounds and a careful comparison shows they are currently in agreement with the Standard Model, see Fig. 51.

### 9.2.3 New Particle Production

In general there are two cases for models in which new particles are produced.

1. The model has only a few new particles, mainly produced as s-channel resonances. Examples include: Z-prime models; little Higgs models; small extra dimension models, ....
2. The model has a large number of new particles. Examples include: SUSY; UED; little Higgs models with T-parity, ....

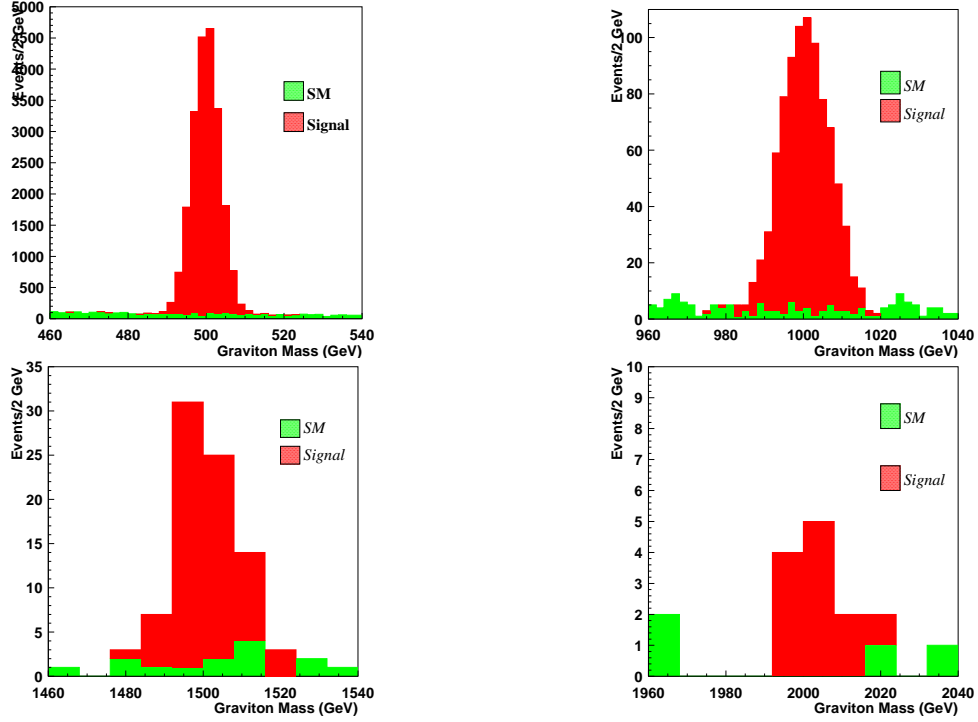


Figure 52: Example of resonant graviton production at the LHC for  $\sqrt{s} = 14$  GeV taken from Ref. [27].

In the first type of model the main signal is the production of  $s$ -channel resonances while in the second class of models the signals are more varied and complex.

#### 9.2.4 Resonance Production

The easiest and cleanest signal in hadron collisions is the production of an  $s$ -channel resonance which decays to  $e^+e^-$  or  $\mu^+\mu^-$ . Resonances in this and other channels are possible in: Little Higgs models;  $Z'$  models; UED; Small Extra Dimensions. Backgrounds can be removed using sideband subtraction.

**Example V: Resonant Graviton Production** The best channel,  $e^+e^-$ , gives a reach of order 2 TeV depending on the cross section for the LHC running at  $\sqrt{s} = 14$  GeV. Other channels  $\mu^+\mu^-$ ,  $gg$ , and  $W^+W^-$  are possible. If the graviton is light enough the angular distribution of the decay products can be used to measure the spin of the resonance. An example of the dilepton mass spectrum in this model is shown in Fig. 52.

A lot of models predict hadronic resonances. This is much more problematic due to the mass resolution which smears out narrow resonances and the often huge QCD backgrounds. Although background subtraction can be used the ratio of the signal to background is often tiny, for example Fig. 53 shows the measured  $Z \rightarrow b\bar{b}$  peak at the Tevatron. 53

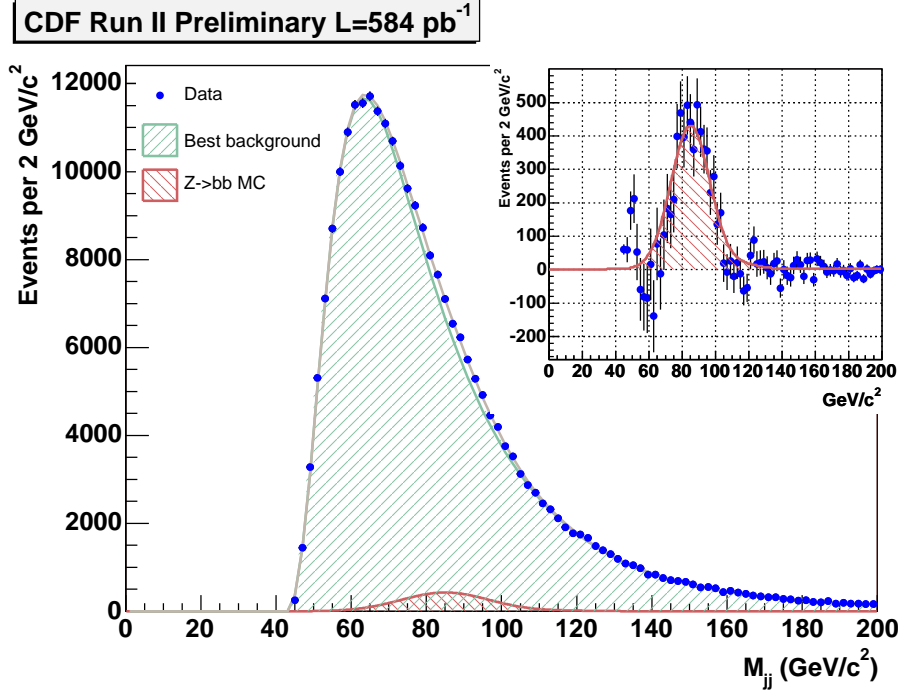


Figure 53: Dijet mass spectrum for bottom quark jets at the Tevatron taken from Ref. [28].

### 9.2.5 SUSY-like models

Most of the other models are “SUSY”-like, *i.e.* they contain: a partner of some kind for every Standard Model particle; often some additional particles such as extra Higgs bosons; a lightest new particle which is stable and a dark matter candidate.

A lot of new particles should be produced in these models. While some particles may be stable,<sup>8</sup> the the majority of these particles decay to Standard Model particles. Therefore we expect to see: charged leptons; missing transverse energy from stable neutral particles or neutrinos; jets from quarks, perhaps with bottom and charm quarks; tau leptons; Higgs boson production; photons; stable charged particles. It is worth noting that seeing an excess of these does not necessarily tell us which model has been observed.

The archetypal model containing large numbers of new particles which may be accessible at the LHC is SUSY. Other models are UED and the Little Higgs Model with T-parity. However, in practice UED is mainly used as a straw-man model for studies trying to show that a potential excess is SUSY.

Two statements which are commonly made are: the LHC will discover the Higgs boson; the LHC will discover low-energy SUSY if it exists. The first is almost certainly true, however the second is only partially true.

In hadron collisions the strongly interacting particles are dominantly produced. Therefore in SUSY squark and gluino production has the highest cross section, for example via the processes shown in Fig. 54.

<sup>8</sup>*i.e.* the decay length of the particle is such that the majority of the particles escape from the detector before decaying. In practice this happens for lifetimes greater than  $10^{-7}$ s.

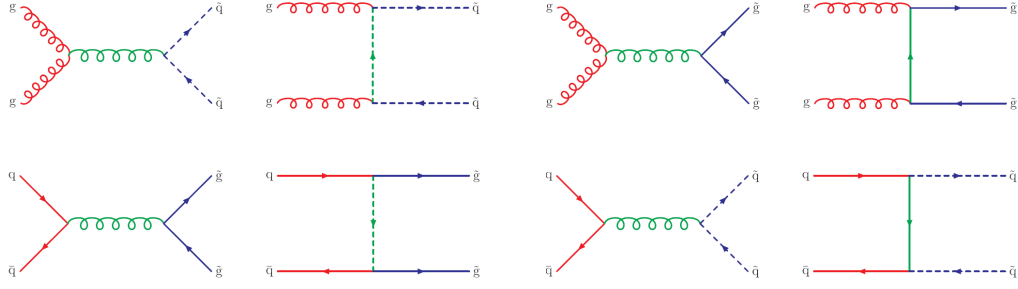


Figure 54: Example SUSY particle production processes.

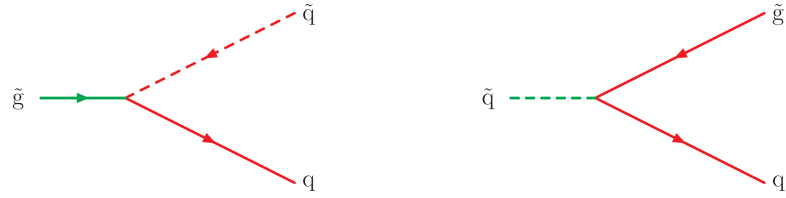


Figure 55: Example strong SUSY particle decays.

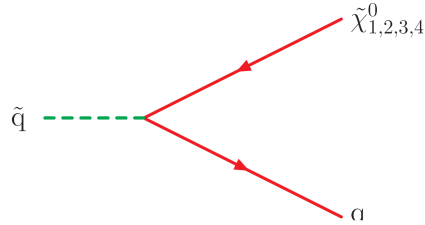


Figure 56: Example weak SUSY particle decays.

These particles then decay in a number of ways. Some of them have strong decays to other strongly interacting SUSY particles, for example via the processes shown in Fig. 55. However the lightest strongly interaction SUSY particle, squark or gluino, can only decay weakly, as shown in Fig. 56. The gluino can only have weak decays with virtual squarks or via loop diagrams. This is the main production mechanism for the weakly interacting SUSY particles.

The decays of the squarks and gluinos will produce lots of quarks and antiquarks. The weakly interacting SUSY particles will then decay giving more quarks and leptons. Eventually the lightest SUSY particle which is stable will be produced. This behaves like a neutrino and gives missing transverse energy. So the signal for SUSY is large numbers of jets and leptons with missing transverse energy. This could however be the signal for many models containing new heavy particles.

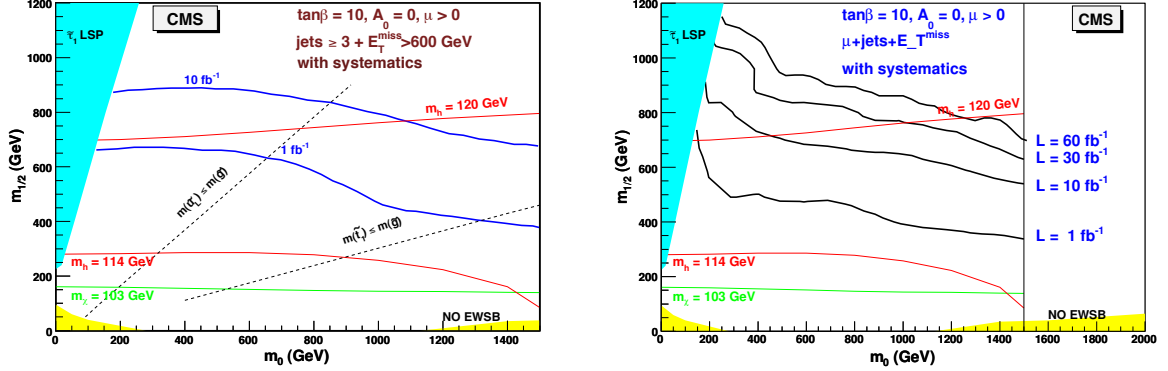


Figure 57: Expected limits in SUSY parameter space for searches using jets and missing transverse energy and jets, leptons and missing transverse energy for the LHC running at  $\sqrt{s} = 14$  TeV taken from Ref. [29].

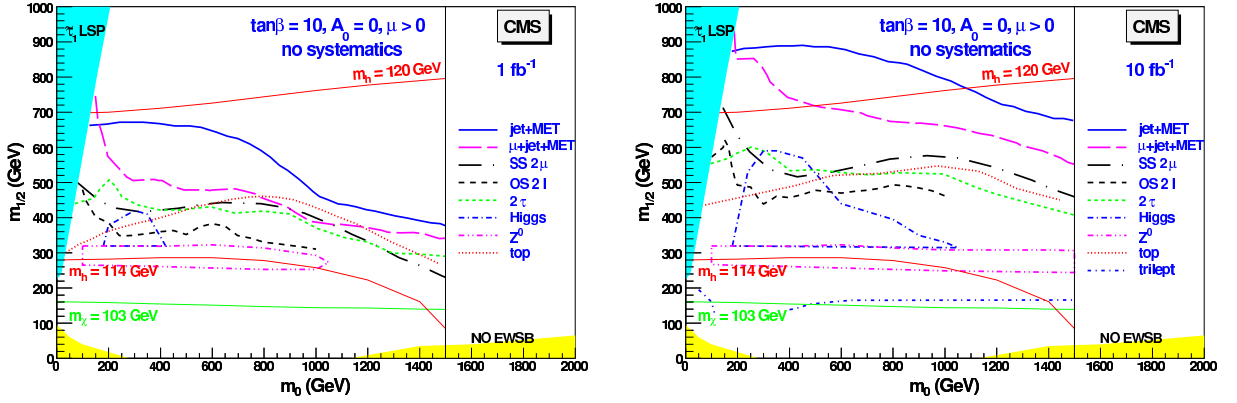


Figure 58: Expected limits in SUSY parameter space for searches using jets, leptons and missing transverse energy for the LHC running at  $\sqrt{s} = 14$  TeV taken from Ref. [29].

All SUSY studies fall into two categories: search studies which are designed to show SUSY can be discovered by looking for a inclusive signatures and counting events; measurement studies which are designed to show that some parameters of the model, usually masses, can be measured.

There is a large reach looking for a number of high transverse momentum jets and leptons, and missing transverse energy, see Figs. 57 and 58. It is also possible to have the production of the  $Z^0$  and Higgs bosons and top quarks. In many cases the tau lepton may be produced more often than electrons or muons.

Once we observe a signal of SUSY there are various approaches to determine the properties of the model. The simplest of these is the effective mass

$$M_{\text{eff}} = \sum_{i=1}^n p_{\perp i}^{\text{jet}} + \cancel{E}_T, \quad (108)$$

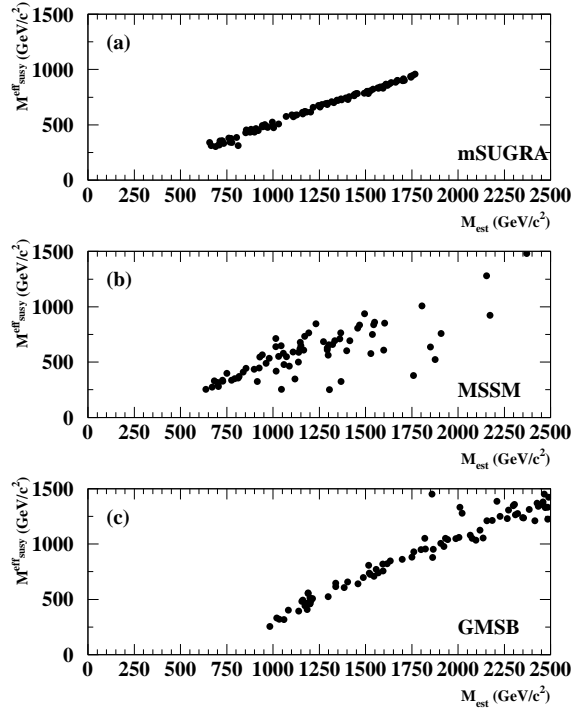


Figure 59: Correlation of the  $M_{\text{eff}}$  variable with the SUSY mass scale in various SUSY models taken from Ref. [30].

which is strongly correlated with the mass of strongly interacting SUSY particles and can be used to measure the squark/gluino mass to about 15%, see Fig. 59.

The analyzes we have just looked at are those that are used to claim the LHC will discover SUSY but this is not really what they tell us. They don't really discover SUSY. What they see is the production of massive strongly interacting particles, this does not have to be SUSY, it could easily be something else. In order to claim that a signal is SUSY we would need to know more about it. SUSY analyzes tend to proceed by looking for characteristic decay chains and using these to measure the masses of the SUSY particles and determine more properties of the model.

Given most of the searches are essentially counting experiments it is important to understand the Standard Model backgrounds which can be challenging, see Fig. 60.

## A Kinematics and Cross Sections

### A.1 Kinematics

The basic language of all phenomenology is that of relativistic kinematics, in particular four-vectors. In hadron collisions because we do not know what fraction of the beam momenta is transferred to the partonic system it is preferable to use quantities, such

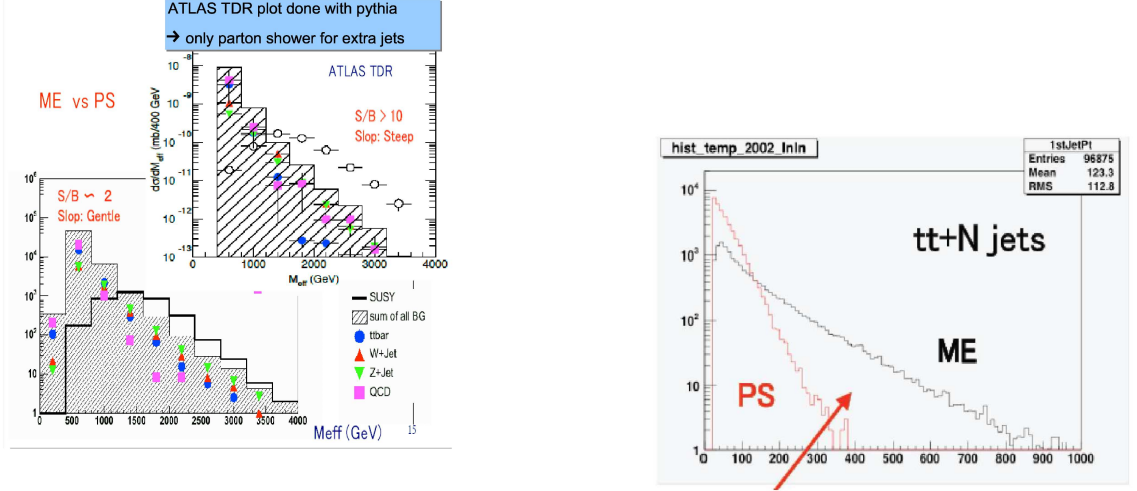


Figure 60: Backgrounds in inclusive SUSY searches.

as the transverse momentum,  $p_\perp$ , with respect to the beam direction which are invariant under longitudinal boosts along the beam direction to describe the kinematics. In addition to the transverse momentum we use the rapidity,  $y$ , and massless pseudorapidity,  $\eta$ ,

$$y = \frac{1}{2} \ln \frac{E + p_z}{E - p_z} \xrightarrow{\text{massless}} \eta = -\ln \tan \frac{\theta}{2}, \quad (109)$$

because rapidity differences are invariant under longitudinal boosts. Particles with small rapidities are produced at an angle close to  $90^\circ$  degrees to the beam direction while particles with large positive (negative) rapidities are travelling in the forward (backward) beam direction. The pseudorapidity is more often used experimentally as it is related to the measured scattering angle.

The four-momentum can be written as

$$p^\mu = (E, p_x, p_y, p_z) = (m_\perp \cosh y, p_\perp \cos \phi, p_\perp \sin \phi, m_\perp \sinh y), \quad (110)$$

where  $m_\perp^2 = p_\perp^2 + m^2$ . The one-particle phase-space element can also be rewritten in terms of  $y$  and  $p_\perp$  as

$$\frac{d^4p}{(2\pi)^4} \delta(p^2 - m^2) \theta(E) = \frac{d^3p}{(2\pi)^2 2E} = \frac{dy d^2p_\perp}{2(2\pi)^3}. \quad (111)$$

## A.2 Cross Sections

The starting point of all collider physics calculations is the calculation of the scattering cross section. The cross section for a  $2 \rightarrow n$  scattering processes,  $a + b \rightarrow 1 \dots n$ , is

$$d\sigma = \frac{(2\pi)^4}{4\sqrt{(p_a \cdot p_b)^2 - m_a^2 m_b^2}} d\Phi_n(p_a + p_b; p_1 \dots p_n) |\overline{\mathcal{M}}|^2, \quad (112)$$

where  $p_{a,b}$  and  $p_{i=1,\dots,n}$  are the momenta of the incoming and outgoing particles, respectively. The matrix element squared  $|\overline{\mathcal{M}}|^2$  is summed/averaged over the spins and colours of the outgoing/incoming particles. The  $n$ -particle phase-space element is

$$d\Phi_n(p_a + p_b; p_1 \dots p_n) = \delta^4 \left( p_a + p_b - \sum_{i=1}^n p_i \right) \prod_{i=1}^n \frac{d^3 p_i}{(2\pi)^3 2E_i}, \quad (113)$$

where  $E_i$  is the energy of the  $i$ th particle. It is conventional to define  $s = (p_a + p_b)^2$ . For massless incoming particles  $4\sqrt{(p_a \cdot p_b)^2 - m_a^2 m_b^2} = 2s$ .

Although modern theoretical calculations involve ever higher multiplicity final states in these lectures we will primarily deal with  $2 \rightarrow 2$  scattering processes in which case

$$\begin{aligned} d\Phi_2(p_a + p_b; p_1, p_2) &= \delta^4(p_a + p_b - p_1 - p_2) \frac{d^3 p_1}{(2\pi)^3 2E_1} \frac{d^3 p_2}{(2\pi)^3 2E_2}, \\ &= \delta(E_a + E_b - E_1 - E_2) \frac{1}{(2\pi)^6 4E_1 E_2} |p_1|^2 d|p_1| d\cos\theta d\phi, \\ &= \frac{1}{8\pi(2\pi)^4} \frac{|p_1|}{\sqrt{s}} d\cos\theta, \end{aligned} \quad (114)$$

where  $|p_1|$  is the magnitude of the three-momenta of either of the outgoing particles and  $\theta$  and  $\phi$  are the polar and azimuthal scattering angles, respectively. The cross section

$$d\sigma = \frac{1}{16\pi s} \frac{|p_1|}{\sqrt{s}} d\cos\theta |\overline{\mathcal{M}}|^2. \quad (115)$$

It is conventional to describe the scattering process in terms of the Mandelstam variables

$$s = (p_a + p_b)^2, \quad t = (p_a - p_1)^2, \quad u = (p_a - p_2)^2. \quad (116)$$

There are only two independent Mandelstam variables

$$s + t + u = m_1^2 + m_2^2 + m_a^2 + m_b^2 \xrightarrow{\text{massless}} 0. \quad (117)$$

In terms of these variables

$$d\sigma = \frac{1}{16\pi s^2} dt |\overline{\mathcal{M}}|^2. \quad (118)$$

### A.3 Cross Sections in Hadron Collisions

In hadron collisions there is an additional complication as the partons inside the hadrons interact. The hadron-hadron cross section is

$$d\sigma_{AB} = \sum_{ab} \int_0^1 dx_1 dx_2 f_{a/A}(x_1, \mu_F^2) f_{b/B}(x_2, \mu_F^2) \hat{\sigma}_{ab}(\hat{s}, \mu_F^2, \mu_R^2), \quad (119)$$

where  $x_{1,2}$  are momentum fractions of the interacting partons with respect to the incoming hadrons,  $\hat{s} = x_1 x_2 s$ ,  $\hat{\sigma}_{ab}(\hat{s}, \mu_F^2, \mu_R^2)$  is the parton-level cross section for the partons  $a$  and  $b$  to produce the relevant final state,  $f_{a/A}(x, \mu_F^2)$  is the parton distribution function (PDF) giving the probability of finding the parton  $a$  in the hadron  $A$ , and similarly for  $f_{b/B}(x, \mu_F^2)$ . The factorization and renormalisation scales are  $\mu_F$  and  $\mu_R$ , respectively.

In hadron collisions we usually denote the variables for partonic process with  $\hat{\phantom{x}}$ , *e.g.*  $\hat{s}$ ,  $\hat{t}$  and  $\hat{u}$  for the Mandelstam variables.



### A.3.1 Resonance production ( $2 \rightarrow 1$ processes)

The simplest example of a hadronic cross section is the production of an  $s$ -channel resonance, for example the  $Z^0$  or Higgs bosons. We assume that the incoming partons are massless so that the 4-momenta of the incoming partons are:

$$p_{a,b} = x_{1,2}(E, 0, 0, \pm E), \quad (120)$$

where  $E$  is beam energy in the hadron–hadron centre-of-mass system of collider such that  $s = 4E^2$ . The Breit-Wigner cross section, *e.g.* for  $Z$  production, is

$$\hat{\sigma}_{q\bar{q} \rightarrow Z^0 \rightarrow \mu^+ \mu^-} = \frac{1}{N_C^2} \frac{12\pi\hat{s}}{M_Z^2} \frac{\Gamma_{q\bar{q}}\Gamma_{\mu^+\mu^-}}{(\hat{s} - M_Z^2)^2 + M_Z^2\Gamma_Z^2}. \quad (121)$$

In the limit that the width is a lot less than the mass

$$\frac{1}{(\hat{s} - M_Z^2)^2 + M_Z^2\Gamma_Z^2} \approx \frac{\pi}{M_Z\Gamma_Z} \delta(\hat{s} - M_Z^2), \quad (122)$$

the *narrow width limit*. In this case the partonic centre-of-mass system is constrained to have  $\hat{s} = M_Z^2$ . The rapidity  $\hat{y}$  of the partonic system and  $\hat{s}$  are related to the momentum fractions  $x_{1,2}$  by

$$\hat{s} = x_1 x_2 s \quad \text{and} \quad \hat{y} = \frac{1}{2} \ln \frac{x_1 + x_2 + x_1 - x_2}{x_1 + x_2 - x_1 + x_2} = \frac{1}{2} \ln \frac{x_1}{x_2}. \quad (123)$$

Inverting these relationships we obtain

$$x_{1,2} = \sqrt{\frac{\hat{s}}{s}} e^{\pm \hat{y}} \quad \text{and} \quad \hat{y} = \frac{1}{2} \ln \frac{x_1^2 s}{\hat{s}} \leq \ln \frac{2E}{\sqrt{\hat{s}}} = \hat{y}_{\max}. \quad (124)$$

This allows us to change the variables in the integration using

$$s dx_1 dx_2 = d\hat{s} d\hat{y}, \quad (125)$$

giving the differential cross section

$$\frac{d\sigma_{AB \rightarrow Z^0 \rightarrow \mu^+ \mu^-}}{d\hat{y}} = \sum_{a,b=q\bar{q}} x_1 f_{q/A}(x_1, \mu_F^2) x_2 f_{\bar{q}/B}(x_2, \mu_F^2) \frac{12\pi^2}{N_C^2 M_Z^3} \Gamma_{q\bar{q}} B_{\mu^+ \mu^-}. \quad (126)$$

### A.3.2 $2 \rightarrow 2$ Scattering Processes

For most  $2 \rightarrow 2$  scattering processes in hadron–hadron collisions it is easier to work in terms of the rapidities  $y_3, y_4$  and transverse momentum,  $p_\perp$ , of the particles. We introduce average (centre-of-mass) rapidity and rapidity difference,

$$\bar{y} = (y_3 + y_4)/2 \quad \text{and} \quad y^* = (y_3 - y_4)/2, \quad (127)$$

which are related to the Bjorken  $x$  values by

$$x_{1,2} = \frac{p_\perp}{\sqrt{2}} (e^{\pm y_3} + e^{\pm y_4}) = \frac{p_\perp}{2\sqrt{s}} e^{\pm \bar{y}} \cosh y^*. \quad (128)$$

Therefore

$$\hat{s} = M_{12}^2 = 4p_\perp^2 \cosh y^* \quad \text{and} \quad \hat{t}, \hat{u} = -\frac{\hat{s}}{2} (1 \mp \tanh y^*).$$

The partonic cross section, assuming all the particles are massless, is

$$\begin{aligned} \hat{\sigma}_{ab \rightarrow 12} &= \frac{1}{2\hat{s}} \int \frac{d^3 p_1}{(2\pi)^3 2E_1} \frac{d^3 p_2}{(2\pi)^3 2E_2} |\overline{\mathcal{M}}_{ab \rightarrow 12}|^2 (2\pi)^4 \delta^4(p_a + p_b - p_1 - p_2), \\ &= \frac{1}{2\hat{s}^2} \int \frac{d^2 p_\perp}{(2\pi)^2} |\overline{\mathcal{M}}_{ab \rightarrow 12}|^2. \end{aligned} \quad (129)$$

Therefore once we include the PDFs, sum over  $a, b$ , and integrate over  $x_{1,2}$  the hadronic cross section is

$$\sigma_{AB \rightarrow 12} = \sum_{ab} \int \frac{dy_1 dy_2 d^2 p_\perp}{16\pi^2 s^2} \frac{f_a(x_1, \mu_F) f_b(x_2, \mu_F)}{x_1 x_2} |\overline{\mathcal{M}}_{ab \rightarrow 12}|^2,$$

including the factor  $1/(1 + \delta_{12})$  for identical final-state particles.

## B Flavour Physics

While most of the interactions in the Standard Model preserve the flavour of quarks and leptons the interaction of fermions with the  $W$  boson can change the flavour of the quarks and violate CP-conservation.

In order to understand the interactions of the quarks with the  $W$  boson we first need to consider the generation of quark masses in the Standard Model. The masses of the quarks come from the Yukawa interaction with the Higgs field

$$\mathcal{L} = -Y_{ij}^d \overline{Q_L^i} \phi d_{Rj}^I - Y_{ij}^u \overline{Q_L^i} \epsilon \phi^* u_{Rj}^I + \text{h.c.}, \quad (130)$$

where  $Y^{u,d}$  are complex  $3 \times 3$  matrices,  $\phi$  is the Higgs field,  $i, j$  are generation indices,  $Q_L^i$  are the left-handed quark doublets and,  $d_R^I$  and  $u_R^I$  are the right down- and up-type quark singlets. When the Higgs field acquires a vacuum expectation value  $\langle \phi \rangle = (0, \frac{v}{\sqrt{2}})$  we get the mass terms for the quarks.

The physical states come from diagonalizing  $Y^{u,d}$  using 4 unitary  $3 \times 3$  matrices,  $V_{L,R}^{u,d}$

$$M_{\text{diag}}^f = V_L^f Y^f V_R^{f\dagger} \frac{v}{\sqrt{2}}. \quad (131)$$

The interaction of the  $W^\pm$  and the quarks is given by

$$\mathcal{L}_W = -\frac{g}{\sqrt{2}} \left[ \bar{d}_L^I \gamma^\mu W_\mu^- u_L^I + \bar{u}_L^I \gamma^\mu W_\mu^+ d_L^I \right]. \quad (132)$$

The interaction with the mass eigenstates,  $f_L^M = V_L^f f_L^I$ , is

$$\mathcal{L}_W = -\frac{g}{\sqrt{2}} \left[ \bar{d}_L^M \gamma^\mu W_\mu^- V_{\text{CKM}}^\dagger u_L^M + \bar{u}_L^M \gamma^\mu W_\mu^+ V_{\text{CKM}} d_L^M \right], \quad (133)$$

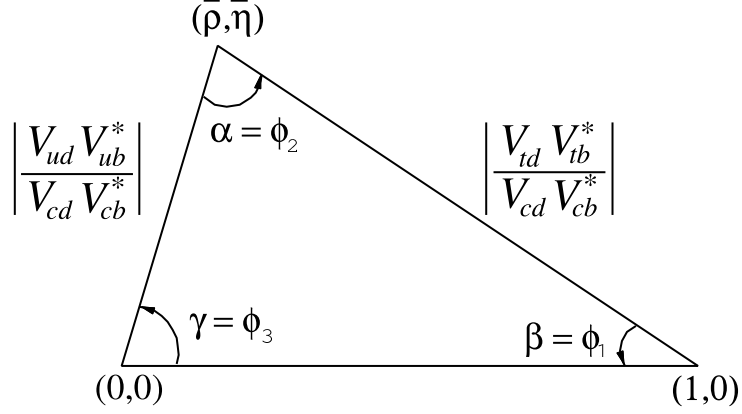


Figure 61: Unitary triangle.

where the Cabibbo-Kobayashi-Maskawa (CKM) matrix

$$V_{\text{CKM}} \equiv V_L^u C V_L^{d\dagger} = \begin{pmatrix} V_{ud} & V_{us} & V_{ub} \\ V_{cd} & V_{cs} & V_{cb} \\ V_{td} & V_{ts} & V_{tb} \end{pmatrix}, \quad (134)$$

is a  $3 \times 3$  unitary matrix.

The CKM matrix can be parameterized in terms of three mixing angles,  $(\theta_{12}, \theta_{13}, \theta_{23})$  and one phase,  $\delta$ ,

$$V_{\text{CKM}} = \begin{pmatrix} c_{12}c_{13} & s_{12}c_{13} & s_{13}e^{-i\delta} \\ -s_{12}c_{23} - c_{12}s_{23}s_{13}e^{i\delta} & c_{12}c_{23} - s_{12}s_{23}s_{13}e^{i\delta} & s_{23}c_{13} \\ s_{12}s_{23} - c_{12}c_{23}s_{13}e^{i\delta} & -c_{12}s_{23} - s_{12}c_{23}s_{13}e^{i\delta} & c_{23}c_{13} \end{pmatrix}, \quad (135)$$

where  $s_{ij} = \sin \theta_{ij}$  and  $c_{ij} = \cos \theta_{ij}$ . As experimentally  $s_{13} \ll s_{23} \ll s_{12} \ll 1$  it is convenient to use the Wolfenstein parameterization:  $s_{12} = \lambda$ ;  $s_{23} = A\lambda^2$ ; and  $s_{13}e^{i\delta} = A\lambda^3(\rho + i\eta)$ .

In which

$$V_{\text{CKM}} = \begin{pmatrix} 1 - \frac{1}{2}\lambda^2 & \lambda & A\lambda^3(\rho - i\eta) \\ -\lambda & 1 - \frac{1}{2}\lambda^2 & A\lambda^2 \\ A\lambda^3(1 - \rho - i\eta) & -A\lambda^2 & 1 \end{pmatrix} + \mathcal{O}(\lambda^4). \quad (136)$$

If we assume that the neutrinos are massless there is no mixing for leptons. We now know that the neutrinos have small masses so there is mixing in the lepton sector. The analogy of the CKM matrix is the Maki-Nakagawa-Sakata (MNS) matrix  $U_{\text{MNS}}$ .

A number of unitarity triangles can be constructed using the properties of the CKM matrix. The most useful one is

$$V_{ud}V_{ub}^* + V_{cd}V_{cb}^* + V_{td}V_{tb}^* = 0, \quad (137)$$

which can be represented as a triangle as shown in Fig. 61. The area of all the unitary

triangles is  $\frac{1}{2}J$ , where  $J$  is the Jarlskog invariant, a convention-independent measure of CP-violation,

$$J = \text{Im}\{V_{ud}V_{cs}V_{us}^*V_{cd}^*\}. \quad (138)$$

There are a large number of measurements which constrain the parameters in the unitarity triangle. They all measure different combinations of the parameters and over-constrain the location of the vertex of the unitarity triangle.

The magnitudes of the CKM elements control the lengths of the sides:

1.  $|V_{ud}|$  is accurately measured in nuclear beta decay;
2.  $|V_{cd}|$  can be measured using either semi-leptonic charm meson decays or using neutrino DIS cross sections;
3.  $|V_{ub}|$  is measured using inclusive and exclusive semi-leptonic B meson decays to light mesons  $B \rightarrow X_u \ell \bar{\nu}$  or  $B \rightarrow \pi \ell \bar{\nu}$ ;
4.  $|V_{cb}|$  is measured using inclusive and exclusive semi-leptonic B meson decays to charm mesons  $B \rightarrow X_C \ell \bar{\nu}$  or  $B \rightarrow D \ell \bar{\nu}$ .

The CKM matrix elements which give the length of the remaining side can only be measured in loop-mediated processes. The most important of these, FCNCs, have already been discussed in the context of BSM physics in Section 9.1.4. These also gives rise to  $B - \bar{B}$  mixing and oscillations, via the Feynman diagrams shown in Fig. 62.



Figure 62: Feynman diagrams giving  $B^0 - \bar{B}^0$  and  $B_s^0 - \bar{B}_s^0$  oscillations.

The oscillation probability is

$$P_{\text{oscillation}} = \frac{e^{-\Gamma t}}{2} \left[ \cosh \left( \frac{\Delta\Gamma t}{2} \right) + \cos(\Delta m t) \right], \quad (139)$$

where  $\Gamma$  is the average width of the mesons,  $\Delta\Gamma$  is the width difference between the mesons and  $\Delta m$  is the mass difference of the mesons. For both  $B_d$  and  $B_s$  mesons the  $\Delta m$  term dominates. From the box diagram

$$\Delta m_q = -\frac{G_F^2 m_W^2 \eta_B m_{B_q} B_{B_q} f_{B_q}^2}{6\pi^2} S_0 \left( \frac{m_t^2}{m_W^2} \right) (V_{tq}^* V_{tb})^2. \quad (140)$$

The decay constant  $f_{B_q}$  can be measured from leptonic decays  $B_q \rightarrow \ell^+ \nu_\ell$  but  $B_{B_q}$  comes from lattice QCD results. The QCD correction  $\eta_B \sim \mathcal{O}(1)$ .

The B-factories have studied  $B^0 - \bar{B}^0$  mixing in great detail giving

$$\Delta m_d = 0.507 \pm 0.005 \text{ps}^{-1}. \quad (141)$$

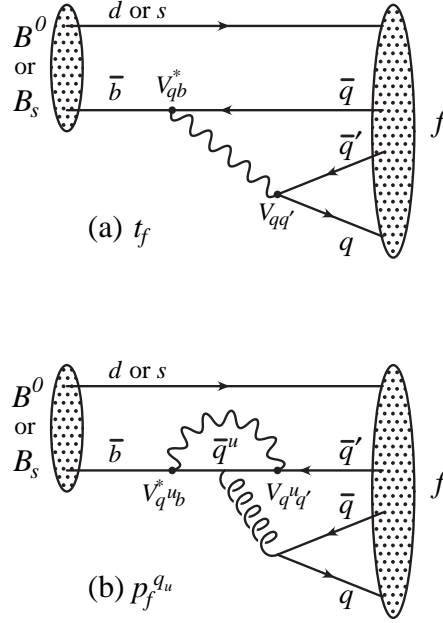


Figure 63: Examples of tree and penguin mediated processes, taken from Ref. [8].

It is important to measure both  $B_d - \bar{B}_d$  and  $B_s - \bar{B}_s$  mixing as some hadronic uncertainties cancel in the ratio. The rate is  $\propto |V_{ts}V_{tb}^*|^2$  due to the GIM mechanism. However, the high oscillation frequency makes  $B_s - \bar{B}_s$  mixing tricky to observe. The Tevatron observation relied on tagging the flavour of the B meson at production by observing an associated kaon from the fragmentation. The final result is

$$\begin{aligned} \Delta m_s &= 17.77 & \pm 0.10(\text{stat}) & \pm 0.07(\text{sys}), \\ |V_{td}| |V_{ts}| &= 0.2060 & \pm 0.0007(\text{exp}) & \pm 0.008(\text{theo}). \end{aligned} \quad (142)$$

The only source of CP-violation in the Standard Model is the complex phase in the CKM matrix. In order to see any effect we need at least two diagrams for the process with different CP-phases. There are three possibilities: CP-violation in the decay (*direct*); CP-violating in the mixing (*indirect*); CP-violation in the interference between decay and mixing. Example amplitudes are shown in Fig. 63.

The simplest type of CP-violation is direct CP-violation. This is the only possible type of CP-violation for charged mesons and is usually observed by measuring an asymmetry

$$A_{f^\pm} \equiv \frac{\Gamma(M^- \rightarrow f^-) - \Gamma(M^+ \rightarrow f^+)}{\Gamma(M^- \rightarrow f^-) + \Gamma(M^+ \rightarrow f^+)} \xrightarrow{\text{CP conserved}} 0. \quad (143)$$

If CP-symmetry holds, then  $|K_L\rangle = \frac{1}{\sqrt{2}}(|K^0\rangle + |\bar{K}^0\rangle)$  would be a CP-eigenstate with  $|K_L\rangle = |\bar{K}_L\rangle$ . If we take  $|M\rangle = |K_L\rangle$  and  $|f\rangle = |\pi^- e^+ \nu_e\rangle$  the corresponding CP-asymmetry is  $A_{\text{CP}} = (0.327 \pm 0.012)\%$ , which means that  $K_L$  is not a CP-eigenstate and there is CP-violation. There are many possible modes which measure different combinations of the angles in the unitarity triangle. The observed flavour and CP-violation is consistent with the Standard Model, i.e. the description by the CKM matrix, see Fig. 64.

There is one final area of flavour physics which is important. The matter in the universe consists of particles and not antiparticles. There are three Sakharov conditions required for this to happen:

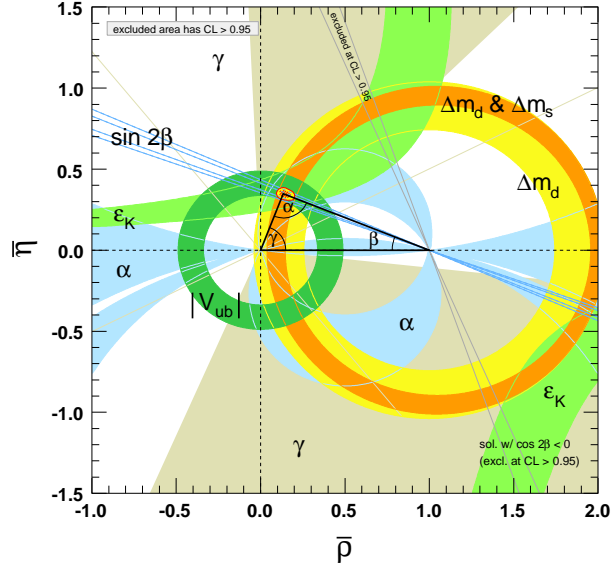


Figure 64: Experimental measurement of the unitarity triangle taken from Ref. [8].

1. baryon number violation;
2. C-symmetry and CP-symmetry violation;
3. interactions out of thermal equilibrium.

There are non-perturbative effects in the SM which violate baryon number. However, the amount of CP-violation in the quark sector is not enough to give the observed matter-antimatter asymmetry, there might be more in the lepton sector, otherwise we need a new physics source of CP-violation.

## References

- [1] F. Halzen and A. D. Martin, *Quarks and Leptons: An Introductory Course in Modern Particle Physics*, . ISBN-9780471887416.
- [2] V. D. Barger and R. J. N. Phillips, *Collider Physics*, . Redwood City, USA: Addison-Wesley (1987) 592 P. (Frontiers in Physics, 71).
- [3] R. K. Ellis, W. J. Stirling, and B. R. Webber, *QCD and Collider Physics*, *Camb. Monogr. Part. Phys. Nucl. Phys. Cosmol.* **8** (1996) 1–435.
- [4] G. Dissertori, I. G. Knowles, and M. Schmelling, *Quantum Chromodynamics: High energy experiments and theory*, . Oxford, UK: Clarendon (2003) 538 p.
- [5] J. F. Gunion, H. E. Haber, G. L. Kane, and S. Dawson, *The Higgs Hunter's Guide*, *Front. Phys.* **80** (2000) 1–448.

- [6] G. P. Salam, *Towards Jetography*, *Eur. Phys. J.* **C67** (2010) 637–686, [arXiv:0906.1833].
- [7] A. Buckley *et. al.*, *General-purpose event generators for LHC physics*, arXiv:1101.2599.
- [8] **Particle Data Group** Collaboration, K. Nakamura *et. al.*, *Review of particle physics*, *J. Phys.* **G37** (2010) 075021.
- [9] **OPAL** Collaboration, G. Abbiendi *et. al.*, *Measurement of event shape distributions and moments in  $e^+e^- \rightarrow \text{hadrons}$  at 91-209 GeV and a determination of  $\alpha_s$* , *Eur. Phys. J.* **C40** (2005) 287–316, [hep-ex/0503051].
- [10] **H1 and ZEUS** Collaboration, F. D. Aaron *et. al.*, *Combined Measurement and QCD Analysis of the Inclusive  $ep$  Scattering Cross Sections at HERA*, *JHEP* **01** (2010) 109, [arXiv:0911.0884].
- [11] J. M. Campbell, J. W. Huston, and W. J. Stirling, *Hard Interactions of Quarks and Gluons: A Primer for LHC Physics*, *Rept. Prog. Phys.* **70** (2007) 89, [hep-ph/0611148].
- [12] **CDF** Collaboration, T. A. Aaltonen *et. al.*, *Measurement of  $d\sigma/dy$  of Drell-Yan  $e^+e^-$  pairs in the  $Z$  Mass Region from  $p\bar{p}$  Collisions at  $\sqrt{s} = 1.96$  TeV*, *Phys. Lett.* **B692** (2010) 232–239, [arXiv:0908.3914].
- [13] **D0** Collaboration, V. M. Abazov *et. al.*, *Measurement of the shape of the boson transverse momentum distribution in  $p\bar{p} \rightarrow Z/\gamma^* \rightarrow e^+e^- + X$  events produced at  $\sqrt{s} = 1.96$ -TeV*, *Phys. Rev. Lett.* **100** (2008) 102002, [arXiv:0712.0803].
- [14] C. Anastasiou, L. J. Dixon, K. Melnikov, and F. Petriello, *High precision QCD at hadron colliders: Electroweak gauge boson rapidity distributions at NNLO*, *Phys. Rev.* **D69** (2004) 094008, [hep-ph/0312266].
- [15] J. R. Ellis, M. K. Gaillard, and G. G. Ross, *Search for Gluons in  $e^+e^-$  Annihilation*, *Nucl. Phys.* **B111** (1976) 253.
- [16] R. K. Ellis, D. A. Ross, and A. E. Terrano, *The Perturbative Calculation of Jet Structure in  $e^+e^-$  Annihilation*, *Nucl. Phys.* **B178** (1981) 421.
- [17] A. Gehrmann-De Ridder, T. Gehrmann, E. W. N. Glover, and G. Heinrich, *Second-order QCD corrections to the thrust distribution*, *Phys. Rev. Lett.* **99** (2007) 132002, [arXiv:0707.1285].
- [18] **CDF** Collaboration, T. Aaltonen *et. al.*, *Measurement of the Inclusive Jet Cross Section at the Fermilab Tevatron  $p$ - $p$ bar Collider Using a Cone-Based Jet Algorithm*, *Phys. Rev.* **D78** (2008) 052006, [arXiv:0807.2204].
- [19] **CDF** Collaboration, T. Aaltonen *et. al.*, *First Run II Measurement of the  $W$  Boson Mass*, *Phys. Rev.* **D77** (2008) 112001, [arXiv:0708.3642].

- [20] V. Buescher and K. Jakobs, *Higgs boson searches at hadron colliders*, *Int. J. Mod. Phys. A* **20** (2005) 2523–2602, [[hep-ph/0504099](#)].
- [21] K. Cheung, W.-Y. Keung, and T.-C. Yuan, *Collider Phenomenology of Unparticle Physics*, *Phys. Rev. D* **76** (2007) 055003, [[arXiv:0706.3155](#)].
- [22] **ATLAS** Collaboration, S. Ferrag, *Proton structure impact on sensitivity to extra-dimensions at LHC*, [hep-ph/0407303](#).
- [23] **UA1** Collaboration, G. Arnison *et. al.*, *Experimental Observation of Events with Large Missing Transverse Energy Accompanied by a Jet Or a Photon(s) in  $p\bar{p}$  Collisions at  $\sqrt{s} = 540\text{-GeV}$* , *Phys. Lett. B* **139** (1984) 115.
- [24] J. R. Ellis and H. Kowalski, *Supersymmetric Particles at the CERN  $p\bar{p}$  Collider*, *Nucl. Phys. B* **246** (1984) 189.
- [25] **Bern-CERN-Copenhagen-Orsay-Pavia-Saclay** Collaboration, P. Bagnaia *et. al.*, *Observation of Electrons Produced in Association with Hard Jets and Large Missing Transverse Momentum in  $p\bar{p}$  Collisions at  $\sqrt{s} = 540\text{ GeV}$* , *Phys. Lett. B* **139** (1984) 105.
- [26] S. D. Ellis, R. Kleiss, and W. J. Stirling, *Missing Transverse Energy Events and the Standard Model*, *Phys. Lett. B* **158** (1985) 341.
- [27] B. C. Allanach, K. Odagiri, M. A. Parker, and B. R. Webber, *Searching for narrow graviton resonances with the ATLAS detector at the Large Hadron Collider*, *JHEP* **09** (2000) 019, [[hep-ph/0006114](#)].
- [28] J. Donini *et. al.*, *Energy Calibration of  $b$ -Quark Jets with  $Z \rightarrow b\bar{b}$  Decays at the Tevatron Collider*, *Nucl. Instrum. Meth. A* **596** (2008) 354–367, [[arXiv:0801.3906](#)].
- [29] **CMS** Collaboration, G. L. Bayatian *et. al.*, *CMS technical design report, volume II: Physics performance*, *J. Phys. G* **34** (2007) 995–1579.
- [30] D. R. Tovey, *Measuring the SUSY mass scale at the LHC*, *Phys. Lett. B* **498** (2001) 1–10, [[hep-ph/0006276](#)].